8-2016

Blood-Tissue Barriers and Autoantibodies in Neurodegenerative Disease Pathogenesis: An Approach to Diagnostics and Disease Mechanism

Eric Luria Goldwaser
Rowan University

BLOOD-TISSUE BARRIERS AND AUTOANTIBODIES IN NEURODEGENERATIVE DISEASE PATHOGENESIS:

AN APPROACH TO DIAGNOSTICS AND DISEASE MECHANISM

Eric Luria Goldwaser, B.S.

A Dissertation submitted to the Graduate School of Biomedical Sciences, Rowan University in partial fulfillment of the requirements for the Ph.D. Degree.

Stratford, New Jersey 08084

August 2016

Table of Contents

Acknowledgements

Reflecting upon my growth comes most naturally in retrospect, and not by the milestones achieved, but by a new appreciation garnered for past events and experiences. As a 12-year old studying for my bar mitzvah, I was told that I had to donate a percentage of my proceeds to a charity of my choosing. It was an easy decision to pick the National Multiple Sclerosis Society, in honor of my aunt "Tia Maida", who had been living with MS for as long as I can remember. I felt helpful, like I was really making a difference to "raise money for research toward a cure", with the couple hundred dollars worth of a donation. Not until a few years later did I begin to take an active interest in science and medicine. In college, I was given the opportunity to work in Dr. Sudhir Nayak's molecular genetics lab for two years using *C. elegans* as a model system. I quickly learned how little a couple hundred dollars worth of lab supplies actually stretched, and it became clear to me that my efforts are much better suited at devoting my time, rather than my money, to scientific pursuits.

As I now finish up my tenure in the PhD program, I realize my clinical experiences of third year medical school are fast approaching. Come July, I wholly expect to find my re-entry into medical school refreshing and equally challenging. For me, the transition will be most difficult in that I feel I will always want to keep one foot in the lab and the other in the hospital. This bridge can become more of a tightrope for the physician-scientist at times (so they say…), however I realize that I have never truly left the lab from seven years ago.

At some point several things happened over the last three years for me: my hair was legitimately longer than my girlfriend's, when I type the letter "p" into my search bar "Pandora" has been replaced by "PubMed", and I often mistake my house key for my lab key when I am the first one in or last one out of lab. I think there is something significant to be said about each of them. I will let the amateur psychoanalyst in each of us interpret as they may.

It is impossible for me to proportion my thanks amongst those who have supported my growth over the years with the actual appreciation that I have. To my mentors who (for lack of better judgement) have given me a chance to prove my worth, I forever am grateful for that opportunity – Dr. Nayak in college, and Dr. Ellis in medical school were the first. Dr. Ellis lectured to my class during the second month into my medical biochemistry class; unfortunately, many students (not myself however) had ceased to attend classes long prior. I can wholeheartedly admit that these lectures were a vacation from the norm. One of the few professors who love to teach and emit their knowledge with such ability that it made me excited to have him again during graduate school for genetics. (What really drew me to Dr. Ellis, however, was his charming dog Max; and my offer as a dog sitter still stands indefinitely!).

Dr. Barone lectured to my second year medical school class during our neurology block, and I was immediately drawn to his incredible intellect and ability to teach – from complex neurological phenomenon down to basic clinical physical examination procedures. Over my vacation times, he graciously allowed me a shadowing opportunity, where I was able to interact with his patient population (predominantly MS patients) and help out around the office. I became a co-investigator on his clinical study testing trekking poles as alternatives to assisted walking devices typically used to help gait in the MS population. As an introduction into the world of clinical research, I found the direct and immediate patient applicability highly motivating, and a great juxtaposition to my time to come in the lab. He has been an instrumental mentor in helping me to grow my interest in neurology and clinical neurosciences, and I look forward to diving head first into clinical neurology and neuroimmunology in the years to come.

Dr. Nagele has never told me to call him Dr. Bob, even though everyone else does, and so I continue to properly refer to him as Dr. Nagele. His reputation amongst medical students is one of extreme admiration, reverence, and all-around wholesome

godliness – this is no exaggeration. Needless to say, along with my interest in neuroscience, I was very excited to set up a rotation in his lab. In fact, I found most topics in medical sciences to be tediously monotonous, save biochemistry, genetics, neuroscience, neurology, pathology, and psychiatry. I felt from my first encounters with Dr. Nagele that we were quite compatible in our out-of-the-lab hobbies, like all things related to Derren Brown, Malcolm Gladwell, The West Wing, and the GOP. Over the years I am immensely glad to have fostered the relationship we have. I know I will take much of the life lessons and lab lessons he has taught me, and will cherish them for the rest of my days. I cannot say enough about the experiences he has given me, and am confident that my return to medical school will (unfortunately for him) not mean the end of our relationship.

To the others from lab who have helped me with experiments, showed me the ropes, and became an integral part of my life (for better or worse), I owe tremendous amount of praise to them – Nimish, Abhi, George, and Cassie. They also deserve a fair amount of credit for putting up with my antics and peculiarities, which is not an easy task for most people. From days on end at conferences, to ever-lasting nights out, I could not have handpicked a better bunch of comrades to help me through this PhD.

Mary truly is the "lab mom", in the strictest sense of the title. She finally understands that just because I ask "What will happen to me if I drink this…" it does not mean that I have any intentions of actually doing so. Her humor and my sarcasm have been met with much awkward silences for other rotating students who don't understand our unique dialogues, but she will always share a special place in my memories. I think I am one of the few who have seen her optimistic side, but it has helped me through some long nights and failed experiments, so to Mary, I owe a boundless amount of thanks.

"We are like dwarfs sitting on the shoulders of giants.
We see more, and things that are more distant, than

they did, not because our sight is superior or because we are taller than they, but because they raise us up, and by their great stature add to ours." – John of Salisbury, 1159.

To Sagar, who never let me down, and has always been there for me. If everyone in the world could have a best friend like him, wars would end tomorrow, and unpunctuality would be a criminal offense. He is a man among boys – "Sutaria for President".

To my family, I owe everything. My parents have shown me they are my biggest fans throughout my life. As a kid, they traveled to my thousands of soccer games across the country, and have always supported my ambitious endeavors. Now, they travel to my poster presentations and talks at conferences and research days. "Coach Alberto" has brought my soccer teams to championships a number of times, and has taught me that humility and perseverance above all else, is what makes a champion. He will never stop being my coach, as I will never stop learning from him. My mom, the brilliant artist (www.indieartworks.com), was so inspired after a tour of the lab one day that she created a painting called "the cell" – and it is a masterpiece that I look very much forward to displaying for the world to see. (Cue Celine Dion "Because you loved me"). I am truly blessed to have such loving and committed parents, and know fully that I owe them more than I could ever express. (They don't know it, but *I* secretly am *their* biggest fan.). My brothers, Ari and Elan, each have helped me grow in very different ways. It is a special bond between a middle child and their siblings. From Shabbat dinners to impromptu Atlantic City trips and everything in between, I am thankful for always having them by my side. We have a blast in any situation we find ourselves – countdown to crazy horse monument completion is only thirty years by the way! Mark your calendars!

And finally, to Becca, my statistically significant partner ($p<10^{-\infty}$), I could not imagine how different my journey would be without her. To keep me updated on soccer games when I was unable to watch, to remind me to eat or sleep (or cut my hair), and to just keep me sane – her presence was always felt, even when we were not physically together. Her care, love, and support fuel me. Even though it does not do it justice, from the bottom of my heart I want you to know how truly amazing of a person you are. In the words of one of the greats, "I want to thank you for just being you".

> *"You have brains in your head. You have feet in your shoes. You can steer yourself any direction you choose. You're on your own. And you know what you know. And YOU are the one who'll decide where to go..." – Dr. Seuss, Oh the places you'll go!*

Abstract

Brain homeostasis can be affected in a number of ways that lead to gross anatomical, cellular, and molecular disturbances giving rise to diseases like Alzheimer's disease (AD) and related dementias. Unfortunately, the mechanistic pathoetiology of AD's hallmark features of cerebral amyloid plaque buildup and neuronal death are still disputed. Using human brain AD sections, immunohistochemistry experiments revealed internalized surface proteins, co-localized to an expanded lysosomal compartment. Other stains for amyloid-$\beta_{1\text{-}42}$ ($A\beta_{42}$) and various immunoglobulin (Ig) species displayed them leaking out of the cerebrovasculature through a dysfunctional blood-brain barrier (BBB), binding to neurons in the vicinity, and localizing to intracellular vesicles presumably en route to lysosomal degradation. To more clearly elucidate this process, a cell culture model system was established and assayed for aspects of an autoantibody (aAb)-mediated enhancement of amyloid internalization.

In a pilot study investigating the role of inhaled anesthetics on the BBB as an acute irritant, we were able to demonstrate the leakage of IgG into the cerebral cortex. As in our AD models and pathological slides, the aAbs bound to subsets of neurons and were increased in regions of BBB breakdown. The extent was directly proportional to the age of the animal, which parallels the incidence of post-operative delirium seen in the clinical setting, thus suggesting a potential link.

Lastly, the ability to assay BBB integrity clinically has remained elusive, yet is invaluable for pre-symptomatic diagnoses and potential treatments. In a previously published study using a diabetic young pig model, pathological changes were demonstrated in the brain parenchyma that faithfully recapitulated AD-type changes. The retinas of these pigs were also investigated for regions of blood-retinal barrier (BRB) leakage and neuronal pathology in the ganglion cell layer. This allows for a juxtaposed comparison between the BBB and the BRB, and opens up doors to use the BRB clinically as a surrogate system to detect ongoing BBB pathology. Taken together, these studies broaden the landscape of knowledge surrounding AD and other neurological diseases, providing new perspectives on pathogenesis, diagnosis, and treatment efforts.

Chapter I

Introduction/Background

INTRODUCTION

The role of the blood-brain barrier and cerebrovasculature in development of the two most common forms of dementias.

Dementia: The most feared disorder by the elderly population.

A survey carried out in 500 individuals aged fifty years and older in the United Kingdom revealed that dementia is the most feared disease by about 70% (news agencies 2014, The Press Association 2014). The second was cancer, by only 10% (news agencies 2014, The Press Association 2014). The Diagnostic and Statistical Manual (DSM) - 5th edition stratifies dementia into nine subtypes of neurocognitive disorders (NCDs). These include: Alzheimer's disease (AD), frontotemporal lobar degeneration, Lewy body disease, vascular disease (previously vascular dementia, VaD), traumatic brain injury, substance/medication-induced, HIV infection, prion disease, and Parkinson's disease. AD and VaD (also known as vascular cognitive impairment) comprise 60-80% and 15-20% of the total NCD cases, respectively. As the overwhelming majority of the cases, AD afflicts one in nine individuals over the age of 65. Presently about 5.3 million Americans are suffering from AD. Compared to the most prevalent fatal diseases, only in the case of AD is the number of deaths steadily increasing. The seven-fold increase in fear of dementia over cancer in the elderly population can perhaps be attributed to the lack of effective treatment coupled with inevitability of outcome. This absence of adequate medical intervention is largely due to a poor understanding of the pathogenesis and etiology of most types of

NCDs, AD included. Here we present selected studies that have demonstrated an abnormal cerebrovasculature as the inciting factor in two of the most prevalent dementias, AD and VaD. We also address some of the controversies that have prevented adequate recognition of the key role of the abnormal cerebrovasculature in etiology of these diseases.

Abnormalities of the cerebrovasculature may contribute to impaired brain homeostasis, neurodegeneration, and ultimately dementia.

The phrase "abnormal cerebrovasculature" is terminology intended to blanket all kinds of perturbations to blood vessels in the cerebral cortex of the brain. Other terminologies implying damage to cerebral blood vessels include blood-brain barrier compromise / breach / permeability, bleeding (micro/mini), cerebral hemorrhage, cerebral amyloid angiopathy, arteriosclerosis, and more (Deramecourt et al. 2012).

Given the importance of maintaining a strictly regulated microenvironment in the brain, it is essential to control exactly what enters and leaves the brain. Thus, the fluid that bathes the central nervous system, the cerebrospinal fluid (CSF), is not merely an ultrafiltrate of blood, but the result of a dynamic interplay between the blood and all of its components and the cellular entities that prevent or facilitate transport into the brain. In most parts of the cerebral cortex and hippocampus, the cerebrovasculature prevents free exchange of blood components between the neurons and the general circulation (Abbott et al. 2010, Hawkins and Davis 2005). This

barrier function is due to the presence of tight junctions between neighboring vascular endothelial cells that line the walls of cerebral blood vessels.

The monolayer of brain microvascular endothelial cells that forms the tight junctions that serve as the physical barrier is emphatically referred to as the "blood-brain barrier" (BBB). Other cellular structures and associations such as astrocytic foot processes, pericytes, basement membrane, and tight junction proteins further strengthen this barrier and are collectively, along with neurons, called the "neurovascular unit". Acting as a hindrance to the passage of blood-borne pathogens, rampant post-prandial glucose levels, soluble immune effector molecules, and cells, the primary function of the BBB is to preserve an optimal brain homeostasis, an essential prerequisite for the normal functioning of neurons operating in a complex electrochemical environment (Abbott et al. 2010, Hawkins and Davis 2005, Kalaria 2010, Reese and Karnovsky 1967).

AD: The most prevalent type of dementia, characterized by progressive, multifactorial neurodegeneration.

AD is a neurodegenerative disorder characterized by a progressive and irreversible decline in memory and cognition in the elderly. Degenerative changes found in the AD brain consist of a loss of neurons and disruption of neuronal circuits in cortical and hippocampal brain regions (Braak and Braak 1991, Gomez-Isla et al. 1997, Mirra et al. 1991, Selkoe 2002, Wisniewski, Wisniewski, and Wen 1985). Amyloid plaques (APs) and neurofibrillary tangles (NFTs) in the brain parenchyma are considered to

be key microscopic pathological hallmarks of AD. More recently, radiological scan studies have demonstrated enhanced levels of amyloid-$\beta_{1\text{-}42}$ ($A\beta_{42}$) peptides in the brains of both AD and control subjects (Klunk et al. 2004). Observations like these corroborate AD as an aging-associated progressive disease where the pathogenesis could have started decades prior to the onset of overt clinical symptoms (Blennow, de Leon, and Zetterberg 2006). In addition to extracellular amyloid deposits referred to APs, extensive intraneuronal $A\beta_{42}$ deposits have been reported in both AD and age-matched control cortices and hippocampi as well as in various animal models (D'Andrea et al. 2001, Nagele, Clifford, et al. 2011, Nagele et al. 2002, Gouras et al. 2000, Wirths and Bayer 2012).

Increasing age is the most important risk factor for AD. Aging is associated with significant changes in physical and metabolic activities. Receding cortical volume, cerebral atrophy, lacunar infarction, and compromised BBB are some of the well-recognized changes in aging brains (Mooradian 1988, Enzinger et al. 2005, Jeong et al. 2015). In fact, in a longitudinal study carried out on 85 year-old demented and non-demented controls, Skoog and colleagues reported a leaky BBB in individuals that later developed dementia (Skoog et al. 1998). In addition, metabolic disorders such as diabetes mellitus and dyslipidemia, particularly type 2 diabetes and hypercholesterolemia, are also associated with aging and have been regarded as additional risk factors for AD (Carlsson 2010, Craft 2009, Ohara et al. 2011). Furthermore, diabetes, hypertension, hyperlipidemia, and cardiovascular diseases are widely recognized as comorbid diseases associated with aging (Davis, Chung, and

Juarez 2011). Vascular inflammation and increased oxidative stress are also reported in aging population (El Assar, Angulo, and Rodriguez-Manas 2013). With millions of identified AD cases and additional tens of millions suffering from comorbid diseases with AD, the exact impact and cost is hard to predict. For the year 2014, AD was estimated to cost $214 billion in the US. Unfortunately, no cure exists for AD, and the few drugs that are available show mild efficacy at symptomatic management. This unmet medical need is due in some part to the fact that the pathogenesis of AD is not clearly understood, and key features remain embroiled in controversy amongst experts in the field.

AD has as unknown etiology but numerous hypotheses.

Even one hundred years since its discovery, the pathogenesis of AD remains elusive and highly contested. Although the presence of amyloid (senile) plaques and NFTs is well recognized, how and why they appear in the brain is still unclear. These pathological features form the basis for the two most prominent hypotheses describing AD pathogenesis: the amyloid hypothesis and tau hypothesis. The amyloid hypothesis is based on the deposition or accumulation of $A\beta_{42}$ peptides generated during the amyloidogenic pathway of amyloid precursor protein (APP) processing by β- and γ-secretases. The function of APP and $A\beta_{42}$ peptides in the brain is still unknown. Thought to be involved in synaptic formation early in neurogenesis and throughout life, excess amyloid may aggregate and accumulate as

insoluble fibrils, eventually impinging on cytoplasmic volume and disturbing cellular function.

NFTs are generated from the hyper-phosphorylated form of the Tau protein. Tau belongs to the class of proteins known as "microtubule associated proteins". Its function is to promote microtubule assembly and stabilization, and it is found in all nucleated cells. In AD pathology, Tau becomes hyper-phosphorylated by various kinases, such as glycogen synthase kinase-3. Hyper-phosphorylated Tau forms NFTs, instead of promoting microtubule stability. The structural imbalances that ensue cause a spiraling, or corkscrew appearance of axonal processes, irreparable neuronal damage, and fibrillar aggregates that disrupt cellular transport and architecture. These so-named "neurofibrillary tangles" are left as remnants within dead neurons. The Tau hypothesis states that as NFT production progresses, cellular transport mechanisms and structural supports collapse, culminating in damage and cell death. $A\beta_{42}$ oligomers have been found to associate with microtubules and can contribute to the breakdown of the microtubule integrity. It is well established that the NFT formation occurs as a downstream event, and amyloid aggregation stimulates a cascade of cellular pathways culminating in various kinase activation states.

Aside from these leading hypotheses, other associations are also gaining interest. For example, apolipoprotein E (APOE) is present on chylomicrons and intermediate-density lipoproteins (Evans et al. 1997, Sando et al. 2008). It plays a role in the catabolism of triglycerides present in lipoprotein complexes. However, an isoform of

APOE, derived from the ε4 allele, has been widely accepted as a genetic risk factor for the late-onset variant of AD (Evans et al. 1997, Sando et al. 2008, Corder et al. 1993). Alternatively, the cholinergic hypothesis attributes aberrant cholinergic firing as a causative factor in AD pathogenesis (Terry and Buccafusco 2003). Numerous abnormalities associated with choline metabolism have also been reported in the cholinergic neurons of elderly and AD patients. Moderate alleviation of AD symptoms using cholinergic drugs lends credence to this hypothesis. More recently, an abnormal cerebrovasculature has also been implicated in AD pathology (Kalaria 2010, Breteler 2000, de la Torre 2002). Efficient vasoreactivity in brain blood vessels is vital to meet the strict oxygen and glucose demands of the brain. Any modifications in the brain vasculature could impair normal brain homeostasis leading to neurodegenerative changes and impaired function (de la Torre 2002, Breteler 2000, Kalaria 2010).

The role of a permeable BBB in AD pathology is highly debated.

As mentioned above, an abnormal cerebrovasculature has been described using various terminologies - BBB compromise/breach/permeability, bleeding (micro/mini), cerebral hemorrhage, cerebral amyloid angiopathy, and arteriosclerosis. The association between BBB breach and AD is not a new concept (Erickson and Banks 2013, Bowman and Quinn 2008, Farrall and Wardlaw 2009, Rosenberg 2014). The integrity of the BBB has been questioned and linked to AD pathology for over three decades by several groups. To assess the functionality of the BBB, albumin or immunoglobulin (Ig) G levels in CSF and plasma/serum have been compared to

demonstrate the extent of BBB integrity. Albumin and IgG are normally absent in brain parenchyma, as they cannot freely cross the BBB. Thus, their appearance in the CSF indicates an increased BBB permeability. Radiologic imaging studies using computed tomography or magnetic resonance imaging have been employed to analyze BBB integrity (Bowman and Quinn 2008, Farrall and Wardlaw 2009, Rosenberg 2014, Erickson and Banks 2013). Immunohistological studies aimed at detecting extravasated IgG and albumin within the brain parenchyma have also been widely employed to survey the status of the BBB. Estimations provided by albumin quotients, IgG indices, and imaging studies can be carried out in vivo, while histological studies are limited to post-mortem tissue. Investigators supporting and refuting the role of an impaired BBB in AD pathology can be found in similar proportions.

In vivo studies of BBB compromise indirectly support its tie to AD and VaD

Albumin quotients and IgG indices are used to identify BBB leak. Alafuzoff's group first assayed albumin levels in the CSF and serum after others demonstrated its potential use in evaluating BBB integrity (Alafuzoff et al. 1983, Tibbling, Link, and Ohman 1977). They found significantly higher levels of albumin in CSF of multi-infarct dementia (a subtype of VaD) and AD (then characterized as "senile dementia of Alzheimer type" or "SDAT") compared to controls (Alafuzoff et al. 1983). Another study conducted by Elovaara and others measured nephelometric readings of immunoglobulins and serum protein ratios in the CSF of age-matched controls and AD patients – ambulatory and institutionalized (Elovaara et al. 1985). They reported

increased CSF/serum ratios for both albumin and IgG in both types of AD patients compared to controls. In another effort, an increased mean albumin ratio in AD patients compared to healthy controls was shown (Blennow et al. 1990). An interesting study using patients with major depression and AD of early and late onset was conducted by Hampel and colleagues, in which they reported lower levels of serum albumin and IgG in patients with AD and major depression (Hampel, Kotter, and Moller 1997). Among all patient groups, those with late-onset AD or major depression also demonstrated a significantly lower level of serum albumin compared to early onset AD patients (Hampel, Kotter, and Moller 1997). They also reported pathological CSF/serum ratios of albumin and IgG in both AD and major depression patients compared to controls (Hampel, Kotter, and Moller 1997). Along these same lines, Wada and colleagues compared AD patients to controls and showed significantly elevated levels of CSF albumin and albumin quotients in the AD cohort (Wada 1998).

Further support for the "BBB hypothesis" came from a longitudinal study of 85 year-olds for three years (Skoog et al. 1998). Of the 65 individuals at the beginning of this study, 13 were diagnosed with AD, 14 with VaD, and 2 with other dementias. Seven individuals developed dementia during the remainder of the study, while the other 29 remained non-demented. The authors reported an increased mean CSF/serum albumin ratio in AD and dementia patients compared to that of controls. Most interestingly, three of the non-demented women that later developed dementia had a higher CSF/serum albumin ratio compared to those who did not develop dementia,

suggesting BBB breakdown as an upstream event prior to symptom manifestation. In a similar prospective analysis, Bowman and colleagues conducted a one-year follow-up study on 36 mild to moderate AD patients (Bowman et al. 2007). Using a CSF-albumin index, they reported an increased extent of BBB compromise in eight of these patients. Additionally, the authors were able to successfully correlate the CSF-albumin index with rates of disease progression using a Mini-Mental State Examination and annual Clinical Dementia Rating sum-of-boxes change and annual ventricular volume change (Bowman et al. 2007). With respect to the CSF/plasma albumin ratio, Algotsson and Winblad also reported a greater incidence of BBB breach in male AD patients compared to female AD patients (Algotsson and Winblad 2007). They suggested gender biases for CSF/serum albumin ratio and plasma creatinine levels. More recently, Chalbot and colleagues have described a greater sensitivity for CSF secretory Ca^{2+}-dependent phospholipase A_2 ($sPLA_2$) activity in detecting BBB compromise when compared to that derived from the albumin quotient (Chalbot et al. 2011). By measuring $sPLA_2$ activity, they detected a greater incidence of BBB compromise in AD patients compared to healthy and non-demented controls. Taken together, these studies suggest a connection between BBB integrity and AD pathology. However, investigations carried out by other teams failed to observe the presence of a compromised BBB in AD patients (Kay et al. 1987, Mecocci et al. 1991, Frolich et al. 1991). Caution must be taken given the number of confounding factors that may contribute to dissenting results, but the data as a whole trend toward favoring a BBB component that is still in need of an optimized blood or CSF assay for more precise detection.

Histological studies can directly confirm BBB breakdown in AD.

Using histological sections taken from AD and control brains, the integrity of the BBB has been widely tested by detecting the presence of blood components in the brain interstitium that are normally confined to the vasculature. With an intact BBB, immunohistochemistry confirms that the brain parenchyma is largely devoid of IgG and albumin. Wisniewski and Kozlowski first utilized the local leakage of IgG and albumin to assess BBB integrity in brain samples (Wisniewski and Kozlowski 1982). They reported perivascular leakage of these components in SDAT brain sections. The extent of leakage was severe in regions demonstrating widespread signs of AD pathology. They also reported weak immunoreactivity in control brains and in brain regions devoid of amyloid plaques, emphasizing a temporal and spatial relationship between local BBB breakdown and the presence of AD-related pathology. DeReuck described a greater prevalence of cerebrovascular lesions, micro- or mini-bleeds in regions of AD brains that demonstrated cerebral amyloid angiopathy compared to controls (De Reuck 2012). Their work also reported mini-bleeds (microscopic, often subclinical, bleeding) in the age-matched controls (De Reuck 2012).

On the contrary, there are several histological reports that have failed to detect any significant difference in the extent of BBB breach. Using SDAT and multi-infarct dementia brain samples, Alafuzoff and colleagues did not observe any difference in BBB permeability between the demented and non-demented age-matched control groups (Alafuzoff et al. 1987). In AD and non-demented controls, Rozemuller's

group observed variations in the immunoreactivity of plasma proteins (Rozemuller et al. 1988). They associated this difference to the fixation period during tissue processing rather than an abnormal BBB (Rozemuller et al. 1988). Munoz and co-workers also failed to find evidence of BBB breach in AD and multi-infarct dementia patients (Munoz et al. 1997). Along these lines, Tomaimoto et al., reported an increased BBB breach in white matter lesions in cerebrovascular disease compared to AD (Tomimoto et al. 1996).

Imaging studies are inconclusive and limited by their ability to resolve the microvasculature.

Several groups have used computed tomography (CT), positron emission tomography (PET), and magnetic resonance imaging (MRI) for detecting BBB breaches in AD and control brains. In spite of employing these sophisticated techniques, all of these groups have failed to observe any substantial evidence of BBB breach in AD and dementia patients (Erickson and Banks 2013, Rosenberg 2012). Recently, Montagne and colleagues demonstrated aging-associated BBB breaches in the hippocampus (Montagne et al. 2015). Using advanced dynamic contrast-enhanced MRI capable of quantifying regional BBB permeability in vivo, the investigators demonstrated increased BBB compromise in aging individuals (Montagne et al. 2015). Additionally, they reported accelerated BBB compromise in the hippocampus of patients with mild cognitive impairment, a well-recognized early stage of AD.

Abnormal cerebrovasculature and impaired BBB are detectable in AD brains using immunohistochemistry.

Our group has examined brain samples from clinically confirmed AD and age-matched non-demented controls to investigate the state of the cerebrovasculature and integrity of the BBB. Utilizing immunohistochemistry, we have mainly studied the extravasation of plasma components such as IgG, C1q, and Aβ peptides (Nagele, Clifford, et al. 2011, Clifford et al. 2007). In accord with other studies, we have also taken advantage of perivascular leakage of these plasma components and used this feature as a tissue biomarker for BBB compromise. In most cases, these leak clouds were found surrounding or near the leaky blood vessels (termed source blood vessels) or their origins could be easily traced. In AD brains, we have observed a greater incidence and extent of focal perivascular leakage of IgG, C1q, and $A\beta_{42}$ peptides (Clifford et al. 2007). The AD cortex and hippocampus had the greatest extent and number of leaky blood vessels (Nagele, Clifford, et al. 2011). However, these were sometimes coincident with adjacent regions that lacked leakage of plasma components and thus appeared to be largely normal. As reported by Wisniewski and Kozlowski, we have also frequently observed some extent of local BBB breach in age-matched controls (Wisniewski and Kozlowski 1982, Nagele, Clifford, et al. 2011). We were further able to measure an increased incidence of cerebral amyloid angiopathy in the AD cerebrovasculature, in support of work done by Wisniewski, Kozlowski, and De Reuck (De Reuck 2012, Wisniewski and Kozlowski 1982, Clifford et al. 2008). Lastly, we also demonstrated an increased incidence of

perivascular leakage from blood vessels that concomitantly exhibited a greater extent of cerebral amyloid angiopathy (Clifford et al. 2008).

We have also investigated the integrity of the BBB in several animal models: Swiss Webster mice, Sprague Dawley rats, and Yorkshire domestic pigs. In mice, we were able to induce chronic BBB compromise by periodically injecting *Pertussis* toxin (Clifford et al. 2007). Upon immunohistological examination of these brains, perivascular IgG leak clouds were evident and comparable to those seen in the human AD cortex. Recently, Sprague Dawley rats at different ages were used to study the effects of inhaled anesthetics, such as Sevoflurane and Isoflurane, on the BBB and cerebrovasculature (Acharya et al. 2015). Older rats exposed to Sevoflurane showed the greatest extent of BBB breach as represented by IgG extravasation. At the regions of IgG leakage in these rats, the histological picture was again similar to that of AD (Acharya et al. 2015, Clifford et al. 2008, Nagele, Clifford, et al. 2011). Lastly, we showed compromise in BBB structural and functional integrity in Yorkshire domestic pigs with long-term diabetes mellitus and hypercholesterolemia, both well-known risk factors for dementia (Acharya et al. 2013). The permeability of the BBB in these animals was increased and IgG leak clouds were prominent, once again corroborating findings in AD and further supporting diabetes as a potent risk factor for AD through its effects on the vasculature (Acharya et al. 2013). Based on these studies, we conclude that immunohistochemistry is the most reliable and direct method to detect and quantify BBB compromise. Unfortunately, this approach comes with the obvious limitations that it is reserved for postmortem tissues. In contrast to

the work of Rozemuller, we have not seen differences in immunoreactivity due to fixation technique and chemicals used [59].

Reservations limiting the role of BBB in AD pathology.

Investigators working in the areas of BBB and AD are split into camps that support or refute the purported role of the BBB in AD pathology. As mentioned above, our studies have strongly suggested that the BBB is compromised during AD pathogenesis. Here, we offer plausible explanations for some of the reports that continue to question the role of the BBB in AD pathology. First is the occurrence of BBB breach in apparently healthy control individuals (Nagele, Clifford, et al. 2011). In a recent study using Sprague Dawley rats, we observed an aging-associated increase in BBB permeability (Acharya et al. 2015). Likewise, in healthy pigs that served as age-matched controls for diabetic and hypercholesterolemic pigs, we demonstrated some extent of BBB compromise (Acharya et al. 2013). In humans, one requirement for sporadic AD is advanced age. Even after the diagnosis of AD, cognitive abilities continue to decline at a variable pace over a period of four to eight years on average. Recent studies now suggest that AD-related pathology may be initiated as early as two to three decades prior to symptomatic presentation and clinical diagnosis (Blennow, de Leon, and Zetterberg 2006). Thus, in a disease as prevalent as AD, it is likely that many apparently healthy individuals often used in studies as age-matched non-demented controls are, in fact, harboring AD-related neurodegenerative changes. As such, they are actually asymptomatic (or pre-symptomatic) AD patients, and are not true controls at all. Starr and colleagues

reported a similar extent of BBB leakage between AD and non-demented older controls, giving further support for an aging-associated BBB compromise (Starr et al. 2009). Aging certainly plays a significant role on the permeability of the BBB globally, but many questions still obviously remain, like the importance of location and extent in the onset of dementia as it relates to BBB breakdown. Based on these data, we conclude that the permeability of the BBB increases with aging and AD, with variations in the location and extent of leak ultimately determining the site and rate of progression of the pathology and when telltale symptoms will emerge.

The second controversy stems from the failure to detect a significant indication of BBB breach in AD patients using imaging studies. This may be due to the limited resolution and sensitivity of this approach (Jellinger and Attems 2007). The brain contains many blood vessels of varying sizes, and current and widely used imaging techniques are not capable of detecting ongoing vascular leakage at the microscopic level within the microvasculature as reported by De Reuck (De Reuck 2012). This concept is illustrated in figure 1. To this point, the subclinical and apparently asymptomatic micro-bleeds require a degree of sensitivity outside the threshold of detection by currently available radiological imaging modalities. These bleeds are, however, readily detected in immunohistochemical preparations of postmortem tissues.

The third controversy is the selective appearance of BBB compromise in regions of pathology in AD patients. Bowman and colleagues reported an increased CSF-

albumin index in only eight out of 36 AD patients (Bowman et al. 2007). In this case, it is possible that the extent of BBB compromise in the remaining AD patients may not yet have reached a level in the brain tissue that is reflected by a detectable threshold of CSF-albumin index. In diabetic and hypercholesterolemic pigs, we have also observed regional variations in $A\beta_{42}$ loading by cortical pyramidal neurons, apparently paralleling the varied extent of local BBB breach in darapladib-treated and control pigs (Acharya et al. 2013). In fact, in AD brains, it is common to observe groups of adjacent pyramidal neurons, presumably supported by the same local vascular network, at similar stages of intra-neuronal amyloid loading. Individual variations, particularly those occurring in different regions of the same brain, is a major problem for all human studies, as it is very difficult to account for all the necessary confounds. Moreover, it becomes an extremely arduous task to find older individuals with only one type of chronic disease. Besides AD, aging is frequently associated with a wide variety of other chronic illnesses – diabetes, cancer, cardiovascular diseases, inflammation, traumatic brain injury, etc. It is likely that the aforementioned agonal and comorbid states play a crucial role in contributing to individual and case-to-case variations that have a tendency to lend confusion to our understanding of the disease process, a towering problem for the forward progress of research and medicine in general.

BACKGROUND

BBB breakdown and neuron-binding immunoglobulin (Ig) G is a novel "two-hit hypothesis" that could contribute to AD initiation and progression.

Tying together the new model to strengthen the old

As mentioned previously, the two microscopic pathological hallmarks of AD are APs and NFTs. Previous studies carried out by our group and others have shed light on the generation of these $A\beta_{42}$-containing plaques in relation to BBB compromise. This work has led us to propose a mechanistic explanation for the generation of amyloid plaques, the intraneuronal origin of $A\beta_{42}$ peptides, and the pathophysiological mechanisms leading to BBB compromise.

The current amyloid hypothesis suggests that $A\beta_{42}$ is directly and gradually deposited in the extracellular spaces within the brain to form APs, and does not include the progressive deposition and intracellular accumulation of $A\beta_{42}$ inside neurons, particularly pyramidal neurons, despite the fact that it has been repeatedly reported in human, pig, and various mouse transgenic models (Clifford et al. 2007, D'Andrea et al. 2001, Gouras et al. 2000, Nagele et al. 2002, Wirths and Bayer 2012, Nagele, Clifford, et al. 2011, D'Andrea and Nagele 2006, D'Andrea et al. 2002). In addition, the prevailing thinking assumes that neurons are the main source of the amyloid and secrete it into the extracellular space to form plaques. However, for some reason, much less attention is given to the possibility that, under conditions of BBB

breakdown, the peripheral circulation is a major source of the $A\beta_{42}$ that is found within neurons and plaques during AD pathogenesis (Clifford et al. 2008, Nagele, Clifford, et al. 2011). In fact, the inverse relationship between the number of plaques observed and number of local pyramidal neurons in any given region of the cortex is highly suggestive that plaques may actually represent the remnants of dead neurons (D'Andrea et al. 2001, Nagele, Clifford, et al. 2011, Nagele et al. 2002). Additional support for a neuronal origin of amyloid plaques includes the following: (1) plaques are most abundant in brain regions that are normally populated by the cell bodies of neurons, especially pyramidal neurons (D'Andrea and Nagele 2006, D'Andrea et al. 2002, D'Andrea et al. 2001, Nagele, Clifford, et al. 2011, Nagele et al. 2002); (2) the size of plaques in the cerebral cortex of AD brains is directly proportion to the size of local neurons from which they are presumably derived (D'Andrea and Nagele 2006, D'Andrea et al. 2002, D'Andrea et al. 2001, Nagele, Clifford, et al. 2011, Nagele et al. 2002); (3) plaques contain numerous intracellular proteins that are known to be somewhat resistant to lysosomal degradation such as cathepsin D, ubiquitin, and tau (D'Andrea et al. 2001, Zhang, Sheng, and Qin 2009, Ihara, Morishima-Kawashima, and Nixon 2012); and (4) plaques contain neuronal mRNAs and DAPI (4′,6-diamidino-2-phenylindole)-positive nuclear remnants (D'Andrea et al. 2001, Ginsberg et al. 2000). All of the above hint at remnants of degenerated cellular structures within Aβ42-containing amyloid plaques (D'Andrea et al. 2001). Since intact pyramidal neurons in AD brains also show selective and often extensive accumulation of $A\beta_{42}$ peptides, we have concluded that the degeneration and eventual

lysis of a neuron harboring intracellular deposits of $A\beta_{42}$ peptides can result in the generation of a single dense-core amyloid plaque (D'Andrea et al. 2001).

A key feature of intraneuronal deposition of $A\beta_{42}$ is its selectivity for pyramidal neurons in AD brains. We have proposed that this selectivity is due to the fact that most pyramidal neurons in the cerebral cortex highly express the α7 nicotinic acetylcholine receptor (α7nAChR). Earlier studies carried out by Wang and colleagues, have demonstrated a high binding affinity between α7nAChR and $A\beta_{42}$ (Wang, Lee, Davis, et al. 2000, Wang, Lee, D'Andrea, et al. 2000). In support of this, histological studies have revealed a selective accumulation of $A\beta_{42}$ peptides in neurons that express α7nAChR in the AD cerebral cortex and hippocampus (Nagele et al. 2002). Using SK-N-MC neuroblastoma cells that over-express α7nAChR, it was also demonstrated that α7nAChR and $A\beta_{42}$ are co-localized in these cells (Nagele et al. 2002). In vitro experiments carried out on α7nAChR-transfected SK-N-MC cells also shed light on the role that α7nAChR plays in endocytosis of exogenous $A\beta_{42}$. When these cells were treated with an inhibitor of endocytosis and an antagonist of α7nAChR, they failed to demonstrate $A\beta_{42}$ accumulation (Nagele et al. 2002). Moving to a mouse in vivo model system, researchers used fluorescein isothiocyanate (FITC)-tagged $A\beta_{42}$ peptides to track their internalization in the mouse brain (Clifford et al. 2007). Here, FITC-tagged $A\beta_{42}$ peptides were introduced into the general circulation by tail vein injection. The BBB of these mice was compromised by injecting *Pertussis* toxin. Consequently, these mice demonstrated selective

accumulation of FITC-tagged $A\beta_{42}$ peptide in cortical pyramidal and hippocampal hilar neurons (Clifford et al. 2007).

Without exception, all brain regions showing AD-related pathological changes contain neurons that are IgG-positive (Acharya et al. 2015, Acharya et al. 2013, Nagele, Clifford, et al. 2011). Western analysis has been used to confirm the presence of brain-reactive aAbs in all mammals tested thus far, including cow, pig, rat and mouse, with their numbers in any one individual in the thousands (Acharya et al. 2013, Nagele, Clifford, et al. 2011). The ability to translate the simple binary output of a Western blot into a complex microarray plate with nearly 10,000 human proteins has highlighted the potential utility of autoantibodies for disease diagnostics (Han et al. 2012, Nagele, Han, et al. 2011, DeMarshall et al. 2015). We are now able to stratify selective profiles of aAbs as biomarkers significant for age, sex, and disease state (Nagele et al. 2013). In addition, we have shown, using adult mouse brain slice cultures, that some brain-reactive autoantibodies are able to induce $A\beta_{42}$ internalization in pyramidal neurons (Nagele, Clifford, et al. 2011).

As mentioned above, in the event of a BBB compromise, various plasma components such as $A\beta_{42}$ peptides and IgG can enter the brain tissue. We have demonstrated the selective binding of IgG to pyramidal neurons in the cerebral cortex and hippocampus in regions of BBB breach in both AD and age-matched non-demented control brains (Nagele, Clifford, et al. 2011). In studies using adult mouse brain slice cultures, we also showed that the extent to which $A\beta_{42}$ accumulates in pyramidal neurons is

increased when treated with human serum that includes brain-reactive IgG aAbs, and sera from different individuals varied in their potency for driving intraneuronal $A\beta_{42}$ accumulation (Nagele, Clifford, et al. 2011). Taken together, these studies favor the idea that intraneuronal accumulation of $A\beta_{42}$ in pyramidal neurons is triggered and driven by local BBB compromise, which allows access of brain-reactive IgG aAbs to targets on the surfaces of local neurons and induces chronic endocytosis of bound IgG. At the same time, the influx of soluble monomeric and oligomeric $A\beta_{42}$ peptides from the peripheral circulation into the brain tissue coupled to their selective binding to α7nAChRs on the surfaces of the same pyramidal neurons that also bind IgG, suggests that these events may drive $A\beta_{42}$ into these cells via endocytosis.

The second hallmark of AD pathology, NFTs, is usually associated with advanced stages of AD pathology. In contrast to APs, there is a scarcity of studies that demonstrate a direct correlation between BBB compromise and NFTs. But, there are several studies that have reported $A\beta_{42}$-mediated initiation of NFTs. For example, primary neurons treated with 20 μM of $A\beta_{42}$ demonstrated significantly increased levels of phosphorylated Tau (Thr 235) (Koh, Noh, and Kim 2008). More recently, Nery and colleagues have demonstrated the association between $A\beta_{42}$ fibrils, Glycogen Synthase Kinase-3β activity and phosphorylation of Tau protein in zebra fish (Nery et al. 2014). The 5dpf larva of zebra fish injected with $A\beta_{42}$ peptide demonstrated weaker avoidance of aversive stimuli compared to controls (Nery et al. 2014). But, on treatment with lithium chloride, an inhibitor of kinase activity, the escape response to stimuli was significantly improved. Similarly, the intraventricular

injection of $A\beta_{42}$ also increased Tau phosphorylation at Ser202 and Thr205 that was inhibited by lithium chloride treatment (Nery et al. 2014). Lithium has recently gained much attention as a potential AD treatment. Many other kinases in the cell are also stimulated by $A\beta_{42}$, which again points to the role of $A\beta_{42}$ in promoting production of hyper-phosphorylated Tau protein. Although not directly linked to breakdown of the BBB, hyper-phosphorylated Tau protein is a downstream substrate to many of the phosphorylating agents activated by $A\beta_{42}$, which enters the brain parenchyma in the first place through a defective BBB and thus may trigger these events.

VaD and its close ties to AD may in fact represent similar pathoetiologies.

Accounting for roughly one of every five cases of dementia, VaD is the second most common cause of dementia or subtype of NCD, behind AD (Roman 2004). Symptoms include a sudden onset of memory dysfunction, immediate history of unsteady gait, loss of executive function, and loss of bowel or bladder control, temporally related to radiologic findings of blood vessel pathology, stroke in particular (Venkat, Chopp, and Chen 2015, Roman 2004). Upon identification of these symptoms, patients undergo neuroimaging tests, and in most cases, these symptoms are associated with one or more types of cerebrovascular lesions in the corresponding areas of the brain. Most of these investigations reveal extravasation of blood components from larger blood vessels as a common theme, with concomitant step-wise deterioration of neurological and neurocognitive function in the affect brain

region. Thus, the designation of VaD arose as a category of dementia because it was possible to directly link the condition to pathological changes in brain blood vessels that are large enough to resolve using imaging. Because large vessels serve larger blocks of brain tissue, pathological changes associated with VaD are acute rather than deterioration or loss of function as seen in AD patients. Neuroimaging, clinical presentations, and a detailed patient history are used for the diagnosis of VaD, an otherwise difficult condition to distinguish from AD. Using CT and MRI, pathology in larger vessels may be found which can cause tissue infarction in cortical, subcortical, or lacunar distributions. Moreover, hemorrhages in the intracerebral, lobar, subarachnoid, and white matter areas are readily detected using standard radiologic modalities, which can help to categorize the VaD (Venkat, Chopp, and Chen 2015, Roman 2004). However, currently used neuroimaging tools have limited sensitivity in detecting mild but chronic types of cerebrovascular lesions, leakage, and ischemic manifestations from smaller vessel pathology (Jellinger and Attems 2007). These so-called micro-bleeds occur in smaller vessels that serve smaller blocks of brain tissue so that, by themselves, they are insufficient to cause overt clinical symptoms as suddenly as that of typical VaD. In this case, the microvascular pathology is generally below the resolution limit of typical imaging methods; and, as such, the contribution of the vasculature to this condition can only be confirmed at autopsy (Roman 2004). The conspicuous overlap in the microvascular pathology of AD and macrovascular pathology of VaD suggests a common mechanistic underpinning, again lending credence to the vasculature as an upstream landmark by which to categorize both conditions.

There is a scarcity of research that points to BBB compromise as a causal factor in VaD. Mecocci and colleagues did, however, report significantly increased CSF albumin and an albumin ratio in multi-infarct dementia, a type of VaD (Mecocci et al. 1991). Similarly, in a three-year follow-up study with 85 year-old individuals, Skoog and colleagues found a significantly increased CSF/serum albumin ratio in VaD patients compared to that of age-matched non-demented controls (Skoog et al. 1998). Some of the animal models of VaD have demonstrated incidences of BBB compromise (Venkat, Chopp, and Chen 2015). Not surprisingly, the majority of reports aimed at understanding the development of VaD implicate lesions in the larger blood vessel for its pathoetiology.

Usually the symptomatology, extent of leakage, and brain region will determine the severity and appearance of the disease phenotype. Unfortunately, there are several instances in which the regions of vascular pathology are not clearly evident. This creates a dilemma when giving a diagnosis that determines the treatment. For example, the comorbidities of VaD and AD have brought about much confusion among investigators in the field. As reported by Barker and colleagues, out of 382 dementia patients, 294 demonstrated pathological changes similar to AD and VaD as shown by histological analysis (Barker et al. 2002). Neuropathological studies conducted similar to that of Barker's group have also demonstrated a high degree of overlap between AD and VaD (Breteler 2000, Craft 2009). These comparable neuropathological and vascular changes between VaD and AD could be the result of

common risk factors, namely aging, hypertension, DM, hyperlipidemia, stroke, and cardiac disease (Barker et al. 2002, Kalaria 2010, Snowdon 1997, Snowdon et al. 1997). In conclusion, VaD and AD are similar in that they both display vascular pathologies, with the major difference between the two being primarily related to the size of the vessels affects and whether the symptoms evolve more gradually (as in AD) or in a more acute fashion (as in VaD).

A damaged BBB and cerebrovasculature underlies a continuum between AD and VaD.

Presently, AD and VaD are the two most common types of dementia accounting for up to 95% of all dementias. Unfortunately, no single hypothesis currently is able to explain all of the facets associated with their pathology. Historically, an abnormal cerebrovasculature has been associated with dementia. Here we have tried to bring to the forefront and underscore the role of the BBB and abnormal cerebrovasculature in the initiation and progression of AD and VaD, aligning these conditions along a continuum of vascular demise, rather than considering them as two distinct and altogether separate pathological entities. Studies carried out by various groups using CT and MRI have clearly demonstrated vascular leakage in the patients suffering from VaD. In most cases, the clinical symptoms correlate with the infarcted or damaged brain regions. On the contrary, these neuroimaging techniques have failed to detect comparable levels of vascular compromise in AD. For this reason, many have questioned the involvement of the abnormal cerebrovasculature in AD pathology. Based on histological studies carried out by our group and others in AD

brains, we propose that the vascular lesions in the AD brain are subacute and affected blood vessels are too small to be resolved using currently employed neuroimaging and other *in vivo* imaging techniques. As the chronically compromised microvasculature perturbs brain homeostasis, it may be more accurate to refer to AD as "microvascular dementia".

We believe that AD- and VaD-associated vascular changes are incurred as a result of more than one type of insult (Figure 1). Aging, diabetes, hypertension, dyslipidemia-associated comorbid conditions, and trauma may increase one's vulnerability for an abnormal cerebrovasculature. The incidentally impaired BBB is only one of the many contributing factors. But it occurs as an important fulcrum by which the rest of the mechanism pivots and proceeds. Our research has invariably pointed to chronic cerebrovasculature leakage as the common upstream event in the pathogenesis of AD and VaD. Unfortunately, the currently employed in vivo techniques are unable to detect these microvascular lesions, thus calling for technical improvements that will make their detection possible. In our opinion, the inability to detect, locate, and quantify BBB compromise in vivo is the greatest challenge. Being able to detect BBB compromise and leaky vasculature at subacute levels would be helpful for early diagnosis, prognosis, and treatment success. Therapeutic efforts aimed at strengthening the BBB at early stages of AD and VaD pathogenesis could be the most promising treatment strategy for preventing AD and other types of NCDs.

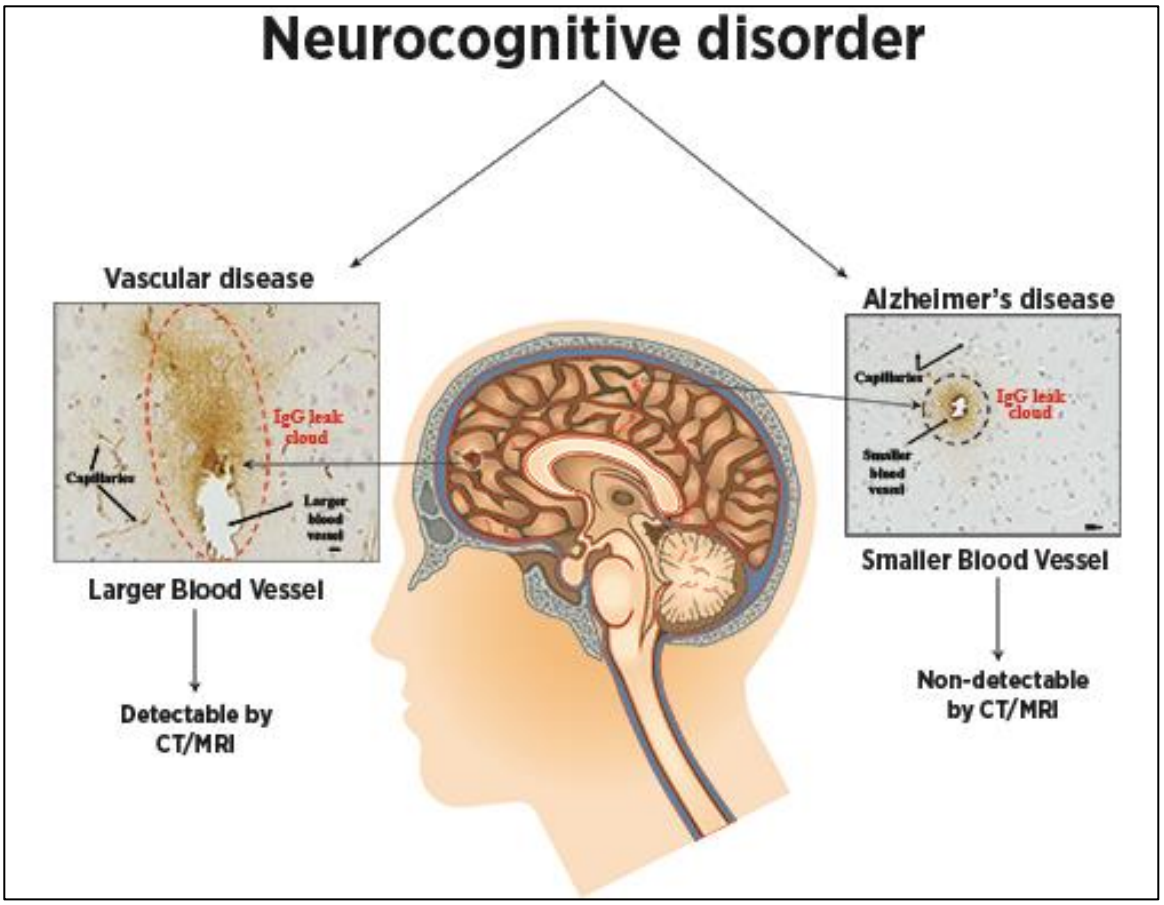
Neurocognitive disorder
Vascular disease
IgG leak cloud
Capillaries
Larger blood vessel
Larger Blood Vessel
Detectable by CT/MRI
Alzheimer's disease
Capillaries
IgG leak cloud
Smaller blood vessel
Smaller Blood Vessel
Non-detectable by CT/MRI

Figure 1: Abnormal cerebrovasculature and BBB breakdown results in extravasation of plasma components and is common to both VaD and AD. In VaD, cerebrovascular lesions result in an acute leakage of greater volumes of plasma components from larger blood vessels. In AD, chronic focal leakage of plasma components occurs in smaller blood vessels. The smaller blood vessels lack tunics and are dependent on endothelial cells, pericytes, astrocytic foot processes, and basement membrane for the containment of plasma components. Failure to do so is referred to as BBB breakdown. The volume of blood components exuding from larger blood vessels in VaD is more readily and easily detected by currently employed neuroimaging techniques. However, in the case of smaller blood vessel leaks, as is the case with AD, this volume is below the detectable threshold for radiological imaging, and can only be visualized in postmortem brain (Goldwaser 2015).

Post-operative delirium may be linked to the effect anesthetics have on the BBB

General anesthesia refers to a state of unconsciousness in a patient achieved by medications for amnestic, analgesic, muscle paralytic, and sedative purposes. This is performed prior to surgeries and procedures that would otherwise produce intolerable pain and discomfort to the patient. In addition, it allows for optimized conditions for a surgeon to operate in that the patient is paralyzed and unresponsive to stimuli that would impede the procedure.

Properties of commonly used anesthetic agents have been studied. One of the most important parameters is reported as minimum alveolar concentration (MAC), which denotes the percentage of atmosphere that is anesthetic in the stream of air delivered to the patient (Acharya et al. 2015, Maldonado 2008). Other factors generally related to a particular anesthetic are its ability to dissolve in gas or lipid, distribute throughout the body, etc.

Sevoflurane and isoflurane have been extensively studied in all of the aforementioned factors, and are two of the most commonly used inhaled anesthetics used in the operating room. However, cognitive dysfunctions that may arise as a result of undergoing general anesthesia have not been extensively studied. Most common anesthesia-related symptoms during the first day post-operatively is vomiting, nausea, sore throat, and incisional pain (Maldonado 2013). Deaths attributable to general anesthesia occur in 1 out of 100,000 patients. Perhaps the most pervasive of post-

operative side effects, however, is post-surgical (operative) delirium (POD). The rate of POD ranges from 10-74% depending on the type of surgery and population under study, however delirium itself occurs in up to 50% of elderly inpatients.

This condition constitutes a neurobehavioral syndrome with altered attention, awareness, and cognition that often develops acutely in response to a systemic, secondary insult (Association 2013). Current literature disputes the pathophysiologic connection between general anesthesia and POD, however several models do exist, likely occurring concomitantly. Some recent studies aimed at surveying the effect anesthetics may have on the BBB, shedding light on yet another condition that may be rooted in cerebrovascular dysfunction (Dittmar et al. 2012, Heinemann 2008, Hu et al. 2014, Sprung et al. 2016, Tetrault et al. 2008, Thal et al. 2012, Zhao et al. 2014). Most studies however, fail to use a single anesthetic agent when inducing their animal into a surgical-plane anesthesia. Although polypharmacy is the rule in the operating room, it may be helpful to begin stratifying all agents used in terms of their respective abilities to damage the BBB functional integrity.

BBB demise and AD-like pathological changes are noted in a pig model of diabetes.

Diabetes mellitus (DM) is a metabolic disorder characterized by abnormally high blood glucose levels, and exists as two major types. Type 1 is described by hyperglycemia and insulin deficiency resulting from immune-mediated destruction of

the insulin-producing beta (β)-cells residing in the islet of Langerhans of the pancreas. This pathoetiology is responsible for only 5-10% of the total diabetic population (CDC, National diabetes fact sheet, 2011). Type 2 DM, primarily caused by insulin resistance, accounts for about 90% of DM cases, and more commonly develops in older individuals. Presently, one in eleven Americans is diagnosed with DM, while one in three adults is considered pre-diabetic. On the global scale, 346 million individuals are diagnosed with DM, and in the year 2010, 10.9 million Americans in the age group of 65 years and older were diabetic (CDC, National diabetes fact sheet, 2011). This age group also accounts for the elderly demographic at risk to be diagnosed with Alzheimer's disease (AD) ("2012 Alzheimer's disease facts and figures," 2012). Epidemiologic studies hinting at the close connection between DM and AD have increased dramatically in number, according to the recent literature.

AD is the most prevalent neurodegenerative disease and the most common cause of dementia in the elderly. One in nine Americans aged 65 years and older is diagnosed with AD. Among major leading causes of death in America, AD is the only chronic disease with an increasing number of fatalities. The 99.6% failure rate for AD drugs in clinical trials has been both unfortunate and disheartening (Cummings JL 2014). In light of this, the field as a whole is in desperate need of a breakthrough, and serious attention to novel potential drug targets may provide new opportunities for successful therapeutic intervention. One promising and accessible target that has thus far received little attention is the brain vasculature. A number of recent studies have

suggested a pivotal role for an impaired blood vasculature in the pathogenesis of both AD and DM. Here, we present some of the evidence supporting the possibility that an abnormal cerebrovasculature is a common feature of AD and DM, which may explain why DM is now listed among the most important risk factors for AD.

Blood-tissue barrier systems serve similar functional roles in immunoprivileged sites.

Diabetes mellitus (DM) and hypercholesterolemia (HC), now considered major risk factors for AD, have been linked to a chronic inflammatory state resulting in increased BBB permeability. In a previous study, a DMHC porcine model treated with darapladib, an inhibitor of lipoprotein-associated phospholipase A_2 (LpPLA2) activity, and demonstrated decreased DMHC-mediated BBB permeability and brain $A\beta_{42}$ deposition (Acharya et al. 2013). This fascinating discovery set the stage for a follow-up study targeting another blood-tissue barrier system found in the ocular system – the blood-retina barrier (BRB). It was important, then, to use the same model system, in fact the same animals, to study if DMHC and darapladib had similar effects on the BRB. The translational scientific relevance of such a study is that the BRB can be tested clinically using ophthalmologic tools for breaches and abnormalities in individual layers of the retina known as a fluorescein angiogram. With the establishment of a correlated pair of vascular structures, the BRB may serve as a surrogate system to detect concomitant ongoing BBB dysfunction, years before clinical symptoms present. Such a finding will open up the doors to pre-symptomatic

detection and treatment options, otherwise rendered unavailable and ineffective by the time symptoms present and a neurodegenerative disease is diagnosed.

Epidemiological and neuropathological evidence supports a close association between DM, aging, dementia, and AD.

Several studies have demonstrated a greater incidence of cognitive decline in individuals with DM. Longitudinal studies carried out in Hashimaya, a small town in Japan, have strongly established DM as a risk factor for AD (Ohara et al. 2011). Similar research in the United States, like the Rotterdam and Rochester studies, has also pointed to DM as a risk factor for AD (Ott et al. 1996, Leibson et al. 1997). Individuals diagnosed with DM at an earlier age have a greater chance of developing AD compared to those who became diabetic at age 65 or older (Carlsson 2010, Xu, Qiu, et al. 2009, Xu et al. 2007, Xu, von Strauss, et al. 2009). Similarly, metabolic syndrome, a constellation of metabolic conditions that heighten the risk for stroke, coronary artery diseases, and type 2 DM, also increases the prevalence of AD (Carlsson 2010, Yaffe et al. 2004). A five-year prospective study carried out by Yaffe and colleagues has revealed an increased incidence of cognitive decline in individuals with metabolic syndrome (Yaffe et al. 2004).

A number of neuropathological changes are common to DM and AD. A state of chronic hyperglycemia in DM patients results in glycosylation of various receptors, leading to the formation of "receptors for advanced glycation end products" (RAGE)

(Taguchi 2009). Several studies have reported an affinity between Aβ peptides and RAGE, an interaction that has been purported to trigger and propagate chronic brain inflammation (Taguchi 2009, Yan et al. 1996). Higher levels of RAGE in neurons populating AD brains further bolster a causal role for RAGE in AD pathology (Yan et al. 1996). DM and AD are also often recognized as comorbid diseases since pathological changes such as hyperinsulinemia, glucose intolerance, hyperglycemia, insulin resistance, atherosclerosis, hypertension, and adiposity are common in afflicted patients (Carlsson 2010, Craft 2009, Kalaria 2010, Sims-Robinson et al. 2010). Aging, hypercholesterolemia, inflammation, and obesity are additional risk factors associated with both AD and DM (Carlsson 2010, Craft 2009, Kalaria 2010, Sims-Robinson et al. 2010, Bowman, Kaye, and Quinn 2012).

An abnormal cerebrovasculature is common in DM and dementias.

Cerebrovascular disease is a general term most often used to describe the consequences of an unhealthy and abnormally functioning brain vasculature. As the largest and most evolutionarily advanced part of the human brain, the cerebral cortex requires a profuse and steady supply of blood for normal functioning. Blood vessels of different kinds and sizes (structural hierarchies) are available to meet this demand.

It is not surprising that vascular abnormalities are more readily detectable when they involve larger blood vessels, as they can be more readily visualized by currently available neuroimaging techniques. Using MRI, increased deep white matter lesions, cerebral atrophy, subcortical brain atrophy, white matter hyperintensities,

hippocampal and amygdalar atrophy, and lacunar infarctions have been found to be more prevalent in type 2 DM patients compared to controls (den Heijer et al. 2003). The extent of damage and specific brain regions where these changes occur dictate the nature of the symptomatology. Acute and extensive leakage of blood components can be detected using MRI and CT, as in VaD cases. However, currently employed neuroimaging techniques fail to detect subacute or subclinical lesions/leakages (Snowdon DA 1997, Ikram MA 2011, Starr et al. 2009).

As in other parts of the body, capillaries in the brain exchange oxygen and nutrients for waste and carbon dioxide. These tiny vessels have a relatively simple architecture in that they lack the rather elaborate organization of circumferential tunics composed of smooth muscle layers and connective tissue that is typical of larger arterioles, venules, and all other blood vessels greater in size. Instead, capillaries are lined by a monolayer of vascular endothelial cells that serves as a functional barrier between the blood and the brain, i.e. the BBB. Continuous tight junctions that form between adjacent brain vascular endothelial cells are the main structural correlate of this barrier, and a number of tight junction proteins, including claudin -5, -3, and -12, occludin, zonula occludens (ZO) -1 and -2, and Vascular Endothelial - Cadherin, are known to be involved in their assembly and maintenance. Pericytes, astrocytic foot processes, and endothelial basement membranes also appear to support the structure and function of the BBB, although the exact nature of their individual contributions are unknown and currently under investigation. Along with neurons, this complex is often referred to as the neurovascular unit, which is currently depicted as a functional

entity that conveys information to and from the vasculature and neurons in connection (Abbott NJ 2010, Zlokovic 2008).

As in AD, there is a rapidly growing body of evidence implicating a dysfunctional BBB as responsible, at least in part, for many conditions, including epilepsy, multiple sclerosis, Parkinson's disease, depression, and schizophrenia (Suit YT 2014, Patel JP 2015, Michalak Z 2012, Hammer C 2013). This makes it reasonable to implicate BBB breakdown as a common mechanistic link in the initiation and progression of many, if not all, common neurocognitive disorders, with the nature of the symptoms being dictated by the exact brain location and severity of the BBB compromise.

Increased BBB permeability is apparent in diabetic patients and animal models.

Several studies have reported increased BBB permeability in diabetic patients. Starr and colleagues (Starr et al. 2003) used gadolinium and MRI to show significant increases in BBB permeability in type 2 diabetic patients compared to age-matched controls. They also reported significantly increased BBB permeability in the deeper brain regions (basal ganglia), more so than in the superficial areas (cortex), but other brain regions failed to show similar changes in these diabetic subjects.

In streptozotocin-induced diabetic rats Huber and colleagues observed an increased BBB permeability for smaller molecules (sucrose, 342 Da) compared to larger molecules (inulin, 5000 Da) (Huber, VanGilder, and Houser 2006). The observed increase in BBB permeability was region specific, with the midbrain demonstrating

the greatest extent of BBB compromise. Furthermore, levels of BBB permeability increased directly with time after induction of diabetes. They also reported that insulin treatment was effective in curtailing BBB compromise, especially at earlier stages of DM. In another study, BBB functional integrity was diminished in streptozotocin-treated diabetic rats (Hawkins et al. 2007). Interestingly, this increased BBB permeability was coincident with lowered expression of occludin and ZO-1 proteins. Upon receiving insulin treatment, hyperglycemia and BBB permeability were successfully attenuated. These streptozotocin-treated rats also showed increased matrix metalloproteinase activity in their plasma. Altered matrix metalloproteinase activity has been reported in various neurodegenerative diseases such as AD and epilepsy (Mizoguchi, Yamada, and Nabeshima 2011, Mizoguchi and Yamada 2013, Wang et al. 2014).

As in the in vivo animal studies, the presence of blood components that are normally absent in the brain parenchyma are commonly used as indicators of BBB compromise, with IgG and albumin leakage being the two most widely used for this purpose. As previously mentioned, Wisniewski and Kozlowski first reported extensive perivascular leakage of IgG and albumin in AD brain samples compared to controls (Wisniewski and Kozlowski 1982). In agreement with these early reports, additional work revealed an increased prevalence of micro- or mini-bleeds, a type of cerebrovascular lesion, in AD brains compared to controls (De Reuck 2012). Neuroradiological modalities employed gadolinium-diethylenetriamine pentaacetic acid (Gd-DTPA) and MRI to demonstrate the presence of a compromised BBB even

at an early stage of AD (Starr et al. 2009). In this study, however, they failed to demonstrate any significant difference in the extent of BBB compromise between AD and age-matched controls. Given the recent understanding that AD pathology can be ongoing decades before symptoms manifest and the disease is diagnosed, this finding is not surprising. The ability to accurately establish a "pathologically controlled" non-AD cohort, rather than a "symptomatically controlled" non-AD cohort, will be crucial to proper interpretation of these findings. Unfortunately, at present, it is impossible to detect accruing AD pathology early on in the disease development in vivo, even though such findings are readily uncovered on post-mortem brain tissue.

Popular rodent models of AD are inadequate for studying vascular changes and early stages of AD pathology.

Over 100 rodent models are available for studies on AD (http://www.alzforum.org/research-models). Each of these models were developed for the purpose of studying one or more aspects of AD-associated neurodegenerative changes or pathological features of the disease, such as amyloid plaques, neurofibrillary tangles, reactive gliosis, neuronal loss, synaptic loss, long-term depression/long-term potentiation, and cognitive decline. Unfortunately, these animals do not live long enough to develop the same types of aging-associated changes in the brain vasculature that afflict humans, including BBB breakdown, and therefore do not naturally develop AD-associated pathologies within their relatively short lifespan. Using radiotracers and endogenous mouse IgG leakage as markers of BBB compromise, vascular integrity and BBB function were tested in six of the most

commonly used rodent models of AD (Bien-Ly et al. 2015). During this study, the authors failed to observe significant incidence of BBB breach in these mouse models compared to the controls. This report supports our earlier studies carried out in Tg2576 mice (unpublished data).

Symptoms associated with AD emerge after many years of progressive neurodegeneration. The best hope for being able to effectively treat this disease almost certainly lies in early intervention. The implementation of early treatments, in turn, will depend on early diagnoses as well as our ability to definitively identify causal factors that drive the early stages of disease initiation. Based on the translational studies carried out by our group and others, cerebrovascular breakdown appears to be one of the common early triggers of AD that is rarely considered while designing animal models to recapitulate human pathology. Instead, the most widely used animal models of AD involve forced neuronal overexpression of mutant genes that does not occur during disease pathogenesis in humans. This provides a likely explanation for the observation that most AD models fail to show BBB leak (Bien-Ly et al. 2015). One must also consider that the structural hierarchy of affected vessels exhibiting BBB compromise seen in the much larger human brain is virtually absent in the mouse brain.

A porcine model is better suited to mimic human AD, and establishes a link between BBB compromise and the onset of AD-related pathology.

In a recent study, we investigated the question of whether or not chronic BBB compromise could lead to pathological changes consistent with early-stage AD using a pig model (Acharya et al. 2013). This animal model was originally developed as a model to study the pathogenesis of atherosclerosis in the great vessels, but was subsequently found to also increase BBB permeability, thus enabling relatively long-term studies of the effects of chronic BBB breakdown on the brain (Acharya et al. 2013). HC is often comorbid in humans with DM, which also serves as its own independent risk factor for developing AD and VaD (Carlsson 2010, Taguchi 2009, Kalaria 2010, Sims-Robinson et al. 2010, Ledesma and Dotti 2012, Luchsinger and Gustafson 2009, Harris 1991, Shepardson, Shankar, and Selkoe 2011). An association between HC and cognitive decline has also been strongly supported by epidemiological, neuropathological, and animal studies (Shepardson, Shankar, and Selkoe 2011, Jiang et al. 2012). It was even possible to increase the number and size of amyloid plaques by feeding a cholesterol-rich diet to AD transgenic mice (Refolo et al. 2000).

Histopathological analyses of DMHC porcine brains showed an increased incidence of BBB breach as visualized by a significantly higher level of free IgG present in the brain parenchyma compared to controls (Acharya et al. 2013). The extravasation of IgG occurred primarily in arterioles, with little evidence of significant leaks from venules or capillaries. Interestingly, extravasated IgG was also found to selectively target the surfaces of pyramidal neurons resident in the cerebral cortex. Along with the IgG leakage significant for AD-like pathology, the DMHC pigs also exhibited a

greater density of $A\beta_{42}$-positive neurons compared to controls (Acharya et al. 2013). Most importantly, pyramidal neurons accumulating $A\beta_{42}$ also demonstrated IgG co-labeling, perhaps alluding to a common mechanistic underpinning shared by these two events. An "antibody-mediated internalization" phenomenon of $A\beta_{42}$ is the current focus of a novel mechanism proposed and investigated for the pathogenesis of AD (Nagele, Clifford, et al. 2011). In addition, the vasculature in the DMHC pigs revealed increased instances of cerebral amyloid angiopathy and "corkscrew dendrites" in association with pyramidal cells, two key histopathological hallmark features of AD brains (Acharya et al. 2013, Nagele, Clifford, et al. 2011).

Curtailing vascular inflammation that favors BBB compromise should be a major therapeutic target.

An important outcome of the above-mentioned DMHC porcine study was in revealing the beneficial effects of darapladib, a potent anti-inflammatory inhibitor of lipoprotein-associated phospholipase A_2 developed by GlaxoSmithKline, on BBB functional integrity (Acharya NK 2013). Treatment of DMHC pigs with darapladib resulted in a reduction of AD-associated pathological hallmarks described above, and included a diminution of IgG leakage from blood vessels and a decreased number of amyloid-burdened pyramidal neurons compared to untreated DMHC controls (Acharya NK 2013). Essentially, darapladib successfully rescued the animals from the AD phenotype that was otherwise observed in controls, and restored the pathological indices measured back to control levels. By inhibiting the BBB

breakdown, this drug contributed to the proper maintenance of the cortical microenvironment in DMHC pigs. This suggests that darapladib may have similar utility in both diabetic and non-diabetic humans, and may also reduce the incidence and magnitude of the neurodegenerative changes triggered by chronic DMHC.

These outcomes are also in agreement with previous studies that implicate abnormalities in the cerebrovasculature in the pathogenesis of AD and VaD. Furthermore, we have recently found that the efficacy of darapladib in inhibiting vascular anomalies rooted in inflammation may also extend to another common affliction of the diabetic population – diabetic retinopathy (manuscript submitted). Here, key pathological features of diabetic retinopathy, such as edematous plexiform layers and shrinkage of various cellular layers, were evident in the same DMHC porcine model. Müller cell activation also alluded towards the pathological state and incurred cellular damage. We have shown increased blood-retinal barrier permeability, as visualized by IgG binding to ganglion cells of the retina, which closely resembled the situation where pyramidal cells in the cerebral cortex displayed IgG-positivity within or near regions of BBB breach. As in the cerebral cortex, pathological changes observed in the retinal layers of DMHC pigs were curtailed by darapladib to near control levels in the cohort of DMHC pigs. This finding further lends credence to the concept that chronic inflammatory changes in the walls of blood vessels within the brain can trigger BBB breakdown, initiating a cascade of pathological events that culminates in AD and perhaps other neurodegenerative diseases. It also suggests that darapladib and other agents that can block vascular

inflammation should be investigated and evaluated for their capacity to assuage the rampant neurodegeneration accompanying these diseases.

Darapladib has utility to restore BBB functionality in the DMHC pig model.

Lipoprotein-associated phospholipase-A_2 (Lp-PLA_2), also known as platelet-activating factor acetylhydrolase or type VIIA PLA2, is a calcium-independent phospholipase A_2. Lp-PLA_2 mediates the production of bioactive inflammatory mediators lysophosphatidyl choline and oxidized nonesterified fatty acids, two key players in the pathoetiology of atherosclerotic plaques and foam cell migration and accumulation. In humans, Lp-PLA_2 is secreted by leukocytes and is associated with circulating LDL and macrophages in atherosclerotic plaques, with plausible roles in the pro-thrombotic state seen when over-activated (Acharya NK 2013). There already exist many studies suggesting a causative role for Lp-PLA_2 in the development of atherosclerosis, and that inhibition of Lp-PLA_2 could decrease the hallmarks of acute plaque instability. Two such agents are being explored in clinical trials, rilapladib and dirapladib, for these purposes. Both drugs have similar efficacies and pharmacodynamics profiles, and are well tolerated.

In a previous study, we built a porcine model comorbid with DM and HC to elucidate the role of Lp-PLA2 in BBB instability, and subsequent intracellular $A\beta_{42}$ deposition. Pigs qualify as a good candidate model system for several reasons with our purposes in mind. Firstly, they have a plasma lipoprotein profile that is similar to that in humans. Furthermore, diabetic pigs develop ketotic states and gain weight to a lesser

degree that do non-diabetic ones. Taken together, this animal model shows advanced, human-like cardiovascular situations better than others available.

The BRB can act as a surrogate system to study concomitant BBB damage.

The BRB is of different ontogenetic origins than the BBB, however the functions of both are largely analogous. For example, the endothelial cell monolayer hallmarking the BBB is of mesenchymal origin, where angioblasts migrate to the neural parenchyma and form the eventual blood-tissue barrier under the influence and maintenance of astrocytic differentiation factors (Cunha-Vaz 1979). The retinal pigment epithelium (RPE) is derived, in contrast to the BBB, from the embryonic neuroectoderm and forms an outer monolayer in the ocular system during neuroembryonic development to partition body fluids from the immune-privileged retina. Although morphologically and developmentally distinct, the strikingly similar permeability properties of each blood-tissue barrier system lend credence to a comparative study aimed at surveying responses of each system to disease and then treatment (Cunha-Vaz et al. 1979).

A porcine model system was used in our study for a multitude of reasons, but perhaps most pervasive is the fact that mammals (humans) and pigs possess similarly arranged vasculature with barrier functions (specifically the inner BRB, iBRB). Meanwhile, neural retina structures of other species like equine and rabbits are largely devoid of such vascular beds (Frohlich 2002, Frydkjaer-Olsen et al. 2016). This discrepancy

holds true only for the iBRB, while the outer BRB (oBRB) is formed by the RPE, compartmentalizing the neural retina (in the neural tunic) from the fenestrated vascular system of the overlying choroid (vascular tunic). In essence, the iBRB is most identical to the endothelial BBB, whereas epithelial cells, not endothelial cells, establish the oBRB. These RPE cells in the eye are not influenced by astrocytes, again differentiating them from the contrasting BBB endothelial cells (Cunha-Vaz, Bernardes, and Lobo 2011).

When assessing carrier properties of the BBB and BRB, similarities of drug permeation and transport systems do exist. The epithelial oBRB parallels the drug permeation and transport systems in the BBB, expressing the same efflux pumps, like GLUT-1 and transcytosis proteins, even though the cell types vary greatly (Strauss 2016). When considering the similarities on a cellular and molecular level, the two systems overlap widely and demonstrate many shared aspects, such as specific tight junctional proteins, like occludins and claudins. These proteins make up the actual barrier structures, endothelial vascular beds, and are key players contributing to the immunologically privileged statuses. Again, although many differences are present between the BBB and BRB, similarities are well documented and established, and allow for interesting comparative studies aimed at assessing possible structural and clinically relevant surrogacies.

Clinical analysis remains for the most part elusive when it comes to the BBB, however ophthalmological tools, like fluorescein angiography, enable insight into

current states and functionality of the BRB. The implications of such a correlative discovery open the doors for BRB analysis to act in surrogacy for BBB pathology, which is vastly accepted as an underlying, and even necessary, component to many neurodegenerative diseases.

Vascular diseases, diabetic retinopathy, and the BRB

DM is an overwhelmingly prevalent disorder in the American population with strong correlations to obesity, chronic inflammation, and subsequent vascular demise. Previous studies have pointed to the role VEGF may play in permeabilizing the BRB, as higher levels of this protein are found in the vitreous fluid of patients with DR. Many of these findings further posit that VEGF induces such a state by a number of distinct mechanisms that are not mutually exclusive. Other studies have implicated proteins and hormones like growth hormone, insulin-like growth factor-1 (IGF-1), PKC, TGF-β, and pigment epithelium derived factor in the progression of DR from a standpoint of structural BRB changes.

The BRB is an essential component to maintain health of the retina, and loss of its integrity precedes neoangiogenesis in the implicated area. BRB breakdown, a hallmark of DR, is the number one cause of blindness in working-age Americans, with 20.1% of type I and 25.4% of type II diabetic patients presenting with macular edema (Muthusamy et al. 2014, Phillips et al. 2008, Runkle and Antonetti 2011). VEGF expression and its receptors are upregulated by six months of experimentally induced DM in the animal model. Presence of these proteins confers a strong

permeabilizing agent that increases prior to neovascularization. IGF-1 and its respective binding proteins are observed later in the disease process (Antonetti and Wolpert 2003). This aberrant endocrine process culminating in increased IGF-1 secretion prompted pituitary ablation procedures to decrease overall IGF-1 production successfully. FGF was noted to affect vascular permeability and neovascularization by increasing VEGF production in endothelial cells of the BRB. PDGF and its receptors are observed in the RPE in membranes to promote remodeling of the vascular network housed in the BRB.

Diabetes-induced BRB breakdown was noted to correlate with increased ROS formation alongside VEGF and uPAR. Similarly, treatment with a NOS inhibitor and peroxynitrite scavenger to reduce ROS formation inhibited the increased VEGF expression and uPAR, thereby preventing BRB breakdown. This study points to oxidative stress playing an integral role in the beginning stages of BRB breakdown from diabetic processes (El-Remessy et al. 2013).

AD-related changes to vision and the eye are well known and documented. However, previous reports fail to implicate the BRB as an underlying and necessary component to the pathoetiology of such conditions. Much effort is being devoted now to understanding the role the BBB plays in AD, and many neurodegenerative diseases of the like. Perhaps more focus should be on the vasculature, as this study alludes to, as being a fundamental early (perhaps the earliest) sign of imminent pathology like DR and AD.

The significance of DM, HC, and aging to vascular diseases is their relevance to actual vascular compromise that undoubtedly accompanies them (Figure 2). It is well documented that the chronic inflammatory states left by DM and HC have on the vasculature is disastrous, but never has it been taken to include the BRB similarly to as it does with the BBB. Clinical examinations using ophthalmoscopes and routine tools found in the ophthalmologist office are capable of surveying the BRB for signs of DR, however other techniques can be employed to take a more accurate view into the functional workings of the BRB itself. Vitreous fluid can be subject of investigation in the clinical setting when vitrectomy is used to treat various disease states and can be sampled for presence of circulating systemic growth factors. Albumin, a blood protein made exclusively in the liver, has been found elevated about twofold in DR patients, clearly underlying the breakdown of the BRB. Vitreous fluorometry and fluorescein angiography allows for retinal leakage mapping assessing structural capacities of the BRB.

In this study, we have shown that such contexts can be extrapolated to the BBB, as shown in the same pigs used in the 2013 paper where the BBB and subsequent cortical pyramidal neurons were studied. With this concept we are able to use the BRB in the clinical setting, as a surrogate for BBB analysis, which remains inevitably and outstandingly elusive for practical purposes to study. Furthermore, the non-invasive and minimally invasive procedures used by the ophthalmologist allow for routine screening to be employed at looking into the vascular integrity of the BRB,

and staking claims with degrees of accuracy as to the functionality of the BBB, a necessary and sufficient component to confer neurodegenerative disease states like AD and dementias of the like.

Diagnostic implications of pre-symptomatic disease states are founded in the vasculature.

Much investigatory effort and money is being devoted to pre-symptomatic diagnostics when it comes to neurodegenerative diseases. Owing to the futility of many pharmaceutical companies in treating full-blown AD, likely because at the time symptoms present, much of the pathology is already rampant in the brain, it has come to light that the onset of symptoms is preceded by pathology for many years. Breakdown of the BRB can be visualized, and is able to demonstrate the earliest observable changes accompanying DR. The extent to which the BRB is damaged correlates strongly with eventual vision loss. There is a clear analogous relationship between the BRB with DR and the BBB with AD. Housed within the ganglion cell layer of the retina is the vasculature that provides metabolic support for the inner layers of the retina that extends down to the outer plexiform layer. The outer retina, mostly the photoreceptors, receives nutrients via diffusion from the vascularized coroidocapillaries across the RPE; as mentioned previously, these retinal vessels in conjunction with the RPE form the oBRB. This level of compartmentalization around the neural retina forms an immunologically privileged tissue and provides a degree of regulation about fluid and metabolite fluxes into the tightly controlled microenvironment of the eye.

Fluorescein angiography is one of the most frequent examinations performed by the ophthalmologist. The BRB regulates the microenvironment of the retina and provides transport function of ciliary epithelia in an effort to maintain the vitreous, retina, and posterior segment of the eye some of the few 'immunoprivileged sites' in the body. Methods of clinical evaluations are performed by vitreous fluorometry to generate a retinal leakage map. This provides insight into the influx and efflux systems present in the BRB by means of fluorescein presence following IV injection. The path the fluorescein takes to enter the vitreous humor of the eye is either anteriorly from the ciliary body and aqueous humor, or posteriorly through the retinal and choroidal vessels traversing the BRB. In DR, the BRB is compromised in the posterior section BRB, allowing access to the vitreous humor. Vitreous fluorometry is a sensitive and quantitative method that depicts changes in the BRB and is used clinically to detect disease presence, not necessarily specific disease identity. On the contrary, such a technique would show promise in detecting treatment efficacy and effectiveness in terms of BRB integrity re-establishment.

Clinical implications of such a finding would allow for non-invasive techniques, like fluorescein angiography for instance, to observe the microvasculature in the ocular system as a surrogate for simultaneously occurring pathology in the BBB. Taken together, these connections shed light on a well-known association between AD-induced changes in the ocular system and vision, perhaps elucidating a common underlying etiology founded in the structural integrity of the vasculature.

Furthermore, by expounding on the mechanistic connection between the BRB, DM, and DR, we are able to more clearly understand an even deeper-seeded root between neurodegenerative diseases like AD, dementia, and the BBB.

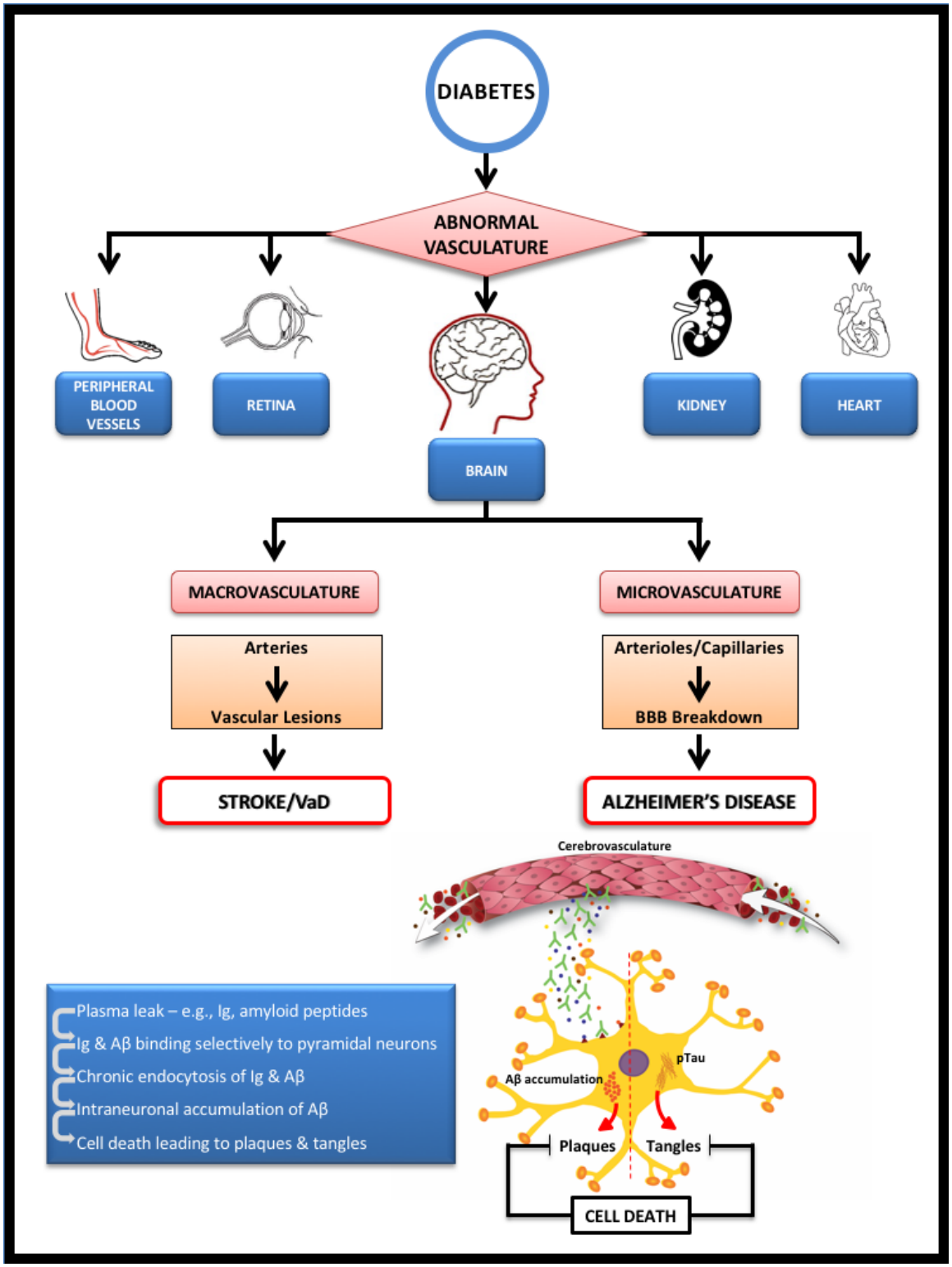
DIABETES
ABNORMAL VASCULATURE
PERIPHERAL BLOOD VESSELS
RETINA
BRAIN
KIDNEY
HEART
MACROVASCULATURE
MICROVASCULATURE
Arteries
Vascular Lesions
Arterioles/Capillaries
BBB Breakdown
STROKE/VaD
ALZHEIMER'S DISEASE
Cerebrovasculature
Plasma leak – e.g., Ig, amyloid peptides
Ig & Aβ binding selectively to pyramidal neurons
Chronic endocytosis of Ig & Aβ
Intraneuronal accumulation of Aβ
Cell death leading to plaques & tangles
Aβ accumulation
pTau
Plaques
Tangles
CELL DEATH

Figure 2 – Diabetes induces blood-brain barrier breakdown, triggering Alzheimer's disease neurodegenerative changes.

Many complications of DM are related to a globally impaired vascular integrity, spanning vessel hierarchy and structure from large to small, and resulting in conditions like peripheral neuropathy, retinopathy, nephropathy, and coronary artery disease. These vascular abnormalities extend throughout the body, and include the supply to the cortical and deep brain structures. Here, macrovascular lesions of the arterial blood supply result in stroke and VaD. On the other hand, chronic leakage of plasma components from the microvasculature occurs at the level of arterioles and capillaries as a result of BBB breakdown and contributes to the pathogenesis and development of AD. Following BBB breakdown, various plasma components, including Ig species (IgG) and amyloid peptides ($A\beta_{42}$), leak out and bind to pyramidal neurons in regions of vascular compromise. Chronic BBB leakage drives binding of Ig and Aβ to neuronal surfaces, followed by their internalization and accumulation, leading to neuronal damage, synaptic loss, cell death, and the appearance of plaques and tangles as pathological hallmarks commonly observed at autopsy. DM = diabetes mellitus; AD = Alzheimer's disease; BBB = blood-brain barrier; Ig = immunoglobulin; $A\beta_{42}$ = amyloid-$\beta_{1\text{-}42}$; VaD = Vascular dementia.

REFERENCES

Abbott, N. J., A. A. Patabendige, D. E. Dolman, S. R. Yusof, and D. J. Begley. 2010. "Structure and function of the blood-brain barrier." *Neurobiol Dis* 37 (1):13-25. doi: 10.1016/j.nbd.2009.07.030.

Abbott NJ, Patabendige AAK, Dolman DEM, Yusof SR, Begley DJ. 2010. "Structure and function of the blood-brain barrier." *Neurobiology of Disease* 37:13-25.

Acharya, N. K., E. C. Levin, P. M. Clifford, M. Han, R. Tourtellotte, D. Chamberlain, M. Pollaro, N. J. Coretti, M. C. Kosciuk, E. P. Nagele, C. Demarshall, T. Freeman, Y. Shi, C. Guan, C. H. Macphee, R. L. Wilensky, and R. G. Nagele. 2013. "Diabetes and hypercholesterolemia increase blood-brain barrier permeability and brain amyloid deposition: beneficial effects of the LpPLA2 inhibitor darapladib." *J Alzheimers Dis* 35 (1):179-98. doi: 10.3233/JAD-122254.

Alafuzoff, I., R. Adolfsson, G. Bucht, and B. Winblad. 1983. "Albumin and immunoglobulin in plasma and cerebrospinal fluid, and blood-cerebrospinal fluid barrier function in patients with dementia of Alzheimer type and multi-infarct dementia." *J Neurol Sci* 60 (3):465-72.

Alafuzoff, I., R. Adolfsson, I. Grundke-Iqbal, and B. Winblad. 1987. "Blood-brain barrier in Alzheimer dementia and in non-demented elderly. An immunocytochemical study." *Acta Neuropathol* 73 (2):160-6.

Algotsson, A., and B. Winblad. 2007. "The integrity of the blood-brain barrier in Alzheimer's disease." *Acta Neurol Scand* 115 (6):403-8. doi: 10.1111/j.1600-0404.2007.00823.x.

Antonetti, D. A., and E. B. Wolpert. 2003. "Isolation and characterization of retinal endothelial cells." *Methods Mol Med* 89:365-74. doi: 10.1385/1-59259-419-0:365.

Association, American Psychiatric. 2013. *Diagnostic and statistical manual of mental disorders: DSM-5*. Washington, D.C.: American Psychiatric Association.

Barker, W. W., C. A. Luis, A. Kashuba, M. Luis, D. G. Harwood, D. Loewenstein, C. Waters, P. Jimison, E. Shepherd, S. Sevush, N. Graff-Radford, D. Newland, M. Todd, B. Miller, M. Gold, K. Heilman, L. Doty, I. Goodman, B. Robinson, G. Pearl, D. Dickson, and R. Duara. 2002. "Relative frequencies of Alzheimer disease, Lewy body, vascular and frontotemporal dementia, and hippocampal sclerosis in the State of Florida Brain Bank." *Alzheimer Dis Assoc Disord* 16 (4):203-12.

Bien-Ly, N., C. A. Boswell, S. Jeet, T. G. Beach, K. Hoyte, W. Luk, V. Shihadeh, S. Ulufatu, O. Foreman, Y. Lu, J. DeVoss, M. van der Brug, and R. J. Watts. 2015. "Lack of Widespread BBB Disruption in Alzheimer's Disease Models: Focus on Therapeutic Antibodies." *Neuron* 88 (2):289-97. doi: 10.1016/j.neuron.2015.09.036.

Blennow, K., M. J. de Leon, and H. Zetterberg. 2006. "Alzheimer's disease." *Lancet* 368 (9533):387-403. doi: S0140-6736(06)69113-7 [pii] 10.1016/S0140-6736(06)69113-7 [doi].

Blennow, K., A. Wallin, P. Fredman, I. Karlsson, C. G. Gottfries, and L. Svennerholm. 1990. "Blood-brain barrier disturbance in patients with Alzheimer's disease is related to vascular factors." *Acta Neurol Scand* 81 (4):323-6.

Bowman, G. L., J. A. Kaye, M. Moore, D. Waichunas, N. E. Carlson, and J. F. Quinn. 2007. "Blood-brain barrier impairment in Alzheimer disease: stability and functional significance." *Neurology* 68 (21):1809-14. doi: 10.1212/01.wnl.0000262031.18018.1a.

Bowman, G. L., J. A. Kaye, and J. F. Quinn. 2012. "Dyslipidemia and blood-brain barrier integrity in Alzheimer's disease." *Curr Gerontol Geriatr Res* 2012:184042. doi: 10.1155/2012/184042.

Bowman, G. L., and J. F. Quinn. 2008. "Alzheimer's disease and the Blood-Brain Barrier: Past, Present and Future." *Aging health* 4 (1):47-55. doi: 10.2217/1745509X.4.1.47.

Braak, H., and E. Braak. 1991. "Demonstration of amyloid deposits and neurofibrillary changes in whole brain sections." *Brain Pathol* 1 (3):213-6.

Breteler, M. M. 2000. "Vascular involvement in cognitive decline and dementia. Epidemiologic evidence from the Rotterdam Study and the Rotterdam Scan Study." *Ann N Y Acad Sci* 903:457-65.

Carlsson, C. M. 2010. "Type 2 diabetes mellitus, dyslipidemia, and Alzheimer's disease." *J Alzheimers Dis* 20 (3):711-22. doi: 10.3233/JAD-2010-100012.

Chalbot, S., H. Zetterberg, K. Blennow, T. Fladby, N. Andreasen, I. Grundke-Iqbal, and K. Iqbal. 2011. "Blood-cerebrospinal fluid barrier permeability in Alzheimer's disease." *J Alzheimers Dis* 25 (3):505-15. doi: 10.3233/JAD-2011-101959.

Clifford, P. M., G. Siu, M. Kosciuk, E. C. Levin, V. Venkataraman, M. R. D'Andrea, and R. G. Nagele. 2008. "Alpha7 nicotinic acetylcholine receptor expression

by vascular smooth muscle cells facilitates the deposition of Abeta peptides and promotes cerebrovascular amyloid angiopathy." *Brain Res* 1234:158-71. doi: S0006-8993(08)01811-8 [pii] 10.1016/j.brainres.2008.07.092 [doi].

Clifford, P. M., S. Zarrabi, G. Siu, K. J. Kinsler, M. C. Kosciuk, V. Venkataraman, M. R. D'Andrea, S. Dinsmore, and R. G. Nagele. 2007. "Abeta peptides can enter the brain through a defective blood-brain barrier and bind selectively to neurons." *Brain Res* 1142:223-36. doi: S0006-8993(07)00127-8 [pii] 10.1016/j.brainres.2007.01.070 [doi].

Corder, E. H., A. M. Saunders, W. J. Strittmatter, D. E. Schmechel, P. C. Gaskell, G. W. Small, A. D. Roses, J. L. Haines, and M. A. Pericak-Vance. 1993. "Gene dose of apolipoprotein E type 4 allele and the risk of Alzheimer's disease in late onset families." *Science* 261 (5123):921-3.

Craft, S. 2009. "The role of metabolic disorders in Alzheimer disease and vascular dementia: two roads converged." *Arch Neurol* 66 (3):300-5. doi: 10.1001/archneurol.2009.27.

Cummings JL, Morstorf T, Zhong K. 2014. "Alzheimer's disease drug-development pipline: few candidates, frequent failures." *Alzheimers Res Ther* 6 (4):37.

Cunha-Vaz, J. 1979. "The blood-ocular barriers." *Surv Ophthalmol* 23 (5):279-96.

Cunha-Vaz, J., R. Bernardes, and C. Lobo. 2011. "Blood-retinal barrier." *Eur J Ophthalmol* 21 Suppl 6:S3-9. doi: 10.5301/ejo.2010.6049.

Cunha-Vaz, J. G., M. F. Goldberg, C. Vygantas, and J. Noth. 1979. "Early detection of retinal involvement in diabetes by vitreous fluorophotometry." *Ophthalmology* 86 (2):264-75.

D'Andrea, M. R., and R. G. Nagele. 2006. "Targeting the alpha 7 nicotinic acetylcholine receptor to reduce amyloid accumulation in Alzheimer's disease pyramidal neurons." *Curr Pharm Des* 12 (6):677-84.

D'Andrea, M. R., R. G. Nagele, H. Y. Wang, and D. H. Lee. 2002. "Consistent immunohistochemical detection of intracellular beta-amyloid42 in pyramidal neurons of Alzheimer's disease entorhinal cortex." *Neurosci Lett* 333 (3):163-6.

D'Andrea, M. R., R. G. Nagele, H. Y. Wang, P. A. Peterson, and D. H. Lee. 2001. "Evidence that neurones accumulating amyloid can undergo lysis to form amyloid plaques in Alzheimer's disease." *Histopathology* 38 (2):120-34. doi: his1082 [pii].

Davis, J. W., R. Chung, and D. T. Juarez. 2011. "Prevalence of comorbid conditions with aging among patients with diabetes and cardiovascular disease." *Hawaii Med J* 70 (10):209-13.

de la Torre, J. C. 2002. "Alzheimer disease as a vascular disorder: nosological evidence." *Stroke* 33 (4):1152-62.

De Reuck, J. L. 2012. "The significance of small cerebral bleeds in neurodegenerative dementia syndromes." *Aging Dis* 3 (4):307-12.

DeMarshall, C. A., M. Han, E. P. Nagele, A. Sarkar, N. K. Acharya, G. Godsey, E. L. Goldwaser, M. Kosciuk, U. Thayasivam, B. Belinka, R. G. Nagele, and Investigators Parkinson's Study Group. 2015. "Potential utility of autoantibodies as blood-based biomarkers for early detection and diagnosis of Parkinson's disease." *Immunol Lett* 168 (1):80-88. doi: 10.1016/j.imlet.2015.09.010.

den Heijer, T., S. E. Vermeer, E. J. van Dijk, N. D. Prins, P. J. Koudstaal, A. Hofman, and M. M. Breteler. 2003. "Type 2 diabetes and atrophy of medial temporal lobe structures on brain MRI." *Diabetologia* 46 (12):1604-10. doi: 10.1007/s00125-003-1235-0.

Deramecourt, V., J. Y. Slade, A. E. Oakley, R. H. Perry, P. G. Ince, C. A. Maurage, and R. N. Kalaria. 2012. "Staging and natural history of cerebrovascular pathology in dementia." *Neurology* 78 (14):1043-50. doi: 10.1212/WNL.0b013e31824e8e7f.

Dittmar, M. S., W. Petermichl, F. Schlachetzki, B. M. Graf, and M. Gruber. 2012. "Isoflurane induces endothelial apoptosis of the post-hypoxic blood-brain barrier in a transdifferentiated human umbilical vein endothelial cell model." *PLoS One* 7 (6):e38260. doi: 10.1371/journal.pone.0038260.

El Assar, M., J. Angulo, and L. Rodriguez-Manas. 2013. "Oxidative stress and vascular inflammation in aging." *Free Radic Biol Med* 65:380-401. doi: 10.1016/j.freeradbiomed.2013.07.003.

El-Remessy, A. B., T. Franklin, N. Ghaley, J. Yang, M. W. Brands, R. B. Caldwell, and M. A. Behzadian. 2013. "Diabetes-induced superoxide anion and breakdown of the blood-retinal barrier: role of the VEGF/uPAR pathway." *PLoS One* 8 (8):e71868. doi: 10.1371/journal.pone.0071868.

Elovaara, I., A. Icen, J. Palo, and T. Erkinjuntti. 1985. "CSF in Alzheimer's disease. Studies on blood-brain barrier function and intrathecal protein synthesis." *J Neurol Sci* 70 (1):73-80.

Enzinger, C., F. Fazekas, P. M. Matthews, S. Ropele, H. Schmidt, S. Smith, and R. Schmidt. 2005. "Risk factors for progression of brain atrophy in aging: six-year follow-up of normal subjects." *Neurology* 64 (10):1704-11. doi: 10.1212/01.WNL.0000161871.83614.BB.

Erickson, M. A., and W. A. Banks. 2013. "Blood-brain barrier dysfunction as a cause and consequence of Alzheimer's disease." *J Cereb Blood Flow Metab* 33 (10):1500-13. doi: 10.1038/jcbfm.2013.135.

Evans, D. A., L. A. Beckett, T. S. Field, L. Feng, M. S. Albert, D. A. Bennett, B. Tycko, and R. Mayeux. 1997. "Apolipoprotein E epsilon4 and incidence of Alzheimer disease in a community population of older persons." *JAMA* 277 (10):822-4.

Farrall, A. J., and J. M. Wardlaw. 2009. "Blood-brain barrier: ageing and microvascular disease--systematic review and meta-analysis." *Neurobiol Aging* 30 (3):337-52. doi: 10.1016/j.neurobiolaging.2007.07.015.

Frohlich, E. 2002. "[Structure and function of blood-tissue barriers]." *Dtsch Med Wochenschr* 127 (49):2629-34. doi: 10.1055/s-2002-35932.

Frolich, L., J. Kornhuber, R. Ihl, J. Fritze, K. Maurer, and P. Riederer. 1991. "Integrity of the blood-CSF barrier in dementia of Alzheimer type: CSF/serum ratios of albumin and IgG." *Eur Arch Psychiatry Clin Neurosci* 240 (6):363-6.

Frydkjaer-Olsen, U., R. Soegaard Hansen, R. Simo, J. Cunha-Vaz, T. Peto, and J. Grauslund. 2016. "Correlation between Retinal Vessel Calibre and Neurodegeneration in Patients with Type 2 Diabetes Mellitus in the European Consortium for the Early Treatment of Diabetic Retinopathy (EUROCONDOR)." *Ophthalmic Res* 56 (1). doi: 10.1159/000444396.

Ginsberg, S. D., S. E. Hemby, V. M. Lee, J. H. Eberwine, and J. Q. Trojanowski. 2000. "Expression profile of transcripts in Alzheimer's disease tangle-bearing CA1 neurons." *Ann Neurol* 48 (1):77-87.

Goldwaser, E. L., Acharya, N. K., Nagele, R. G. 2015. "Cerebrovascular and blood-brain barrier compromise: A mechanistic link between Vascular disease and Alzheimer's disease subtypes of Neurocognitive disorders." *J Parkinsons Dis Alzheimer Dis* 2 (2):10.

Gomez-Isla, T., R. Hollister, H. West, S. Mui, J. H. Growdon, R. C. Petersen, J. E. Parisi, and B. T. Hyman. 1997. "Neuronal loss correlates with but exceeds neurofibrillary tangles in Alzheimer's disease." *Ann Neurol* 41 (1):17-24. doi: 10.1002/ana.410410106.

Gouras, G. K., J. Tsai, J. Naslund, B. Vincent, M. Edgar, F. Checler, J. P. Greenfield, V. Haroutunian, J. D. Buxbaum, H. Xu, P. Greengard, and N. R. Relkin. 2000. "Intraneuronal Abeta42 accumulation in human brain." *Am J Pathol* 156 (1):15-20.

Hammer C, Stepniak B, Schneider A, Papiol S, Tantra M, Begemann M, Siren A-L, Pardo AL, Sperling S, Mohd Jofrry S, Gurvich A, Jensen N, Ostmeier K, Lunder F, Probst C, Martens H, Gillis M, Saher G, Assogna F, Spalletta G, Stocker W, Schulz TF, Nave K-A, Ehrenreich H. 2013. "Neuropsychiatric disease relevance of circulating anti-NMDA receptor autoantibodies depends on blood-brain barrier integrity." *Molecular Psychiatry*:1-7.

Hampel, H., H. U. Kotter, and H. J. Moller. 1997. "Blood-cerebrospinal fluid barrier dysfunction for high molecular weight proteins in Alzheimer disease and major depression: indication for disease subsets." *Alzheimer Dis Assoc Disord* 11 (2):78-87.

Han, M., E. Nagele, C. DeMarshall, N. Acharya, and R. Nagele. 2012. "Diagnosis of Parkinson's disease based on disease-specific autoantibody profiles in human sera." *PLoS One* 7 (2):e32383. doi: 10.1371/journal.pone.0032383.

Harris, M. I. 1991. "Hypercholesterolemia in diabetes and glucose intolerance in the U.S. population." *Diabetes Care* 14 (5):366-74.

Hawkins, B. T., and T. P. Davis. 2005. "The blood-brain barrier/neurovascular unit in health and disease." *Pharmacol Rev* 57 (2):173-85. doi: 10.1124/pr.57.2.4.

Hawkins, B. T., T. F. Lundeen, K. M. Norwood, H. L. Brooks, and R. D. Egleton. 2007. "Increased blood-brain barrier permeability and altered tight junctions in experimental diabetes in the rat: contribution of hyperglycaemia and matrix metalloproteinases." *Diabetologia* 50 (1):202-11. doi: 10.1007/s00125-006-0485-z.

Heinemann, U. 2008. "New dangers of anesthesia: isoflurane induced opening of the blood-brain barrier (Commentary on Tetrault et al.)." *Eur J Neurosci* 28 (7):1329. doi: 10.1111/j.1460-9568.2008.06500.x.

Hu, N., D. Guo, H. Wang, K. Xie, C. Wang, Y. Li, C. Wang, C. Wang, Y. Yu, and G. Wang. 2014. "Involvement of the blood-brain barrier opening in cognitive decline in aged rats following orthopedic surgery and high concentration of sevoflurane inhalation." *Brain Res* 1551:13-24. doi: 10.1016/j.brainres.2014.01.015.

Huber, J. D., R. L. VanGilder, and K. A. Houser. 2006. "Streptozotocin-induced diabetes progressively increases blood-brain barrier permeability in specific brain regions in rats." *Am J Physiol Heart Circ Physiol* 291 (6):H2660-8. doi: 10.1152/ajpheart.00489.2006.

Ihara, Y., M. Morishima-Kawashima, and R. Nixon. 2012. "The ubiquitin-proteasome system and the autophagic-lysosomal system in Alzheimer disease." *Cold Spring Harb Perspect Med* 2 (8). doi: 10.1101/cshperspect.a006361.

Ikram MA, Van der Iugt A, Niessen WJ, Krestin GP, Koudstaal PJ, Hofman A, Breteler MMB, Vernooij, MW. 2011. "The Rotterdam Scan Study: design and update up to 2012." *Eur J Epidemiol* 26:811-824.

Jellinger, K. A., and J. Attems. 2007. "Neuropathological evaluation of mixed dementia." *J Neurol Sci* 257 (1-2):80-7. doi: 10.1016/j.jns.2007.01.045.

Jeong, S. K., J. H. Lee, D. H. Nam, J. T. Kim, Y. S. Ha, S. Y. Oh, S. H. Park, S. H. Lee, N. Hur, H. S. Kwak, and G. H. Chung. 2015. "Basilar artery angulation in association with aging and pontine lacunar infarction: a multicenter observational study." *J Atheroscler Thromb* 22 (5):509-17. doi: 10.5551/jat.26245.

Jiang, X., M. Guo, J. Su, B. Lu, D. Ma, R. Zhang, L. Yang, Q. Wang, Y. Ma, and Y. Fan. 2012. "Simvastatin blocks blood-brain barrier disruptions induced by elevated cholesterol both in vivo and in vitro." *Int J Alzheimers Dis* 2012:109324. doi: 10.1155/2012/109324.

Kalaria, R. N. 2010. "Vascular basis for brain degeneration: faltering controls and risk factors for dementia." *Nutr Rev* 68 Suppl 2:S74-87. doi: 10.1111/j.1753-4887.2010.00352.x.

Kay, A. D., C. May, N. M. Papadopoulos, R. Costello, J. R. Atack, J. S. Luxenberg, N. R. Cutler, and S. I. Rapoport. 1987. "CSF and serum concentrations of albumin and IgG in Alzheimer's disease." *Neurobiol Aging* 8 (1):21-5.

Klunk, W. E., H. Engler, A. Nordberg, Y. Wang, G. Blomqvist, D. P. Holt, M. Bergstrom, I. Savitcheva, G. F. Huang, S. Estrada, B. Ausen, M. L. Debnath, J. Barletta, J. C. Price, J. Sandell, B. J. Lopresti, A. Wall, P. Koivisto, G. Antoni, C. A. Mathis, and B. Langstrom. 2004. "Imaging brain amyloid in Alzheimer's disease with Pittsburgh Compound-B." *Ann Neurol* 55 (3):306-19. doi: 10.1002/ana.20009.

Koh, S. H., M. Y. Noh, and S. H. Kim. 2008. "Amyloid-beta-induced neurotoxicity is reduced by inhibition of glycogen synthase kinase-3." *Brain Res* 1188:254-62. doi: 10.1016/j.brainres.2007.10.064.

Ledesma, M. D., and C. G. Dotti. 2012. "Peripheral cholesterol, metabolic disorders and Alzheimer's disease." *Front Biosci (Elite Ed)* 4:181-94.

Leibson, C. L., W. A. Rocca, V. A. Hanson, R. Cha, E. Kokmen, P. C. O'Brien, and P. J. Palumbo. 1997. "Risk of dementia among persons with diabetes mellitus: a population-based cohort study." *Am J Epidemiol* 145 (4):301-8.

Luchsinger, J. A., and D. R. Gustafson. 2009. "Adiposity, type 2 diabetes, and Alzheimer's disease." *J Alzheimers Dis* 16 (4):693-704. doi: 10.3233/JAD-2009-1022.

Maldonado, J. R. 2008. "Pathoetiological model of delirium: a comprehensive understanding of the neurobiology of delirium and an evidence-based approach to prevention and treatment." *Crit Care Clin* 24 (4):789-856, ix. doi: 10.1016/j.ccc.2008.06.004.

Maldonado, J. R. 2013. "Neuropathogenesis of delirium: review of current etiologic theories and common pathways." *Am J Geriatr Psychiatry* 21 (12):1190-222. doi: 10.1016/j.jagp.2013.09.005.

Mecocci, P., L. Parnetti, G. P. Reboldi, C. Santucci, A. Gaiti, C. Ferri, I. Gernini, M. Romagnoli, D. Cadini, and U. Senin. 1991. "Blood-brain-barrier in a geriatric population: barrier function in degenerative and vascular dementias." *Acta Neurol Scand* 84 (3):210-3.

Michalak Z, Lebrun A, DiMiceli M, Rousset M, Crespel A, Coubes P, Henshall DC, Lerner-Natoli M, Rigau V. 2012. "IgG leakage may contribute to neuronal dysfunction in drug-refractory epilepsies with blood-brain barrier disruption." *J Neuropathol Exp Neurol* 71 (9):826-838.

Mirra, S. S., A. Heyman, D. McKeel, S. M. Sumi, B. J. Crain, L. M. Brownlee, F. S. Vogel, J. P. Hughes, G. van Belle, and L. Berg. 1991. "The Consortium to Establish a Registry for Alzheimer's Disease (CERAD). Part II. Standardization of the neuropathologic assessment of Alzheimer's disease." *Neurology* 41 (4):479-86.

Mizoguchi, H., and K. Yamada. 2013. "Roles of matrix metalloproteinases and their targets in epileptogenesis and seizures." *Clin Psychopharmacol Neurosci* 11 (2):45-52. doi: 10.9758/cpn.2013.11.2.45.

Mizoguchi, H., K. Yamada, and T. Nabeshima. 2011. "Matrix metalloproteinases contribute to neuronal dysfunction in animal models of drug dependence, Alzheimer's disease, and epilepsy." *Biochem Res Int* 2011:681385. doi: 10.1155/2011/681385.

Montagne, A., S. R. Barnes, M. D. Sweeney, M. R. Halliday, A. P. Sagare, Z. Zhao, A. W. Toga, R. E. Jacobs, C. Y. Liu, L. Amezcua, M. G. Harrington, H. C. Chui, M. Law, and B. V. Zlokovic. 2015. "Blood-brain barrier breakdown in the aging human hippocampus." *Neuron* 85 (2):296-302. doi: 10.1016/j.neuron.2014.12.032.

Mooradian, A. D. 1988. "Effect of aging on the blood-brain barrier." *Neurobiol Aging* 9 (1):31-9.

Munoz, D. G., T. Erkinjuntti, S. Gaytan-Garcia, and V. Hachinski. 1997. "Serum protein leakage in Alzheimer's disease revisited." *Ann N Y Acad Sci* 826:173-89.

Muthusamy, A., C. M. Lin, S. Shanmugam, H. M. Lindner, S. F. Abcouwer, and D. A. Antonetti. 2014. "Ischemia-reperfusion injury induces occludin phosphorylation/ubiquitination and retinal vascular permeability in a VEGFR-2-dependent manner." *J Cereb Blood Flow Metab* 34 (3):522-31. doi: 10.1038/jcbfm.2013.230.

Nagele, E., M. Han, C. Demarshall, B. Belinka, and R. Nagele. 2011. "Diagnosis of Alzheimer's disease based on disease-specific autoantibody profiles in human sera." *PLoS One* 6 (8):e23112. doi: 10.1371/journal.pone.0023112.

Nagele, E. P., M. Han, N. K. Acharya, C. DeMarshall, M. C. Kosciuk, and R. G. Nagele. 2013. "Natural IgG autoantibodies are abundant and ubiquitous in human sera, and their number is influenced by age, gender, and disease." *PLoS One* 8 (4):e60726. doi: 10.1371/journal.pone.0060726.

Nagele, R. G., P. M. Clifford, G. Siu, E. C. Levin, N. K. Acharya, M. Han, M. C. Kosciuk, V. Venkataraman, S. Zavareh, S. Zarrabi, K. Kinsler, N. G. Thaker, E. P. Nagele, J. Dash, H. Y. Wang, and A. Levitas. 2011. "Brain-reactive autoantibodies prevalent in human sera increase intraneuronal amyloid-beta(1-42) deposition." *J Alzheimers Dis* 25 (4):605-22. doi: 10.3233/JAD-2011-110098.

Nagele, R. G., M. R. D'Andrea, W. J. Anderson, and H. Y. Wang. 2002. "Intracellular accumulation of beta-amyloid(1-42) in neurons is facilitated by the alpha 7 nicotinic acetylcholine receptor in Alzheimer's disease." *Neuroscience* 110 (2):199-211. doi: S0306452201004602 [pii].

Nery, L. R., N. S. Eltz, C. Hackman, R. Fonseca, S. Altenhofen, H. N. Guerra, V. M. Freitas, C. D. Bonan, and M. R. Vianna. 2014. "Brain intraventricular injection of amyloid-beta in zebrafish embryo impairs cognition and increases

tau phosphorylation, effects reversed by lithium." *PLoS One* 9 (9):e105862. doi: 10.1371/journal.pone.0105862.

news agencies. 2014. "Older people are more scared of dementia than cancer, poll finds." http://www.telegraph.co.uk/news/health/elder/11008905/Older-people-are-more-scared-of-dementia-than-cancer-poll-finds.html.

Ohara, T., Y. Doi, T. Ninomiya, Y. Hirakawa, J. Hata, T. Iwaki, S. Kanba, and Y. Kiyohara. 2011. "Glucose tolerance status and risk of dementia in the community: the Hisayama study." *Neurology* 77 (12):1126-34. doi: 10.1212/WNL.0b013e31822f0435.

Ott, A., R. P. Stolk, A. Hofman, F. van Harskamp, D. E. Grobbee, and M. M. Breteler. 1996. "Association of diabetes mellitus and dementia: the Rotterdam Study." *Diabetologia* 39 (11):1392-7.

Patel JP, Frey BN. 2015. "Disruption in the Blood-Brain Barrier: The Missing Link between Brain and Body Inflammation in Bipolar Disorder?" *Neural Plast.* 2015:708306.

Phillips, B. E., L. Cancel, J. M. Tarbell, and D. A. Antonetti. 2008. "Occludin independently regulates permeability under hydrostatic pressure and cell division in retinal pigment epithelial cells." *Invest Ophthalmol Vis Sci* 49 (6):2568-76. doi: 10.1167/iovs.07-1204.

Reese, T. S., and M. J. Karnovsky. 1967. "Fine structural localization of a blood-brain barrier to exogenous peroxidase." *J Cell Biol* 34 (1):207-17.

Refolo, L. M., B. Malester, J. LaFrancois, T. Bryant-Thomas, R. Wang, G. S. Tint, K. Sambamurti, K. Duff, and M. A. Pappolla. 2000. "Hypercholesterolemia accelerates the Alzheimer's amyloid pathology in a transgenic mouse model." *Neurobiol Dis* 7 (4):321-31. doi: 10.1006/nbdi.2000.0304.

Roman, G. C. 2004. "Facts, myths, and controversies in vascular dementia." *J Neurol Sci* 226 (1-2):49-52. doi: 10.1016/j.jns.2004.09.011.

Rosenberg, G. A. 2012. "Neurological diseases in relation to the blood-brain barrier." *J Cereb Blood Flow Metab* 32 (7):1139-51. doi: 10.1038/jcbfm.2011.197.

Rosenberg, G. A. 2014. "Blood-Brain Barrier Permeability in Aging and Alzheimer's Disease." *J Prev Alzheimers Dis* 1 (3):138-139. doi: 10.14283/jpad.2014.25.

Rozemuller, J. M., P. Eikelenboom, W. Kamphorst, and F. C. Stam. 1988. "Lack of evidence for dysfunction of the blood-brain barrier in Alzheimer's disease: an immunohistochemical study." *Neurobiol Aging* 9 (4):383-91.

Runkle, E. A., and D. A. Antonetti. 2011. "The blood-retinal barrier: structure and functional significance." *Methods Mol Biol* 686:133-48. doi: 10.1007/978-1-60761-938-3_5.

Sando, S. B., S. Melquist, A. Cannon, M. L. Hutton, O. Sletvold, I. Saltvedt, L. R. White, S. Lydersen, and J. O. Aasly. 2008. "APOE epsilon 4 lowers age at onset and is a high risk factor for Alzheimer's disease; a case control study from central Norway." *BMC Neurol* 8:9. doi: 10.1186/1471-2377-8-9.

Selkoe, D. J. 2002. "Alzheimer's disease is a synaptic failure." *Science* 298 (5594):789-91. doi: 10.1126/science.1074069298/5594/789 [pii].

Shepardson, N. E., G. M. Shankar, and D. J. Selkoe. 2011. "Cholesterol level and statin use in Alzheimer disease: I. Review of epidemiological and preclinical studies." *Arch Neurol* 68 (10):1239-44. doi: 10.1001/archneurol.2011.203.

Sims-Robinson, C., B. Kim, A. Rosko, and E. L. Feldman. 2010. "How does diabetes accelerate Alzheimer disease pathology?" *Nat Rev Neurol* 6 (10):551-9. doi: 10.1038/nrneurol.2010.130.

Skoog, I., A. Wallin, P. Fredman, C. Hesse, O. Aevarsson, I. Karlsson, C. G. Gottfries, and K. Blennow. 1998. "A population study on blood-brain barrier function in 85-year-olds: relation to Alzheimer's disease and vascular dementia." *Neurology* 50 (4):966-71.

Snowdon, D. A. 1997. "Aging and Alzheimer's disease: lessons from the Nun Study." *Gerontologist* 37 (2):150-6.

Snowdon, D. A., L. H. Greiner, J. A. Mortimer, K. P. Riley, P. A. Greiner, and W. R. Markesbery. 1997. "Brain infarction and the clinical expression of Alzheimer disease. The Nun Study." *JAMA* 277 (10):813-7.

Snowdon DA, Greiner LH, Mortimer JA, Riley KP, Greiner PA, Markesbery WR. 1997. "Brain infarction and the clinical expression of Alzheimer disease. The Nun Study." *JAMA* 277 (10):813-817.

Sprung, J., R. O. Roberts, D. S. Knopman, D. M. Olive, J. L. Gappa, V. L. Sifuentes, T. L. Behrend, J. D. Farmer, T. N. Weingarten, A. C. Hanson, D. R. Schroeder, R. C. Petersen, and D. O. Warner. 2016. "Association of Mild Cognitive Impairment With Exposure to General Anesthesia for Surgical and Nonsurgical Procedures: A Population-Based Study." *Mayo Clin Proc* 91 (2):208-17. doi: 10.1016/j.mayocp.2015.10.023.

Starr, J. M., A. J. Farrall, P. Armitage, B. McGurn, and J. Wardlaw. 2009. "Blood-brain barrier permeability in Alzheimer's disease: a case-control MRI study." *Psychiatry Res* 171 (3):232-41. doi: 10.1016/j.pscychresns.2008.04.003.

Starr, J. M., J. Wardlaw, K. Ferguson, A. MacLullich, I. J. Deary, and I. Marshall. 2003. "Increased blood-brain barrier permeability in type II diabetes demonstrated by gadolinium magnetic resonance imaging." *J Neurol Neurosurg Psychiatry* 74 (1):70-6.

Strauss, O. 2016. "Pharmacology of the retinal pigment epithelium, the interface between retina and body system." *Eur J Pharmacol*. doi: 10.1016/j.ejphar.2016.03.066.

Suit YT, Bullock KM, Erickson MA, Zhang J, Banks WA. 2014. "Alpha synuclein is transported into and out of the brain by the blood-brain barrier." *Peptides* 62:197-202.

Taguchi, A. 2009. "Vascular factors in diabetes and Alzheimer's disease." *J Alzheimers Dis* 16 (4):859-64. doi: D170H786448862N3 [pii]10.3233/JAD-2009-0975.

Terry, A. V., Jr., and J. J. Buccafusco. 2003. "The cholinergic hypothesis of age and Alzheimer's disease-related cognitive deficits: recent challenges and their implications for novel drug development." *J Pharmacol Exp Ther* 306 (3):821-7. doi: 10.1124/jpet.102.041616.

Tetrault, S., O. Chever, A. Sik, and F. Amzica. 2008. "Opening of the blood-brain barrier during isoflurane anaesthesia." *Eur J Neurosci* 28 (7):1330-41. doi: 10.1111/j.1460-9568.2008.06443.x.

Thal, S. C., C. Luh, E. V. Schaible, R. Timaru-Kast, J. Hedrich, H. J. Luhmann, K. Engelhard, and C. M. Zehendner. 2012. "Volatile anesthetics influence blood-brain barrier integrity by modulation of tight junction protein expression in traumatic brain injury." *PLoS One* 7 (12):e50752. doi: 10.1371/journal.pone.0050752.

The Press Association. 2014. "Dementia 'more feared than cancer' by older patients." http://www.nursingtimes.net/nursing-practice/specialisms/older-people/dementia-more-feared-than-cancer-by-older-patients/5073567.article.

Tibbling, G., H. Link, and S. Ohman. 1977. "Principles of albumin and IgG analyses in neurological disorders. I. Establishment of reference values." *Scand J Clin Lab Invest* 37 (5):385-90. doi: 10.1080/00365517709091496.

Tomimoto, H., I. Akiguchi, T. Suenaga, M. Nishimura, H. Wakita, S. Nakamura, and J. Kimura. 1996. "Alterations of the blood-brain barrier and glial cells in white-matter lesions in cerebrovascular and Alzheimer's disease patients." *Stroke* 27 (11):2069-74.

Venkat, P., M. Chopp, and J. Chen. 2015. "Models and mechanisms of vascular dementia." *Exp Neurol*. doi: 10.1016/j.expneurol.2015.05.006.

Wada, H. 1998. "Blood-brain barrier permeability of the demented elderly as studied by cerebrospinal fluid-serum albumin ratio." *Intern Med* 37 (6):509-13.

Wang, H. Y., D. H. Lee, M. R. D'Andrea, P. A. Peterson, R. P. Shank, and A. B. Reitz. 2000. "beta-Amyloid(1-42) binds to alpha7 nicotinic acetylcholine receptor with high affinity. Implications for Alzheimer's disease pathology." *J Biol Chem* 275 (8):5626-32.

Wang, H. Y., D. H. Lee, C. B. Davis, and R. P. Shank. 2000. "Amyloid peptide Abeta(1-42) binds selectively and with picomolar affinity to alpha7 nicotinic acetylcholine receptors." *J Neurochem* 75 (3):1155-61.

Wang, X. X., M. S. Tan, J. T. Yu, and L. Tan. 2014. "Matrix metalloproteinases and their multiple roles in Alzheimer's disease." *Biomed Res Int* 2014:908636. doi: 10.1155/2014/908636.

Wirths, O., and T. A. Bayer. 2012. "Intraneuronal Abeta accumulation and neurodegeneration: lessons from transgenic models." *Life Sci* 91 (23-24):1148-52. doi: 10.1016/j.lfs.2012.02.001.

Wisniewski, H. M., and P. B. Kozlowski. 1982. "Evidence for blood-brain barrier changes in senile dementia of the Alzheimer type (SDAT)." *Ann N Y Acad Sci* 396:119-29.

Wisniewski, K. E., H. M. Wisniewski, and G. Y. Wen. 1985. "Occurrence of neuropathological changes and dementia of Alzheimer's disease in Down's syndrome." *Ann Neurol* 17 (3):278-82. doi: 10.1002/ana.410170310.

Xu, W. L., E. von Strauss, C. X. Qiu, B. Winblad, and L. Fratiglioni. 2009. "Uncontrolled diabetes increases the risk of Alzheimer's disease: a population-based cohort study." *Diabetologia* 52 (6):1031-9. doi: 10.1007/s00125-009-1323-x.

Xu, W., C. Qiu, M. Gatz, N. L. Pedersen, B. Johansson, and L. Fratiglioni. 2009. "Mid- and late-life diabetes in relation to the risk of dementia: a population-based twin study." *Diabetes* 58 (1):71-7. doi: 10.2337/db08-0586.

Xu, W., C. Qiu, B. Winblad, and L. Fratiglioni. 2007. "The effect of borderline diabetes on the risk of dementia and Alzheimer's disease." *Diabetes* 56 (1):211-6. doi: 10.2337/db06-0879.

Yaffe, K., A. Kanaya, K. Lindquist, E. M. Simonsick, T. Harris, R. I. Shorr, F. A. Tylavsky, and A. B. Newman. 2004. "The metabolic syndrome, inflammation, and risk of cognitive decline." *JAMA* 292 (18):2237-42. doi: 10.1001/jama.292.18.2237.

Yan, S. D., X. Chen, J. Fu, M. Chen, H. Zhu, A. Roher, T. Slattery, L. Zhao, M. Nagashima, J. Morser, A. Migheli, P. Nawroth, D. Stern, and A. M. Schmidt. 1996. "RAGE and amyloid-beta peptide neurotoxicity in Alzheimer's disease." *Nature* 382 (6593):685-91. doi: 10.1038/382685a0.

Zhang, L., R. Sheng, and Z. Qin. 2009. "The lysosome and neurodegenerative diseases." *Acta Biochim Biophys Sin (Shanghai)* 41 (6):437-45.

Zhao, J., J. Hao, X. Fei, X. Wang, Y. Hou, and C. Deng. 2014. "Isoflurane inhibits occludin expression via up-regulation of hypoxia-inducible factor 1alpha." *Brain Res* 1562:1-10. doi: 10.1016/j.brainres.2014.03.025.

Zlokovic, BV. 2008. "The blood-brain barrier in health and chronic neurodegenerative disorders." *Neuron* 57:178-201.

ATTRIBUTIONS

Figure 1. We would like to thank Ms. Tara Askin, senior graphic designer/multimedia specialist, Academic Technology at the Rowan University School of Osteopathic Medicine, for her help in the preparation of the illustration used for figure 1.

Figure 2. We would like to thank Abhirup Sarkar, PhD candidate, for his contributions in the graphic design of figure 2.

Chapter II

Rationale

RATIONALE

Given the contentious nature of an underlying mechanism for the pathoetiology of Alzheimer's disease (AD), it is of utmost importance to understand how the proposed hallmarks that define the disease develop and progress. Past evidence has directed the mechanism to contain an involvement of autoantibody (aAb)-mediated endocytosis of the alpha 7 nicotinic acetylcholine receptor (α7nAChR)-$A\beta_{42}$ complex, and my efforts will be focused on elucidating the pathway by which $A\beta_{42}$ may enter the cholinergic neurons specifically expressing the α7nAChR (Nagele et al. 2002, D'Andrea 2001, Nagele et al. 2011, Wang et al. 2012, Wang et al. 2000).

The elderly population is at risk for many conditions, including not only AD, but others like atherosclerosis, coronary artery disease, and post-operative delirium (POD) (Vasilevskis et al. 2012, Xie et al. 2014). Much dispute exists in current literature as to a mechanism that causes POD, however the onset of the delirious episode is routinely found secondary to a systemic disturbance or an inciting event or cause, such as exposure to toxins, drugs, or general anesthesia. With much overlap to symptoms of AD during the delirious episode, the condition is further characterized by a neurobehavioral syndrome that may or may not resolve, with restlessness and irritability, delusional thoughts, and limited mental capacities or cognition (Association 2013). In the young pediatric or elderly population, the episode of delirium can be especially long lasting, even irreversible, in these vulnerable populations (Deiner and Silverstein 2009, Maldonado 2013). Taking into account

similar symptomatic manifestations of AD, along with histopathological sections of human AD brains that consistently show blood-brain barrier (BBB) breaches, we chose to assess the phenomenon of POD from a vascular standpoint. The objective of this portion of my dissertation will be to focus on the mechanism of such delirious episodes, in hopes of gaining a clearer understanding that will shed light on the undefined mechanism of POD.

As previously mentioned, the BBB plays an integral part in maintaining homeostasis of the brain. The effects of diabetes mellitus (DM) and hypercholesterolemia (HC) on the vasculature and propagation of amyloid-based neurodegenerative diseases has been recently published (Acharya et al. 2013). The BBB was shown to be of utmost importance in the disease manifestation, and subsequent influx of aAb into the brain and $A\beta_{42}$ into the neurons was measured to gauge the extent of neurodegenerative progression. Pigs induced to have DM and HC were used as a model system to study the pharmacological effect that a certain drug could have on BBB modification in these chronic disease states. A treatment group with darapladib, a lipoprotein-associated phospholipase A_2 inhibitor, was used in the pig model to illustrate the effects of chronic DM and HC on increased BBB permeability leading to neuronal pathology. A natural follow-up study that presented was to gauge a functionally and structurally analogous vascular bed housed in the ocular system known as the blood-retina barrier (BRB) (Cunha-Vaz 1979, Cunha-Vaz, Bernardes, and Lobo 2011, Cunha-Vaz et al. 1979). The BRB is making its way into the realm of diagnostics for neurodegenerative disorders, as it shares many features with the brain, but can be

assayed very readily for disease-associated changes. More specifically, efforts to better categorize the BRB, especially as it relates to BBB dysfunction, in the chronic disease state will be the emphasis of this project.

REFERENCES

Acharya, N. K., E. C. Levin, P. M. Clifford, M. Han, R. Tourtellotte, D. Chamberlain, M. Pollaro, N. J. Coretti, M. C. Kosciuk, E. P. Nagele, C. Demarshall, T. Freeman, Y. Shi, C. Guan, C. H. Macphee, R. L. Wilensky, and R. G. Nagele. 2013. "Diabetes and hypercholesterolemia increase blood-brain barrier permeability and brain amyloid deposition: beneficial effects of the LpPLA2 inhibitor darapladib." *J Alzheimers Dis* 35 (1):179-98. doi: 10.3233/JAD-122254.

Association, American Psychiatric. 2013. *Diagnostic and statistical manual of mental disorders: DSM-5*. Washington, D.C.: American Psychiatric Association.

Cunha-Vaz, J. 1979. "The blood-ocular barriers." *Surv Ophthalmol* 23 (5):279-96.

Cunha-Vaz, J., R. Bernardes, and C. Lobo. 2011. "Blood-retinal barrier." *Eur J Ophthalmol* 21 Suppl 6:S3-9. doi: 10.5301/ejo.2010.6049.

Cunha-Vaz, J. G., M. F. Goldberg, C. Vygantas, and J. Noth. 1979. "Early detection of retinal involvement in diabetes by vitreous fluorophotometry." *Ophthalmology* 86 (2):264-75.

D'Andrea, M. R., Nagele, R. G., Wang, H-Y., Peterson, P. A., Lee, D. H. 2001. "Evidence that neurones accumulating amyloid can undergo lysis to form amyloid plaques in Alzheimer's disease." *Histopathology* 38:120-134.

Deiner, S., and J. H. Silverstein. 2009. "Postoperative delirium and cognitive dysfunction." *Br J Anaesth* 103 Suppl 1:i41-46. doi: 10.1093/bja/aep291.

Maldonado, J. R. 2013. "Neuropathogenesis of delirium: review of current etiologic theories and common pathways." *Am J Geriatr Psychiatry* 21 (12):1190-222. doi: 10.1016/j.jagp.2013.09.005.

Nagele, R. G., P. M. Clifford, G. Siu, E. C. Levin, N. K. Acharya, M. Han, M. C. Kosciuk, V. Venkataraman, S. Zavareh, S. Zarrabi, K. Kinsler, N. G. Thaker, E. P. Nagele, J. Dash, H. Y. Wang, and A. Levitas. 2011. "Brain-reactive autoantibodies prevalent in human sera increase intraneuronal amyloid-beta(1-42) deposition." *J Alzheimers Dis* 25 (4):605-22. doi: 10.3233/JAD-2011-110098.

Nagele, R. G., M. R. D'Andrea, W. J. Anderson, and H. Y. Wang. 2002. "Intracellular accumulation of beta-amyloid(1-42) in neurons is facilitated by the alpha 7 nicotinic acetylcholine receptor in Alzheimer's disease." *Neuroscience* 110 (2):199-211. doi: S0306452201004602 [pii].

Vasilevskis, E. E., J. H. Han, C. G. Hughes, and E. W. Ely. 2012. "Epidemiology and risk factors for delirium across hospital settings." *Best Pract Res Clin Anaesthesiol* 26 (3):277-87. doi: 10.1016/j.bpa.2012.07.003.

Wang, H. Y., K. Bakshi, M. Frankfurt, A. Stucky, M. Goberdhan, S. M. Shah, and L. H. Burns. 2012. "Reducing amyloid-related Alzheimer's disease pathogenesis by a small molecule targeting filamin A." *J Neurosci* 32 (29):9773-84. doi: 10.1523/JNEUROSCI.0354-12.2012.

Wang, H. Y., D. H. Lee, M. R. D'Andrea, P. A. Peterson, R. P. Shank, and A. B. Reitz. 2000. "beta-Amyloid(1-42) binds to alpha7 nicotinic acetylcholine receptor with high affinity. Implications for Alzheimer's disease pathology." *J Biol Chem* 275 (8):5626-32.

Xie, Z., C. A. Swain, S. A. Ward, H. Zheng, Y. Dong, N. Sunder, D. W. Burke, D. Escobar, Y. Zhang, and E. R. Marcantonio. 2014. "Preoperative cerebrospinal fluid beta-Amyloid/Tau ratio and postoperative delirium." *Ann Clin Transl Neurol* 1 (5):319-328. doi: 10.1002/acn3.58.

Chapter III

Sevoflurane and isoflurane induce structural changes in brain vascular endothelial cells and increase blood-brain barrier permeability: Possible link to postoperative delirium and cognitive decline

ABSTRACT

A large percentage of patients subjected to general anesthesia at 65 years and older exhibit postoperative delirium (POD). Here, we test the hypothesis that inhaled anesthetics (IAs), such as Sevoflurane and Isoflurane, act directly on brain vascular endothelial cells (BVECs) to increase blood-brain barrier (BBB) permeability, thereby contributing to POD. Rats of young (3-5 months), middle (10-12 months) and old (17-19 months) ages were anesthetized with Sevoflurane or Isoflurane for 3 hours. After exposure, some were euthanized immediately; others were allowed to recover for 24 hours before sacrifice. Immunohistochemistry was employed to monitor the extent of BBB breach, and scanning electron microscopy (SEM) was used to examine changes in the luminal surfaces of BVECs. Quantitative immunohistochemistry revealed increased BBB permeability in older animals treated with Sevoflurane, but not Isoflurane. Extravasated immunoglobulin G showed selective affinity for pyramidal neurons. SEM demonstrated marked flattening of the luminal surfaces of BVECs in anesthetic-treated rats. Results suggest an aging-linked BBB compromise resulting from exposure to Sevoflurane. Changes in the luminal surface topology of BVECs indicate a direct effect on the plasma membrane, which may weaken or disrupt their BBB-associated tight junctions. Disruption of brain homeostasis due to plasma influx into the brain parenchyma and binding of plasma components (e.g., immunoglobulins) to neurons may contribute to POD. We propose that, in the elderly, exposure to some IAs can cause BBB compromise that disrupts

brain homeostasis, perturbs neuronal function and thereby contributes to POD. If unresolved, this may progress to postoperative cognitive decline and later dementia.

INTRODUCTION

Nearly 60,000 patients undergo general anesthesia every day with the hope of alleviating chronic diseases and improving their quality of life (Brown et al., 2010; Nadelson et al., 2014). Unfortunately, after exposure to anesthetics, a large percentage of elderly patients at age 65 and older exhibit postoperative delirium (POD), and many subsequently develop postoperative cognitive decline (POCD), which may be linked to later dementia (Ansaloni et al., 2010; Inouye et al., 2014; Neufeld et al., 2013; Rudolph and Marcantonio, 2011). In the US, the number of affected individuals continues to rise because the elderly are the fastest growing segment of our population (Howden and Meyer, 2011; Brown and Purdon, 2013; Leslie et al., 2008; Neufeld and Thomas, 2013). POD is characterized by an acute, fluctuating onset of attention disturbance and cognitive change in patients who may otherwise lack a history of neurocognitive manifestations (Bedford, 1955; Burns et al., 2004; Strom et al., 2014). As multifactorial disorders, POD and POCD have been associated with a variety of somatic factors as well as medication intoxication or withdrawal (Strom et al., 2014; van Munster and de Rooij, 2014). Advanced age and exposure to inhaled anesthetics have been widely implicated as risk factors (Bedford, 1955; Brown and Purdon, 2013; Neufeld and Thomas, 2013; Strom et al., 2014).

Although the underlying mechanisms of POD and POCD are unknown (Maldonado, 2013), emerging evidence suggests a common mechanistic link. Aging is a known predisposing factor in a number of vascular pathologies, including chronic vascular

inflammation, atherosclerosis, amyloid angiopathy, hyalinosis and hypertension (Clifford et al., 2008; Kalaria, 2010; Rouhl et al., 2012; Vasilevko et al., 2010). The blood vessels in the brain are not spared from these anomalies. Brain vascular endothelial cells (BVECs) line the luminal surfaces of these vessels and contribute both structurally and functionally to the blood-brain barrier (BBB). These cells are held together at their margins by extensive tight junctions associated with prominent tight junctional folds or ridges. The BBB is thought to be further supported by the basement membrane of BVECs, pericytes, and the end-feet of astrocytes (Abbott et al., 2010; Zlokovic, 2008). It regulates the movement of various biomolecules into and out of the brain, which is crucial for establishing and maintaining brain homeostasis and enabling the normal functioning of the neurons and glia within their microenvironment in the brain. Factors or conditions that disrupt BBB function can trigger a transient or chronic leakage of plasma components into the brain tissue, thereby disrupting brain homeostasis and triggering disease states (Abbott et al., 2010; Zlokovic, 2008). Several neurodegenerative diseases, most notably Alzheimer's disease (AD), exhibit BBB breakdown as a consistent pathological feature that likely contributes to both disease initiation and progression (Nagele et al., 2011).

In the present study, we tested the hypothesis that exposure to commonly used inhalation anesthetics disrupts BBB integrity, causing an influx of plasma components into the brain that locally disrupts brain homeostasis. To investigate this, young (3-5 months), middle-aged (10-12 months) and old (17-19 months) rats were

subjected to either Sevoflurane or Isoflurane anesthesia for 3 hours and then were sacrificed immediately or first allowed to recover for 24 hours. Using immunohistochemistry (IHC) and immunoglobulin G (IgG) as a tissue biomarker of BBB leak, we compared the functional integrity of BBB between control animals and those exposed to anesthesia with or without 24 hour of recovery. Results showed an increased BBB permeability and influx of plasma components into the brain tissue in Sevoflurane-treated animals, but not in those exposed to Isoflurane, compared to controls. Extravasated IgG showed selective affinity for the surfaces of pyramidal neurons. Scanning electron microscopy revealed an increased incidence of BVEC degeneration and death within the walls of brain blood vessels along with a marked flattening of their luminal surfaces and stretching of tight junctional ridges at their margins. The BBB of older and anesthetic-treated older rats appeared to be most sensitive to disruption, and Sevoflurane was more effective than Isoflurane in promoting BBB compromise and luminal surface changes in BVECs. These data link aging-associated decline in BBB functional integrity to the increased vulnerability of brain blood vessels in older animals to the effects of anesthesia. Extrapolation of this data to humans leads us to suggest that, particularly in the elderly, exposure to certain types of anesthetics causes a rapid, transient breakdown of the BBB, which results in a critical loss of brain homeostasis and disruption of neuronal function that could, at least in part, account for the expression of symptoms that characterize delirium. Furthermore, if BBB function is not completely restored in elderly patients suffering from POD, we suggest that they are at increased risk for subsequently developing POCD and perhaps even dementia.

EXPERIMENTAL PROCEDURE

Rodents

Wild-type Sprague Dawley rats (Harlan Laboratories, Inc.) were maintained on *ad libitum* food and water in an AAALAC-accredited vivarium with a 12-hour light/dark cycle. Animal use was approved by the RowanSOM IACUC.

Animal treatment

Young (3-5 months), middle-aged (10-12 months) and older (17-19 months) rats were subjected to Sevoflurane (1-3%) or Isoflurane (1-3%) for 3 hours. Anesthesia was first induced by exposing rats in an induction chamber to about 3% Sevoflurane or Isoflurane. Once surgical plane anesthesia was attained, they were removed from the induction chamber and put on a heat pad (T/Pump by Stryker, Kalamazoo, MI). Surgical plane anesthesia was maintained by supplying the anesthetics via nose cones. The concentration of the anesthetics was gradually lowered but the animal was not allowed to either progress to deeper sleep or to regress to wakeful states. The state of anesthesia was constantly monitored by testing for the pedal withdrawal reflex (toe pinch) and by pinching the tail. In addition, animal vital signs such as rate and depth of respiration were monitored and maintained (at 32 ± 3 respirations per minute) by regulating the mixture of anesthetic and oxygen. Body temperature was maintained by a heated pad and by covering the body. A calibrated Midmark Matrx VMR® table top anesthesia machine with a VIP 3000 well-fill style vaporizer was used to supply Sevoflurane (Sevothesia^{TM}; Butler Schein^{TM,} Dublin, OH; NDC: 11695-0501-2) and

Isoflurane (Isothesia™; Butler Schein™, Dublin, OH; NDC 11695-6776-2) with oxygen as the carrier gas. Separate vaporizers for Sevoflurane and Isoflurane were acquired and used as each rodent received only one type of anesthetic. The concentration of anesthetic required for maintaining surgical plane anesthesia varied between the age groups and individuals. Non-recovery rats were euthanized at the end of third hour by exsanguination - the animal was perfused with phosphate-buffered saline (PBS) followed by freshly prepared 4% paraformaldehyde in PBS. Recovery rats were first allowed to recover for 24 hours after the 3-hour exposure to anesthetic and were euthanized by CO_2 asphyxiation. The control group included rats of all three age groups that were not exposed to either anesthetic and were euthanized by CO_2 asphyxiation. To achieve the best preservation of the brain tissue, all animals were fixed by perfusion using freshly prepared 4% paraformaldehyde in PBS. Brains were quickly removed and, using a brain block, coronal sections were cut anteroposteriorly for bright-field microscopy, IHC, and scanning electron microscopy. Left hemispheres were sliced into 4mm thick sections for IHC; right hemispheres were sliced into 2 mm thick sections for scanning electron microscopy. From the left hemispheres a total of four tissue blocks were generated - anterior, middle, posterior and cerebellar. Anterior, middle and posterior tissue blocks comprising different regions of cerebral cortex were the primarily focus of this study.

Tissue preparation, immunohistochemistry and scanning electron microscopy

Brain tissues for IHC were fixed in 4% paraformaldehyde and prepared for routine embedding in paraffin and sectioning as described previously (Nagele et al., 2011).

Sections representing each brain region (anterior, middle and posterior) were randomly selected for detection of extravasated IgG using IHC. IHC was performed using the protocol and reagents described previously (Nagele et al., 2011). To detect IgG, biotinylated anti-rat IgG (Vector Laboratories, BA-9400, 1:20 in Dako antibody diluent) was used as the primary antibody (Acharya et al., 2013; Nagele et al., 2011). Cortical regions from each section were photographed using a Nikon FXA microscope, and images were analyzed using NIS-Elements Imaging Software (Nikon Instruments Inc. USA). For scanning electron microscopy, brain tissue was fixed in 4% paraformaldehyde, rinsed in PBS, and post-fixed with 1% osmium tetroxide. After washing in buffer, tissues were first dehydrated in ethanol followed by amyl acetate. Samples were then dried using carbon dioxide in an E3100 critical point dryer (Quorum Technologies, USA) and rendered conductive by coating with a thin (~40Å) layer of gold using an EMS 150R S sputter coater (Quorum Technologies, USA). Tissues were examined using JEOL NeoScope JCM-5000 scanning electron microscope.

Determination of the density of leaking cortical blood vessels

The effects of age and inhalation anesthetics on the functional integrity of the BBB were assessed by counting blood vessels (arteries, veins and capillaries) with associated perivascular IgG-positive leak clouds and measuring the extent of the leak in the cerebral cortex (Figs. 1-2). Extravasation of IgG has been widely used as a biomarker of BBB breach (Acharya et al., 2013; Jin et al., 2010; Kuang et al., 2004; Nagele et al., 2011). For each image, the area of the cerebral cortex and the number

of cortical blood vessels exhibiting perivascular leak clouds were quantified. For each animal, the total number of leaking blood vessels per unit area of cortex was determined. Data from individual animals of the same age and treatment groups were averaged and used for comparisons. Only perivascular leak clouds displaying the source blood vessel were included in the analysis.

Determination of the extent of BBB breach in cortical blood vessels

A relative scoring system based on the area of IgG extravasation was used to quantify the extent of BBB breach (Fig. 2) (Acharya et al., 2013). Normally, IgG in the cerebral cortex is contained within local blood vessels (Fig. 1A-B and 2A). Under conditions of BBB breakdown, IgG is able to extravasate and form perivascular leak clouds, which take on a brown color in IHC preparations. The interaction of IgG with cognate epitopes present on the exposed surfaces of brain tissue components also causes immunostaining of pyramidal neurons, axons, dendrites and synapses within tissue sections (Figs. 2C-F). The area and intensity of each perivascular leak cloud were considered to be directly proportional to the extent of BBB breach (Fig. 2). Investigators were blinded as to the identity of the specimens during image analysis.

Statistics

Using Student's *t* test, statistical significance was calculated and a $p < 0.05$ was considered statistically significant. Variation within each treatment group was represented by standard error.

RESULTS

Inhalation anesthetics increase BBB permeability in the rat

To assess the effects of anesthetics on the functional integrity of the BBB, IHC was used to detect the leak of plasma components from blood vessels into the cerebral cortex of anesthetic-treated and control rats (Fig. 1). IgG, which is normally absent in the brain interstitial space, was used as a biomarker of plasma leak and therefore BBB compromise. Results revealed the leakage of plasma components from cortical blood vessels (mostly small arterioles) in both Sevoflurane- and Isoflurane-treated animals, with extravasated IgG highlighting the presence of perivascular leak clouds (Figs. 1C, 1E-H). Perivascular leak clouds were clearly more prominent in the cerebral cortex of older rodents (Figs. 1G-H) than in young- and middle-aged animals (Figs. 1A-F), suggesting that the BBB of older animals is more sensitive to the disruptive effects of anesthetics. In addition, perivascular leak clouds in the cerebral cortex of Sevoflurane-treated rats (Figs. 1E, G-H) were more extensive than those in Isoflurane-treated rats (Figs. 1C, F). These findings imply that Sevoflurane is more disruptive than Isoflurane to BBB functional integrity. Immunohistochemical controls were used to confirm the specificity of the anti-IgG antibody staining reaction (Fig 1I).

Synergistic effect of anesthetic exposure and aging on increasing BBB permeability

We next sought to quantify the separate effects of Sevoflurane and Isoflurane on the density of vessels exhibiting BBB compromise in the cerebral cortex and the extent of

the plasma leak emanating from these vessels. To accomplish this, we first established a scoring system that could be used to measure the relative extent of BBB leak from cortical blood vessels based on specific features of perivascular leak clouds as shown in figure 2. Using this system, a score of 0 corresponds to no detectable leak (Fig. 2A), whereas scores of 1-3 reflect a progressive increase in the size (and thus extent) of the perivascular leak cloud (Figs. 2B-F). A maximum score of three reflects the largest IgG-positive perivascular leak clouds, with IgG-labeled neurons either within it or in its immediate vicinity (Figs. 2E-F). Selective binding of IgG to neurons was consistently observed in the brains of both control animals and those subjected to Sevoflurane or Isoflurane anesthesia. Interestingly, non-neuronal cells were IgG-negative, suggesting that brain-reactive autoantibodies in the blood primarily target the pyramidal neurons that are dominant in the cerebral cortex (Figs. 2E-F). Quantification revealed an age-dependent increase in BBB permeability in control animals that were not exposed to anesthetics, as evidenced by increases in both the density of cerebrocortical blood vessels exhibiting BBB leaks and the extent or amount of material leaking from these vessels (Figs. 3A-B). Likewise, the older group of animals subjected to Sevoflurane anesthesia showed a dramatic and significant increase in the density and extent of vascular leak compared to controls (Figs. 3A-B). By contrast, older animals exposed to Isoflurane for 3 hour failed to show any significant age-related differences in either the density or extent of vascular leaks. Taken together, these data indicate that, in rodents, Sevoflurane is much more effective than Isoflurane in enhancing BBB permeability (Figs. 3A-B). In addition, similar measurements carried out on animals following 24 hour of recovery from

anesthesia revealed that this interval was insufficient for full functional recovery of BBB integrity in older rats, as the measurements of the density and extent of vascular leaks were still comparable among recovery and non-recovery rats (Figs. 3A-B).

Sevoflurane and Isoflurane induce dramatic structural changes in the luminal surfaces of BVECs that may be linked to BBB compromise

The quantitative IHC data described above shows that BBB breakdown and the leak of plasma components into the brain tissue are already well underway at the conclusion of the 3-hour treatment period. This suggests that the response of the BBB to exposure to inhalation anesthetics is rapid. To investigate the origin and nature of this rapid response, we next sought to determine if Sevoflurane and Isoflurane exert a direct effect on the BVECs that are essential for the structural and functional integrity of the BBB. To address this, we examined the effects of these anesthetics on the luminal surface morphology of rat BVECs *in vivo* using scanning electron microscopy. Isolated rat brains were sliced to permit direct access to the interior of the brain blood vessels as well as to visualize the luminal surfaces of BVECs. Figure 4A shows a SEM image of a transverse section through a leptomeningeal artery of a control animal, which was tilted to provide a view of the BVECs that form the inner lining of the vessel. Closer examination of the luminal surfaces of BVECs revealed long rows of discrete cytoplasmic ridge-like protrusions or tight junctional folds at the margins of individual BVECs that delineate the location of BBB-associated tight junctions (Fig. 4B). These are best seen when viewed from directly overhead (Fig. 4C). In arterioles, these tight junctional folds

most likely provide the extra membrane necessary for expansion or stretching of BVECs without compromising the structural integrity of tight junctions during systolic dilation (Fig. 4C). In larger arterioles, BVECs are highly elongated and the BBB-associated cytoplasmic protrusions are oriented parallel to the long axis of the vessel, presumably to minimize turbulence during rapid blood flow (Fig. 4C). Also, the intervening luminal surface of BVECs displays numerous small microvilli (Fig. 4C).

Exposure of animals to 3 hours of Sevoflurane or Isoflurane caused a dramatic and generalized overall flattening of the luminal surfaces of BVECs in rats of all age groups (Figs. 4D and 5). Tight junctional folds at the margins of most BVECs were collapsed and flattened. This was often accompanied by a loss of the numerous small microvilli seen on BVECs of controls (e.g., compare Fig. 4C with D and 5E with F). We also observed numerous holes at the margins of BVECs that appeared to be true holes in the BVEC layer (e.g., Fig. 4D). However, whether or not these structures correspond to real gaps in the BBB and underlying basal lamina and thus focal sites of BBB leak is unknown.

Exposure to Sevoflurane and Isoflurane can be toxic to BVECs

Analysis of the luminal surface morphology of BVECs also revealed some variations in the individual responses of BVECs to Sevoflurane and Isoflurane. Interestingly, the most severely affected BVECs were most frequently found in regions where blood vessels exhibited a sharp directional deviations or branching. Severely affected BVECs in these regions exhibited luminal surface membranes that were often

"pockmarked" with small holes, some of which were also located at cell margins in regions of BBB-associated tight junction folds (Fig. 6A). These were not specimen preparation artifacts since numerous adjacent BVECs in these same preparations often completely lacked these structural anomalies.

We also found that exposure to either Sevoflurane or Isoflurane led to the death of some BVECs (Fig. 6), although the underlying reason for the differential sensitivity of BVECs to the anesthetics used here remains to be established. For example, figure 6A shows two dying cells exhibiting unusually smooth luminal surface membranes, one with small holes scattered over the surface and the other with these holes restricted to the cell margin in the region of tight junctional folds. The next stage in the death of BVECs is the stripping of the entire luminal surface membrane from the cell, thereby exposing an easily identified cell nucleus apparently still held in place by residual cytoplasmic components (Figs. 6B-C). Eventually, the nucleus and much of the residual cytoplasm are stripped off, presumably by the shearing action of continued blood flow (Fig. 6D). It is reasonable to predict that the death of BVECs creates gaps in the integrity of the BVEC layer and thus the BBB. However, whether sites of BVEC death actually correspond to focal regions of BBB leak in brain blood vessels remains to be demonstrated, and the relative contribution of BVEC loss to the extent of BBB leak still needs to be defined.

Vascular integrity and surface morphology of BVECs failed to recover within 24 hour of anesthetic treatment

We next asked if the effects of these anesthetics on the BBB integrity and the surface morphology of BVECs are reversed within 24 hours. This was tested by allowing animals to recover for 24 hours after the conclusion of the 3-hour exposure to Sevoflurane or Isoflurane. Quantitative IHC failed to show any significant reduction in the density of leaking vessels or in the extent of their leakage after a 24-hour recovery period, most notably in the Sevoflurane-treated animals (Fig. 3). This was corroborated by examination of the luminal surface topographies of BVECs using SEM. BVECs in young- and middle-aged animals appeared to be more comparable to controls after 24 hours of recovery than those in older animals (data not shown). We also monitored the emergence from anesthesia and orientation of the recovery rats. Interestingly, the emergence of rodents from anesthesia during the post-anesthesia period was clearly faster in Sevoflurane-treated animals compared to Isoflurane, with rats exposed to Isoflurane being more lethargic and subdued.

FIGURES

Fig 1: Effects of Sevoflurane and Isoflurane on BBB permeability

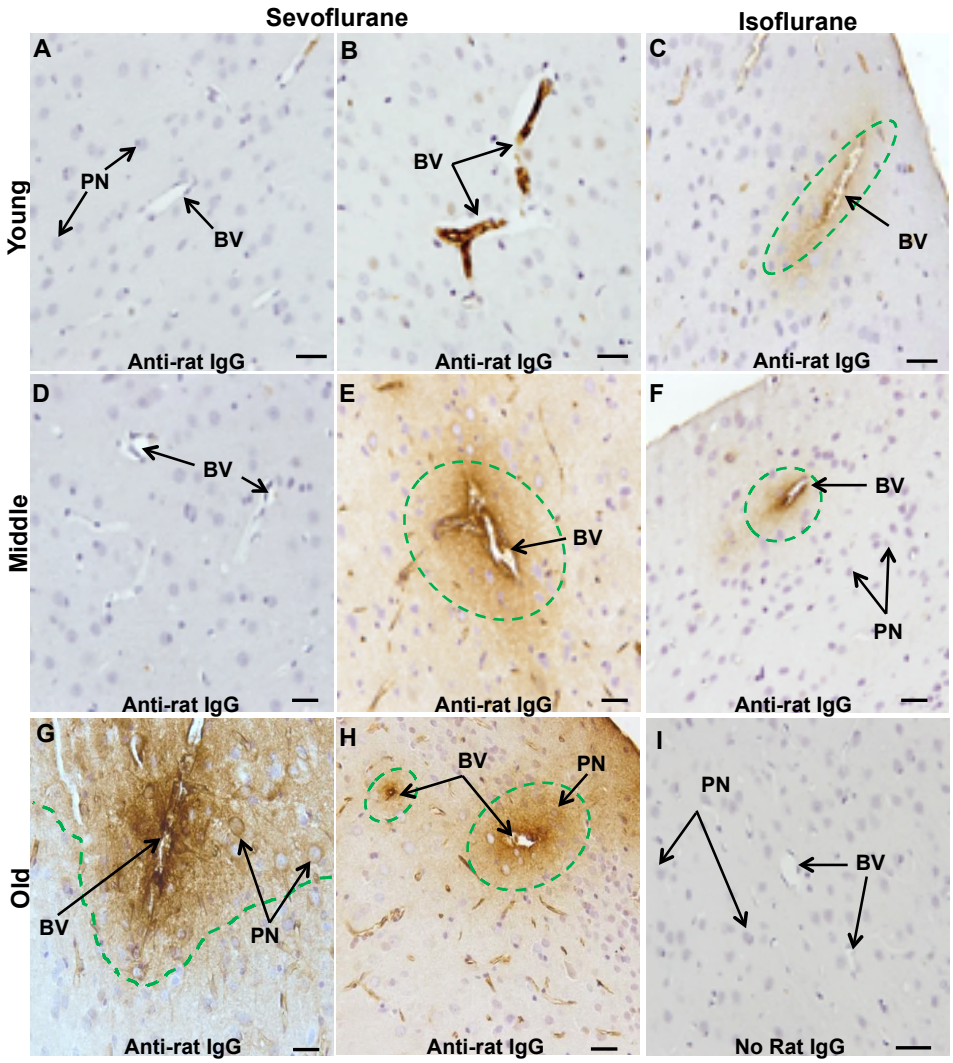

Figure 1: Age-dependent effects of Sevoflurane and Isoflurane on BBB permeability.

Histological sections of the cerebral cortex of young (**A-C**), middle-aged (**D-F**) and older (**G-I**) rats subjected to Sevoflurane or Isoflurane anesthesia for 3 hours were immunostained to reveal BBB leak from blood vessels and the influx of IgG into the brain tissue. The most prominent leaks were observed in the cerebral cortex of older rats exposed to Sevoflurane (**G-H**). (**I**) An IHC control section treated with blocking sera only to confirm the specificity of the anti-IgG antibody used to detect interstitial, extravasated IgG. PN - pyramidal neuron; BV - blood vessel. Scale bar = 100μm.

Fig 2: Scoring system to determine extent of anesthetic-induced BBB leak

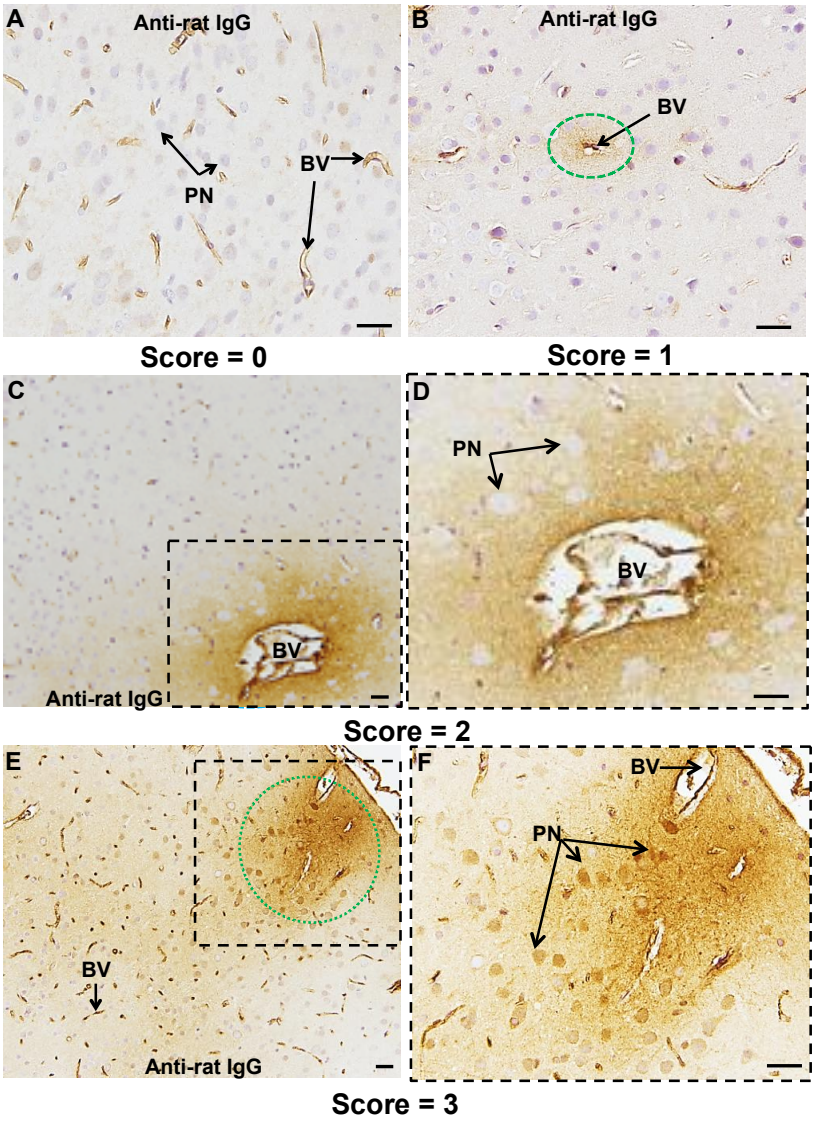

Figure 2: Scoring system to quantify the extent of anesthetic-induced BBB leak.

The extent of BBB leak from each blood vessel was assigned a score ranging from 0-3 based on the appearance of perivascular leak clouds. (**A**) A score of 0 corresponds to no detectable leak. (**B-F**) Scores ranging from 1-3 reflect a progressive increase in the size of leak clouds, which is also taken to reflect the extent of the leak. (**E-F**) A score of three indicates a large IgG-positive perivascular leak cloud that also contains IgG-positive neurons within or near the leak cloud. (**D** and **F**) Enlarged regions of **C** and **E**, respectively. PN - pyramidal neurons; BV - blood vessels. Scale bar = 100μm.

Fig 3. Effects of Sevoflurane and Isoflurane on the density and extent of BBB leaks

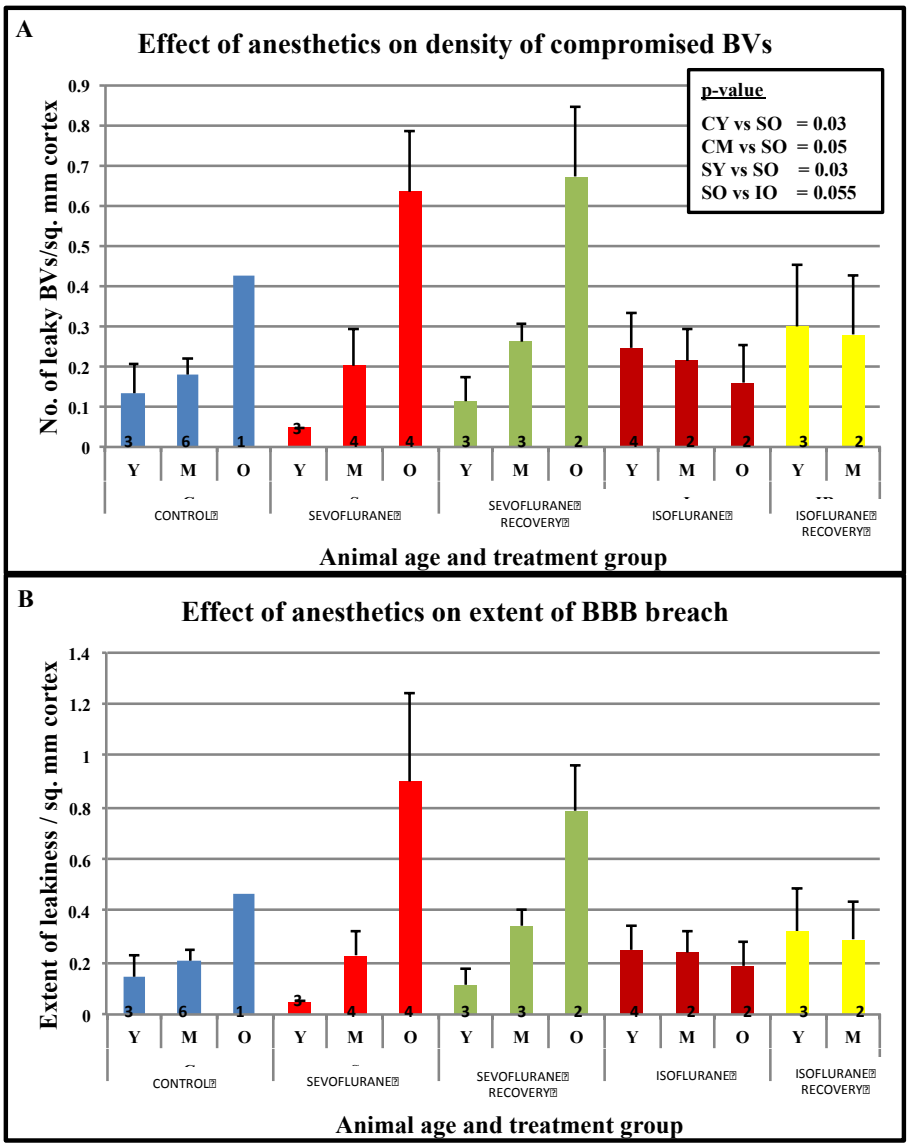

Figure 3: Quantification of the effects of Sevoflurane and Isoflurane exposure and age on the density and extent of BBB leaks.

(**A**) The density of blood vessels with demonstrable BBB leaks was determined by counting the total number of leaking blood vessels per unit area of cerebral cortex. (**B**) The extent of BBB leak was quantified using the scoring system described and illustrated in Fig. 2. Control animals showed a gradual, age-dependent increase in BBB permeability, as evidenced by increases in both the density of blood vessels in the cerebral cortex with detectable BBB leaks and the extent of leak from these vessels. Older animals subjected to Sevoflurane showed more dramatic increases in the density and extent of blood vessel leaks compared to controls and Isoflurane. A period of 24 hours was insufficient for recovery of BBB functional integrity from either Sevoflurane or Isoflurane. Y - young; M - middle; O - old; S - Sevoflurane; I – Isoflurane; p (*) $\leq$ 0.05. n = sample size at bottom of bar.

Fig 4: Sevoflurane causes dramatic flattening of the luminal surfaces of BVECs revealed by SEM

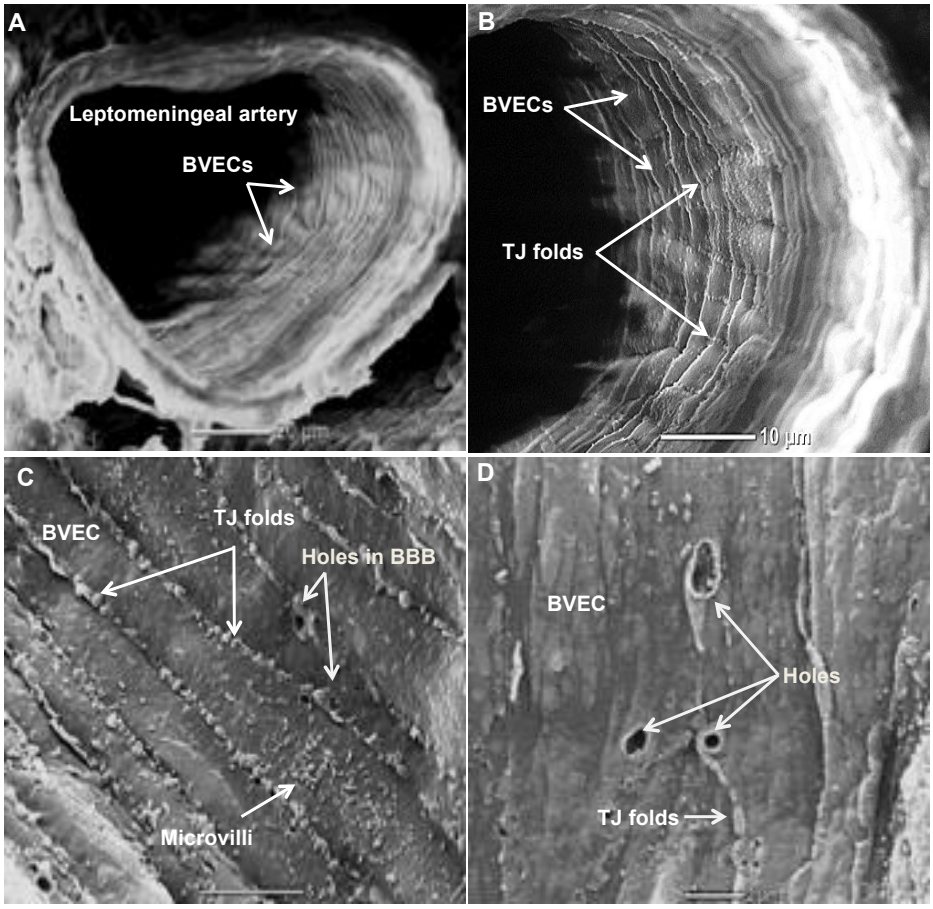

Figure 4: Sevoflurane causes dramatic flattening of the luminal surfaces of BVECs.

(A) Scanning electron microscopic image of a transverse section through a rat leptomeningeal artery of a control rat. (**B**) Enlarged portion of (A) showing the luminal surfaces of BVECs and long rows of discrete cytoplasmic protrusions that delineate the location of BBB-associated tight junctional folds at the cell margins of BVECs. (**C**) Higher magnification showing extensive, ridge-like protrusions of cytoplasm overlying BBB-associated tight junctional folds and oriented parallel to the long axis of the vessel. Between these junctional folds, the luminal surface displays numerous small microvilli. (**D**) Exposure of animals to Sevoflurane for 3 hours caused a dramatic overall flattening of the luminal surfaces of BVECs, including the marginal tight junctional folds associated with BBB tight junctions and a loss of small microvilli. Holes were often observed at cell margins between adjacent BVECs. BVEC - brain vascular endothelial cell; BBB TJ - blood-brain barrier tight junctions.

Fig 5: Sevoflurane and Isoflurane cause comparable flattening of the luminal surfaces of BVECs

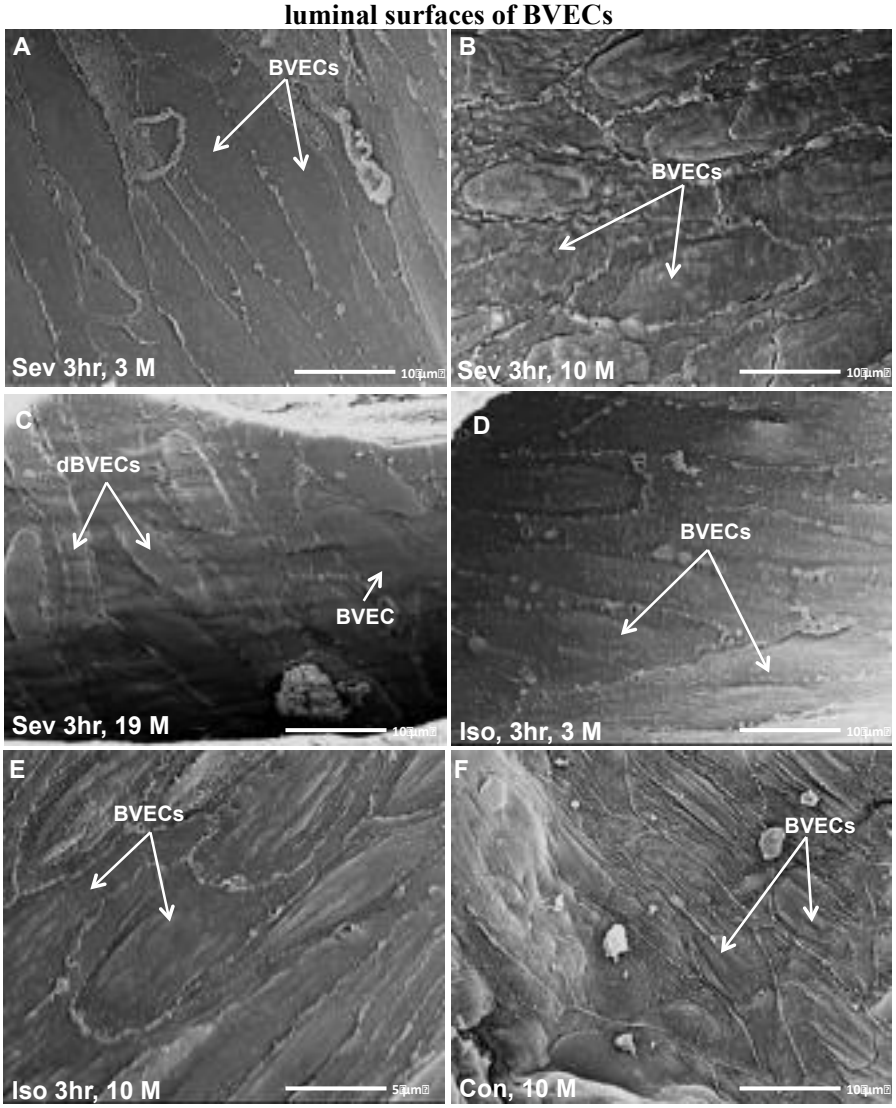

Figure 5: Sevoflurane and Isoflurane cause comparable flattening of the luminal surfaces of BVECs.

SEM images showing the luminal surfaces of BVECs lining the walls of brain blood vessels. Sevoflurane (**A-C**) caused changes in the luminal surface topography of BVECs that ranged from a pronounced surface flattening (**A**) to wrinkling (**B**). Scattered BVECs appeared to be dying as revealed by defects in their surface membranes, which were tightly opposed to underlying nuclei. Isoflurane (**D-E**) also caused comparable flattening of the luminal surface membranes of BVECs, whereas the luminal surfaces of BVECs in controls showed prominent marginal ridges/folds as well as small microvilli scattered over the cell surface (**F**). BVECs - brain vascular endothelial cells; dBVECs - dying or dead BVECs.

Fig 6: Sevoflurane and Isoflurane can induce BVEC death resulting in focal BBB breakdown

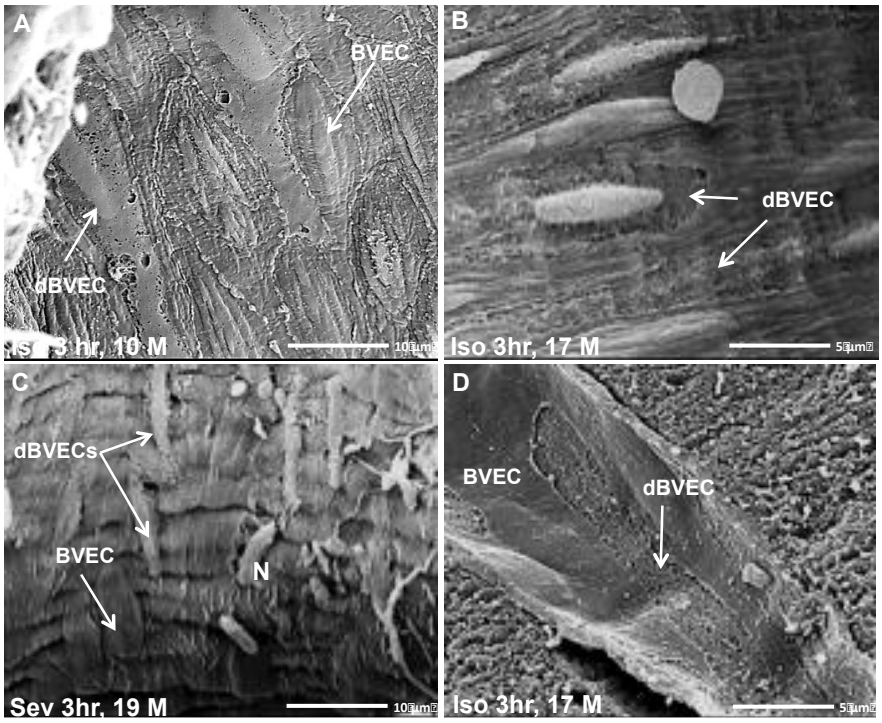

Figure 6: Sevoflurane and Isoflurane can induce the death of BVECs, resulting in focal BBB breakdown.

(**A**) The luminal surface membranes of some BVECs scattered throughout the walls of blood vessels were often "pockmarked" with holes, especially at cell margins in the vicinity of BBB-associated tight junctional folds. This appears to be the first indication of impending cell death. (**B**) Next, the luminal surface membrane is completely stripped from the BVEC, exposing a nucleus presumably still held in place by residual cytoplasmic fibers. (**C**) BVECs at branch points of blood vessels are apparently most vulnerable to the effects of Sevoflurane and Isoflurane. (**D**) A large capillary showing the remnant of a dead BVEC with the nucleus stripped off by the shear forces of normal blood flow. dBVEC - dying or dead BVEC.

Fig 7: Illustration

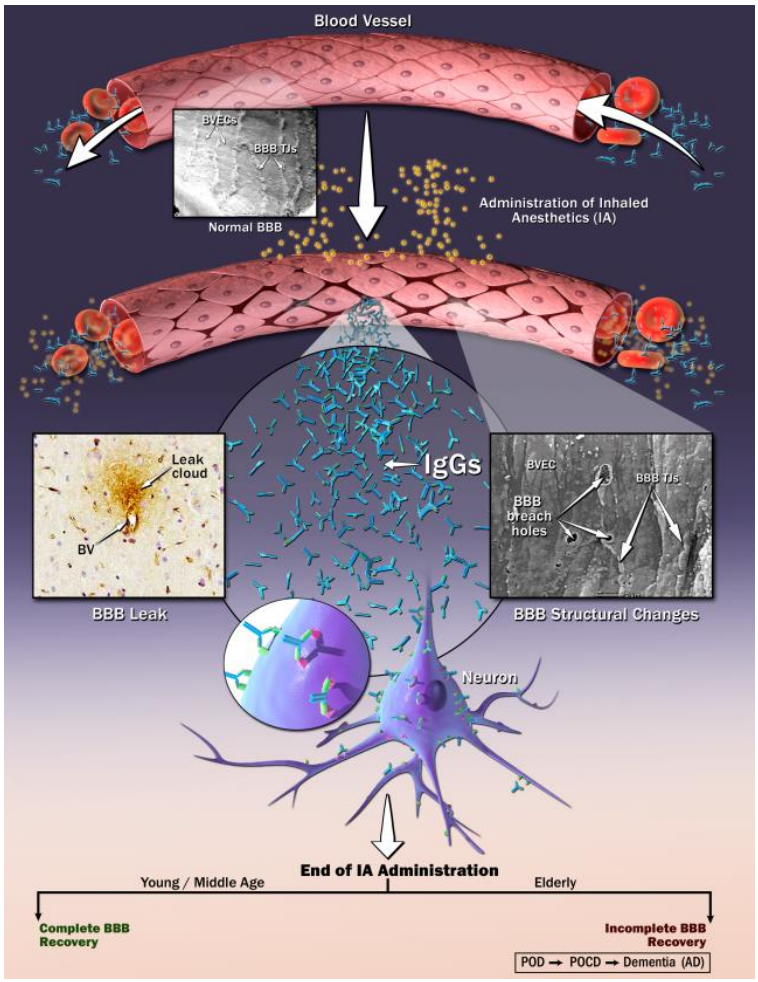

Figure 7: Diagram showing a proposed mechanism of anesthetic-induced BBB breakdown and its potential mechanistic relationship to POD, postoperative cognitive decline and dementia.

Here, we propose that the combination of BBB breakdown, plasma entry into the brain tissue, and the selective binding of brain-reactive IgGs to pyramidal neurons act together to contribute to disruption of normal neuronal activity and collectively elicit the symptoms that define POD. Further, we suggest that failure to completely restore BBB function following surgery, which appears to be most prevalent in the elderly, leads to POCD in the short-term and, if unresolved in the long-term, can favor the development of dementia. Thus, BBB breakdown may provide a common mechanistic link between POD, POCD and dementia.

DISCUSSION

The present study shows that some commonly used inhalation anesthetics, such as Sevoflurane, rapidly cause increased BBB permeability in blood vessels in the rat cerebral cortex as demonstrated by the influx of IgG into the brain parenchyma, most notably in older animals. We also show a differential response of the BBB to specific inhalation anesthetics; with Sevoflurane having a much greater effect on increasing BBB permeability than Isoflurane. Given that the cerebral cortex is normally immunoprivileged, the presence of IgG in the brain parenchyma was used as a biomarker of BBB compromise. Small arteries and arterioles within the brain exhibited a greater extent of leak than small veins, venules and capillaries, and were often surrounded by perivascular clouds of leaked IgG-immunopositive material, indicative of BBB breakdown. This apparent selectivity for arteries and arterioles is expected, since both are under considerably more hydrostatic pressure than their associated small veins, venules and capillaries.

Anesthetics compromise BBB function through their rapid and direct effects on BVECs

The underlying mechanisms through which anesthetics can trigger BBB permeability are unknown, but a temporal link to immediate and dramatic morphological changes in the luminal surfaces of BVECs described here suggests that a direct effect of the anesthetics on these cells may be involved. In support of this, we show using scanning electron microscopy that exposure to Sevoflurane or Isoflurane induced an

overall flattening of the luminal surfaces of BVECs. This was most conspicuous at the boundaries between adjacent BVECs, with flattening and collapse of the tight junctional folds found in this region. Although Sevoflurane and Isoflurane are known to be potent vasodilators, whether or not this contributes to the observed flattening of tight junctional folds between adjacent BVECs is unknown (Iida et al., 1998).

The present study also shows that, in older animals, Sevoflurane was more effective than Isoflurane in generating these effects based on structural changes in BVECs, measurements of the relative density of leaking blood vessels and the overall extent of vascular leakage in the brain parenchyma. In surgical settings, Sevoflurane is usually selected over Isoflurane, since in humans the average time to emergence, response to commands, orientation and hospital stay is shorter (Sahu et al., 2011; Scholz et al., 1996). In our hands, Sevoflurane appears to behave similarly in rats; Sevoflurane-treated animals were quicker to recover and orient themselves compared Isoflurane-treated animals; the latter were more lethargic and subdued for a longer time period following the conclusion of anesthesia. If these phenotypes do in fact relate to the underlying BBB breaches following the inhaled anesthetic administration, then the next step would be to determine if the recovery in behavior correlates with recovery in BBB breakdown.

The age of the animal was found to be a key factor in determining the magnitude of the response of the BBB to exposure to a particular anesthetic. For example, despite the fact that Sevoflurane and Isoflurane exposure resulted in dramatic differences in

the degree of BVEC luminal surface flattening among animals at different ages, the oldest animals in the Sevoflurane-treated group clearly showed the greatest degree of BBB permeability as well as the least recovery at 24 hours post-anesthesia. Indeed, we found that 24 hours of recovery was generally insufficient for complete restoration of BBB functional integrity and normal BVEC luminal surface morphology in all age groups tested, but most notably in older animals. Extrapolating this to humans suggests that, in elderly patients planning to undergo surgery and exposure to inhalation anesthetics, there may be a long-term benefit in purposely choosing a less potent, slower-acting anesthetic over a more potent faster-acting one. The basis of this decision comes from the concept that the less potent anesthetic would presumably pose less risk for BBB compromise and, hopefully, minimizes subsequent POD, which is supported by the data presented here. Rates of POD have not been studied extensively in humans for several reasons, not least important is the difficulty in standardizing anesthetic use while administering a cocktail of varying polypharmaceuticals. Also complicating these studies is the lack of consistently used and validated tools for assessing POD. Further studies will be needed to identify specific anesthetics for use in surgery that are less disruptive to BBB function and thus better able to help patients to avoid postoperative manifestations such as POD, postoperative cognitive decline and perhaps even subsequent dementias. For example, in this context, the data presented here would support the choice of Isoflurane over Sevoflurane for use in elderly patients.

Anesthetic-mediated death of BVECs contributes to BBB compromise

Scanning electron microscopy revealed single and small clusters of dying and dead BVECs in animals treated with Sevoflurane or Isoflurane, with an increased prevalence in Sevoflurane-treated animals (Figs. 6). Since these cells were relatively few and often surrounded by numerous other cells that appeared normal, it can be suggested that they were, for some unknown reason, more vulnerable to anesthetic treatment than surrounding cells. Not surprisingly, dying and dead BVECs were clearly more abundant in 24-hour recovery group of animals, suggesting that it may take some time for affected BVECs to finally succumb to the effects of anesthetics (Figs. 6). Some features associated with the death of BVECs have been reported in earlier studies of rats treated with a hypertonic arabinose solution (Lossinsky et al., 1995) as well as in spontaneously hypertensive rats (Hazama et al., 1979). Regardless of the underlying reason for the observed death of BVECs, there is no doubt that their loss leaves a physical gap in the BBB that apparently does not get rectified within 24 hours. It is unknown if or how such gaps are repaired as well as the time frame for repair, but replacement of a lost BVEC with another derived from circulating endothelial progenitor cells originating in the bone marrow is one possibility (Kaneko et al., 2012; Peplow, 2014; Wei et al., 2010). Further work will be needed to test this repair mechanism as well as to investigate any potential therapeutic utility of stimulating such cell replacements.

Agreement of data with results of prior studies

Our data agrees with a study by Tetrault et al., who demonstrated a dose-dependent breakdown of the BBB by Isoflurane in the cerebral cortex and thalamus in cats

(Tetrault et al., 2008). Likewise, Hu et al. showed BBB compromise in 18-month-old Wistar rats that had undergone orthopedic surgery under Sevoflurane (Hu et al., 2014). However, the experimental design of the present study differs from that of these earlier studies in two important ways. First, Tetrault et al. also treated the cats with a muscle relaxant and other anesthetics in addition to Isoflurane. The use of multiple compounds makes it difficult to definitively attribute the observed effects on the BBB solely to Isoflurane (Tetrault et al., 2008). In the present study, in an effort to more directly link the individual effects to Sevoflurane or Isoflurane, we avoided the use of additional agents with the exception of an obligatory brief use of CO_2 for euthanizing recovery and control rats. Second, Hu et al. carried out an orthopedic surgical procedure in their Sevoflurane-treated rats (Hu et al., 2014). It is known that surgical trauma, among other things, can induce expression of CCL2 by vascular endothelial cells, which can influence BBB permeability by facilitating transendothelial migration of macrophages into the brain parenchyma (Dzenko et al., 2005). This introduces another variable that makes it difficult to distinguish the relative contributions of the inhalation anesthetics from the response to the surgical procedure on the observed outcomes. To avoid this, no surgical procedures were carried out in the present study. The results of all of these studies, however, differ from that published recently by Thal et al., as they failed to detect any effect of Isoflurane or Sevoflurane on inflicting brain edema, BBB compromise, or alteration in the expression of tight junction proteins associated with the BBB in young C57B16N mice (Thal et al., 2012). Although it is certainly possible that the mouse responds differently than the rat and larger mammals to these anesthetics, the fact that

this study was focused only on younger mice might have contributed to the different outcomes. Lastly, in the present study, we were also mindful of the increasing frequency of aging-associated chronic vascular changes and comorbidities that can afflict very old animals (Popescu et al., 2009; Shah and Mooradian, 1997; Zeevi et al., 2010). Such chronic states can have significant impact on our experimental outcomes and can confuse interpretations of data (Popescu et al., 2009; Shah and Mooradian, 1997; Zeevi et al., 2010). For this reason, we decided against including extremely old rats in our study.

BBB breakdown - a common theme linking POD, postoperative cognitive decline and eventual dementia

About 50% of the elderly patients who undergo general anesthesia develop POD, and only half of these POD patients regain normal cognition on the second day (Neufeld et al., 2013). In the context of the present study, this suggests that entry of plasma components into the brain parenchyma through anesthesia-induced increased BBB permeability results in disruption of the brain homeostasis. This acutely altered brain homeostasis could trigger neuronal dysfunction, leading to a manifestation of symptoms that collectively defines POD. During patient recovery, partial or complete restoration of BBB function, depending on the age and vascular health status of the individual, would be expected to correspond to partial or complete loss of POD symptoms. Furthermore, failure to completely recover BBB function, which may occur preferentially in elderly POD patients, could set into motion a long-term pathological progression that transgresses POD, leading to postoperative cognitive

decline and perhaps even dementia in the long-term as depicted in figure 7. In the present study, we also demonstrate that some blood-borne IgGs have selective affinity for pyramidal neurons in the cerebral cortex. This binding of extravasated IgG to pyramidal neurons may also be disruptive to neuronal function and even trigger further pathological changes via the crosslinking and internalization of key surface membrane proteins. For example, we have previously reported that IgG binds selectively to amyloid-beta$_{1-42}$ (Abeta42)-burdened pyramidal neurons located in regions of pathology in the cerebral cortex of Alzheimer's disease patients (Nagele et al., 2011). We tested the possible mechanistic relationship between neuronal IgG binding and intraneuronal Abeta42 deposition in adult mouse brain slice cultures and demonstrated that IgG binding to pyramidal neurons enhances chronic endocytosis and selective intraneuronal deposition of Abeta42 in these cells (Nagele et al., 2011). The fact that BBB breakdown and selective binding of IgG to neurons are common events that occur in the brains of inhalation anesthetic-treated older rats and human Alzheimer's disease patients leads us to propose that BBB compromise may be a common and requisite mechanistic link. Similar results and conclusions implicating BBB compromise and selective IgG binding to neurons in chronic epilepsy were reported in a study carried out on human temporal lobe epileptic tissues and in a rat model of epilepsy (Michalak et al., 2012).

This study has some obvious limitations. The first is the small sample size of the group of older rats, due to their limited availability and long waiting periods for their delivery. This had a negative impact on statistical significance in spite of an easily

discerned pattern of the effects of these inhalation anesthetics on BBB integrity. In addition, the treatment of the animals with anesthetics as carried out in the present study fails to match the induction of general anesthesia in humans, as we did not use any intravenous anesthetic agent, opioids, or muscle relaxants. Of course, in part, this was done purposefully in an effort to more clearly attribute the observed effects to a single agent, i.e., Sevoflurane or Isoflurane. Lastly, the selection of a single recovery point was subsequently found to be limiting since our data clearly revealed that 24 hours was insufficient for full recovery of BBB functional integrity, even in young and middle aged rodents. Further studies using larger numbers of rats from all age group that are allowed to recover for longer time periods will be needed.

Conclusions and perspectives

The data presented here show that some inhalation anesthetics can increase BBB permeability, particularly in older subjects. In addition, we show that Sevoflurane has a greater effect on increasing BBB permeability in a rat model, and that older Sevoflurane-treated animals failed to regain BBB integrity within 24 hours of exposure to anesthetic, as judged by the persistent presence of IgG in the brain parenchyma as a biomarker of vascular leak. These findings advocate for the identification and selection of inhalation anesthetics that are less disruptive to the BBB in the elderly, since individuals in this age group are most vulnerable to BBB breakdown and thus POD. From this study, it is clear that both anesthetics directly alter the luminal surface morphologies of BVECs, particularly in regions of BBB-associated tight junctional folds. Furthermore, the more severe effects of Sevoflurane

on BVEC luminal surface morphology suggest that these changes are sufficient to exceed some threshold required for breach of BBB integrity. Based on these findings, we propose that BBB breakdown induced by some inhalation anesthetics perturbs brain homeostasis due to the influx of plasma components into the brain parenchyma. For example, IgG, a plasma component normally blocked from entry into the brain by the BBB, was found to extravasate into brain parenchyma predominantly in Sevoflurane-treated animals. The observed selective binding of this IgG to neurons may further exacerbate neuronal dysfunction and thereby contribute to emergence of symptoms associated with POD. Furthermore, we suggest that failure to completely restore BBB function following surgery, which appears to be most prevalent in the elderly, could lead to postoperative cognitive decline in the short-term and, if unresolved, may favor the later development of dementia in the long-term (Fig. 7). Therefore, maintenance of proper BBB function is crucial for preventing the occurrence and escalation of postoperative delirium.

REFERENCES

A, H.L.M.a.M.J., 2011. 2010 Census Summary File 1. Vol., ed.^eds. U.S. CENSUS BUREAU, USA.

Abbott, N.J., Patabendige, A.A., Dolman, D.E., Yusof, S.R., Begley, D.J., 2010. Structure and function of the blood-brain barrier. Neurobiol Dis. 37**,** 13-25.

Acharya, N.K., Levin, E.C., Clifford, P.M., Han, M., Tourtellotte, R., Chamberlain, D., Pollaro, M., Coretti, N.J., Kosciuk, M.C., Nagele, E.P., Demarshall, C., Freeman, T., Shi, Y., Guan, C., Macphee, C.H., Wilensky, R.L., Nagele, R.G., 2013. Diabetes and hypercholesterolemia increase blood-brain barrier permeability and brain amyloid deposition: beneficial effects of the LpPLA2 inhibitor darapladib. J Alzheimers Dis. 35**,** 179-98.

Ansaloni, L., Catena, F., Chattat, R., Fortuna, D., Franceschi, C., Mascitti, P., Melotti, R.M., 2010. Risk factors and incidence of postoperative delirium in elderly patients after elective and emergency surgery. Br J Surg. 97**,** 273-80.

Bedford, P.D., 1955. Adverse cerebral effects of anaesthesia on old people. Lancet. 269**,** 259-63.

Brown, E.N., Lydic, R., Schiff, N.D., 2010. General anesthesia, sleep, and coma. N Engl J Med. 363**,** 2638-50.

Brown, E.N., Purdon, P.L., 2013. The aging brain and anesthesia. Curr Opin Anaesthesiol. 26**,** 414-9.

Burns, A., Gallagley, A., Byrne, J., 2004. Delirium. J Neurol Neurosurg Psychiatry. 75**,** 362-7.

Clifford, P.M., Siu, G., Kosciuk, M., Levin, E.C., Venkataraman, V., D'Andrea, M.R., Nagele, R.G., 2008. Alpha7 nicotinic acetylcholine receptor expression by vascular smooth muscle cells facilitates the deposition of Abeta peptides and promotes cerebrovascular amyloid angiopathy. Brain Res. 1234**,** 158-71.

Dzenko, K.A., Song, L., Ge, S., Kuziel, W.A., Pachter, J.S., 2005. CCR2 expression by brain microvascular endothelial cells is critical for macrophage transendothelial migration in response to CCL2. Microvasc Res. 70**,** 53-64.

Hazama, F., Ozaki, T., Amano, S., 1979. Scanning electron microscopic study of endothelial cells of cerebral arteries from spontaneously hypertensive rats. Stroke. 10**,** 245-52.

Hu, N., Guo, D., Wang, H., Xie, K., Wang, C., Li, Y., Wang, C., Wang, C., Yu, Y., Wang, G., 2014. Involvement of the blood-brain barrier opening in cognitive decline in aged rats following orthopedic surgery and high concentration of sevoflurane inhalation. Brain Res. 1551**,** 13-24.

Iida, H., Ohata, H., Iida, M., Watanabe, Y., Dohi, S., 1998. Isoflurane and sevoflurane induce vasodilation of cerebral vessels via ATP-sensitive K+ channel activation. Anesthesiology. 89**,** 954-60.

Inouye, S.K., Westendorp, R.G., Saczynski, J.S., 2014. Delirium in elderly people. Lancet. 383**,** 911-22.

Jin, A.Y., Tuor, U.I., Rushforth, D., Kaur, J., Muller, R.N., Petterson, J.L., Boutry, S., Barber, P.A., 2010. Reduced blood brain barrier breakdown in P-selectin deficient mice following transient ischemic stroke: a future therapeutic target for treatment of stroke. BMC Neurosci. 11**,** 12.

Kalaria, R.N., 2010. Vascular basis for brain degeneration: faltering controls and risk factors for dementia. Nutr Rev. 68 Suppl 2**,** S74-87.

Kaneko, Y., Tajiri, N., Shinozuka, K., Glover, L.E., Weinbren, N.L., Cortes, L., Borlongan, C.V., 2012. Cell therapy for stroke: emphasis on optimizing safety and efficacy profile of endothelial progenitor cells. Curr Pharm Des. 18**,** 3731-4.

Kuang, F., Wang, B.R., Zhang, P., Fei, L.L., Jia, Y., Duan, X.L., Wang, X., Xu, Z., Li, G.L., Jiao, X.Y., Ju, G., 2004. Extravasation of blood-borne immunoglobulin G through blood-brain barrier during adrenaline-induced transient hypertension in the rat. Int J Neurosci. 114**,** 575-91.

Leslie, D.L., Marcantonio, E.R., Zhang, Y., Leo-Summers, L., Inouye, S.K., 2008. One-year health care costs associated with delirium in the elderly population. Arch Intern Med. 168**,** 27-32.

Lossinsky, A.S., Vorbrodt, A.W., Wisniewski, H.M., 1995. Scanning and transmission electron microscopic studies of microvascular pathology in the osmotically impaired blood-brain barrier. J Neurocytol. 24**,** 795-806.

Maldonado, J.R., 2013. Neuropathogenesis of delirium: review of current etiologic theories and common pathways. Am J Geriatr Psychiatry. 21**,** 1190-222.

Michalak, Z., Lebrun, A., Di Miceli, M., Rousset, M.C., Crespel, A., Coubes, P., Henshall, D.C., Lerner-Natoli, M., Rigau, V., 2012. IgG leakage may contribute to neuronal dysfunction in drug-refractory epilepsies with blood-brain barrier disruption. J Neuropathol Exp Neurol. 71**,** 826-38.

Nadelson, M.R., Sanders, R.D., Avidan, M.S., 2014. Perioperative cognitive trajectory in adults. Br J Anaesth. 112**,** 440-51.

Nagele, R.G., Clifford, P.M., Siu, G., Levin, E.C., Acharya, N.K., Han, M., Kosciuk, M.C., Venkataraman, V., Zavareh, S., Zarrabi, S., Kinsler, K., Thaker, N.G., Nagele, E.P., Dash, J., Wang, H.Y., Levitas, A., 2011. Brain-reactive autoantibodies prevalent in human sera increase intraneuronal amyloid-beta(1-42) deposition. J Alzheimers Dis. 25**,** 605-22.

Neufeld, K.J., Leoutsakos, J.M., Sieber, F.E., Wanamaker, B.L., Gibson Chambers, J.J., Rao, V., Schretlen, D.J., Needham, D.M., 2013. Outcomes of early delirium diagnosis after general anesthesia in the elderly. Anesth Analg. 117**,** 471-8.

Neufeld, K.J., Thomas, C., 2013. Delirium: definition, epidemiology, and diagnosis. J Clin Neurophysiol. 30**,** 438-42.

Peplow, P.V., 2014. Growth factor- and cytokine-stimulated endothelial progenitor cells in post-ischemic cerebral neovascularization. Neural Regen Res. 9**,** 1425-9.

Popescu, B.O., Toescu, E.C., Popescu, L.M., Bajenaru, O., Muresanu, D.F., Schultzberg, M., Bogdanovic, N., 2009. Blood-brain barrier alterations in ageing and dementia. J Neurol Sci. 283**,** 99-106.

Rouhl, R.P., Damoiseaux, J.G., Lodder, J., Theunissen, R.O., Knottnerus, I.L., Staals, J., Henskens, L.H., Kroon, A.A., de Leeuw, P.W., Tervaert, J.W., van Oostenbrugge, R.J., 2012. Vascular inflammation in cerebral small vessel disease. Neurobiol Aging. 33**,** 1800-6.

Rudolph, J.L., Marcantonio, E.R., 2011. Review articles: postoperative delirium: acute change with long-term implications. Anesth Analg. 112**,** 1202-11.

Sahu, D.K., Kaul, V., Parampill, R., 2011. Comparison of isoflurane and sevoflurane in anaesthesia for day care surgeries using classical laryngeal mask airway. Indian J Anaesth. 55**,** 364-9.

Scholz, J., Bischoff, P., Szafarczyk, W., Heetel, S., Schulte, J., 1996. [Comparison of sevoflurane and isoflurane in ambulatory surgery. Results of a multicenter study]. Anaesthesist. 45 Suppl 1**,** S63-70.

Shah, G.N., Mooradian, A.D., 1997. Age-related changes in the blood-brain barrier. Exp Gerontol. 32**,** 501-19.

Strom, C., Rasmussen, L.S., Sieber, F.E., 2014. Should general anaesthesia be avoided in the elderly? Anaesthesia. 69 Suppl 1**,** 35-44.

Tetrault, S., Chever, O., Sik, A., Amzica, F., 2008. Opening of the blood-brain barrier during isoflurane anaesthesia. Eur J Neurosci. 28**,** 1330-41.

Thal, S.C., Luh, C., Schaible, E.V., Timaru-Kast, R., Hedrich, J., Luhmann, H.J., Engelhard, K., Zehendner, C.M., 2012. Volatile anesthetics influence blood-brain barrier integrity by modulation of tight junction protein expression in traumatic brain injury. PLoS One. 7**,** e50752.

van Munster, B.C., de Rooij, S.E., 2014. Delirium: a synthesis of current knowledge. Clin Med. 14**,** 192-5.

Vasilevko, V., Passos, G.F., Quiring, D., Head, E., Kim, R.C., Fisher, M., Cribbs, D.H., 2010. Aging and cerebrovascular dysfunction: contribution of hypertension, cerebral amyloid angiopathy, and immunotherapy. Ann N Y Acad Sci. 1207**,** 58-70.

Wei, H.J., Jiang, R.C., Liu, L., Zhang, J.N., 2010. Circulating endothelial progenitor cells in traumatic brain injury: an emerging therapeutic target? Chin J Traumatol. 13**,** 316-8.

Zeevi, N., Pachter, J., McCullough, L.D., Wolfson, L., Kuchel, G.A., 2010. The blood-brain barrier: geriatric relevance of a critical brain-body interface. J Am Geriatr Soc. 58**,** 1749-57.

Zlokovic, B.V., 2008. The blood-brain barrier in health and chronic neurodegenerative disorders. Neuron. 57**,** 178-201.

ATTRIBUTIONS

Authors

Nimish K. Acharya, Ph.D.[1,3]**; Eric L. Goldwaser, B.S**.[1,2,]; Martin M. Forsberg, M.D.[3]; George A. Godsey, B.S.[1,2]; Cristina A. Johnson, M.S.[1,2]; Abhirup Sarkar, M.S.[1,2]; Cassandra DeMarshall, M.S.[1,2]; Mary C. Kosciuk, Ph.D.[1,3]; Jacqueline M. Dash, M.S.[2,3]; Caitlin P. Hale, B.S.[3]; Douglas M. Leonard, D.O. [4]; Denah M. Appelt, Ph.D.[5]; Robert G. Nagele, Ph.D.[1,3]

Affiliations

[1]Biomarker Discovery Center, New Jersey Institute for Successful Aging, Rowan University School of Osteopathic Medicine, Stratford, NJ 08084

[2]Graduate School of Biomedical Sciences, Rowan University, Stratford, NJ 08084

[3]Department of Geriatrics and Gerontology, Rowan University School of Osteopathic Medicine, Stratford, NJ 08084

[4]Department of Psychiatry, Rowan University School of Osteopathic Medicine, Stratford, NJ 08084

[5]Philadelphia College of Osteopathic Medicine, Philadelphia, PA 19131

Funding disclosure

The authors wish to thank the Osteopathic Heritage Foundation and Princeton Institute for Life Sciences for supporting this project.

Running headline

Inhaled anesthetics and blood-brain barrier permeability

Keywords

blood brain barrier, sevoflurane, isoflurane, anesthesia, delirium, postoperative delirium

Abbreviations

BBB – blood-brain barrier, POD – postoperative delirium, POCD – postoperative cognitive decline, IgG – immunoglobulin G

PMID: 25960348

Citation

Acharya NK, Goldwaser EL, Forsberg MM, et al. Sevoflurane and Isoflurane induce structural changes in brain vascular endothelial cells and increase blood-brain barrier permeability: Possible link to postoperative delirium and cognitive decline. Brain Res. 2015; 1620:29-41.

Figure 1. ELG, NKA, GG, AS, MK, JD, CH, CJ, and CD helped to harvest, process, and image tissue from animals.

Figure 2. ELG, NKA, GG, AS, and CD helped to harvest, process, and image tissue from animals.

Figure 3. ELG, NKA, GG, AS, and CD helped in the making of this graph.

Figure 4. ELG, NKA, GG, AS, and CD helped to harvest, process, and image tissue with help from DA.

Figure 5. ELG, NKA, GG, AS, and CD helped to harvest, process, and image tissue with help from DA.

Figure 6. ELG, NKA, GG, AS, and CD helped to harvest, process, and image tissue with help from DA.

Figure 7. We wish to thank Amanda S. Almon, M.F.A. C.M.I. from the Department

of Art at the College of Communication and Creative Arts of Rowan University.

Chapter IV

Chronic diabetes mellitus and hypercholesterolemia disrupt retinal architecture and increase blood-retina barrier permeability

ABSTRACT

Diabetic retinopathy (DR) has been identified as one of the complications of diabetes mellitus (DM). Presently, with increased incidence of obesity, hypercholesterolemia (HC) has also become prevalent. For understanding the impact of DM and HC on cerebrovasculature our group has developed a swine model with DMHC. Using this model, we have demonstrated increased blood-brain barrier (BBB) permeability, selective binding of serum IgG to pyramidal neurons, and deposition of beta-amyloid$_{1-42}$ peptide in these neurons. Increased BBB permeability and associated secondary effects were alleviated by treatment with Darapladib (GlaxoSmithKline, SB480848), an inhibitor of lipoprotein-associated phospholipase A2 (LpPLA$_2$). Here, we have investigated the effect of DMHC on retinal architecture of these DMHC pigs by using histological and immunohistochemistry analyses on their retinal sections. Here, we report increased permeability of the blood-retinal barrier (BRB) with the following structural alterations in retinal architecture: increased leak of plasma components into retinal tissue, selective IgG binding to neurons in the ganglion cell layer, thinning of several retinal layers as a result of cell loss, and increased glial fibrillary acidic protein expression in Müller cells, all of which were curtailed by treatment with Darapladib. Based on these structural changes, we propose that chronic DMHC-induced structural changes in the retina impair BRB integrity and may lead to diabetic retinopathy. Drugs like Darapladib may prove to be useful for alleviating the impact of chronic DMHC on retina.

INTRODUCTION

Diabetic retinopathy is one of the early onsets, long-term complication of diabetes mellitus (DM) (Barber and Antonetti 2003, Cunha-Vaz, Faria de Abreu, and Campos 1975, Klein 2007, Leal et al. 2010). It is also regarded as a primary cause of partial or complete vision loss in these patients (Klein 2007, Yau et al. 2012). Yet, the reason for its onset and the development of its pathology in diabetic patients is still unknown. Earlier studies have demonstrated chronic extravasation of plasma components via a compromised blood-retinal barrier (BRB) in patients with DM and therefore DM has been implicated in the pathogenesis of diabetic retinopathy (Barber and Antonetti 2003, Cunha-Vaz, Faria de Abreu, and Campos 1975, Leal et al. 2010). Recently, we have reported increased blood-brain barrier (BBB) permeability in a porcine model with chronic DM and hypercholesterolemia (HC) (Acharya et al. 2013). This increased BBB permeability is morphologically demonstrated as perivascular leak clouds with selective binding of immunoglobulin G (IgG) to pyramidal neurons in the cerebral cortex along with increased intracellular deposition of the amyloid beta$_{1\text{-}42}$ (Aβ42) peptide in these neurons (Acharya et al. 2013). Upon treatment with Darapladib, a lipoprotein-associated phospholipase A2 inhibitor developed by GlaxoSmithKline to treat atherosclerosis, DMHC animals demonstrated a reduction in BBB permeability, IgG binding and Aβ42 deposition in the cortical pyramidal neurons (Acharya et al. 2013). Using retinal sections from the eyes of this animal model, we have sought to determine disruptive effect of chronic DMHC on the BRB. Similar to the BBB, the BRB is also a functional blood-tissue barrier in eye.

It consists of a monolayer of vascular endothelial cells tasked with restricting the movement of plasma components from the blood into the immune-privileged retina. Hence BRB closely resembles the BBB both structurally and functionally (Steuer et al. 2005).

In this animal model, we have observed a significant alteration in the thicknesses of three retinal layers possibly as a result of cell loss. The chronic state of DMHC also revealed an increased BRB permeability in DMHC pigs since there was a significantly higher incidence of IgG-positive cells within the retinal ganglion cell layer. Normally, the BRB tightly regulates and prevents blood components such as IgG from entering the retina. We also found a significant increase in the expression of glial fibrillary acidic protein (GFAP) by the Müller cells located in the retina of these DMHC pigs. Müller cells are the most abundant type of glial cells in retina (Chang et al. 2007). Increased GFAP expression by Müller cells has been widely used as a biomarker of glial cell activation, which usually occurs in response to injury/inflammation resulting from trauma, disease, or chemical insults (Eng, Ghirnikar, and Lee 2000). Thus, based on these data, we conclude that the chronic state of DMHC impairs BRB integrity. Upon treatment with Darapladib, the pigs with chronic DMHC, demonstrated significant reduction in BRB permeability along with normalization of retinal layer - thickness, number and architecture. These observations suggest the beneficial role of anti-inflammatory drugs like Darapladib in assuaging the chronic effect of DMHC on retina. Furthermore, usage of drugs like

Darapladib need to be further investigated as it has a potential application in the treatment of diabetic retinopathy.

EXPERIMENTAL PROCEDURE

Porcine model, tissue handling, and processing

Details of the DMHC porcine model have been reported previously (Acharya et al. 2013, Wilensky et al. 2008). Briefly, six month old male Yorkshire domestic farm pigs (~25-35 kg) were selected as the animal model for this study. DM was induced in these animals by injecting a single dose of 125 mg/kg Streptozotocin. After three days of DM induction, these animals were put on a hyperlipidemic diet. Throughout the course of the study, blood levels of glucose and cholesterol were closely monitored and maintained at 350-400 mg/dl and 400-800 mg/dl, respectively. One month after induction of DMHC, DMHC pigs were randomly separated into two groups: DMHC and Darapladib-DMHC. The Darapladib-DMHC group received an oral dose (10 mg $kg^{-1}day^{-1}$) of the Lp-PLA_2 inhibitor, Darapladib (SB480848, GlaxoSmithKline). Three of the Yorkshire domestic farm pigs of the same age and sex were refrained from DM induction and hyperlipidemic diet. This group of pigs was used as age-matched normal controls. Darapladib-DMHC pigs received Darapladib treatment for 24 weeks. At the end of treatment, animals from all three groups were euthanized. The eyes were quickly removed within 20 minutes of euthanizing and processed immediately. Animal use and experimental details of this study were approved by the IACUC of the University of Pennsylvania.

Determination of retinal thickness

The remarkably uniform and laminated histological architecture of the retina lends itself well to direct measurements of the thickness of the various layers as shown in figure 1. Using the image analysis software, ImagePro 7.0 (Media Cybernetics, Silver Spring, MD), we measured the thickness of all retinal layers. The thickness of each retinal layer was measured in three separate retinal sections obtained from each animal. In each section, measurements were made at two randomly selected locations in the middle part of retina to minimize regional variability. Results were averaged for each pig. The subject group identity of specimens was blinded and two independent investigators carried out this analysis. In addition, the percentage contribution of each retinal layer to the total thickness of the retina was calculated and compared among the different treatment groups.

Immunohistochemistry (IHC) and bright-field microscopy

Localization of IgG in the cerebral cortex and retina was carried out using IHC as described previously (Acharya et al. 2013, Nagele et al. 2011). Briefly, tissue sections were deparaffinized in xylene and rehydrated in decreasing concentrations of ethanol. The antigenicity of these tissues was enhanced by microwaving in citrate buffer. Sections were treated with 3% H_2O_2 for 10 minutes to quench endogenous peroxidase activity. Tissues were subsequently treated with blocking serum for 30 minutes at room temperature and then probed with anti-swine IgG antibody (Vector Laboratories, Inc, Catalogue # BA-9020; dilution 1:100) for an hour. Sections were then rinsed in PBS, treated with avidin-peroxidase complex (Vectastain ABC Elite kit, Vector Laboratories, Catalogue # PK-6100), washed with PBS, and visualized

with 3-3-diaminobenzidine-4-HCL (DAB)/ H_2O_2 (Imm-PACT-DAB) (Dako, Code K3468). Nuclei were lightly counterstained with hematoxylin. Lastly, tissues were dehydrated in increasing concentrations of ethanol, cleared in xylene and mounted in Permount (Fisher Scientific, USA). The specificity of the IgG antibodies was tested by treating tissue sections with blocking sera only as negative controls. Slides were examined and photographed with a Nikon FXA microscope, and digital images were recorded using a Nikon DXM1200F digital camera and analyzed using NIS-elements software (Nikon, Melville, NY). The evaluator was blinded as to subject group identity of the samples during image analysis.

Immunofluorescence microscopy and image analysis of the retina

Retinal sections were deparaffinized using xylene and rehydrated through a graded series of decreasing concentrations of ethanol. Antigen Unmasking Solution (Vector Laboratories) was used according to the manufacturer's instructions. Slides were then placed in 0.5% Triton X-100 in PBS for 5 minutes. After washing briefly with PBS, they were incubated overnight at 4˚C with rabbit anti-GFAP antibody (dilution 1:200, Sigma, Cat # G3893)**,** washed three times with PBS, and then incubated with Alexa Fluor 488 goat anti-rabbit secondary antibodies (dilution 1:200, Molecular Probes, Life Technology, USA) for 1 hour at room temperature. Sections were thoroughly washed in PBS and then mounted using Vectashield with DAPI (Vector Laboratories, USA). Negative controls were treated with non-immune serum or without primary antibody. Images were taken at 20X magnification on a Nikon Eclipse E800 microscope (Nikon, Melville, NY) equipped with a QImaging Retiga Exi (Qimaging

Burnham, Canada) digital camera. Cells positive for GFAP were counted throughout the thickness of the retina, and then quantified using ImagePro7.0 (Media Cybernetics, Silver Spring, MD). Briefly, a 300 x 300 pixel square area was randomly selected in each retinal section in three contiguous locations across the retina and the positive GFAP area was determined per total area using a fixed threshold. For total cell counts, sections were mounted in Vectashield with DAPI (Vector Laboratories). Cell number was determined by counting the DAPI-positive nuclei in a fixed area. The results of these measurements were then averaged for each section. The evaluator was blinded as to subject group identity of the samples during image analysis.

Using the image analysis software, ImagePro 7.0 (Media Cybernetics, Silver Spring, MD), the total number of IgG positive ganglion cells and total cells in GCL was counted. The percentage of the IgG labeled ganglion cells was then quantified out of total ganglion cells.

Statistics

The Student's *t* test with Welch's correction was used for calculating statistical significance. Variations within each treatment group were represented by either standard deviation or standard error.

RESULTS

In the chronic DMHC pig model, we have reported an increased BBB permeability which results in IgG binding to pyramidal neurons, amyloid deposition, and neurodegenerative changes resembling pathological features of early stage AD (Acharya et al. 2013). We further showed that these changes could be curtailed by treatment with Darapladib. In view of the well-established link between chronic DM and retinal pathology, particularly diabetic retinopathy, and the structural and functional similarities between BBB and BRB, we have investigated the effects of DMHC and Darapladib on the structure of the retina and BRB function in the same DMHC pig model.

Chronic DMHC altered the thickness of the individual retinal layers.

The thickness of individual layers of the retina was measured using Hematoxylin and Eosin stained transverse sections (Fig 1). Chronic DMHC (or Darapladib treatment) failed to demonstrate significant changes in the total thickness of the retina (Figs 1A-D). However, in DMHC pigs we have found a significant decrease in the thickness of several individual layers of retina, namely, ganglion cell layer (GCL), outer nuclear layer (ONL), and inner-segment (IS) / outer-segment (OS) photoreceptor layer compared to controls (Fig 1D-G). By contrast, the inner plexiform layer (IPL) in DMHC animals showed a significant increase in thickness and was more disorganized compared to controls (Fig 1H). This could be the reason for similar

total retinal thickness among treatment groups in spite of significant reduction in the GCL, ONL, and IS/OS thickness. The inner nuclear layer (INL) retained a comparable thickness across all treatment groups (Fig 1I). Most importantly, Darapladib treatment reversed the effects of DM and HC on the thickness of GCL, ONL, and IS/OS layers as their thickness in Darapladib-treated DMHC group was comparable to controls (Figs 1E-G). Darapladib treatment also lowered IPL thickness in DMHC animals to near control levels (Fig 1H).

DMHC reduced the number of cells in the GCL and INL.

The thickness of any given cellular layer in the retina is directly proportional to the number of cells comprising that layer. To determine the effects of chronic DMHC and Darapladib treatment on the cell number within the GCL and INL, we compared the numbers of cells in these layers by counting their nuclei (Figs 2). The state of chronic DMHC has made a significant reduction in the numbers of nuclei and therefore cells within the GCL and INL compared to controls (Figs 2D-E). On the other hand, the total number of cells in both GCL and INL were maintained at control levels under Darapladib treatment (Figs 2D-E).

IgG binds selectively to ganglion cells in the GCL.

In our previous study, looking at the effects of chronic DMHC on the cerebral cortex in these same pigs, we revealed a greater degree of intense IgG-positive staining in cortical pyramidal neurons. This staining demonstrated a compromised BBB (Acharya et al. 2013). In this retinal study, extravasated IgG was detected. Using anti-

pig IgG, retinal sections were immune-stained as previously described. Image analysis of these tissues revealed an increased presence of IgG-positive ganglion cells in the retina of DMHC pigs over controls. These ganglion cells exhibited both cytoplasmic and cell surface IgG labeling (Figs 3A-C). Cells in other retinal layers lacked detectable immuno-labeling with IgG. We calculated the percentage of IgG-positive ganglion cells relative to total ganglion cells in the GCL. Among the treatment groups, DMHC animals had the highest percentage of IgG-positive ganglion cells followed by controls and then the DMHC-Darapladib group (Fig 3D).

DMHC triggers gliosis in the retina.

We have also investigated the effect of chronic DMHC and Darapladib treatment on retinal glial cells. The expression of GFAP in retina was used to access the state of glial cells (Fig 4). GFAP expression was markedly increased in the DMHC retina compared to controls and Darapladib-treated DMHC pigs (Figs. 4A-D). In DMHC retina, GFAP-positive fluorescence extended from the inner- to the outer-limiting membranes, confirming that the observed GFAP expression was predominantly associated with Müller cells (Fig. 4B). The proximal and distal ends of Müller cells positioned within the GCL demonstrated the most intense GFAP expression in the DMHC group (Fig. 4B). However, GFAP immunoreactivity was reduced and confined to the GCL in both control and DMHC-Darapladib animals (Figs 4A-C). We also quantified the intensity of GFAP staining (Fig. 4D). An eight-fold increase in GFAP staining was observed in the DMHC group compared to controls. Darapladib treatment, although, significantly reduced GFAP expression in the Darapladib-treated

DMHC group compared to DMHC animals by nearly three-fold it was significantly elevated in DMHC-Darapladib pigs compared to controls (Fig. 4D).

FIGURES

Fig 1

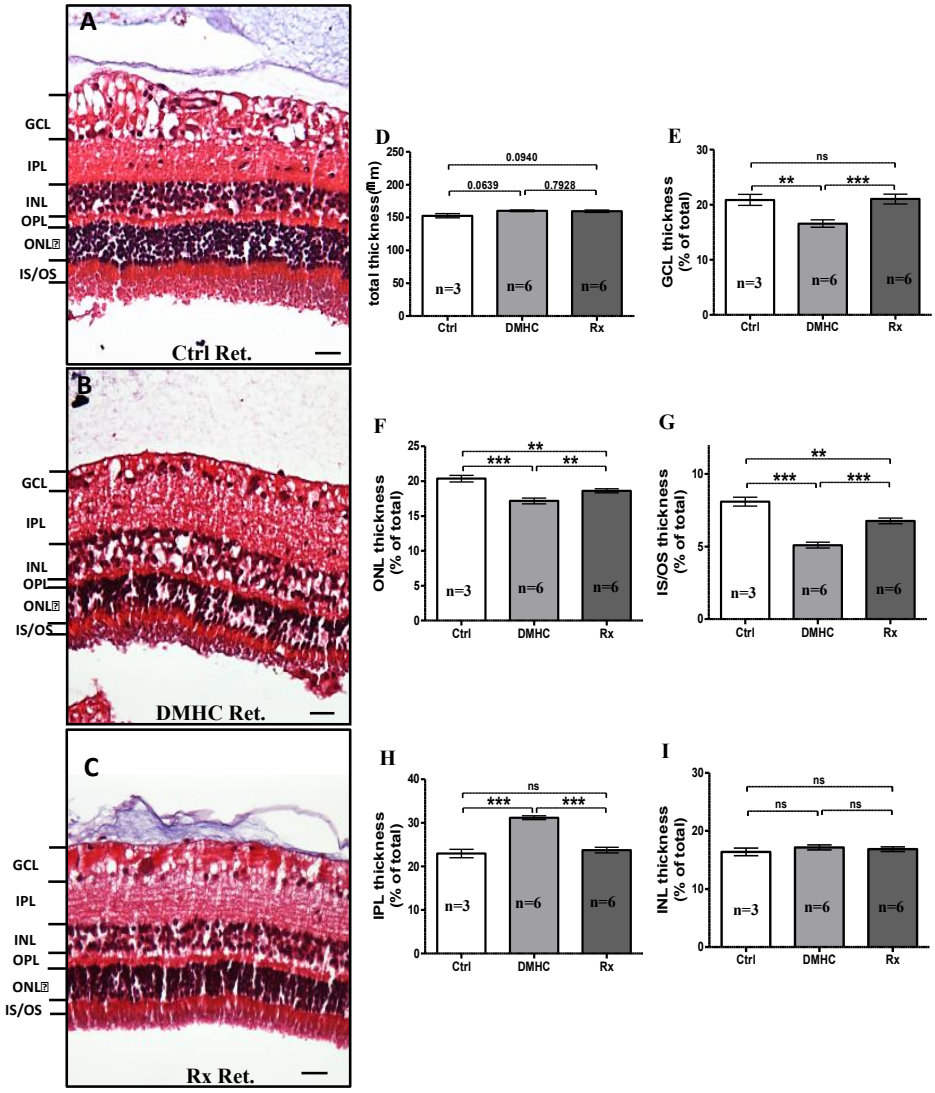

Figure 1: Chronic DMHC and Darapladib treatment modifies thickness of retinal layers.

The effect of DMHC induction and Darapladib treatment on the porcine retina (Ret.) was investigated by carrying out histological analyses of Hematoxylin-Eosin stained retinal sections from all treatment groups - control (Ctrl., A), DMHC (B) and Darapladib-treated DMHC (Rx, C). The thickness of total and individual retinal layers was quantified and the percentage of individual retinal layer thickness in relation to total retinal thickness was calculated and used for comparison. D – Total retinal thickness, E – ganglion cell layer percentage, F - Outer nuclear layer percentage, G - IS/OS – Inner and outer segments of photoreceptors percentage, H - Inner plexiform layer percentage, I - Inner nuclear layer percentage. Scale bar - 50 microns. ns = $p > 0.05$, ** = $p < 0.01$, *** = $p < 0.001$

Fig 2

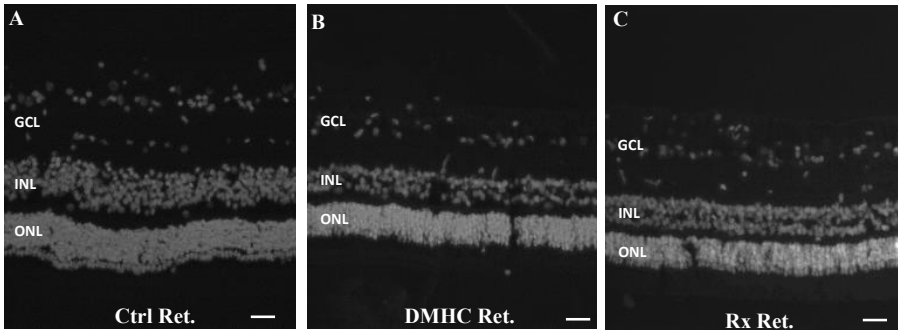
A
GCL
INL
ONL
Ctrl Ret.
B
GCL
INL
ONL
DMHC Ret.
C
GCL
INL
ONL
Rx Ret.

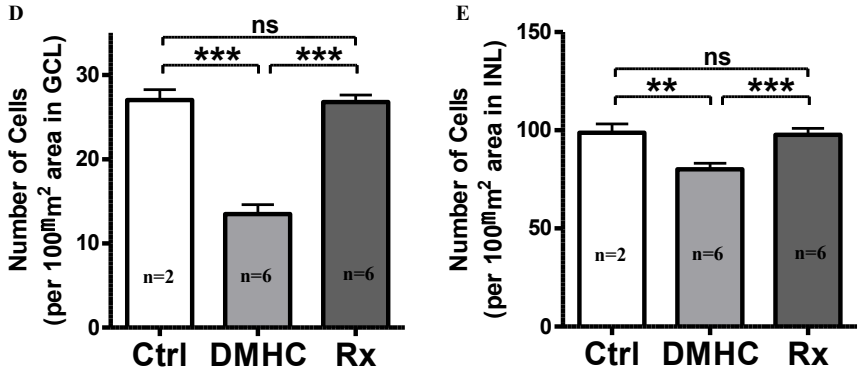
D
Number of Cells
(per 100μm² area in GCL)
ns
***
***
n=2
n=6
n=6
Ctrl
DMHC
Rx
E
Number of Cells
(per 100μm² area in INL)
ns
**
***
n=2
n=6
n=6
Ctrl
DMHC
Rx

Fig 2: DMHC-induced cell loss in the GCL and INL was reversed by Darapladib treatment. Retinal (Ret.) sections from pigs of all treatment groups were prepared with DAPI staining for histological assessment and nuclear count in the GCL and INL for control (Ctrl., **A**), DMHC (**B**) and Darapladib-treated DMHC (Rx, **C**). The number of cells in GCL (**D**) and INL (**E**) was quantified using image analysis. Scale bar - 50 microns, ns = $p > 0.05$, ** = $p < 0.01$, *** = $p < 0.001$

Fig 3

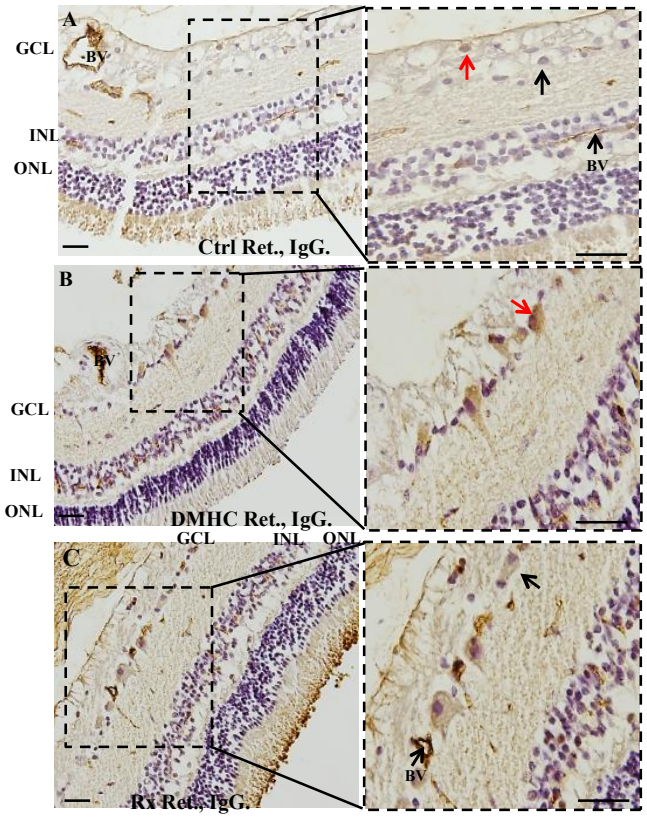
A
GCL
BV
INL
ONL
BV
Ctrl Ret., IgG.
B
BV
GCL
INL
ONL
DMHC Ret., IgG.
GCL
INL
ONL
C
BV
Rx Ret., IgG.

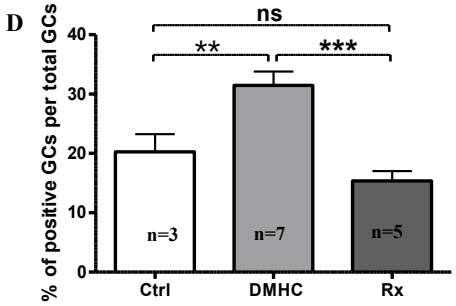
D
% of positive GCs per total GCs
40
30
20
10
0
ns
**
***
n=3
n=7
n=5
Ctrl
DMHC
Rx

Figure 3: DMHC pigs have the highest incidence of IgG-labeled ganglion cells. Retinal (Ret.) sections from pigs of control (Ctrl., A), DMHC (B) and Darapladib treatment (Rx, C) groups were probed with anti-swine IgG antibodies. DMHC pigs demonstrated the highest number of IgG labeled ganglion cells (red arrow). Ganglion cells in the other treatment groups failed to show similar extent of IgG labeling (black arrowhead) (D) The percentage of IgG labeled ganglion cells in the GCL for each treatment group was quantified using Image J software and IHC. Scale bar - 50 microns, ns = $p > 0.05$, ** = $p < 0.01$, *** = $p < 0.001$, BV = Blood vessel.

Fig 4

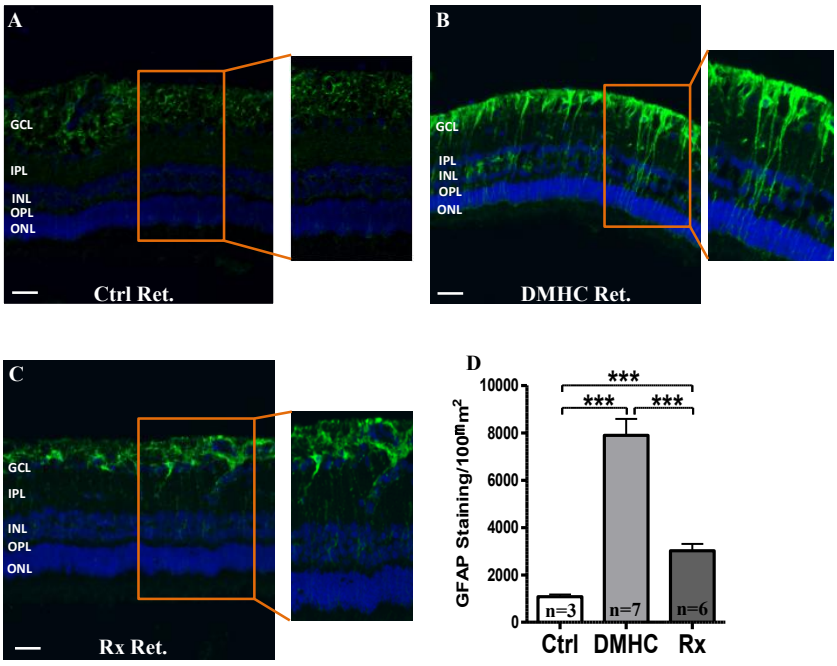
A
GCL
IPL
INL
OPL
ONL
Ctrl Ret.
B
GCL
IPL
INL
OPL
ONL
DMHC Ret.
C
GCL
IPL
INL
OPL
ONL
Rx Ret.
D
GFAP Staining/100μm²
10000
8000
6000
4000
2000
0
***
***
***
n=3
n=7
n=6
Ctrl
DMHC
Rx

Figure 4: DMHC induction and Darapladib treatment modify GFAP expression.

Retinal (Ret.) sections from control (Ctrl., A), DMHC (B) and Darapladib-treated pigs (Rx, C) were probed with anti-GFAP antibody to study its expression by Müller cells. Using ImagePro software and IHC, GFAP expression by pigs from all treatment groups (D) were quantified. GCL - Ganglion cell layer, IPL- Inner plexiform layer, INL - Inner nuclear layer, ONL - Outer nuclear layer, IS/OS – Inner and outer segments of photoreceptors, Scale bar - 50 microns, ns = $p > 0.05$, ** = $p < 0.01$, *** = $p < 0.001$

DISCUSSION

Diabetes mellitus (DM) and hypercholesterolemia (HC) are considered major risk factors for a number of diseases, including diabetic retinopathy and Alzheimer's disease (Barber and Antonetti 2003, Cunha-Vaz, Faria de Abreu, and Campos 1975, Klein 2007, Awad, Gagnon, and Messier 2004, Carlsson 2010, Moroz et al. 2008, Zambon et al. 2010). DM and HC often occur concurrently, and this close interrelationship has been linked to well-known deleterious effects on the vasculature, particularly in the elderly, some of which may have their origins in vascular inflammation (Carlsson 2010, Jiang et al. 2012, Luchsinger and Gustafson 2009, Moroz et al. 2008, Taguchi 2009). In support of this, an earlier study investigating mechanisms of atherosclerosis in a DMHC swine model revealed that Darapladib was capable of blocking the progression of arterial plaques to a higher-risk phenotype by reducing inflammatory macrophage infiltration (Wilensky et al. 2008). Subsequently, we reported increased BBB permeability, selective binding of IgG to cortical pyramidal neurons, and increased intraneuronal deposition of Aβ42 in the cerebral cortex in these same DMHC pigs (Acharya et al. 2013). In support of this claim, a recent placebo-controlled phase IIa study on the efficacy of Darapladib treatment on individuals suffering from diabetic macular edema demonstrated modest improvements in their vision and macular edema within three months of treatment (Staurenghi et al. 2015).

The above-mentioned effects of DMHC on the retina and cortical vasculature prompted us to further investigate its influence on the retina in these animals. In the present study, we observed an increase in the permeability of the BRB in the eyes. Pigs have many similarities in their metabolism and physiology to that of humans. Furthermore, their organs are large enough to be supported by vessels of comparable hierarchy as in humans. For this reason, pigs are an ideal animal model to study abnormalities associated with blood vasculature (Steuer et al. 2005). Also, unlike the rodent models, pigs are naturally vulnerable to atherosclerosis and DM, and can develop cardiovascular anomalies as in humans. Presently, both DM and cardiovascular diseases are reaching epidemic proportions in human population (Carlsson 2010, Matsuzaki et al. 2011, Ohara et al. 2011). During this study though we found that chronic DMHC did not cause changes in the overall thickness of the retina, it was associated with significant decreases in the thicknesses of the GCL, ONL, and IS/ OS layers compared to controls. On the other hand, the IPL demonstrated increased thickness compared to other treatment groups. In addition, image analysis revealed that thinning of the GCL and INL was associated with a reduction in number of cells populating these layers. On treatment with Darapladib, the thicknesses of the GCL, ONL, and IS/OS layers was normalized possibly due to inhibition of cell loss within these layers. Darapladib treatment also maintained IPL thickness comparable to controls.

Several studies carried out in patients and animal models with DM have reported an increased BRB permeability and altered tight junction protein expression in the retina

(Leal et al. 2010, Fan et al. 2014, Goncalves et al. 2012, Goncalves et al. 2014, Klaassen et al. 2009, Saker et al. 2014), corroborating our results. In the present study, a DMHC-associated BRB compromise was evidenced by the selective binding of IgG to ganglion cells within the GCL. IgG is normally excluded from the retinal interstitium and thus, as in the brain, can be used as an effective reporter molecule to identify sites of increased BRB permeability. The effects of chronic binding of IgG on ganglion cell functions are unknown. However, in our previous study that investigated the effects of chronic DMHC on the cerebral cortex in these same pigs, we demonstrated a selective and increased binding of IgG to neurons and intraneuronal Aβ42 peptide deposition in the regions exhibiting a compromised BBB (Acharya et al. 2013). In addition, in a separate study, binding of IgG to cortical pyramidal neurons dramatically increased the accumulation of soluble, exogenous Aβ42 peptide in adult mouse brain slice cultures (Nagele et al. 2011). These results strongly suggest that the influx of IgG into the brain and retina enables its binding to cell surfaces and promotes chronic endocytosis which, in the case of cortical pyramidal neurons, has been linked to intracellular Aβ42 deposition, a feature presumably contributing to AD pathogenesis and progression. In a similar manner, this binding of IgG to ganglion cells may interfere with the normal function of their cytoplasmic processes. Our data suggests a direct link between the influx of plasma components such as IgG into the retina and the reduced thickness and increased cell loss within individual retinal layers. The fact that Darapladib treatment not only curtailed IgG influx into retinal layers but also stabilized the thickness of retinal

layers and cell number further supports a causal link between plasma influx, inflammation, and degenerative changes.

DM has been associated with activation of Müller cells resulting in enhanced levels of GFAP expression in the retina (Barber, Antonetti, and Gardner 2000, Lewis et al. 1988, Mizutani, Gerhardinger, and Lorenzi 1998, Rungger-Brandle, Dosso, and Leuenberger 2000, Tuccari et al. 1986). To further validate the results obtained from the use of the DMHC porcine model, we also looked for any early and telltale signs of diabetic retinopathy such as gliosis (Barber, Antonetti, and Gardner 2000, Mizutani, Gerhardinger, and Lorenzi 1998, Rungger-Brandle, Dosso, and Leuenberger 2000, Tuccari et al. 1986). Increased GFAP expression is widely used as a reliable biomarker of glial cell activation that usually occurs in response to injury resulting from trauma, disease, inflammation or chemical insults (Eng, Ghirnikar, and Lee 2000). In this present study, chronic DMHC was found to enhance gliosis in the retina as evidenced by increased expression of GFAP by Müller cells. Two types of glial cells populate the mammalian retina: Müller cells and astrocytes (Chang et al. 2007). The cell bodies of Müller cells are positioned within the GCL, and their cytoplasmic processes extend to the inner and outer limiting membranes of the retina (Chang et al. 2007, Antonetti et al. 2006, Tuccari et al. 1986, Wilkinson-Berka 2004). Astrocytes however are less abundant in the retina and form a single layer in the GCL with close proximity to the inner limiting membrane (Antonetti et al. 2006, Lewis et al. 1988, Wilkinson-Berka 2004). Under normal, healthy conditions in the retina, GFAP is predominantly expressed by astrocytes, while Müller cells rarely express it

(Barber, Antonetti, and Gardner 2000, Rungger-Brandle, Dosso, and Leuenberger 2000). However, under conditions of DM or retinal injury as shown here, Müller cells become the dominant glial cell type expressing GFAP (Barber, Antonetti, and Gardner 2000, Mizutani, Gerhardinger, and Lorenzi 1998, Rungger-Brandle, Dosso, and Leuenberger 2000, Tuccari et al. 1986). This change hints at ongoing pathological changes resulting from inflammation, oxidation, or degeneration in the retina, possibly as a result of chronic DMHC (Fernandez-Robredo et al. 2005, Goncalves et al. 2014, Yucel et al. 2005). Notably, as the retinas of Darapladib-treated DMHC pigs demonstrated significantly lowered and limited expression of GFAP, it is clear that Darapladib treatment can play a beneficial role in inhibiting or alleviating DMHC-associated pathological changes in the retina.

The present study however has some limitations. First is the sample size in each treatment group. Having additional animals in each treatment groups would have definitely strengthened these observations. On that note, it is important to point out the high cost associated with usage of swine as an animal model. On the other hand, the data obtained from using pigs as our animal model allows us to draw more translational implications to human pathology and treatment, since pig's anatomy are closer to human compared to that of rodents. Additionally, pigs are also prone to naturally acquired DM and obesity. Another limitation is the age of the animals that were used in this study. By the time of euthanasia, the pigs used in the study were about 13 months old. Therefore, this age is not comparable to the phases of life afflicted with DM and AD typically seen in humans. The only reason for selection of

younger pigs is to avoid aging associated comorbid changes on the vasculature. Lastly, the accepted means by which DM is induced more resembles that of Type 1DM rather than Type 2. Obliteration of the β-cells of pancreas by injecting Streptozotocin makes this animal similar to Type 1 DM.

Conclusion and perspectives

DM and HC have become common comorbid conditions in the adult and elderly population (Fryar et al. 2010, Suh et al. 2010). Using a DMHC porcine model, we have reported increased BBB permeability and intraneuronal Aβ42 peptide deposition in the cerebral cortex (Acharya et al. 2013). These changes were reversed by treatment with the LpPLA2 inhibitor, Darapladib (Acharya et al. 2013). In the present study, we report increase in BRB permeability in the retinas of the same DMHC animals, as well as a curtailment of BRB compromise upon Darapladib treatment. In other words, similar effects from DMHC and Darapladib treatment were observed in two separate, but functionally similar blood-tissue barriers. This raises the possibility that detection of BRB compromise in the eye may be predictive of a similar compromise of the BBB in the brain, thus providing diagnostic utility. But, the effect of BRB permeability on retinal architecture and individual layers was poorly investigated. Fluorescein angiograms have been routinely used by ophthalmologists to access functional integrity of the BRB because of the ease and greater predictability for early diagnosis of diabetic retinopathy. Using this technique, BRB breakdown can be detected years ahead of clinical diagnosis of diabetic retinopathy (Cunha-Vaz, Faria de Abreu, and Campos 1975). Since BBB and BRB are

functionally similar, affected by similar stressors and are apparently compromised years prior to the onset of their respective diseases, BRB integrity may prove useful to gauge the overall health of the BBB in the brain. Thus, detecting aberrations in BRB function may help in pre-symptomatic diagnosis of various neurodegenerative diseases in which breakdown of the BBB is thought to be a key component, including Alzheimer's disease, Multiple Sclerosis, and Parkinson's disease. Additionally, our findings support the pursuit of therapeutic strategies aimed at fortifying BRB integrity. Since chronic DMHC leads to significant reductions in the thickness of some retinal layers as a result of cell loss, most notably involving the retinal ganglion cells exhibiting the highest level of IgG labeling. As in the IgG-mediated degenerative changes reported in the cerebral cortex of these animals (Acharya et al. 2013), we propose that chronic IgG binding to ganglion cells may facilitate their death and removal from the ganglion cell layer, and thereby favor the development diabetic retinopathy and/or aid in its progression. A similar scenario may be operating in other ocular deposition diseases, such as age-related macular degeneration (AMD). Since Darapladib has some anti-inflammatory properties and reduces BBB and BRB permeability under conditions of chronic DMHC, this drug may have the beneficial effect in preventing or slowing down progression of diabetic retinopathy and AMD.

REFERENCES

Acharya, N. K., E. C. Levin, P. M. Clifford, M. Han, R. Tourtellotte, D. Chamberlain, M. Pollaro, N. J. Coretti, M. C. Kosciuk, E. P. Nagele, C. Demarshall, T. Freeman, Y. Shi, C. Guan, C. H. Macphee, R. L. Wilensky, and R. G. Nagele. 2013. "Diabetes and hypercholesterolemia increase blood-brain barrier permeability and brain amyloid deposition: beneficial effects of the LpPLA2 inhibitor darapladib." *J Alzheimers Dis* 35 (1):179-98. doi: 10.3233/JAD-122254.

Antonetti, D. A., A. J. Barber, S. K. Bronson, W. M. Freeman, T. W. Gardner, L. S. Jefferson, M. Kester, S. R. Kimball, J. K. Krady, K. F. LaNoue, C. C. Norbury, P. G. Quinn, L. Sandirasegarane, I. A. Simpson, and Jdrf Diabetic Retinopathy Center Group. 2006. "Diabetic retinopathy: seeing beyond glucose-induced microvascular disease." *Diabetes* 55 (9):2401-11. doi: 10.2337/db05-1635.

Awad, N., M. Gagnon, and C. Messier. 2004. "The relationship between impaired glucose tolerance, type 2 diabetes, and cognitive function." *J Clin Exp Neuropsychol* 26 (8):1044-80. doi: 10.1080/13803390490514875.

Barber, A. J., and D. A. Antonetti. 2003. "Mapping the blood vessels with paracellular permeability in the retinas of diabetic rats." *Invest Ophthalmol Vis Sci* 44 (12):5410-6.

Barber, A. J., D. A. Antonetti, and T. W. Gardner. 2000. "Altered expression of retinal occludin and glial fibrillary acidic protein in experimental diabetes. The Penn State Retina Research Group." *Invest Ophthalmol Vis Sci* 41 (11):3561-8.

Carlsson, C. M. 2010. "Type 2 diabetes mellitus, dyslipidemia, and Alzheimer's disease." *J Alzheimers Dis* 20 (3):711-22. doi: 10.3233/JAD-2010-100012.

Chang, M. L., C. H. Wu, Y. F. Jiang-Shieh, J. Y. Shieh, and C. Y. Wen. 2007. "Reactive changes of retinal astrocytes and Muller glial cells in kainate-induced neuroexcitotoxicity." *J Anat* 210 (1):54-65. doi: 10.1111/j.1469-7580.2006.00671.x.

Cunha-Vaz, J., J. R. Faria de Abreu, and A. J. Campos. 1975. "Early breakdown of the blood-retinal barrier in diabetes." *Br J Ophthalmol* 59 (11):649-56.

Eng, L. F., R. S. Ghirnikar, and Y. L. Lee. 2000. "Glial fibrillary acidic protein: GFAP-thirty-one years (1969-2000)." *Neurochem Res* 25 (9-10):1439-51.

Fan, Y., K. Liu, Q. Wang, Y. Ruan, W. Ye, and Y. Zhang. 2014. "Exendin-4 alleviates retinal vascular leakage by protecting the blood-retinal barrier and reducing retinal vascular permeability in diabetic Goto-Kakizaki rats." *Exp Eye Res* 127:104-16. doi: 10.1016/j.exer.2014.05.004.

Fernandez-Robredo, P., D. Moya, J. A. Rodriguez, and A. Garcia-Layana. 2005. "Vitamins C and e reduce retinal oxidative stress and nitric oxide metabolites and prevent ultrastructural alterations in porcine hypercholesterolemia." *Invest Ophthalmol Vis Sci* 46 (4):1140-6. doi: 10.1167/iovs.04-0516.

Fryar, C. D., R. Hirsch, M. S. Eberhardt, S. S. Yoon, and J. D. Wright. 2010. "Hypertension, high serum total cholesterol, and diabetes: racial and ethnic prevalence differences in U.S. adults, 1999-2006." *NCHS Data Brief* (36):1-8.

Goncalves, A., E. Leal, A. Paiva, E. Teixeira Lemos, F. Teixeira, C. F. Ribeiro, F. Reis, A. F. Ambrosio, and R. Fernandes. 2012. "Protective effects of the dipeptidyl peptidase IV inhibitor sitagliptin in the blood-retinal barrier in a type 2 diabetes animal model." *Diabetes Obes Metab* 14 (5):454-63. doi: 10.1111/j.1463-1326.2011.01548.x.

Goncalves, A., C. Marques, E. Leal, C. F. Ribeiro, F. Reis, A. F. Ambrosio, and R. Fernandes. 2014. "Dipeptidyl peptidase-IV inhibition prevents blood-retinal barrier breakdown, inflammation and neuronal cell death in the retina of type 1 diabetic rats." *Biochim Biophys Acta* 1842 (9):1454-63. doi: 10.1016/j.bbadis.2014.04.013.

Jiang, X., M. Guo, J. Su, B. Lu, D. Ma, R. Zhang, L. Yang, Q. Wang, Y. Ma, and Y. Fan. 2012. "Simvastatin blocks blood-brain barrier disruptions induced by elevated cholesterol both in vivo and in vitro." *Int J Alzheimers Dis* 2012:109324. doi: 10.1155/2012/109324.

Klaassen, I., J. M. Hughes, I. M. Vogels, C. G. Schalkwijk, C. J. Van Noorden, and R. O. Schlingemann. 2009. "Altered expression of genes related to blood-retina barrier disruption in streptozotocin-induced diabetes." *Exp Eye Res* 89 (1):4-15. doi: 10.1016/j.exer.2009.01.006.

Klein, B. E. 2007. "Overview of epidemiologic studies of diabetic retinopathy." *Ophthalmic Epidemiol* 14 (4):179-83. doi: 10.1080/09286580701396720.

Leal, E. C., J. Martins, P. Voabil, J. Liberal, C. Chiavaroli, J. Bauer, J. Cunha-Vaz, and A. F. Ambrosio. 2010. "Calcium dobesilate inhibits the alterations in tight junction proteins and leukocyte adhesion to retinal endothelial cells induced by diabetes." *Diabetes* 59 (10):2637-45. doi: 10.2337/db09-1421.

Lewis, G. P., P. A. Erickson, D. D. Kaska, and S. K. Fisher. 1988. "An immunocytochemical comparison of Muller cells and astrocytes in the cat retina." *Exp Eye Res* 47 (6):839-53.

Luchsinger, J. A., and D. R. Gustafson. 2009. "Adiposity, type 2 diabetes, and Alzheimer's disease." *J Alzheimers Dis* 16 (4):693-704. doi: 10.3233/JAD-2009-1022.

Matsuzaki, T., K. Sasaki, J. Hata, Y. Hirakawa, K. Fujimi, T. Ninomiya, S. O. Suzuki, S. Kanba, Y. Kiyohara, and T. Iwaki. 2011. "Association of Alzheimer disease pathology with abnormal lipid metabolism: the Hisayama Study." *Neurology* 77 (11):1068-75. doi: 10.1212/WNL.0b013e31822e145d.

Mizutani, M., C. Gerhardinger, and M. Lorenzi. 1998. "Muller cell changes in human diabetic retinopathy." *Diabetes* 47 (3):445-9.

Moroz, N., M. Tong, L. Longato, H. Xu, and S. M. de la Monte. 2008. "Limited Alzheimer-type neurodegeneration in experimental obesity and type 2 diabetes mellitus." *J Alzheimers Dis* 15 (1):29-44.

Nagele, R. G., P. M. Clifford, G. Siu, E. C. Levin, N. K. Acharya, M. Han, M. C. Kosciuk, V. Venkataraman, S. Zavareh, S. Zarrabi, K. Kinsler, N. G. Thaker, E. P. Nagele, J. Dash, H. Y. Wang, and A. Levitas. 2011. "Brain-reactive autoantibodies prevalent in human sera increase intraneuronal amyloid-beta(1-42) deposition." *J Alzheimers Dis* 25 (4):605-22. doi: 10.3233/JAD-2011-110098.

Ohara, T., Y. Doi, T. Ninomiya, Y. Hirakawa, J. Hata, T. Iwaki, S. Kanba, and Y. Kiyohara. 2011. "Glucose tolerance status and risk of dementia in the community: the Hisayama study." *Neurology* 77 (12):1126-34. doi: 10.1212/WNL.0b013e31822f0435.

Rungger-Brandle, E., A. A. Dosso, and P. M. Leuenberger. 2000. "Glial reactivity, an early feature of diabetic retinopathy." *Invest Ophthalmol Vis Sci* 41 (7):1971-80.

Saker, S., E. A. Stewart, A. C. Browning, C. L. Allen, and W. M. Amoaku. 2014. "The effect of hyperglycaemia on permeability and the expression of junctional complex molecules in human retinal and choroidal endothelial cells." *Exp Eye Res* 121:161-7. doi: 10.1016/j.exer.2014.02.016.

Staurenghi, G., L. Ye, M. H. Magee, R. P. Danis, J. Wurzelmann, P. Adamson, M. M. McLaughlin, and D. M. E. Study Group Darapladib. 2015. "Darapladib, a lipoprotein-associated phospholipase A2 inhibitor, in diabetic macular edema:

a 3-month placebo-controlled study." *Ophthalmology* 122 (5):990-6. doi: 10.1016/j.ophtha.2014.12.014.

Steuer, H., A. Jaworski, B. Elger, M. Kaussmann, J. Keldenich, H. Schneider, D. Stoll, and B. Schlosshauer. 2005. "Functional characterization and comparison of the outer blood-retina barrier and the blood-brain barrier." *Invest Ophthalmol Vis Sci* 46 (3):1047-53. doi: 10.1167/iovs.04-0925.

Suh, D. C., I. S. Choi, C. Plauschinat, J. Kwon, and M. Baron. 2010. "Impact of comorbid conditions and race/ethnicity on glycemic control among the US population with type 2 diabetes, 1988-1994 to 1999-2004." *J Diabetes Complications* 24 (6):382-91. doi: 10.1016/j.jdiacomp.2009.07.001.

Taguchi, A. 2009. "Vascular factors in diabetes and Alzheimer's disease." *J Alzheimers Dis* 16 (4):859-64. doi: 10.3233/JAD-2009-0975.

Tuccari, G., C. Trombetta, M. M. Giardinelli, F. Arena, and G. Barresi. 1986. "Distribution of glial fibrillary acidic protein in normal and gliotic human retina." *Basic Appl Histochem* 30 (4):425-32.

Wilensky, R. L., Y. Shi, E. R. Mohler, 3rd, D. Hamamdzic, M. E. Burgert, J. Li, A. Postle, R. S. Fenning, J. G. Bollinger, B. E. Hoffman, D. J. Pelchovitz, J. Yang, R. C. Mirabile, C. L. Webb, L. Zhang, P. Zhang, M. H. Gelb, M. C. Walker, A. Zalewski, and C. H. Macphee. 2008. "Inhibition of lipoprotein-associated phospholipase A2 reduces complex coronary atherosclerotic plaque development." *Nat Med* 14 (10):1059-66. doi: 10.1038/nm.1870.

Wilkinson-Berka, J. L. 2004. "Diabetes and retinal vascular disorders: role of the renin-angiotensin system." *Expert Rev Mol Med* 6 (15):1-18. doi: 10.1017/S1462399404008129.

Yau, J. W., S. L. Rogers, R. Kawasaki, E. L. Lamoureux, J. W. Kowalski, T. Bek, S. J. Chen, J. M. Dekker, A. Fletcher, J. Grauslund, S. Haffner, R. F. Hamman, M. K. Ikram, T. Kayama, B. E. Klein, R. Klein, S. Krishnaiah, K. Mayurasakorn, J. P. O'Hare, T. J. Orchard, M. Porta, M. Rema, M. S. Roy, T. Sharma, J. Shaw, H. Taylor, J. M. Tielsch, R. Varma, J. J. Wang, N. Wang, S. West, L. Xu, M. Yasuda, X. Zhang, P. Mitchell, T. Y. Wong, and Group Meta-Analysis for Eye Disease Study. 2012. "Global prevalence and major risk factors of diabetic retinopathy." *Diabetes Care* 35 (3):556-64. doi: 10.2337/dc11-1909.

Yucel, I., Y. Akar, G. Yucel, M. A. Ciftcioglu, N. Keles, and M. Aslan. 2005. "Effect of hypercholesterolemia on inducible nitric oxide synthase expression in a rat model of elevated intraocular pressure." *Vision Res* 45 (9):1107-14. doi: 10.1016/j.visres.2004.11.018.

Zambon, D., M. Quintana, P. Mata, R. Alonso, J. Benavent, F. Cruz-Sanchez, J. Gich, M. Pocovi, F. Civeira, S. Capurro, D. Bachman, K. Sambamurti, J. Nicholas, and M. A. Pappolla. 2010. "Higher incidence of mild cognitive impairment in familial hypercholesterolemia." *Am J Med* 123 (3):267-74. doi: 10.1016/j.amjmed.2009.08.015.

ATTRIBUTIONS

Authors

Nimish K Acharya[1,3*], Xin Qi[4,8*], **Eric L Goldwaser[1,2]**, Hao Wu[2,5], Mary C. Kosciuk[1,3], Theresa Freeman[4], Colin H Macphee[6], Robert L Wilensky[7] and Robert G. Nagele[1,3]

Affiliations

[1]Biomarker Discovery Center, New Jersey Institute for Successful Aging, Rowan University School of Osteopathic Medicine, Stratford, NJ 08084, USA

[2]Graduate School of Biomedical Sciences, Rowan University, Stratford, NJ 08084, USA

[3]Department of Geriatrics and Gerontology, Rowan University School of Osteopathic Medicine, Stratford, NJ 08084, USA

[4]Thomas Jefferson University, 1025 Walnut Street, Philadelphia, Pennsylvania 19107, USA

[5]Department of Cell Biology, Rowan University School of Osteopathic Medicine, Stratford, NJ 08084

[6]GlaxoSmithKline, 709 Swedeland Road, King of Prussia, Pennsylvania 19406, USA

[7] Hospital of the University of Pennsylvania, 3400 Spruce Street, 9 Gates, Philadelphia, Pennsylvania 19104, USA

[8]Department of Ophthalmology, the Second Xiangya Hospital of Central South University, Changsha, Hunan, 410011, China

* Authors contributed equally to this project.

Sponsors

GlaxoSmithKline and Osteopathic Heritage Foundations

Financial disclosure

The authors declare competing financial interests: RGN and RLW are recipients of research grants from GlaxoSmithKline; RGN has filed a patent for use of Darapladib in the treatment of neurodegenerative diseases. CHM is an employee of GlaxoSmithKline, the manufacturer of Darapladib.

Short title

Diabetes and retinal architecture

Highlights

1. Chronic diabetes and hypercholesterolemia alters the thicknesses of retinal layers.
2. Diabetes and hypercholesterolemia causes cell loss in ganglion and inner nuclear layers.
3. Diabetes and hypercholesterolemia increases blood-retina barrier permeability and triggers plasma leak and retinal gliosis.
4. Plasma component such immunoglobulin (Ig) G binds specifically to retinal ganglion cells and induces retinal gliosis.

Keywords

Blood-retina barrier, blood-brain barrier, darapladib, lipoprotein-associated phospholipase-A_2 ($LpPLA_2$), diabetes mellitus, cholesterol, retina

Abbreviations

BBB - blood brain barrier, $LpPLA_2$ - lipoprotein-associated phospholipase-A_2, DM – Diabetes mellitus, HC – Hypercholesterolemia

Authors Contribution

RGN, NKA, XQ, TF and ELG conceived and designed the project. RLW and CHM developed, maintained and treated the DMHC pig model. NKA, XQ, ELG, HW, TF, MCK and RGN analyzed and interpreted all data. NKA, XQ, ELG and RGN wrote the manuscript. MCK, XQ, TF and NKA performed the histology and immunohistochemistry. NKA, XQ, and HW carried out the image analyses.

Figure 1. RLW and CHM developed, maintained and treated the DMHC pig model. ELG, NKA, XQ, TF, RGN helped to harvest, process, and image animal tissue for H&E staining. HW helped construct graphical representations of the data.

Figure 2. RLW and CHM developed, maintained and treated the DMHC pig model. ELG, NKA, XQ, TF, RGN helped to harvest, process, and image animal tissue for immunofluorescence staining. HW helped construct graphical representations of the data.

Figure 3. RLW and CHM developed, maintained and treated the DMHC pig model. ELG, NKA, XQ, TF, RGN helped to harvest, process, and image animal tissue for immunohistochemistry staining. HW helped construct graphical representations of the data.

Figure 4. RLW and CHM developed, maintained and treated the DMHC pig model. ELG, NKA, XQ, TF, RGN helped to harvest, process, and image animal tissue for immunofluorescence staining. HW helped construct graphical representations of the data.

Chapter V

Neuron-binding autoantibodies facilitate amyloid-β_{1-42} internalization and contribute to amyloid plaque formation in Alzheimer's disease pathogenesis

ABSTRACT

Aging related neurocognitive disorders such as Alzheimer's disease (AD) are poorly understood from a pathogenic or mechanistic standpoint. However, current literature is directing more attention to the cerebrovasculature that nourishes the brain, especially in the regions related to memory and higher-order cognition. Inherent in the brain vasculature is the blood-brain barrier (BBB), and perturbations in its functional integrity have been noted in aging and in AD, causing influx of plasma components like amyloid proteins and antibodies from the blood. In an effort to better elucidate the consequences of a breached BBB, human AD brain sections were stained with antibodies for amyloid-$\beta_{1\text{-}42}$ ($A\beta_{42}$), immunoglobulin (Ig) -M, -G, -E, and -A, neuronal surface receptors and proteins like GluR -2/3 and -6/7, α7nAChR, Glut1, and Map2. Detection of these proteins in perivascular leak clouds and within vesicles in neuronal and glial cells suggests that they are internalized by chronic endocytosis. This was further confirmed by documentation of the vast expansion of the lysosomal compartment using cathepsin D as a lysosome-specific biomarker. We show that $A\beta_{42}$ and neuron-binding autoantibodies can induce endocytosis independently, however their synergistic action within neurons is a novel hypothesis that can readily account for the observed dramatic increase in amyloid-burdened neurons that is typical for AD pathology. To test this novel hypothesis for $A\beta_{42}$ endocytosis, a cell culture model system was developed using a neuroblastoma cell line that can be stimulated to undergo a neuron-like differentiation in which they take on a number of characteristics of neurons typically found in vivo. These features exhibit a neuronal

morphology, which includes the extension of neurites (axon- and dendrite-like processes) and establish synaptic-appearing connections with neighboring cells. When differentiated cells were treated with physiologic concentrations of $A\beta_{42}$, the baseline levels of $A\beta_{42}$ internalization were measured at various time points over a period of 72 hours. We then examined the effects of serum from the following subjects on the rate and amount of $A\beta_{42}$ internalization: young-aged non-demented control, old-aged non-demented control, and old-age matched AD patient. Results showed that internalization of $A\beta_{42}$ was enhanced in all cases of serum supplementation, and the rate and extent was directly proportional to the neuron-binding capacity of autoantibodies present in each serum sample tested. Taken together, this work supports the idea that the presence of brain-reactive autoantibodies in the serum along with transient or chronic blood-brain barrier breakdown act synergistically to drive a key pathological feature of early-stage AD, that is, excessive intraneuronal accumulation of $A\beta_{42}$, which accelerates and propagates AD progression.

INTRODUCTION

Brain homeostasis can be affected in a number of ways that lead to gross anatomical, cellular, and molecular disturbances in the regions affected. Subsequent neurological, cognitive, and behavioral symptoms are manifest and constitute an array of diseases, including AD. Unfortunately, the mechanistic pathoetiology of AD that culminates in its hallmark features of cerebral amyloid plaque buildup and neuronal death is still disputed. Widely accepted amongst experts in the field, however, is the observation that AD is inextricably linked to aging. In fact, for every five year age bracket above 65, the prevalence of AD doubles, such that up to 50% of those currently 85 years and older have clinically diagnosed AD(Association 2015, Hebert et al. 2013).

Given the pervasiveness and attention that AD has received, coupled with a concerning lack of consensus over long-standing paradigms regarding AD's pathoetiology, a new look from a treatment standpoint may be warranted. In fact, disheartening and unforutnate estimates show a 99.6% failure rate for AD drugs in clinical trials(Cummings JL 2014). In light of this, the field as a whole is in desperate need of a breakthrough, and serious attention to novel potential drug targets may provide new opportunities for successful therapeutic intervention. One promising and accessible target that has thus far received little attention is the brain vasculature, including the blood-brain barrier (BBB).

Cerebrovascular disease is a general term most often used to describe the consequences of an unhealthy and abnormally functioning brain vasculature. Typically, during the transit of blood through the brain vasculature, what leaves the blood and enters into the brain parenchyma is stringently regulated by the BBB, with a relatively small subset of biomolecules being exchanged between brain cells and blood via specialized receptors and transporters (Snyder et al. 2015, Zlokovic 2011). This helps to maintain overall brain homeostasis as well as electrochemical balances that are crucial for normal functioning of neuronal circuitry. Failure to properly control or regulate this exchange, as in instances of local vascular inflammation, atherosclerosis, hemorrhages, or infarctions can lead to an indiscriminant leakage of blood components, including a diverse array of proteins, metabolic byproducts, and sometimes pathogens, into the brain tissue. The BBB is tasked with carefully regulating which blood components enter into the immunoprivileged brain tissue (Abbott et al. 2010, Zlokovic 2008). As in AD, there is a rapidly growing body of evidence implicating a dysfunctional BBB as responsible, at least in part, for many conditions, including epilepsy, multiple sclerosis, Parkinson's disease, depression, and schizophrenia (Sui et al. 2014, Michalak et al. 2012, Dahm et al. 2014, Hammer et al. 2014, Ortiz et al. 2014, Patel and Frey 2015).

Previous research efforts have been dedicated to characterizing the pathway of how extracellular amyloid-$\beta_{1\text{-}42}$ ($A\beta_{42}$), the 42 amino acid product of amyloid precursor protein cleavage and major pathological component of amyloid plaques (APs), enters the neuron as well as elucidating its fate once inside. Curiously, the AD pathology is

often localized in the early stages to regions of the brain associated with learning and memory formation, structures housed in the hippocampus, entorhinal cortex, and other surrounding cortical areas. Treatments had previously been directed towards enhancing cholinergic systems, as AD has been shown to primarily affect these areas. In support of this preference, Wang and colleagues showed that $A\beta_{42}$ binds with greatest affinity to the α7 subtype of nicotinic acetylcholine receptors (α7nAChR) on the neuronal surfaces (Wang et al. 2000). His later work with Nagele and colleagues demonstrated that when α7nAChR-transfected neuroblastoma cells are incubated with human $A\beta_{42}$, they subsequently internalize the receptor-$A\beta_{42}$ complex and begin accumulating insoluble $A\beta_{42}$ (Nagele et al. 2002). Nearly a decade later the role of effects of serum on these neurons was tested in mouse brain organotypic cultures, and it was shown that serum in conjunction with $A\beta_{42}$ has a synergistic effect on increasing the internalization and accumulation of insoluble, non-degradable, fibrillized amyloid aggregates (Nagele, Clifford, et al. 2011).

Synaptic degeneration and APs are well-known to riddle the brain of an Alzheimer's patient on autopsy, and their extent and number is inversely proportional to the number of surviving neurons present (D'Andrea 2001). The origin and pathogenesis of amyloid plaques is highly contested amongst leaders in the field. Previous work has shown the presence of extravasated plasma components such as immunoglobulin (Ig) G and $A\beta_{42}$ in the cerebral cortex and other brain regions implicated in AD (Nagele et al. 2013, Nagele, Clifford, et al. 2011). IgG and $A\beta_{42}$ are found ubiquitously in the blood, and are readily detected and observed emanating radially

from leaky blood vessels in the brain and binding to neurons in their vicinity (Clifford et al. 2007, D'Andrea 2001). Taken together, these observations suggest that the amyloid plaques are derived from the lysis of neurons, which had accumulated $A\beta_{42}$ as it escaped from the general circulation and entered into the brain via a defective blood-brain barrier. Like the binding of Ig to a surface protein, $A\beta_{42}$ binding to the surface of a neuron can induce endocytosis as well. By coupling these two events together, synergistic endocytic effects may occur, and thereby over-burden neurons exposed to both blood components, $A\beta_{42}$ and IgG. Once within the brain parenchyma, these proteins selectively bind to similar, often identical, neurons, distributed throughout the brain, but especially in regions of AD pathology (Nagele, Clifford, et al. 2011).

Both events (that is, $A\beta_{42}$ or Ig binding to neurons) independently may lead to neuronal endocytosis of extracellular amyloid, however the mechanism by which this occurs when coupled together remains to be deciphered, and could shed light on an important mechanisms relating to the pathogenesis of AD, with far-reaching implications. To the extent that AD has been described, the mechanism of AP formation remains unresolved despite their presence being strongly correlated with synaptic degeneration and the eventual disease phenotype. The overall goal of this study is to elucidate the pathogenic consequences at the cellular level that are driven by a compromised cerebrovasculature, particularly the events leading to neuronal dysfunction and death, and AP formation and development.

Here, we present data that links the observations on human brain AD sections to a cell culture model that assesses the consequence of BBB compromise. Upon leakage of soluble blood proteins like Ig and $A\beta_{42}$ into the brain parenchyma, we demonstrate their labeling of neuronal surface proteins as well as APs. The presence of neuron-binding antibodies (i.e. autoantibodies; aAbs) in the blood that can bind to neurons provides a route by which $A\beta_{42}$ can enter the neuron via chronic endocytosis, leading to their entry into the lysosomal complex, where it is fibrillized and thus rendered insoluble and non-degradable, as is seen on AD brain autopsy. This process is not unique to IgG, the most robust and abundant of the immunoglobulins found in the blood, and was shown to occur in other subtypes as well, including Ig -M, -E, and -A. The localization of immunoglobulins within intracellular vesicles along with other neuronal surface proteins suggests that the neuron also internalizes various surface receptor proteins that are bound to neuron-binding aAbs, likely as a removal process that clears cross-linked (and now nonfunctional) proteins from the surface.

We propose that neuron-binding aAbs can trigger antibody (or rather, aAb)-mediated endocytosis, and that $A\beta_{42}$ bound to cell surfaces can enter the cell passively this way, furthering neuronal damage and homeostatic imbalances. Lysosomal compartment expansion would confirm this novel hypothesis. To explore this model, SH-SY5Y cells were used as a cell culture model system. Upon induction of neuronal differentiation, these cells were able to react to aAbs present in the blood of human samples irrespective of age or the presence of disease in these subjects. Coincident with this binding, $A\beta_{42}$ entry and accumulation in these cells was enhanced. A more

precise mechanism of aAb-mediated endocytosis will be needed to elucidate the inner workings of this process, however the far-reaching impact of such a discovery warrants much attention as a means by which extracellular $A\beta_{42}$ accumulates in neurons and facilitates AP formation in the context of AD. Furthermore, these results provide validation for new line of therapeutics aimed primarily at addressing the functionality of a BBB, as the compromised BBB is a pre-requisite factor that initiates the downstream events discussed here.

EXPERIMENTAL PROCEDURE

Human brain sections

Standardized protocol was followed for immunohistochemistry (IHC) experiments and techniques related to its procedure, as previously established (Nagele, Clifford, et al. 2011). In brief, paraffin-embedded human tissues were deparaffinized using xylene and rehydrated through a graded series of decreasing concentrations of ethanol. Antigenicity was then enhanced by microwaving sections in citrate buffer. Endogenous peroxidase was quenched by treating sections with 0.3% H_2O_2 for 30 minutes. Sections were incubated in blocking serum and then treated with primary antibodies at appropriate dilutions for one hour at room temperature. To detect endogenous IgG (and other Ig classes), biotinylated anti-human IgG was used as the primary antibody, and a traditional secondary antibody treatment is foregone. After a thorough rinse in PBS, biotin-labeled secondary antibody was applied for 30 minutes. Sections were treated with avidin-peroxidase complex and visualized with DAB. Sections were lightly counterstained with hematoxylin, dehydrated through increasing concentrations of ethanol, cleared in xylene, and mounted in Permount. Controls consist of brain sections treated with non-immune serum or omission of the primary antibody. Specimens were examined and photographed with a Nikon FXA microscope, and digital images were analyzed using NIS-Elements Imaging Software (Nikon Instruments Inc. USA).

Cell culture experiments

For immunocytochemistry experiments, and aAb and amyloid binding and internalization experiments, SH-SY5Y cells were used. They are an established cell line that can be grown in 10% Fetal Bovine Serum (FBS) in Dulbecco's Minimal Essential Medium (DMEM)/F12 media. Complete media was changed every three days, and cells were split weekly at 80% confluence. These cells can be differentiated after being split into 35mm glass-bottom dishes once they have achieved 60% confluence using 10μM retinoic acid and 0.2% FBS in DMEM/F12 media. Upon differentiation for three days, cells begin to sprout neuron-like processes and establish connections with neurons in the vicinity, at roughly 70% confluence. At this point, they can be assayed using standard immunocytochemistry protocols previously described for neuronal markers of differentiation and surface proteins (Nagele et al. 2002).

In brief, cultures were washed in cation-free Hanks Buffered Salt Solution (HBSS) (without calcium or magnesium) three times, and then fixed in 4% paraformaldehyde (PFA). If the cell surface membrane was to be stripped for internalization assays, three acid washes (0.1M Glycine, pH 2.5) of two minutes each were performed at this point, followed by two more HBSS washes to remove any residual acid prior to fixation. Some cultures were treated with 100nM fluorescein isothiocyanate (FITC)-labeled $A\beta_{42}$ (physiologic concentration) for time points ranging from 30 minutes to 72 hours. Other dishes were treated with $A\beta_{42}$ and human serum obtained from young-aged non-demented control (YC), old-aged non-demented control (OC), and Alzheimer's disease patient blood (AD) at 1:50 dilutions in serum-free media. After

fixation, cells were blocked in 3% BSA (in PBS-T or PBS depending on the assay being performed) and then probed with primary antibody overnight at 4°C or secondary antibodies for one hour at room temperature covered from the light. For human serum containing IgG, anti-human IgG (Sigma laboratories) conjugated to an Alexa-fluor 594 fluorophore was used, in contrast to the FITC-labeled $A\beta_{42}$. Nuclei were counterstained with Hoechst. Nikon Confocal microscopy equipped with epifluorescence was used to capture images and NIS-Elements software to perform image analysis and quantification of signal intensities.

Analysis

Immunohistochemistry experiments of human brain tissue were used for qualitative and observational purposes only. Unpublished work was performed, however, measuring the extent and size of lysosomal vesicles and overall compartment space as a proportion of the neuron using a macros program written for ImageJ software (Rasband 1997-2015). For immunocytochemistry experiments, images captured using Nikon Confocal microscopy NIS-Elements software was used to outline cells manually as a "Region of Interest" (ROI). Approximately ten random images were taken per experiment (i.e. individual dish), and only fully enclosed cells within the 60x field were outlined. Each experiment had roughly counted 80 cells, and then the software was able to determine the fluorescence signal intensity within the ROI, making sure not to include saturating amounts of signal during the establishment of image parameter acquisition. After exporting this data to excel, the summed signal intensity for the FITC (green) channel ($A\beta_{42}$ was FITC-labeled) was divided by the

pixel count (area) of the ROI to determine the signal intensity (FITC-$A\beta_{42}$) per unit area (cell). The summed fluorescence intensity is the most well recognized surrogate measurement used to establish relative protein amount. By stripping the surface membrane off the cells using established protocol (0.1M Glycine acid wash), all signal intensity retrieved therefore represented internalized FITC-$A\beta_{42}$ protein. For experiments aimed at addressing surface bound proteins, no such acid wash was performed, nor was any detergents used throughout the immunocytochemistry procedure.

Statistics

Experiments were done in triplicate and blinded, so as to limit bias and improve reproducibility. Once data was compiled, graphical representations were constructed using a two-tailed Student's *t*-test, and a p-value < 0.05 was considered statistically significant: *, $p<0.05$; **, $p<0.01$; ***, $p<0.001$). Variation within each treatment group was represented by standard deviations of the mean (SEM). Acquisition parameters were determined by the user at the beginning of each experiment and were kept identical for all other images of a given experiment.

RESULTS

A compromised BBB allows an influx of $A\beta_{42}$ peptide into the brain parenchyma, which subsequently binds to pyramidal neurons prior to lysis and amyloid plaque formation in AD brains.

Alzheimer's disease (AD) brain sections show pathologic changes suggesting cerebrovascular and blood-brain barrier (BBB) dysfunction prior to amyloid plaque formation. $A\beta_{42}$ is often observed extravasating from a leaky BBB, subsequently binding to the surfaces of pyramidal neurons, followed by internalization in these cells in AD brains (fig. 1). Cortical amyloid plaques, with the characteristic dense core, are visualized using antibodies to amyloid-$\beta_{1\text{-}42}$ ($A\beta_{42}$) and are a hallmark feature of AD brains on autopsy (fig. 1A). Intraneuronal $A\beta_{42}$ is also seen in neurons apparently on the verge of lysis, which then contributes to amyloid plaque's growth and development. Sections through the microvasculature within the AD brain cortex often reveal the presence of leak clouds, representing sites of plasma leak into the brain parenchyma. Commonly, $A\beta_{42}$ is observed bound to the surfaces of neurons in the vicinity of these damaged blood vessel (fig. 1B-C). Soluble, $A\beta_{42}$ can be detected as a perivascular leak cloud, emanating radially from the point of damage along the BBB of the vessel. Furthermore, some neurons in the vicinity of these leaks exhibit intracellular $A\beta_{42}$ loading. The negative control shows the minimal background noise of the antibody stain used (fig. 1D). Lastly, sections of cerebral cortex from age-matched non-demented control brains stained with antibody to $A\beta_{42}$ often shows the nuclear/peri-nuclear localization of the protein, with little intracellular deposits as

seen in AD brains (fig. 1E). Moreover, a scarcity of amyloid plaques in control brains is also found in these sections.

Immunoglobulins -M, -A, -G, and -E leak out of a damaged BBB and demonstrate neuron- and glia-binding capabilities.

The presence of neuron-binding autoantibodies (aAbs) in the serum is now widely recognized across many fields of neuroscience, and their presence in AD serum has been gaining attention as well. We next asked which classes of immunoglobulin are able to leak into the brain parenchyma from brain blood vessels upon BBB functional compromise in the cerebral cortex of AD patients (fig. 2). The consequence of an antibody binding to the surface of a cell and inducing endocytosis is not novel; however, in this context it does give rise to a completely new mechanism of how $A\beta_{42}$ may enter the neuron that fits well with the hypothesis proposed here. We used appropriate and specific secondary antibodies to probe sections of human brain to detect the presence of the following Igs in the brain parenchyma (extravascular brain tissue): IgM, IgA, IgG, IgE (figs 2A-D).

Endogenous Ig immunoreactivity varied in these brain sections, with IgM reactivity primarily in glia/astrocytes and IgG, IgA, and IgE mostly associated with neurons. Pan Ig, which reacts to IgM, IgA, and IgG simultaneously, generated the most heavily labeled perivascular leak clouds, as expected, compared to the other individual immunoglobulin types. Negative control sections revealed minimal background noise when no secondary antibody was added. These findings confirm that all Ig species

present in the serum readily penetrate the compromised BBB and thereby gain access to the brain parenchyma, and that each Ig type can be detected within leak clouds that are morphologically comparable to those revealed by $A\beta_{42}$ immunostaining. Interestingly, the fact that neurons and glia both bind Ig, but show differential binding, suggest that each of these cell types has its own unique surface antigens that are immunoreactive to blood-borne, brain-reactive aAbs. Furthermore, we show intracellularly localized deposits of Ig as well as the presence of Igs within amyloid plaques (fig. 2B-C) strongly suggesting that these aAbs accumulate gradually within neurons and are later released along with accumulated, fibrillized $A\beta_{42}$ and other cellular proteins upon neuronal lysis.

Lysosomal compartment expansion in AD brains reflects chronic endocytosis of indigestible $A\beta_{42}$.

An expectation is that chronic internalization and accumulation of $A\beta_{42}$ should result in a pronounced expansion of the lysosomal compartment. To test for this in human AD brain, we used cathepsin D (CathD), an enzyme confined to the lysosomal compartment, as a biomarker for lysosomes. IHC with cathepsin D-specific antibody revealed a vast expansion of the lysosomal compartment in neurons in regions of AD-pathology, clearly reflecting the accumulation of indigestible $A\beta_{42}$ aggregates as they are trafficked through endocytosis to their final site of deposition within lysosomes (fig. 3). In neurons in the AD brain cerebral cortex, CathD was localized to the neuronal perikaryon (fig. 3A). Higher magnification images of pyramidal neurons in the cortex of an AD brain, the cells known to be most vulnerable to excessive $A\beta_{42}$

accumulation and cell death, show the vast expansion of the lysosomal compartment located in the perinuclear region, often displacing the nucleus within the cell body. In favorable sections and tissues showing good preservation, individual lysosomal vesicles can sometimes be seen aggregating in the proximal segments of major dendritic trunks extending from the cell body, reflecting an over-burdened waste disposal pathway, and encroachment on the limited space capacity of the neuron cytoplasm. When cells were tested for the presence of other surface receptors, the lysosomal compartment is similarly seen having undergone expansive changes, likely reflecting the chronic endocytic events occurring to these proteins as well (fig 3B). One example of such a surface protein is the α7nAChR which, in IHC preparations, is seen to also accumulate in the perinuclear region and to co-localize within the lysosomal compartment as well, apparently reflecting the consequence of its rampant endocytosis.

Figure 3C shows a consecutive histological section stained for a ubiquitous surface protein (α7nAChR; top) and lysosome (CathD; bottom) to visualize similar staining in the vicinity of a blood vessel, perhaps alluding to a leak phenomenon occurring, resulting in endocytosis of plasma components. In consecutive sections stained for a ubiquitous surface protein as well as CathD, the similar localizations suggest a coalescence of the surface protein within the lysosomal compartment (fig. 3C), likely reflecting the destination of the endocytic route by which surface proteins are internalized with the cellular intent of degradation. In age-matched, non-demented control brains, CathD immunostaining reveals the expected vesicular structures that

account for baseline levels of lysosomal functionality occurring through normal protein turnover and aging (fig. 3D). Note that in CathD staining of control brain slices, the lysosomal compartments of neurons are more evenly dispersed in the cell body, and vesicles are not accumulated or coalesced (packed) to the extent seen in these same cells in AD brains. Within the lysosomal compartment, $A\beta_{42}$ is believed to self-assemble into non-degradable fibrils, accumulating in the cell body and encroaching on the entrance into axonal processes as it grows in mass. These images further support the idea that, upon chronic endocytosis of exogenously supplied $A\beta_{42}$ (that is from the periphery through a compromised BBB) and aAb binding (which induces endocytosis), the affected neuron undergoes vast lysosomal expansion in an attempt to likely rid the cell surface of bound protein.

The presence of internalized neuronal surface proteins supports a global "receptor-stripping" phenomenon as a consequence of aAb and $A\beta_{42}$ binding and endocytosis.

We next asked if the chronic induction of endocytosis via aAb binding also causes the internalization of other cell surface proteins as passive passengers, a phenomenon we have called "receptor-stripping". To resolve this, we used IHC and commercially available antibodies specific for several well-known and abundant neuronal cell surface proteins. Internalized distributions of several surface receptors were seen within neurons in the brain of AD patients. Neuronal cell surface markers such as glutamate receptors GluR2/3 (fig. 4A) and GluR6/7 (fig. 4B), α7nAChR (fig. 4C), and glucose transporter Glut1 (fig. 4D) were detected and imaged to determine their cellular distribution, along with another abundant intracellular neuronal protein,

Map2 (fig. 4E). Results show clearly that many of these neuronal cell surface proteins are detectable within the lysosomal complex, suggesting that chronic $A\beta_{42}$ and aAb binding to the surface may secondarily cause an equally devastating effect of the functional integrity of the neuronal cell surface caused by global "receptor stripping". The Map2 stain however, being an intracellular protein used as a marker of neuronal differentiation, is observed undergoing retrograde vesicular traffic back towards the cell body, presumably from degenerative synaptic changes and dendritic collapse as a result of similar events.

Differentiated cells in culture, unlike their non-differentiated counterparts, exhibit aAb reactivity to human serum, as well as increased $A\beta_{42}$ internalization over time.

A cell culture model system was established to test the hypothesis that $A\beta_{42}$ internalization is enhanced in local neurons following BBB breakdown. In an attempt to recapitulate in vivo conditions, SH-SY5Y neuroblastoma cells were induced to differentiate using retinoic acid, a response highlighted by a change in cell shape more resembling neurons and the extension of axon- and dendrite-like cellular processes. Interestingly, the non-differentiated cells did not display significant aAb reactivity compared to the differentiated ones (fig. 5). Representative micrographs accurately reflecting this observation are shown (fig. 5A), which includes bright field images of live cells in culture (top panels) and fixed cells treated with human serum (bottom panels). Cells in the non-differentiated dish (left) contrasted with those in the differentiated dish (right) in many of the markers used to distinguish successfully differentiated cell types. The differentiated cells contain axonal processes that

interact with processes of adjacent cells (exhibiting synaptic-like formations), as well as a flattened and small cell body compared to the rest of the elongated cell morphology. Figure 5B shows the amount of aAb reactivity as a function of fluorescence intensity, confirming that differentiated cells contain the appropriate cognate receptor targeted by aAbs present in human serum. Serum samples tested were from young-aged non-demented control (YC), old-aged non-demented control (OC), and old-aged matched Alzheimer's disease patient.

Next, differentiated and non-differentiated cells were assayed for baseline $A\beta_{42}$ internalization over time. From previous results, 3 hours was enough time to observe measureable changes in $A\beta_{42}$ internalization. Representative micrographs showing cells at each time point revealed that differentiated cells, like their non-differentiated counterparts, exhibited internalized $A\beta_{42}$, and the extent of $A\beta_4$ accumulation was directly proportional to the time elapsed (fig. 6A). Quantitative assessments of $A\beta_{42}$ accumulation under these conditions support what is shown in the images, and furthermore indicates that that the model system being used displays $A\beta_{42}$ and aAb binding, similar to the results obtained in human AD brain, and that both of these events independently induce endocytosis.

$A\beta_{42}$ internalization is enhanced in the presence of serum containing neuron-binding aAbs directed at neuronal surface proteins.

$A\beta_{42}$ internalization was enhanced when co-administered with human serum containing autoantibodies that target neuronal surface proteins. When differentiated

SH-SY5Y cells were treated in culture with physiologic $A\beta_{42}$ concentrations in the presence of human serum, the extent of amyloid burdening was enhanced over time (fig. 7A). Cells were first induced to differentiate as described above, treated for 3- to 72-hrs with 100nM fluorescein isothiocyanate (FITC)-labeled $A\beta_{42,}$ and then assayed to determine the relative amount of internalized $A\beta_{42}$. Figure 7 shows the internalized $A\beta_{42}$ in these cells over the time points, as graphed according to signal intensity of the FITC channel ($A\beta_{42}$). Quantification of baseline $A\beta_{42}$ internalization (left) and the effects of co-treatment with human serum containing neuron-reactive aAbs (right) are shown. (B) Irrespective of age or disease state, serum obtained from young control (YC), old control (OC), or Alzheimer's disease (AD) patients demonstrate an enhancement of $A\beta_{42}$ internalization. When IgG was purified, which contains antibody and aAb fractions, from AD serum and treated similarly, there was no significant difference in the enhanced extent of $A\beta_{42}$ internalization. These results indicate that internalization of $A\beta_{42}$ was enhanced when co-administered with serum containing neuron-binding aAbs, and that these aAbs are in fact the causative agents. Indeed, these findings suggest that upon BBB breakdown, $A\beta_{42}$ and aAbs leak into the brain parenchyma, both of which induce endocytosis, however the extent is greater in the presence of aAbs.

FIGURES

Fig 1. $A\beta_{42}$ extravasation from a leaky BBB subsequently binds pyramidal neurons and undergoes internalization, and is enhanced in AD brains.

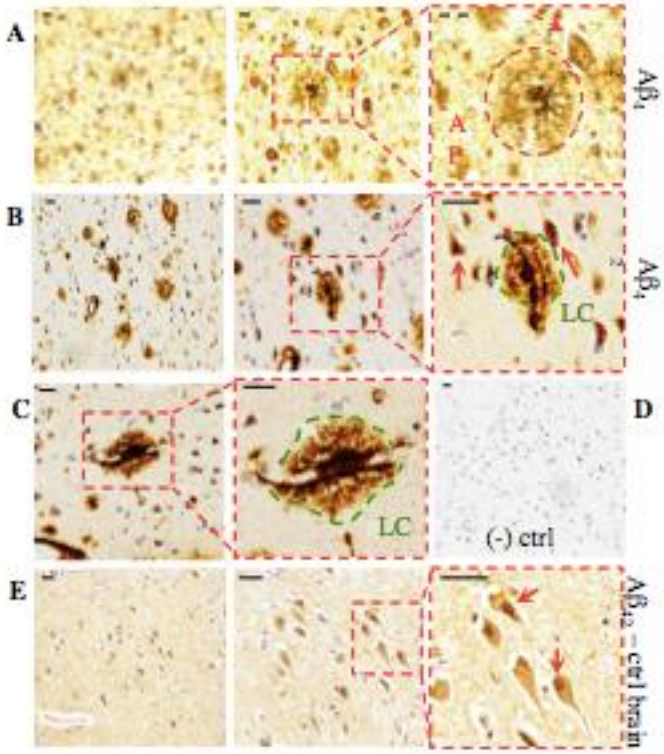

Figure 1: **$A\beta_{42}$ extravasation from a leaky BBB subsequently binds pyramidal neurons and undergoes internalization, and is enhanced in AD brains.**

Alzheimer's disease (AD) brain sections show pathologic changes suggesting cerebrovascular and blood-brain barrier (BBB) dysfunction prior to amyloid plaque formation. A) Cortical amyloid plaques are visualized using antibodies to amyloid-$\beta_{1\text{-}42}$ ($A\beta_{42}$), a hallmark feature of AD brains on autopsy. Intraneuronal $A\beta_{42}$ is also seen in a neuron seemingly on the verge of lysis, which will then contribute to the plaque's growth and development. B) and C) Sections through AD brain cortex show the orientation of a small blood vessel observed from the side, in a longitudinal cut, with the plasma leak cloud emanating radially in all cases. Neurons in the vicinity are shown with intracellular $A\beta_{42}$ loading. D) Low magnification image of a similar AD brain section serving as the negative control for the immunohistochemistry experiments in which $A\beta_{42}$ antibody was omitted. E) Age-matched non-demented control brain section through cortex stained with antibody to $A\beta_{42}$ shows the nuclear localization of the protein, with little intracellular deposits as seen in AD brain. No amyloid plaques are present.

$A\beta_{42}$ = amyloid-$\beta_{1\text{-}42}$; ctrl = control; (-) ctrl = negative control; AP = amyloid plaque; red arrow = intraneuronal amyloid; red dashed circle = amyloid plaque; green dashed circle = perivascular leak cloud; LC = leak cloud; BV = blood vessel

Fig 2. Immunoglobulins leak from points of damaged BBB, and display selectivity and specificity to cell types, varying with class type.

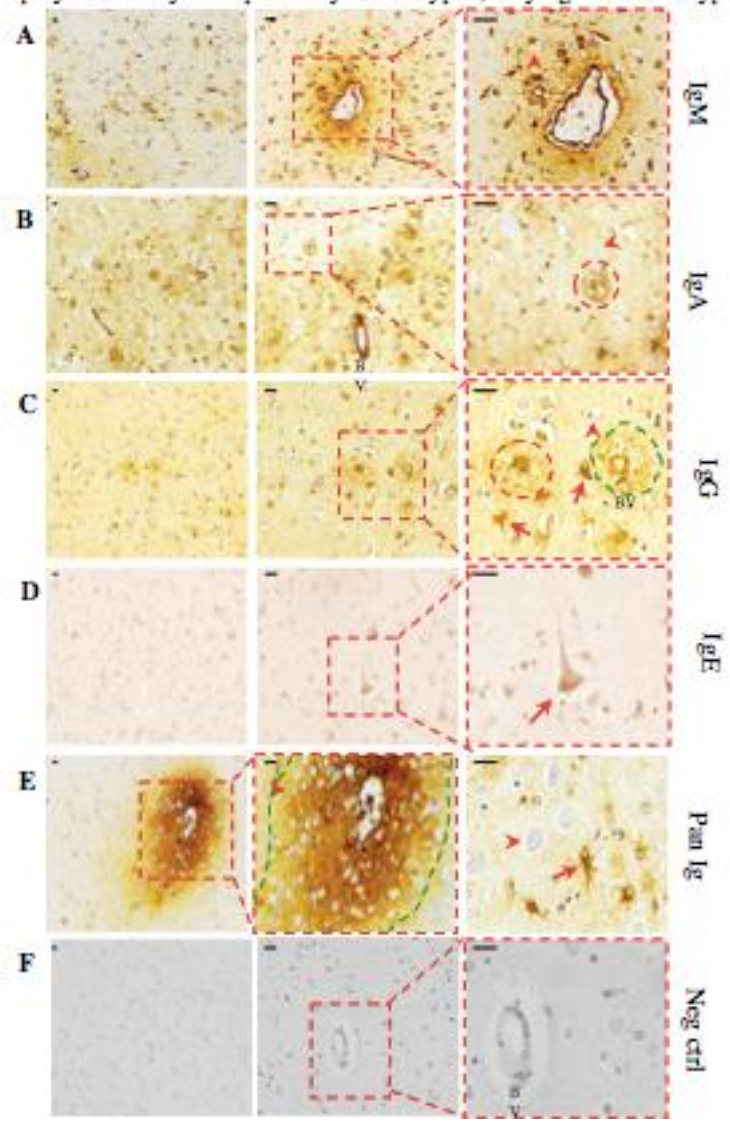

Figure 2: **Immunoglobulins leak from points of damaged BBB, and display selectivity and specificity to cell types, varying with class type.**
Binding of different Ig classes, also leaking from blood vessels with a dysfunctional BBB, were assayed for IgM (A), IgA (B), IgG (C), and IgE (D), Pan Ig (E). Omission of secondary antibody served as a negative control (F). Endogenous Ig varied in reactivity to glia/astrocyte surface protein (IgM, Pan Ig) or neurons (IgG, IgE).
Ig = immunoglobulin; red arrow = Ig-positive cell (neuron/astrocyte); red arrowhead = Ig-negative cell (neuron/astrocyte); red dashed circle = amyloid plaque (visualized Ig antibody); green dashed circle = perivascular leak cloud.

Fig 3. Lysosomal compartment expansion is noted in neurons in AD brains, reflecting chronic endocytosis of insoluble $A\beta_{42}$.

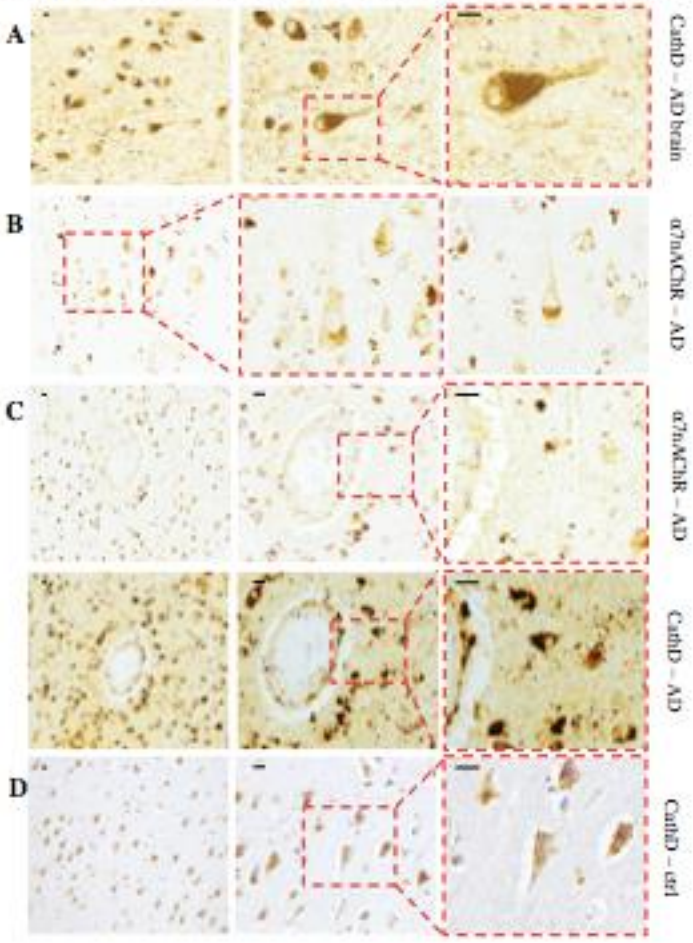

Figure 3: Lysosomal compartment expansion is noted in neurons in AD brains, reflecting chronic endocytosis of insoluble $A\beta_{42}$.

Cathepsin D (CathD), a marker for the lysosomal compartment, is shown to vastly expand in regions of AD-pathology, representing the accumulation of indigestible $A\beta_{42}$ aggregates as they are trafficked through endocytosis. (A) CathD immunoreactivity in neurons populating the cerebral cortex of AD brains expands in the cell body. CathD-positive vesicles can be seen trafficking retrograde down the main dendrite trunk towards the perinuclear lysosomal compartment. (B) Surface protein represented by α7nAChR is seen accumulating in the perinuclear region, likely co-localized within the lysosomal compartment as well, reflecting the consequence of rampant endocytosis. (C) A consecutive section is stained for a ubiquitous surface protein (α7nAChR; top) expressed in pyramidal neurons and lysosome (CathD; bottom) to visualize similar staining in the vicinity of a blood vessel, alluding to the presence of a local leak in the BBB, resulting in endocytosis of plasma components. Age-matched non-demented control brain cortical slices immunostained for lysosomes (D) show the baseline levels of CathD-positive vesicles representing the normal amount and distribution of the lysosomal compartment. Note that with the CathD stain in the control brain slices, the lysosomal compartments are more evenly dispersed in the cell body, and vesicles are not accumulated or coalesced to the extent of that seen in AD brain sections. The $A\beta_{42}$ becomes fibrillized in the lysosomal compartment and is rendered indigestible, accumulating in the cell body and encroaching on axonal processes as it grows in mass.

CathD = Cathepsin D (lysosomal marker); α7nAChR = alpha7 nicotinic acetylcholine receptor (surface receptor).

Fig 4. Internalized neuronal surface proteins are seen in the AD brain.

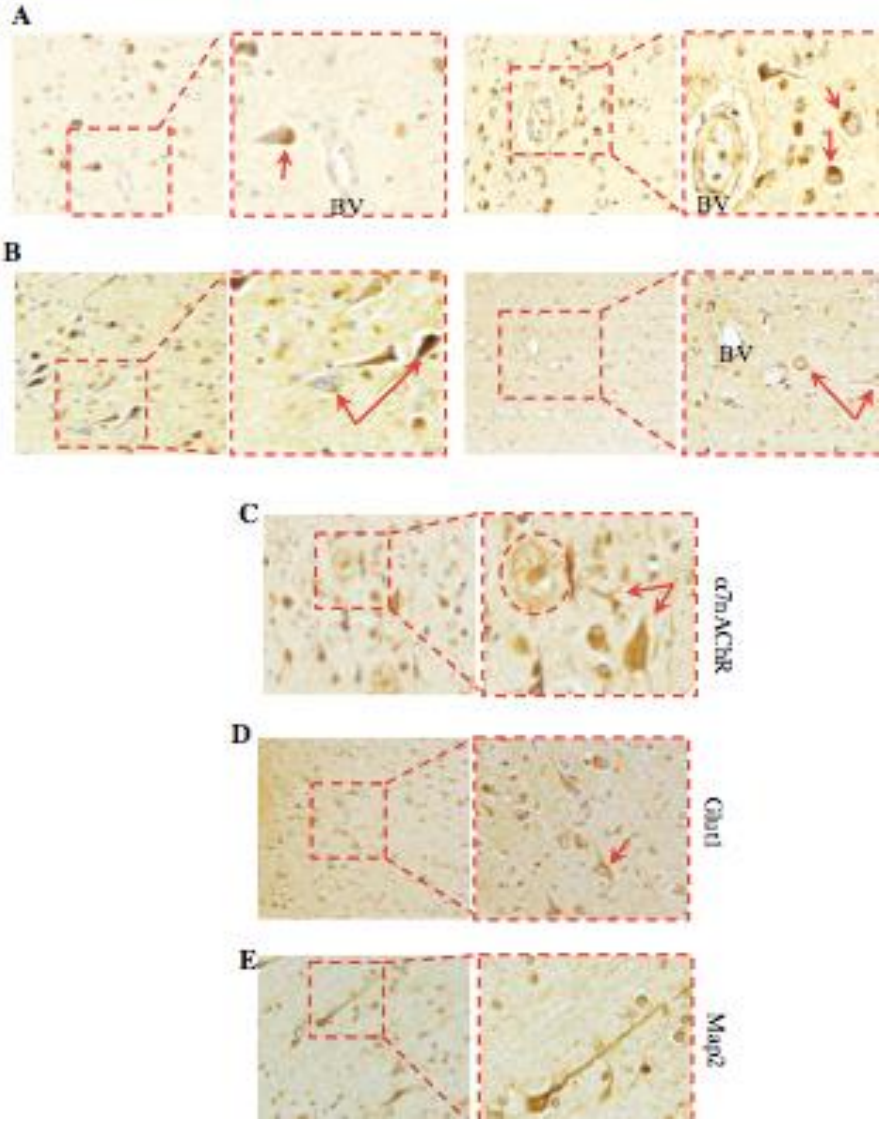

Figure 4: Internalized neuronal surface proteins are seen in the AD brains.

Normally abundant neuronal cell surface marker proteins such as glutamate receptors GluR2/3 (A) and GluR6/7 (B), α7nAChR (C), and glucose transporter Glut1 (D) in AD brains were detected with IHC and imaged to determine their cellular distribution, as well as an intracellular protein, Map2 (E). In all cases, the localization patterns of these proteins appeared to coincide with that of the lysosome compartment. This common localization pattern is likely to reflect the consequence of chronic $A\beta_{42}$ and Ig binding to the neuronal surface, giving rise to the receptor-stripping phenomenon. Map2, however, being an intracellular protein used as a marker of neuronal differentiation, was observed undergoing retrograde vesicular traffic back towards the cell body, presumably from degenerative synaptic changes and dendritic collapse as a result of similar events.

Fig 5. Autoantibody reactivity occurs in the differentiated SH-SY5Y cell line compared to the non-differentiated state.

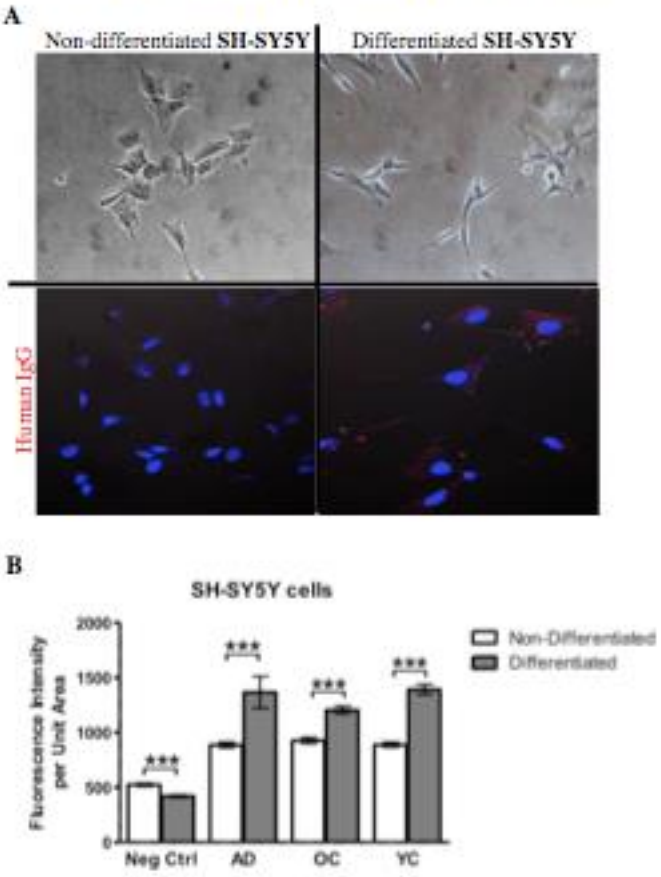

Figure 5: Autoantibody reactivity occurs in the differentiated SH-SY5Y cell line compared to the non-differentiated state.

The cell culture model established using SH-SY5Y human neuroblastoma cell line displays human autoantibody reactivity in the differentiated state. (A) Representative micrographs from SH-SY5Y immunocytochemistry experiments showing that autoantibodies present in human serum from young-age non-demented control (YC), old-age non-demented control (OC), and old-age matched Alzheimer's disease (AD) patient blood are largely non-reactive to undifferentiated cells, but do display binding abilities in the differentiated neuroblastoma cell. (B) Graphical representation of the phenomenon by quantifying signal intensity.

Fig 6. Differentiated cells increase $A\beta_{42}$ internalization over time.

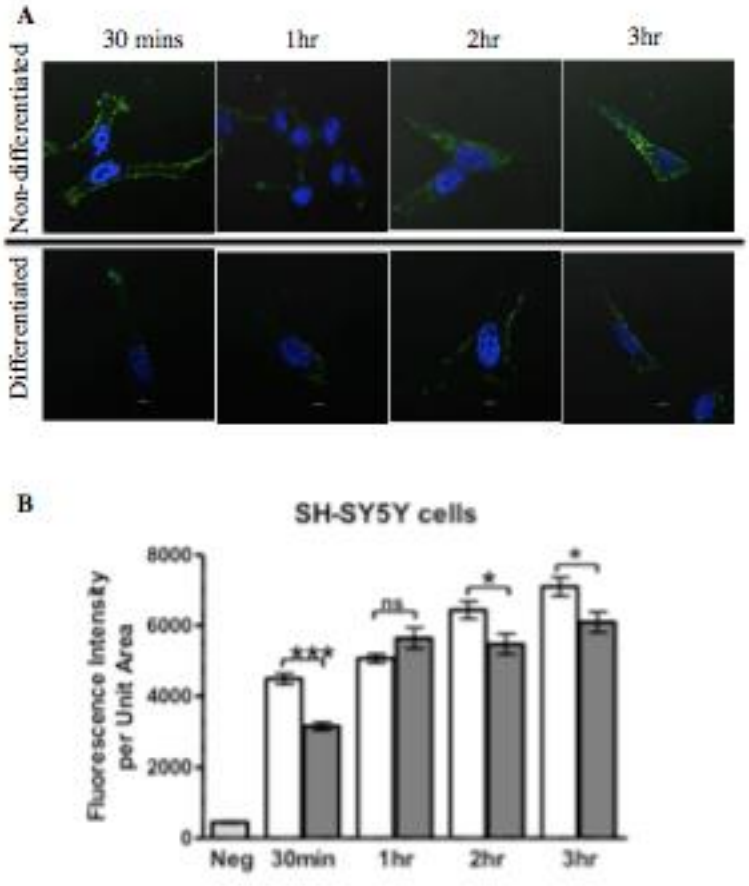

Figure 6: Differentiated cells increase $A\beta_{42}$ internalization over time.

To more faithfully recapitulate in vivo brain physiology, SH-SY5Y cells were differentiated before they were treated with $A\beta_{42}$. 3 hours was determined to be sufficient to detect appreciable $A\beta_{42}$ internalization rates. (A) Representative micrographs of time points and cell states showing that differentiated cells, like their non-differentiated counterparts, exhibited $A\beta_{42}$ intraneuronally, and the extent was directly proportional to the time points observed. (B) Graphical representation of the observed internalized $A\beta_{42}$.

Fig 7. $A\beta_{42}$ internalization was enhanced in the presence of serum with autoantibodies directed at surface proteins.

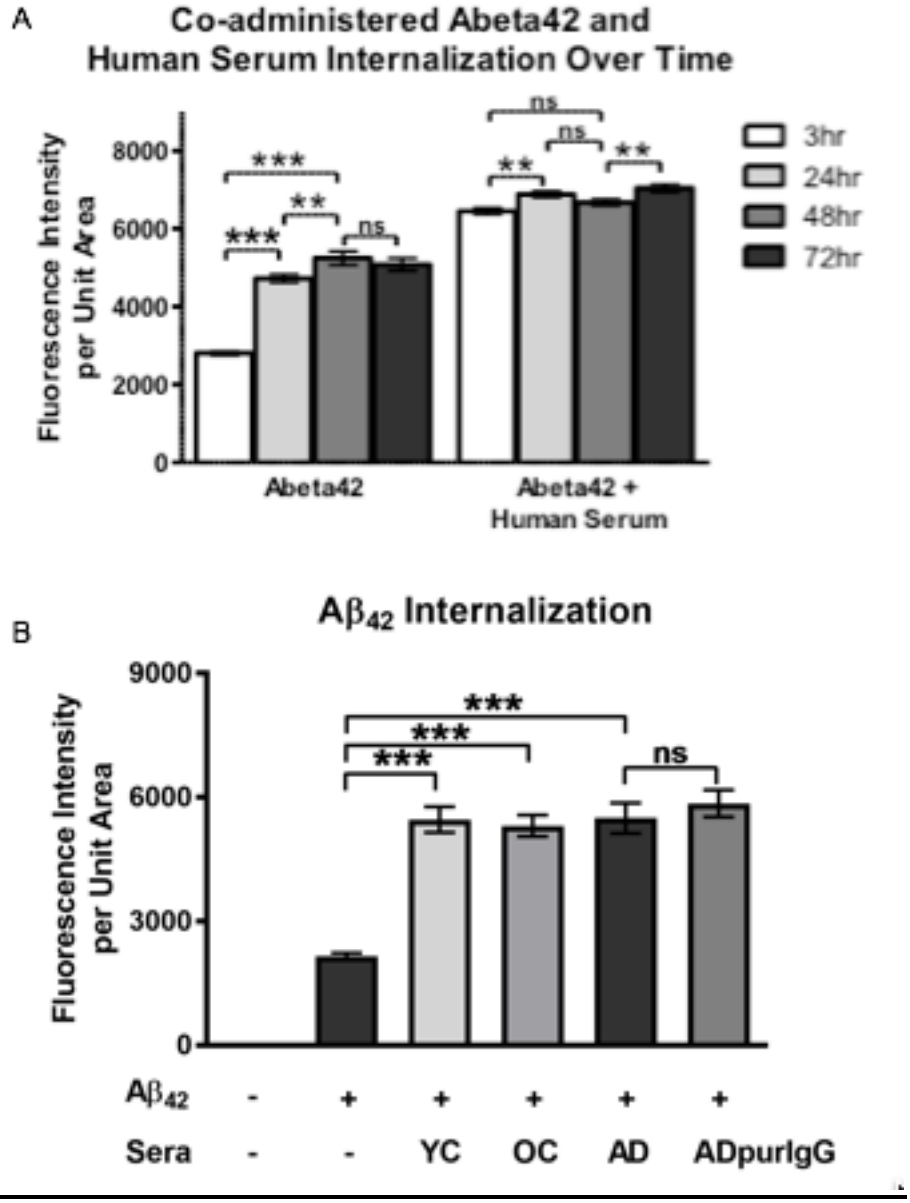

Figure 7: $A\beta_{42}$ internalization was enhanced when co-administered with human serum containing autoantibodies directed to surface proteins.

When differentiated SH-SY5Y cells were treated in culture with physiologic $A\beta_{42}$ concentrations in the presence of human serum, amyloid burdening was enhanced over time. (A) Cells were differentiated and then treated for 3- to 72-hrs with 100nM fluorescein isothiocyanate (FITC)-$A\beta_{42}$ and then assayed for internalized $A\beta_{42}$. Graphical representations show baseline $A\beta_{42}$ internalization over time (left) and upon supplementation with human serum containing neuron-binding aAbs (right). The $A\beta_{42}$ internalization was in fact enhanced when given in conjunction with human serum containing neuron-binding aAb targets. Indeed, these findings suggest that upon BBB breakdown, $A\beta_{42}$ and aAbs leak into the brain parenchyma, both of which induce endocytosis, however the extent is greater in the presence of aAbs. (B) Irrespective of age or disease, aAb presence can induce internalization of $A\beta_{42}$. By purifying the IgG portion of AD serum and treating cells with the antibody fraction only, there is no significant difference in the extent of $A\beta_{42}$ internalization enhancement.

DISCUSSION

Brain homeostasis is of vital importance to cognitive functioning. Cerebral tissue is highly sensitive to noxious conditions, and as such, the vascular integrity is essential to optimize the array of neuronal, and non-neuronal, activities day-to-day. The importance of the BBB function is thought to lie in the access that would otherwise be granted to blood-borne pathogens, if compromised. Similarly, the immune system is kept separated from the central nervous system (CNS) by the same structural impediment. The integrity of the BBB is important in not only maintaining an optimal microenvironment for cells of the CNS to live and function in, but also in the prevention of a wide array of disease processes. A gamut of neurodegenerative conditions is known to have a degree of BBB breach, and the subsequent pathological manifestations that define the disease processes can be measurably debilitating. Just as important as it is for the BBB to stringently control what enters the CNS, it is equally critical that cellular debris and metabolic waste products be shuttled out of the brain parenchyma. If left to accumulate, the glial and neuronal attempts to rid the CSF of such debris by endocytosis would be quickly overwhelmed. This includes $A\beta_{42}$, which, if in high enough concentrations, would be fibrillized and rendered non-digestible within the lysosomal compartments of these cells. Eventually, the amyloid-burdened neurons would become overly taxed and undergo lysis, thereby releasing their cellular contents, including aggregated amyloid fibrils, as a cloud of fibrils currently referred to as an amyloid plaque (AP).

Diseases that have classically been linked to autoantibody (aAb)-mediated internalization of surface proteins have described the process in the context of multiple sclerosis, myasthenia gravis, anti-NMDAR encephalitis, schizophrenia, and others. Generally, however, these diseases do not account for the neuronal accumulation of a protein aggregate as well. Based on examination of human brain sections stained for $A\beta_{42}$ and Ig -M, -G, -A, and -E, it is clear that leakage of peripheral blood components commonly occurs, presumably at areas of BBB breakdown. The effects of the surface-binding capability of all of these aAbs can compound the consequence of this indiscriminant leakage. We demonstrate that these phenomena occur coincidentally and may augment the effect each may have on endocytosis alone. However, given the nature of $A\beta_{42}$ to aggregate at high enough concentration in low pH such as within the lysosomal compartment, these observations enable us to propose the novel mechanism by which internalization of $A\beta_{42}$ may be enhanced to toxic levels within the cell.

In an effort to study the consequences of BBB disruption leading to $A\beta_{42}$ and aAb binding, a cell culture model was established using the human neuroblastoma cell line, SH-SY5Y. These cells were differentiated and found to bind aAbs present in human serum. The identity of these aAbs is not known, however they have been the focus of intense efforts using microarray technologies to further categorize the IgG aAbs present in serum of all individuals, especially for diagnostic purposes (Han et al. 2012, Nagele, Han, et al. 2011, Nagele et al. 2013, DeMarshall et al. 2015). By acknowledging that both events (that is $A\beta_{42}$ and aAb binding to neurons and

induction of endocytosis) occur after BBB breakdown, then a novel hypothesis can be tested as to determining the origin of APs. Lastly, these findings support the use of therapies that target the BBB, and vascular health in general, both now thought to be major players in AD initiation and progression.

REFERENCES

Abbott, N. J., A. A. Patabendige, D. E. Dolman, S. R. Yusof, and D. J. Begley. 2010. "Structure and function of the blood-brain barrier." *Neurobiol Dis* 37 (1):13-25. doi: 10.1016/j.nbd.2009.07.030.

Association, Alzheimer's. 2015. "2015 Alzheimer's Disease Facts and Figures." *Alzheimer's & Dementia* 11 (3):332+.

Clifford, P. M., S. Zarrabi, G. Siu, K. J. Kinsler, M. C. Kosciuk, V. Venkataraman, M. R. D'Andrea, S. Dinsmore, and R. G. Nagele. 2007. "Abeta peptides can enter the brain through a defective blood-brain barrier and bind selectively to neurons." *Brain Res* 1142:223-36. doi: S0006-8993(07)00127-8 [pii]10.1016/j.brainres.2007.01.070 [doi].

Cummings JL, Morstorf T, Zhong K. 2014. "Alzheimer's disease drug-development pipline: few candidates, frequent failures." *Alzheimers Res Ther* 6 (4):37.

D'Andrea, M. R., Nagele, R. G., Wang, H-Y., Peterson, P. A., Lee, D. H. 2001. "Evidence that neurones accumulating amyloid can undergo lysis to form amyloid plaques in Alzheimer's disease." *Histopathology* 38:120-134.

Dahm, L., C. Ott, J. Steiner, B. Stepniak, B. Teegen, S. Saschenbrecker, C. Hammer, K. Borowski, M. Begemann, S. Lemke, K. Rentzsch, C. Probst, H. Martens, J. Wienands, G. Spalletta, K. Weissenborn, W. Stocker, and H. Ehrenreich. 2014. "Seroprevalence of autoantibodies against brain antigens in health and disease." *Ann Neurol* 76 (1):82-94. doi: 10.1002/ana.24189.

DeMarshall, C. A., M. Han, E. P. Nagele, A. Sarkar, N. K. Acharya, G. Godsey, E. L. Goldwaser, M. Kosciuk, U. Thayasivam, B. Belinka, and R. G. Nagele. 2015. "Potential utility of autoantibodies as blood-based biomarkers for early detection and diagnosis of Parkinson's disease." *Immunol Lett* 168 (1):80-8. doi: 10.1016/j.imlet.2015.09.010.

Hammer, C., B. Stepniak, A. Schneider, S. Papiol, M. Tantra, M. Begemann, A. L. Siren, L. A. Pardo, S. Sperling, S. Mohd Jofrry, A. Gurvich, N. Jensen, K. Ostmeier, F. Luhder, C. Probst, H. Martens, M. Gillis, G. Saher, F. Assogna, G. Spalletta, W. Stocker, T. F. Schulz, K. A. Nave, and H. Ehrenreich. 2014. "Neuropsychiatric disease relevance of circulating anti-NMDA receptor autoantibodies depends on blood-brain barrier integrity." *Mol Psychiatry* 19 (10):1143-9. doi: 10.1038/mp.2013.110.

Han, M., E. Nagele, C. DeMarshall, N. Acharya, and R. Nagele. 2012. "Diagnosis of Parkinson's disease based on disease-specific autoantibody profiles in human sera." *PLoS One* 7 (2):e32383. doi: 10.1371/journal.pone.0032383.

Hebert, L. E., J. Weuve, P. A. Scherr, and D. A. Evans. 2013. "Alzheimer disease in the United States (2010-2050) estimated using the 2010 census." *Neurology* 80 (19):1778-83. doi: 10.1212/WNL.0b013e31828726f5.

Michalak, Z., A. Lebrun, M. Di Miceli, M. C. Rousset, A. Crespel, P. Coubes, D. C. Henshall, M. Lerner-Natoli, and V. Rigau. 2012. "IgG leakage may contribute to neuronal dysfunction in drug-refractory epilepsies with blood-brain barrier disruption." *J Neuropathol Exp Neurol* 71 (9):826-38. doi: 10.1097/NEN.0b013e31826809a6.

Nagele, E., M. Han, C. Demarshall, B. Belinka, and R. Nagele. 2011. "Diagnosis of Alzheimer's disease based on disease-specific autoantibody profiles in human sera." *PLoS One* 6 (8):e23112. doi: 10.1371/journal.pone.0023112.

Nagele, E. P., M. Han, N. K. Acharya, C. DeMarshall, M. C. Kosciuk, and R. G. Nagele. 2013. "Natural IgG autoantibodies are abundant and ubiquitous in human sera, and their number is influenced by age, gender, and disease." *PLoS One* 8 (4):e60726. doi: 10.1371/journal.pone.0060726.

Nagele, R. G., P. M. Clifford, G. Siu, E. C. Levin, N. K. Acharya, M. Han, M. C. Kosciuk, V. Venkataraman, S. Zavareh, S. Zarrabi, K. Kinsler, N. G. Thaker, E. P. Nagele, J. Dash, H. Y. Wang, and A. Levitas. 2011. "Brain-reactive autoantibodies prevalent in human sera increase intraneuronal amyloid-beta(1-42) deposition." *J Alzheimers Dis* 25 (4):605-22. doi: 10.3233/JAD-2011-110098.

Nagele, R. G., M. R. D'Andrea, W. J. Anderson, and H. Y. Wang. 2002. "Intracellular accumulation of beta-amyloid(1-42) in neurons is facilitated by the alpha 7 nicotinic acetylcholine receptor in Alzheimer's disease." *Neuroscience* 110 (2):199-211. doi: S0306452201004602 [pii].

Ortiz, G. G., F. P. Pacheco-Moises, M. A. Macias-Islas, L. J. Flores-Alvarado, M. A. Mireles-Ramirez, E. D. Gonzalez-Renovato, V. E. Hernandez-Navarro, A. L. Sanchez-Lopez, and M. A. Alatorre-Jimenez. 2014. "Role of the blood-brain barrier in multiple sclerosis." *Arch Med Res* 45 (8):687-97. doi: 10.1016/j.arcmed.2014.11.013.

Patel, J. P., and B. N. Frey. 2015. "Disruption in the Blood-Brain Barrier: The Missing Link between Brain and Body Inflammation in Bipolar Disorder?" *Neural Plast* 2015:708306. doi: 10.1155/2015/708306.

Rasband, W.S. 1997-2015. "ImageJ." U.S. National Institutes of Health. http://imagej.nih.gov/ij/.

Snyder, H. M., R. A. Corriveau, S. Craft, J. E. Faber, S. M. Greenberg, D. Knopman, B. T. Lamb, T. J. Montine, M. Nedergaard, C. B. Schaffer, J. A. Schneider, C. Wellington, D. M. Wilcock, G. J. Zipfel, B. Zlokovic, L. J. Bain, F. Bosetti, Z. S. Galis, W. Koroshetz, and M. C. Carrillo. 2015. "Vascular contributions to cognitive impairment and dementia including Alzheimer's disease." *Alzheimers Dement* 11 (6):710-7. doi: 10.1016/j.jalz.2014.10.008.

Sui, Y. T., K. M. Bullock, M. A. Erickson, J. Zhang, and W. A. Banks. 2014. "Alpha synuclein is transported into and out of the brain by the blood-brain barrier." *Peptides* 62:197-202. doi: 10.1016/j.peptides.2014.09.018.

Wang, H. Y., D. H. Lee, M. R. D'Andrea, P. A. Peterson, R. P. Shank, and A. B. Reitz. 2000. "beta-Amyloid(1-42) binds to alpha7 nicotinic acetylcholine receptor with high affinity. Implications for Alzheimer's disease pathology." *J Biol Chem* 275 (8):5626-32.

Zlokovic, B. V. 2008. "The blood-brain barrier in health and chronic neurodegenerative disorders." *Neuron* 57 (2):178-201. doi: 10.1016/j.neuron.2008.01.003.

Zlokovic, B. V. 2011. "Neurovascular pathways to neurodegeneration in Alzheimer's disease and other disorders." *Nat Rev Neurosci* 12 (12):723-38. doi: 10.1038/nrn3114.

ATTRIBUTIONS

Authors

Eric L Goldwaser[1, 2], Nimish K Acharya[4], Hao Wu[2], George Godsey[1, 2], Abhirup Sarkar[1, 2], Cassandra DeMarshall[1, 2], Mary Kosciuk[1, 2], and Robert G Nagele[1, 2, 3]

Affiliations

[1]Biomarker Discovery Center, New Jersey Institute for Successful Aging, Rowan University School of Osteopathic Medicine, Stratford, NJ 08084

[2]Graduate School of Biomedical Sciences, Rowan University, Stratford, NJ 08084

[3]Department of Geriatrics and Gerontology, Rowan University School of Osteopathic Medicine, Stratford, NJ 08084

[4]Department of Neurosurgery, University of Pennsylvania, Philadelphia, Pennsylvania, PA 19104

Funding disclosure

The authors wish to thank the Osteopathic Heritage Foundation and the Dean's endowment for primary care research for support of this project.

Running headline

Neuron-binding autoantibodies and amyloid plaques

Figure 1. RGN and MK stained tissue, ELG imaged and analyzed.

Figure 2. RGN and MK stained tissue, ELG imaged and analyzed.

Figure 3. RGN and MK stained tissue, ELG imaged and analyzed.

Figure 4. RGN and MK stained tissue, ELG imaged and analyzed.

Figure 5. ELG, GG, NKA, AS helped in the culturing and maintaining the cell lines, as well as establishing protocol adapted for ICC experiments. ELG imaged, analyzed, and quantified data. HW helped in construction of the graphical representations.

Figure 6. ELG, GG, NKA, AS helped in the culturing and maintaining the cell lines, as well as establishing protocol adapted for ICC experiments. ELG imaged, analyzed, and quantified data. HW helped in construction of the graphical representations.

Figure 7. ELG, GG, NKA, AS helped in the culturing and maintaining the cell lines, as well as establishing protocol adapted for ICC experiments. ELG imaged, analyzed, and quantified data. HW helped in construction of the graphical representations.

Chapter VI

Cellular mechanisms of amyloid plaque formation in Alzheimer's disease involve exogenous amyloid-β_{1-42} internalization by autoantibody-mediated endocytosis

ABSTRACT

The presence of extravasated plasma components such as IgG and $A\beta_{42}$ has been widely reported in the cerebral cortex of AD brains. We investigated the possible role of these plasma components in mediating endocytosis, its link to intraneuronal $A\beta_{42}$ deposition, and the generation of amyloid plaques (APs) in AD brains. Based on a tentative mechanism derived from observations on human AD brains described in detail above, a cell culture model system was established to investigate cellular mechanisms associated with the phenomenon of autoantibody (aAb)-mediated receptor endocytosis. Differentiated SH-SY5Y human neuroblastoma cells were used to test the possibility that IgG aAbs elicit intraneuronal $A\beta_{42}$ accumulation through induction of endocytosis. Immunofluorescence microscopy assessed the internalization of $A\beta_{42}$ and surface proteins and the subcellular trafficking of $A\beta_{42}$. Cells were treated for up to 72-hours with specific antibodies against selected neuronal surface antigens or with serum or purified-IgG from either AD or controls in conjunction with physiologically relevant concentrations of soluble, exogenous $A\beta_{42}$. An array of inhibitors was used to test the requirement for specific types of endocytosis. Dynasore, a dynamin1/2 GTPase inhibitor of clathrin-mediated endocytosis, showed that $A\beta_{42}$ accumulation is predominantly dependent on this pathway of entry into cells. We also demonstrated co-localization of IgG, α7nAChR, and $A\beta_{42}$ that was temporally related to the early endosomal marker, Rab11, and at later time points to the lysosomal marker, LAMP-1. Lastly, results using monovalent F(ab) antibody fragments generated from purified IgG of AD patient serum suggest

that internalization of $A\beta_{42}$ via endocytosis is triggered by the cross-linking capacity of neuron-binding aAbs. Lastly, we have demonstrated aAb-mediated endocytosis and accumulation of serum IgG and $A\beta_{42}$ within the lysosomal compartment of SH-SY5Y cells. Accumulation of these serum components within neurons along with the associated depletion of key surface proteins and signaling receptors on their cell surfaces is thought to disrupt their homeostasis leading to impaired neuronal function, neurotoxicity, progressive intracellular $A\beta_{42}$ accumulation, and ultimately cell death and AP development. Preventing plasma extravasation by restoring the structural and functional integrity of the blood-brain barrier may curtail initiation and progression of AD pathology, and thus is a promising therapeutic target that directly prevents assault from blood-borne factors that trigger and propagate this devastating disease.

INTRODUCTION

The pathogenesis of Alzheimer's disease (AD) is contested amongst leaders in the field. With the growing at-risk population in the U.S., it is of utmost importance to elucidate the mechanism of this dire affliction more clearly. Previous work has shown the presence of extravasated plasma components such as immunoglobulin (Ig) G and β-amyloid$_{42}$ (Aβ_{42}) in the cerebral cortex and other brain regions implicated in AD pathology in these patients (Clifford et al. 2008, Clifford et al. 2007, D'Andrea 2001, Nagele et al. 2002, Nagele et al. 2003, Wang et al. 2000). These proteins are observed bound to similar neurons, mostly pyramidal neurons, distributed throughout the brain. Both events independently may lead to heightened neuronal endocytosis, however the mechanism by which this occurs when coupled together remains to be deciphered, but could shed light on an important mechanism to the pathogenesis of AD, with far-reaching implications (Hammer et al. 2014, Carey et al. 2005, Kuboyama et al. 2015).

Previous studies have shown that Aβ_{42} leaks out from the cerebrovasculature in regions where the blood-brain barrier (BBB) is structurally and functionally compromised (Acharya et al. 2013, Bouras et al. 2005, Goldwaser 2015, Nagele, Clifford, et al. 2011, Zhao et al. 2015, Zlokovic 2011, 2008). Along with other blood components such as IgG and complement, these proteins will bind to neuronal surfaces and are internalized to yield similar intracellular distributions, suggesting a linked mechanistic underpinning to the internalization events that would otherwise

ensue independently. By looking for other markers of neuronal surface protein internalization (i.e. a phenomenon that we refer to as receptor-stripping), and an expansion of the cell's waste disposal system (lysosomal compartment), a broader picture of the means by which $A\beta_{42}$ can enter a neuron and accumulate within cells are further elucidated. The subsequent fate of $A\beta_{42}$ as indigestible, fibrillized aggregates represents the transition to diseased neurons en route to necrosis, making it extremely important to fully understand these upstream events. Since there are limits to the information that can be extracted from observations of pathological brain tissues in a post-mortem state, it is helpful to recruit or develop living cell models to test key aspects of this process.

Diseases that have classically been shown to involve autoantibody (aAb)-mediated internalization of surface proteins include multiple sclerosis, myasthenia gravis, anti-NMDAR encephalitis, schizophrenia, and others (Hammer et al. 2014, Leech et al. 2007, Sui et al. 2014, Terryberry, Thor, and Peter 1998, Whitton 2007, Zlokovic 2008). Although the immune system is thought to be involved in some aspects of these diseases, none of them, unlike AD, have accumulation of exogenous protein aggregates (e.g., $A\beta_{42}$ or alpha-synuclein) within neurons and the surrounding brain interstitium as a key pathological feature. Differentiated SH-SY5Y neuroblastoma cells, which were previously demonstrated to exhibit features of neurons including neuronal process extension, bind $A\beta_{42}$, and react to aAbs in human serum, were used to test our hypothesis. The ability for differentiated cells to bind aAb in the serum of young control, old control, and AD patient versus non-differentiated cells may point

for the evolutionary need to develop a barrier (a blood-brain barrier) between the blood and the brain that can sequester aAbs away from the brain and thereby prevent their contact with neurons in the brain.

The cell contains multiple mechanisms to internalize exogenous substances and also to clear materials adherent to their surface membranes that potentially interfere with the normal functions and fluidity characteristics of this membrane (Doherty and McMahon 2009, Elkin, Lakoduk, and Schmid 2016). To date, multiple researchers have suggested that $A\beta_{42}$ may undergo different types of endocytosis depending on its structure and solubility (Carey et al. 2005, Chyung and Selkoe 2003, Cossec et al. 2010, Jang et al. 2015, Kandimalla et al. 2009, Koo and Squazzo 1994, Kuboyama et al. 2015, Lana et al. 2016). For instance, $A\beta_{42}$ can exist in monomeric, oligomeric, or fibrillized forms, and there is no consensus as to which form exists in vivo, and if the transition from one form to another also constitutes different endocytic mechanisms or reflects different endpoints of their storage within cells. To this end, we have examined the dynamic aspects of $A\beta_{42}$ binding to neuronal surfaces and its subsequent internalization using several endocytosis inhibitors, like Dynasore (Dyn), Genistein (Gen), Cytochalasin D (CytD), and Phenylarsine oxide (PAO). Dynasore, an inhibitor of dynamin1/2 needed for clathrin-mediated endocytosis, showed greatest effect at inhibiting $A\beta_{42}$ entry into the cell. Curiously, however, internalization was rescued when treated in conjunction with AD serum sample, suggesting a new approach to $A\beta_{42}$ internalization in a more physiological context.

Here, we study the effects of monovalent antibodies to demonstrate that autoantibody (aAb)-mediated internalization of surface components and $A\beta_{42}$ requires cross-linking of surface proteins bound to aAb prior to endocytosis. Also, as shown in similar studies for other neurological conditions (e.g., NMDAR-mediated schizophrenia, restoration of the aAb crosslinking function using anti-F(ab) antibodies can rescue aAb-mediated endocytosis of surface-bound proteins) (Hughes et al. 2010).

Thousands of aAbs are typically present in human sera, and these can be used for diagnostic purposes (DeMarshall et al. 2015, Han et al. 2012, Harris and Sadiq 2014, Mecocci et al. 1995, Nagele, Han, et al. 2011, Nagele et al. 2013, Roche et al. 2008, Schott et al. 1996, Singh and Fudenberg 1989). From a mechanistic standpoint, however, we are interested in knowing the cognate receptors to which the aAbs bind on the surface of neurons in the presence of $A\beta_{42}$ that could participate in the enhanced endocytosis observed in vivo. Protein microarray platforms have been extensively used for the purpose of characterizing the aAb profiles present in serum, and has enabled a high throughput experiment for assaying potential biomarkers of disease shared between the cohorts' serum tested.

In summary, we demonstrate here that exogenous $A\beta_{42}$ entry into neurons is enhanced when IgG aAbs from serum are also present in the milieu and binds to the surfaces of the same neuron. The mechanism by which this occurs seems to be through classical dynamin-dependent, clathrin-mediated endocytosis pathway that is trafficked to the lysosome. In high enough concentrations within lysosomes, the $A\beta_{42}$ aggregates and

fibrillizes, and is rendered non-digestible. Continual entry into the lysosomal compartment along with the lack of degradation translates into progressive accumulation of $A\beta_{42}$. This is a key step in the process leading to cell death and AP formation. Lastly, we show that cross-linking of surface aAbs is a required event that precedes internalization of receptor-aAb complexes, and facilitates $A\beta_{42}$ internalization as well into the endosome-lysosome system. We have also identified some novel biomarkers that may have pathogenic implications as candidate surface proteins to which aAbs react and thus trigger the $A\beta_{42}$ internalization and accumulation process.

EXPERIMENTAL PROCEDURE

Cell culture experiments

For immunocytochemistry experiments, and aAb and amyloid binding and internalization experiments, SH-SY5Y cells were used. They are an established cell line that can be grown in 10% Fetal Bovine Serum (FBS) in Dulbecco's Minimal Essential Medium (DMEM)/F12 media. Complete media was changed every three days, and cells were split weekly at 80% confluence. These cells can be differentiated after being split into 35mm glass-bottom dishes once they have achieved 60% confluence using 10μM retinoic acid and 0.2% FBS in DMEM/F12 media. Upon differentiation for three days, cells begun to sprout neuron-like processes and established connections with neurons in the vicinity, at roughly 70% confluence. At this point, they can be assayed using standard immunocytochemistry protocols previously described for neuronal markers of differentiation and surface proteins (Nagele et al. 2002). In brief, cultures were washed in cation-free Hanks Buffered Salt Solution (HBSS) (without calcium or magnesium) three times, and then fixed in 4% paraformaldehyde (PFA). If the cell surface membrane was to be stripped for internalization assays, three acid washes (0.1M Glycine, pH 2.5) of two minutes each were performed at this point, followed by two more HBSS washes to remove any residual acid prior to fixation. Some cultures were treated with 100nM fluorescein isothiocyanate (FITC)-labeled $A\beta_{42}$ (physiologic concentration) for time points ranging from 30 minutes to 72 hours. Other dishes were treated with $A\beta_{42}$ and human serum obtained from young-aged non-demented control (YC), old-aged non-

demented control (OC), and Alzheimer's disease patient blood (AD) at 1:50 dilutions in serum-free media. After fixation, cells were blocked in 3% BSA (in PBS-T or PBS depending on the assay being performed) and then probed with primary antibody overnight at 4°C or secondary antibodies for one hour at room temperature covered from the light. For human serum containing IgG, anti-human IgG (Sigma laboratories) conjugated to an Alexa-fluor 594 fluorescent signal was used, in contrast to the FITC-labeled $A\beta_{42}$. Nuclei were counterstained with Hoechst. Nikon Confocal microscopy equipped with epifluorescence was used to capture images and NIS-Elements software to perform image analysis and quantification of signal intensities.

Analysis

Immunohistochemistry experiments of human brain tissue were used for qualitative and observational purposes only. Unpublished work was performed, however, measuring the extent and size of lysosomal vesicles and overall compartment space as a proportion of the neuron using a macros program written for ImageJ software (Rasband 1997-2015). For immunocytochemistry experiments, images captured using Nikon Confocal microscopy NIS-Elements software was used to outline cells manually as a "Region of Interest" (ROI). Approximately ten random images were taken per experiment (i.e. individual dish), and only fully enclosed cells within the 60x field were outlined. Each experiment had roughly counted 80 cells, and then the software was able to determine the fluorescence signal intensity within the ROI, making sure not to include saturating amounts of signal during the establishment of image parameter acquisition. After exporting this data to excel, the summed signal

intensity for the FITC (green) channel ($A\beta_{42}$ was FITC-labeled) was divided by the pixel count (area) of the ROI to determine the signal intensity (FITC-$A\beta_{42}$) per unit area (cell). The summed fluorescence intensity is the most well recognized surrogate measurement used to establish relative protein amount. By stripping the surface membrane of the cells using established protocol (0.1M Glycine acid wash), all signal intensity retrieved therefore represented internalized FITC-$A\beta_{42}$ protein. For experiments aimed at addressing surface bound proteins, no such acid wash was performed, nor was any detergents used throughout the immunocytochemistry procedure.

Statistics

Experiments were done in triplicate and blinded, so as to limit bias and improve reproducibility. Once data was compiled, graphical representations were constructed using a two-tailed Student's *t*-test, and a p-value < 0.05 was considered statistically significant: *, $p<0.05$; **, $p<0.01$; ***, $p<0.001$). Variation within each treatment group was represented by standard deviations of the mean (SEM). Acquisition parameters were determined by the user at the beginning of each experiment and were kept identical for all other images of a given experiment.

Human protein microarrays

To detect and identify autoantibodies in human sera, we used *Invitrogen's* ProtoArray v5.0 Human Protein Microarrays (Cat. *No.* PAH0525020, *Invitrogen*, Carlsbad, CA, USA), each containing 9,486 unique human protein antigens

(www.invitrogen.com/proto0array). All proteins were expressed as GST fusion proteins in insect cells, purified under native conditions, and spotted in duplicate onto nitrocellulose-coated glass slides. Arrays were probed with serum, processed and scanned according to the manufacturer's instructions. Briefly, microarrays were blocked using Blocking Buffer (Cat. *No. PA055*, *Invitrogen*) and each was incubated with serum diluted to 1:500 in washing buffer. After washing, arrays were probed with anti-human IgG (H+L) conjugated to AlexaFluor 647 (Cat. *No.* A-21445, Invitrogen) diluted 1: 2,000 in washing buffer. Arrays were then washed, dried, and immediately scanned with a GenePix 4000B Fluorescence Scanner (*Molecular Devices*, Sunnyvale, CA, USA).

Microarray data analysis

Fluorescence data was acquired by aligning the *Genepix Array List* (GAL) onto the microarray using the *Genepix Pro* analysis software. The resulting *Genepix Results* (GPR) files were imported into Invitrogen's *Prospector 5.2* for analysis. Positive hits were determined by a Z-Factor greater than 0.4, and a minimum signal intensity of 1500 RFU, which allow for stringent biomarker selection and minimizes the amount of false positives. Autoantibodies were sorted into descending order by difference of prevalence, and the top 50 most differentially expressed autoantibodies were chosen as potential candidate biomarkers.

RESULTS

Differentiated SH-SY5Y cells can be used as a model system to test for aAb-mediated $A\beta_{42}$ endocytosis.

Upon differentiation of SH-SY5Y human neuroblastoma cells with retinoic acid (RA) for 72 hours, cells were surveyed for the expression of various neuronal marker proteins indicative of neuronal differentiation (Fig. 1). Immunocytochemistry and confocal microscopy revealed that (Fig. 1A) α7nAChR, (Fig. 1B) SV2, (Fig. 1C) Map2, and (Fig. 1D) Tau6 were all expressed and distributed within cells as expected. Moreover, axon-like neuronal processes were present amongst and between cultured cells upon differentiation, further supporting the differentiated status and tendency to assume many of the properties of neurons. The effect of RA on $A\beta_{42}$ was also tested to minimize bias and as an added control to validate future experiments using this cell culture system (Supp. Fig. 1). Using double immunofluorescence confocal microscopy, results show that $A\beta_{42}$ is endocytosed at similar rates when RA is included in the treatment medium. Representative micrographs (Supp. Fig. 1A) show similar morphology and $A\beta_{42}$ localization. No statistical significance is achieved when differentiated cells are given RA throughout the course of $A\beta_{42}$ treatment (Supp. Fig. 1B), as in experiments detailed below.

$A\beta_{42}$ is trafficked through the endosome-lysosome pathway after internalization.

To assess the fate of internalized $A\beta_{42}$, differentiated SH-SY5Y cells were treated with FITC-$A\beta_{42}$ at physiologic concentrations of 100nM in serum free media for 3-,

24-, 48-, or 72-hours (Fig. 2). At the specified time interval, cells were fixed and processed for confocal microscopy using standard immunocytochemistry protocols. Representative micrographs show cells from the 72-hour experiment with $A\beta_{42}$ (green) co-localized with the lysosome (red), as detected using LAMP-1 antibody showing a yellow color signifying an overlay of the green and red channels (Fig. 2, top panel). At the same time point, $A\beta_{42}$ did not co-localize with the early endosome marker Rab-11 (red), as seen in the lower panel as two separate colors – green and red (Fig. 2, bottom panel). The reverse was true for earlier time points, reflecting that with increased time, $A\beta_{42}$ is shuttled through the endosome first and subsequently ends its transit through the cell in the lysosome.

$A\beta_{42}$ internalization is enhanced when co-administered with human serum.

As mentioned above, human serum and $A\beta_{42}$ have been shown to leak in to the brain parenchyma and bind to neurons. To study the effects secondary to BBB breach, we treated our cell model system with both of these components and assayed for internalized FITC-$A\beta_{42}$ (Fig. 3). Human serum from young non-demented control, old-aged non-demented control, and old-aged matched AD patient blood was added into the culture treatment media containing physiologically relevant levels of $A\beta_{42}$. Each of the serum samples was demonstrated to possess neuron-binding aAbs. Differentiated SH-SY5Y cells were treated for up to 72 hours with $A\beta_{42}$ in the presence or absence of human serum or α7nAChR antibodies as a positive control. Results showed that treatment with human serum or α7nAChR antibodies dramatically enhanced $A\beta_{42}$ internalization in cells as a function of time. Treatment

with human serum (Fig. 3D) significantly raised intracellular $A\beta_{42}$ levels at each time point, and continued to do so for the entire 72-hour maximal time interval. The effect that an antibody directed against a known cell surface receptor (α7nAChR) was found to be more potent than that of the whole human serum (Fig. 3C), although there was a significant drop in levels of $A\beta_{42}$ after 48 hours of treatment. It is possible that this effect is due to progressive depletion of this receptor from the cell surface which, upon reduction of the rate of entry, allows cells sufficient time and resources to clear or degrade some of the internalized $A\beta_{42}$ while it is still in the more soluble and degradable monomeric or oligomeric states. If so, the continued but slower rate of entry of $A\beta_{42}$ would be expected to continue, especially if the route of its entry into the cells is not completely dependent on antibody crosslinking events taking place on the cell surface.

Lysosomal compartment expansion occurs over time in our cell model, consistent with what has been observed to occur in human AD brains.

In human AD brain sections, we showed in previous work that the lysosomal compartment undergoes a vast expansion, presumably as an effect of vesicles containing non-digestible $A\beta_{42}$ continually coalescing and fusing over time. This idea that chronic endocytosis of $A\beta_{42}$ occurs and drives $A\beta_{42}$ accumulation in the lysosomal compartment was confirmed here by observations on our cell culture model at the end of the 72-hour treatment period (Fig. 4). Here, differentiated cells were treated for 3- or 72-hours with FITC-$A\beta_{42}$ with or without AD serum. Immunocytochemistry was carried out to detect LAMP-1, a lysosomal marker.

Comparing each group as a function of time, it is clear that the lysosomal expansion occurs in this cell model, thus mimicking in vivo findings and strengthening the likelihood that such a mechanism is also operating in vivo.

IgG aAb fraction present in human serum enhances the internalization of Aβ$_{42}$.

To investigate the effects of IgG aAbs present in human serum on Aβ$_{42}$ internalization, IgG purification procedures were performed. IgG was purified from AD serum using a spin-column chromatography according to manufacturer's protocol and was confirmed by SDS-PAGE (Supp. Fig. 2) and absorption at 280nm. The IgG purified from AD serum was then tested against AD serum without IgG as well as an antibody to a known surface receptor, α7nAChR, for their ability to drive internalization of Aβ$_{42}$. The amount of internalized FITC-Aβ$_{42}$ was quantified based on signal intensity per unit area, and plotted on the representative bar graph (Fig. 5). In the group treated with 100nM Aβ$_{42}$ alone, baseline internalized Aβ$_{42}$ is compared to that treated with α7nAChR antibody, purified IgG from AD subjects, or AD serum with IgG selectively removed (IgG-depleted AD serum). The greatest degree of Aβ$_{42}$ internalization was achieved using purified IgG from AD serum. Roughly 50% of the enhancement in Aβ$_{42}$ signal was lost when Aβ$_{42}$ was co-administered with AD serum depleted of IgG. These findings suggest that the aAb fraction of serum is largely responsible for the Aβ$_{42}$ internalization observed in these cells.

aAb-mediated Aβ$_{42}$ internalization proceeds through classic receptor-mediated endocytosis mechanisms.

Inhibitors for caveolin-mediated endocytosis, clathrin-independent and clathrin-dependent endocytosis, macropinocytosis, and phagocytosis were employed to investigate the method of internalization utilized by $A\beta_{42}$ in the context of aAb supplementation (Fig. 6). 0.01% DMSO was used as a control (Fig. 6A). Cytochalasin D (CytD) at low concentrations inhibits actin polymerization, effectively blocking macropinocytosis and phagocytosis (Fig. 6B). Phenylarsine oxide (PAO) is an inhibitor of macropinocytosis and phagocytosis (Fig. 6C). Genistein (Gen) inhibits caveolae-mediated uptake, a clathrin-independent mechanism (Fig. 6D). Lastly, Dynasore (Dyn), a specific inhibitor of dynamin1/2 GTPase, inhibits clathrin-mediated endocytosis (Fig. 6E). Differentiated cells were treated with inhibitor for up to two hours prior to wash and co-treatment of cells with FITC-$A\beta_{42}$ and AD serum. In the control group, $A\beta_{42}$ internalization (Fig. 6A, middle bar) was enhanced when co-administered with AD serum (Fig. 6A, right bar), supporting our previous findings. None of the inhibitors except Dyn (Fig. 6E) significantly blocked $A\beta_{42}$ internalization, suggesting that the endocytic mechanism in question relies on dynamin1/2 in a clathrin-dependent fashion. Curiously, when supplemented with AD serum, the Dyn inhibition was overcome. Under these conditions, it appears that it is possible for $A\beta_{42}$ to be internalized via other mechanisms or by more than one mechanism at any one time. However, it is clear that the predominant means of its entry into cells is via classical receptor-mediated endocytic pathway, reliant on dynamin1/2 and clathrin. Representative micrographs of cells from the Dynasore treatment experiments (Fig. 6F) show the resulting differences in $A\beta_{42}$ accumulation under the different treatment parameters. Note the

stark difference in green signal (FITC-$A\beta_{42}$) in the Dynasore treated cells (top far-left) versus the same cells and parameters except for addition of AD serum (top middle-right). Also, a marked difference in the Dyn treated cells with $A\beta_{42}$ and AD serum versus that of the vehicle only is the extent of co-localization, rather than internalization. This is particularly interesting, in that although the $A\beta_{42}$ is seen internalized, the Dyn seemingly prevents the internalization to proceed directly with the aAbs in AD serum. Meanwhile, this phenomenon does recur, as expected, in the vehicle only group. Although $A\beta_{42}$ internalization is restored when AD serum is supplemented, this finding suggests that a different means by which $A\beta_{42}$ enters the cell may be occurring. This data gives rise to novel stimuli (i.e. aAb) for receptor-mediated endocytosis, making use of previously established mechanisms we now call aAb-mediated endocytosis.

aAb-mediated endocytosis requires a cross-linking step to precede internalization.

Antibody-mediated internalization is believed to require cross-linking of surface proteins bound to antibody prior to the triggering of endocytosis. If this step is a required first step in $A\beta_{42}$ internalization, then enzymatic cleavage of the aAbs derived from human serum to produce monovalent F(ab) fragments should block the induction of endocytosis. As performed in similar studies for other neurological conditions, reaction of monovalent aAb fragments with anti-F(ab) antibodies should be capable of restoring aAb cross-linking ability and rescue aAb-mediated endocytosis. Using immobilized papain treatment according to manufacturer's protocol (Pierce Fab Micro Preparation Kit), we successfully digested purified IgG

from AD serum, producing monovalent F(ab) fragments, which was confirmed using SDS-PAGE (Supp. Fig. 3). Next, cells were treated with monovalent F(ab) fragments in conjunction with $A\beta_{42}$. Another treatment included F(ab) fragments supplemented with antibodies directed to the F(ab) fragment, thus restoring cross-linking abilities with the now divalent antibody complex. The data suggests that monovalent antibodies are unable to induce any significant increase in $A\beta_{42}$ internalization compared to $A\beta_{42}$ alone, but when anti-F(ab) antibodies are supplied, cross-linking, and thus internalization, proceeds (Fig. 7).

Microarray data may lead to identification of aAb targets on the surface of neurons, with diagnostic and pathogenic implications.

The identity of the receptors to which the ubiquitous IgG aAbs bind is not known, and will be the focus of future investigations into this novel mechanism for the pathogenesis of the early stages in AD. In an effort to get a glimpse into the expansive repertoire of candidate epitope cognates, human protein microarray technologies were used. The 50 most prevalent aAb targets amongst young-aged non-demented control (green), old-aged non-demented control (blue), and AD patient (yellow) serum were chosen and listed in order of decreasing prevalence (Table 1).

FIGURES

Fig 1. Differentiated SH-SY5Y cell line as a model system.

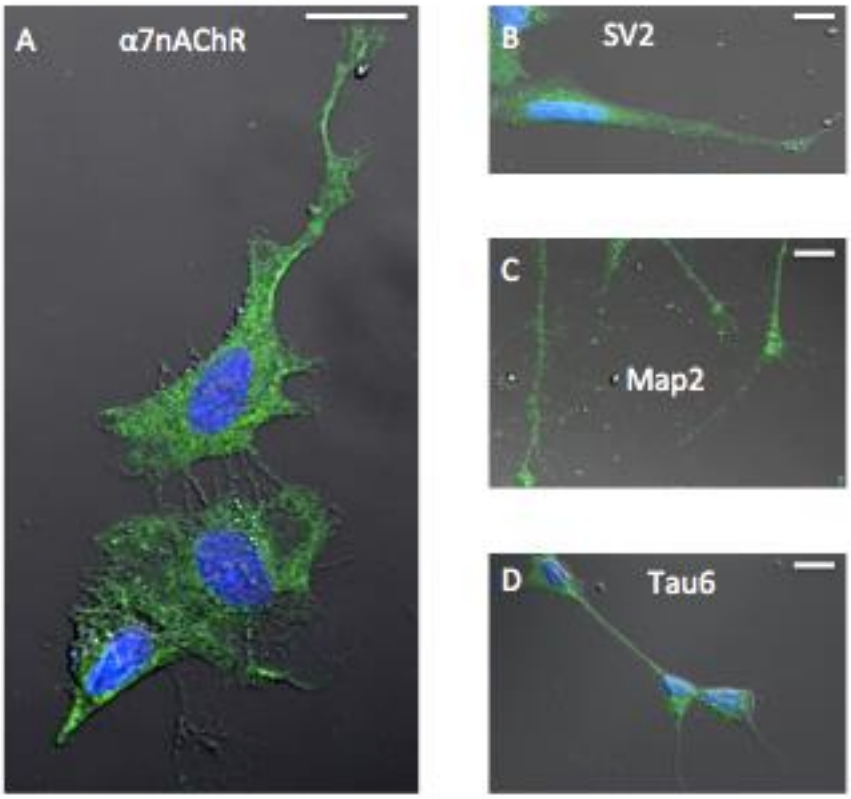

Figure 1: SH-SY5Y cells can be used as a model system for purpose of testing aAb-mediated $A\beta_{42}$ endocytosis.

Upon differentiation with retinoic acid (RA) for 72 hours, cells were surveyed for various neuronal markers of differentiation. Immunocytochemistry and confocal microscopy revealed that (Fig. 1A) α7nAChR, (Fig. 1B) SV2, (Fig. 1C) Map2, and (Fig. 1D) Tau6 were all expressed and appropriately distributed throughout the cell. Moreover, axon- or dendrite-like neuronal processes were present amongst and between cultured cells upon differentiation, further supporting the differentiated status.

Supplemental Fig. 1. Retinoic acid does not effect $A\beta_{42}$ internalization.

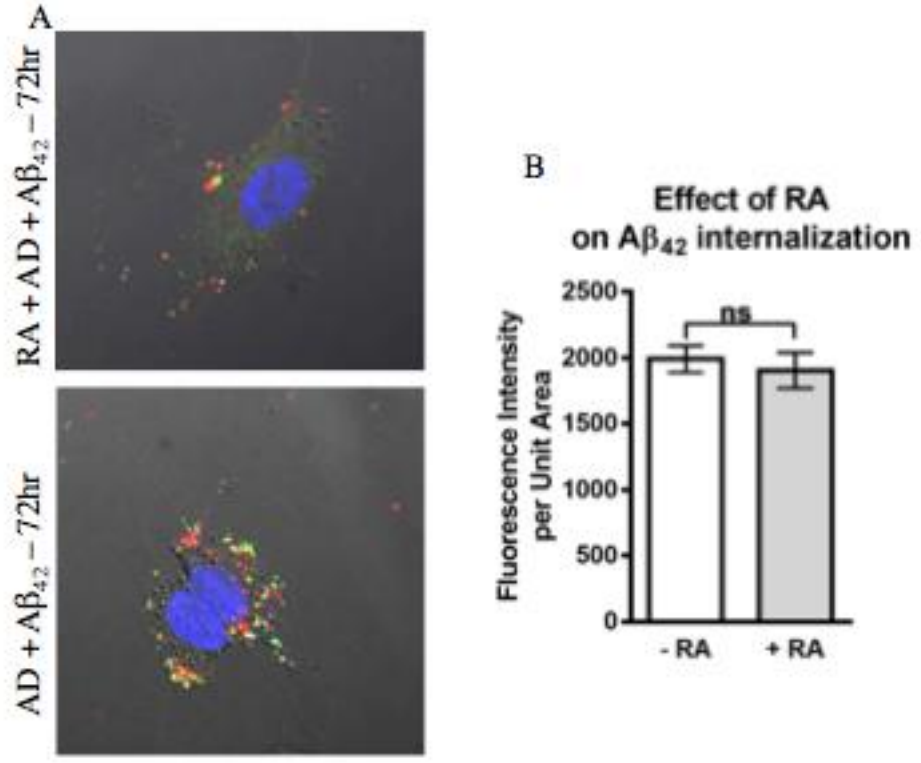

Supplemental Figure 1: RA does not affect $A\beta_{42}$ internalization rates over 72 hours.

The effect of RA on $A\beta_{42}$ internalization was tested to minimize bias and as an added control to validate future experiments using this cell culture system. We show, using double immunofluorescence confocal microscopy that FITC-$A\beta_{42}$ is endocytosed at similar rates regardless of whether or not RA is included in the treatment medium. Representative micrographs (Supp. Fig. 1A) show similar cell morphology and $A\beta_{42}$ localization. No statistically significant differences in $A\beta_{42}$ internalization were noted when differentiated cells are given RA throughout the course of $A\beta_{42}$ treatment (Supp. Fig. 1B), as in future experiments performed.

Fig 2. $A\beta_{42}$ is trafficked through endosome-lysosome pathway upon internalization.

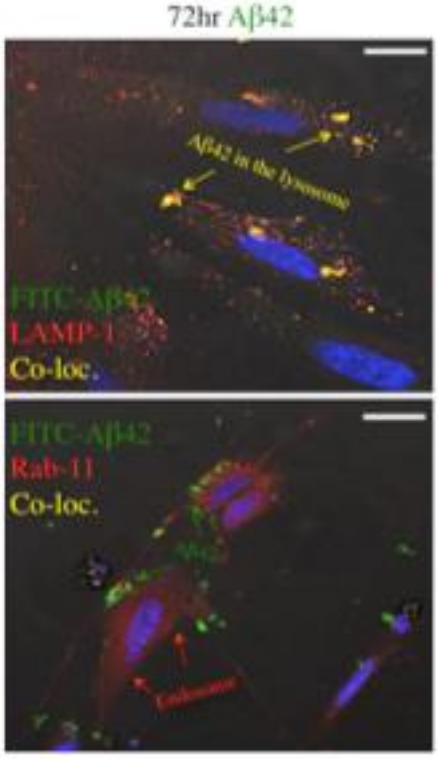

Figure 2: $A\beta_{42}$ is trafficked through the endosome-lysosome pathway after internalization.

Upon internalization, $A\beta_{42}$ is trafficked through the endosome-lysosome pathway en route to attempted degradation in the lysosomal compartment. Differentiated SH-SY5Y cells were treated with 100nM FITC-$A\beta_{42}$ in serum free media for 3-, 24-, 48-, or 72-hours. At completion of the time course, cells were fixed and processed for immunofluorescence confocal microscopy using standard immunocytochemistry protocols. The representative micrographs show cells from the 72-hour experiment with $A\beta_{42}$ (green) co-localized with the lysosome (red), as detected using LAMP-1 antibody showing a yellow color signifying an overlay of the green and red channels (top). At the same time point, $A\beta_{42}$ did not co-localize with the early endosome marker Rab-11 (red), as seen in the lower panel as two separate colors – green and red (bottom).

Fig 3. $A\beta_{42}$ internalization was enhanced in the presence of serum with autoantibodies directed at surface proteins.

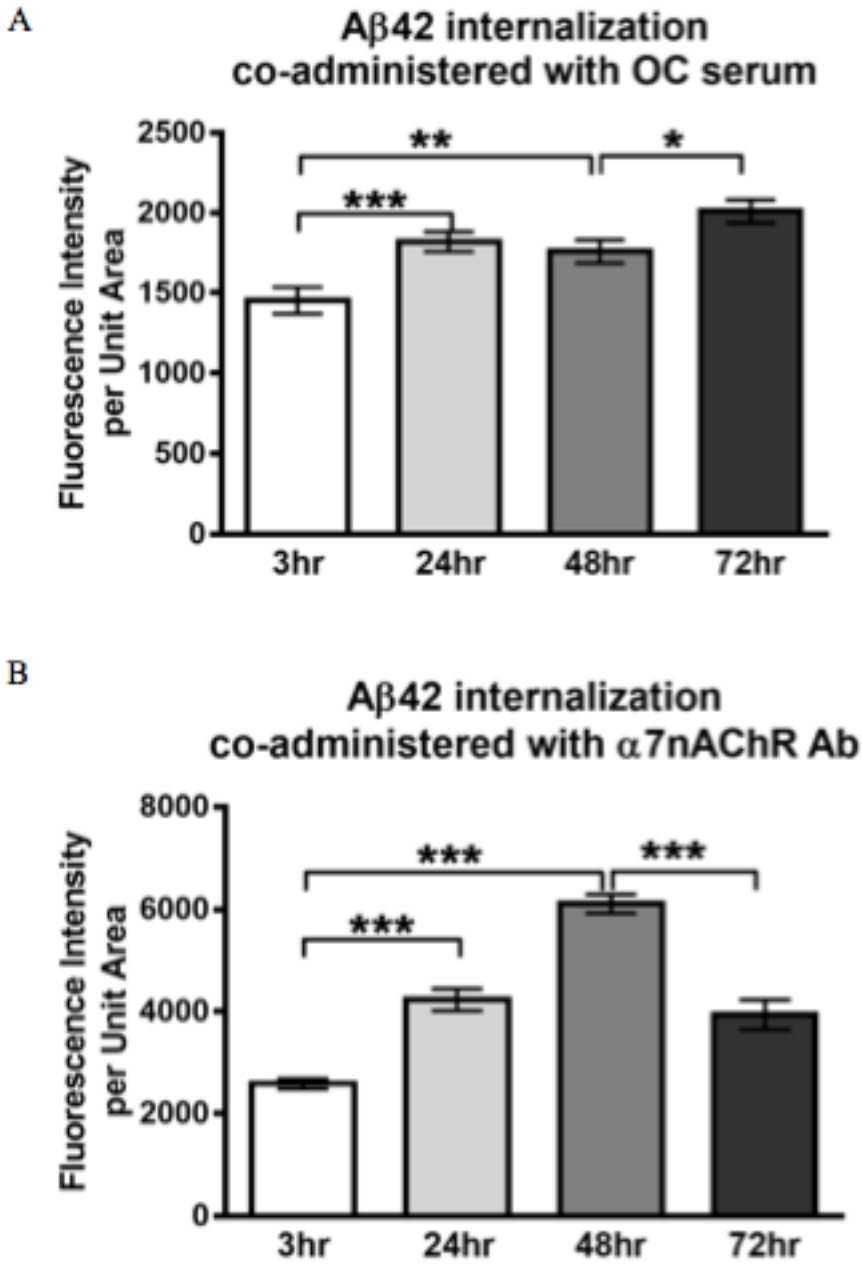

Figure 3: Autoantibodies present in human serum enhance $A\beta_{42}$ internalization.

Differentiated SH-SY5Y cells were treated with $A\beta_{42}$ supplemented with human serum or commercial antibody directed at a known surface receptor, the α7nAChR. Human serum from the old-aged non-demented control was used at 1:50 dilution in serum-free medium, and was supplemented in the culture treatment media containing FITC-$A\beta_{42}$. Cells were incubated for 3-, 24-, 48-, and 72-hours with $A\beta_{42}$ in the presence of human serum or α7nAChR antibodies as a positive control. Graphical representations of the data showed that the presence of human serum (Fig. 3A) significantly raises the levels of intracellular $A\beta_{42}$ compared to controls at each time point, and continues on through 72 hours. By contrast, the effect of an antibody directed towards a known surface receptor (α7nAChR) was more potent than that of adding whole human serum (Fig. 3B), but there is a significant drop in the amount of detectable internalized $A\beta_{42}$ after 48 hours.

Fig 4. Lysosomal compartment expansion occurs with longer incubation with $A\beta_{42}$.

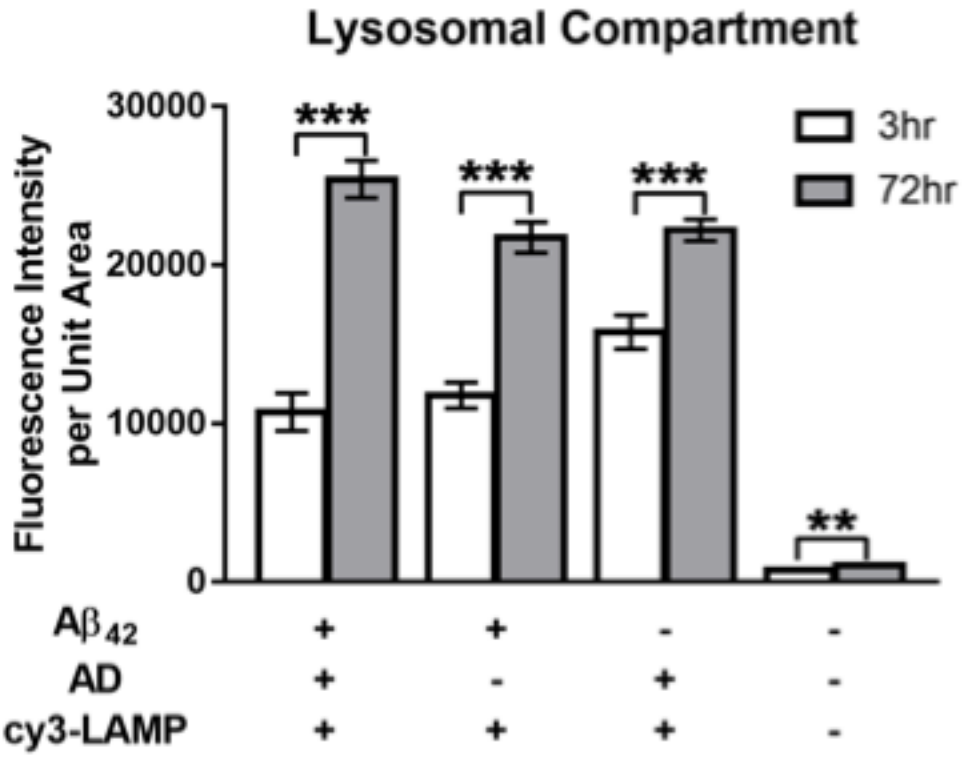

Figure 4: Lysosomal compartment expansion occurs over longer periods of incubation with $A\beta_{42}$.

Neurons in human brain AD sections have been shown to undergo dramatic lysosomal compartment expansion when compared to control brains. This most likely reflects the underlying mechanism of $A\beta_{42}$ endocytosis, and its being rendered non-digestible as it is progressively acidified within the lysosome. As a result of accumulating non-digestible $A\beta_{42}$-positive vesicles, they are forced to coalesce and fuse with one another, effectively taking up more and more of the total cytoplasmic volume in the cell. Differentiated cells were treated for 3- and 72-hours with 100nM FITC-$A\beta_{42}$ with or without human AD serum. Cells were then fixed and immunostained for LAMP-1, a marker for the lysosome. The intensity of the LAMP-1 staining was quantified and graphed (Fig. 4). In all cases, LAMP-1 levels were elevated as a function of time, comparing the 3- and the 72-hour treatments with one another. Interestingly, the most significant change in the relative size of the lysosomal compartment came when cells were treated with both $A\beta_{42}$ and AD serum, in agreement with previous results. This also may reflect a synergistic, or even just compounded, effect that AD serum aAb components have on $A\beta_{42}$ internalization and accumulation within lysosomal vesicles.

Fig 5. $A\beta_{42}$ internalization is enhanced by IgG fraction of AD serum.

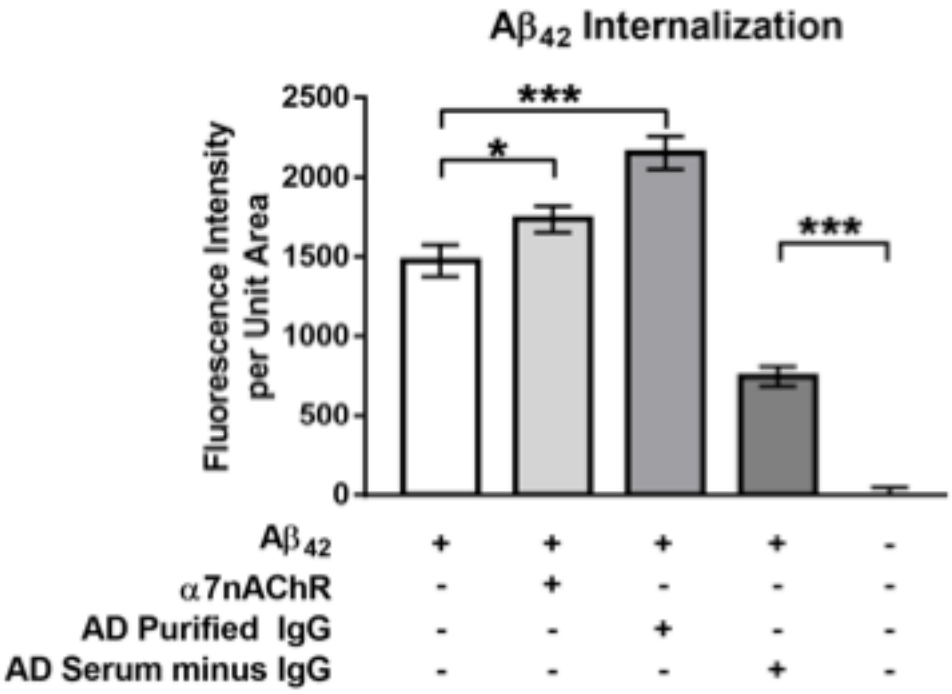

Figure 5: IgG aAbs present in human serum enhance the internalization of $A\beta_{42}$.

IgG purified from AD serum (AD purified IgG) was used alongside AD serum without IgG (AD serum minus IgG), as well as an antibody to a known neuronal surface receptor, α7nAChR. $A\beta_{42}$ internalization was assayed in the context of these parameters and results are shown in Figure 5. The amount of internalized FITC-$A\beta_{42}$ was quantified based on signal intensity per unit area and plotted as shown in the representative bar graph. In the group treated with 100nM $A\beta_{42}$ alone, baseline internalized $A\beta_{42}$ is compared to that with α7nAChR antibody, AD purified IgG, and AD serum without IgG supplementation. These results demonstrate that the IgG fraction of serum, that is the IgG neuron-binding aAb fraction, specifically participates in the enhancement of $A\beta_{42}$ internalization, and no other components in the serum.

Supplemental Fig 2. IgG purified from AD serum using spin-column chromatography.

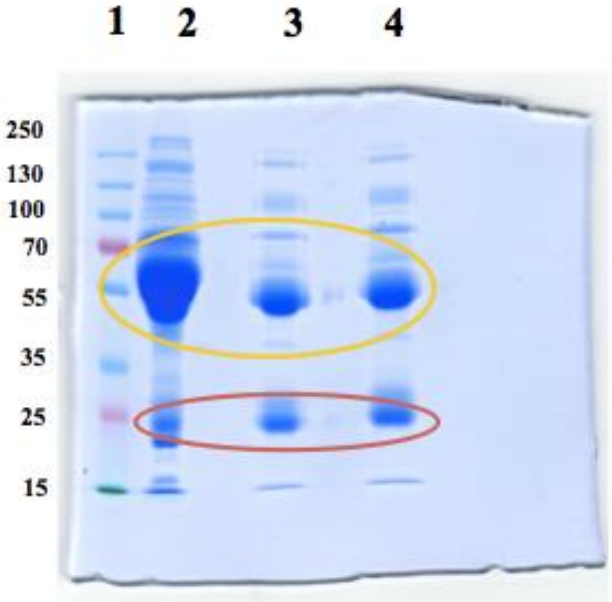

1. **Protein ladder**
2. **Whole serum**
3. **Purified serum 1-13-16**
4. **Purified serum 1-19-16**

Heavy Chain (~ 55 kDa)

Light Chain (~ 20 kDa)

Supplemental Figure 2: Purification of IgG from human serum.

IgG was purified from AD serum using a spin-column chromatography (Pierce Melon Gel IgG Purification Kit) according to manufacturer's protocol and confirmed using SDS-PAGE (Supp. Fig. 2) and absorption at 280nm. The gel shows bands from whole AD serum (lane 2), and IgG purified from the AD serum sample (lanes 3 and 4). Expected yields are roughly 80%. Bands at ~55kDa and ~20kDa correspond to the immunoglobulin heavy and light chains respectively.

Fig. 6. aAb-mediated $A\beta_{42}$ internalization proceeds through classic receptor endocytosis.

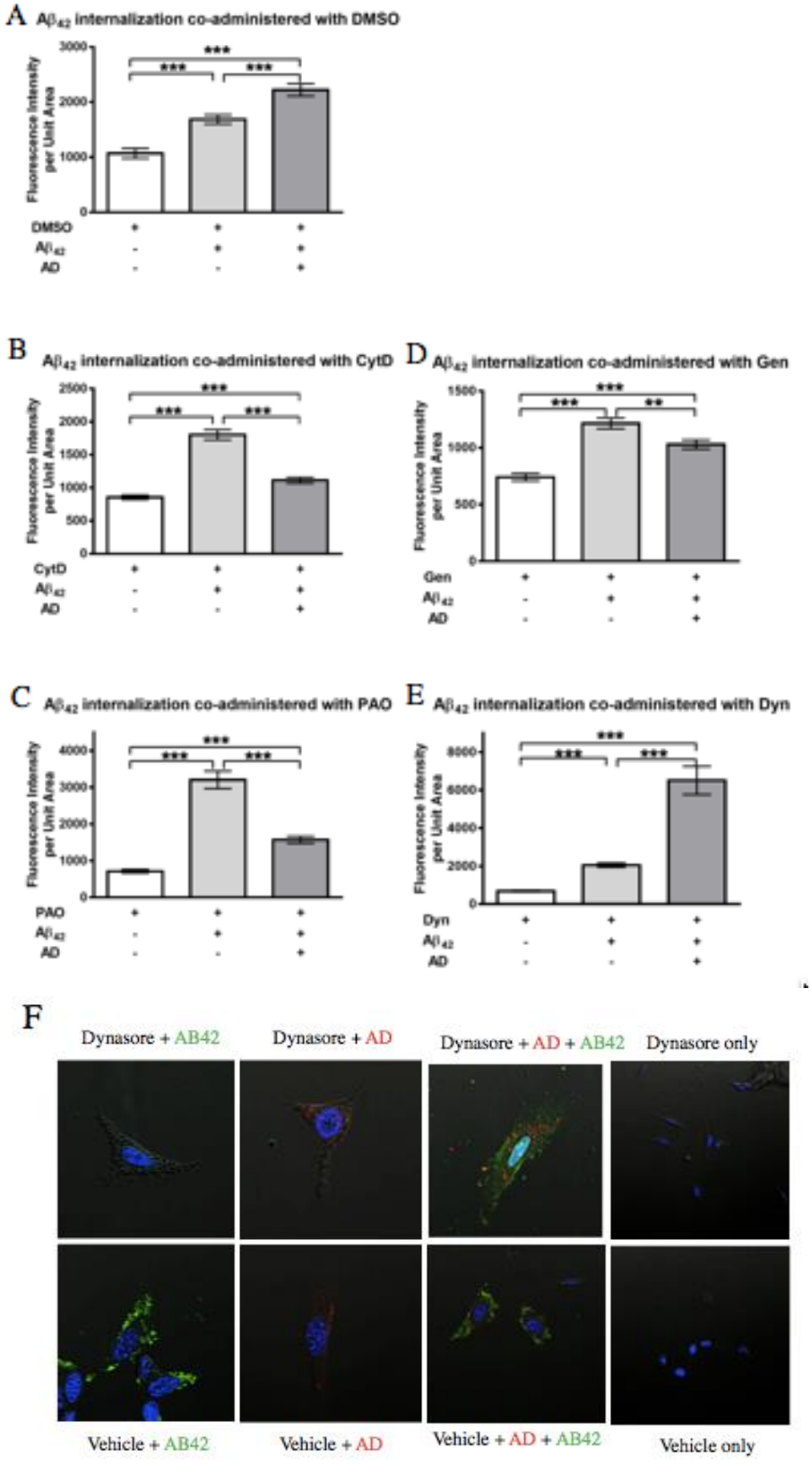

Figure 6: aAb-enhanced $A\beta_{42}$ internalization relies on dynamin1/2 and clathrin-mediated mechanisms predominantly.

Vehicle (0.01% DMSO) was used as a control to show normal endocytosis outcomes of $A\beta_{42}$ or AD serum treatment (Fig. 6A). Cytochalasin D (CytD) at low concentrations inhibits actin polymerization, effectively blocking macropinocytosis and phagocytosis (Fig. 6B). Phenylarsine oxide (PAO) is an inhibitor of macropinocytosis and phagocytosis (Fig. 6C). Genistein (Gen) inhibits caveolae-mediated uptake, a clathrin-independent mechanism (Fig. 6D). Lastly, Dynasore (Dyn), a specific inhibitor of dynamin1/2 GTPase, inhibits clathrin-mediated endocytosis (Fig. 6E). Differentiated cells were treated with inhibitor for up to two hours prior to wash and FITC-$A\beta_{42}$ co-administered with AD serum. Representative micrographs of cells from the Dynasore treatment experiments (Fig. 6F) show the differences in $A\beta_{42}$ accumulation under different treatment parameters. Note the stark difference in green signal (FITC-$A\beta_{42}$) in the Dynasore treated experiment (top far-left) versus the same parameters except for AD serum (top middle-right).

Fig. 7. aAb-mediated endocytosis requires a cross-linking step to precede internalization.

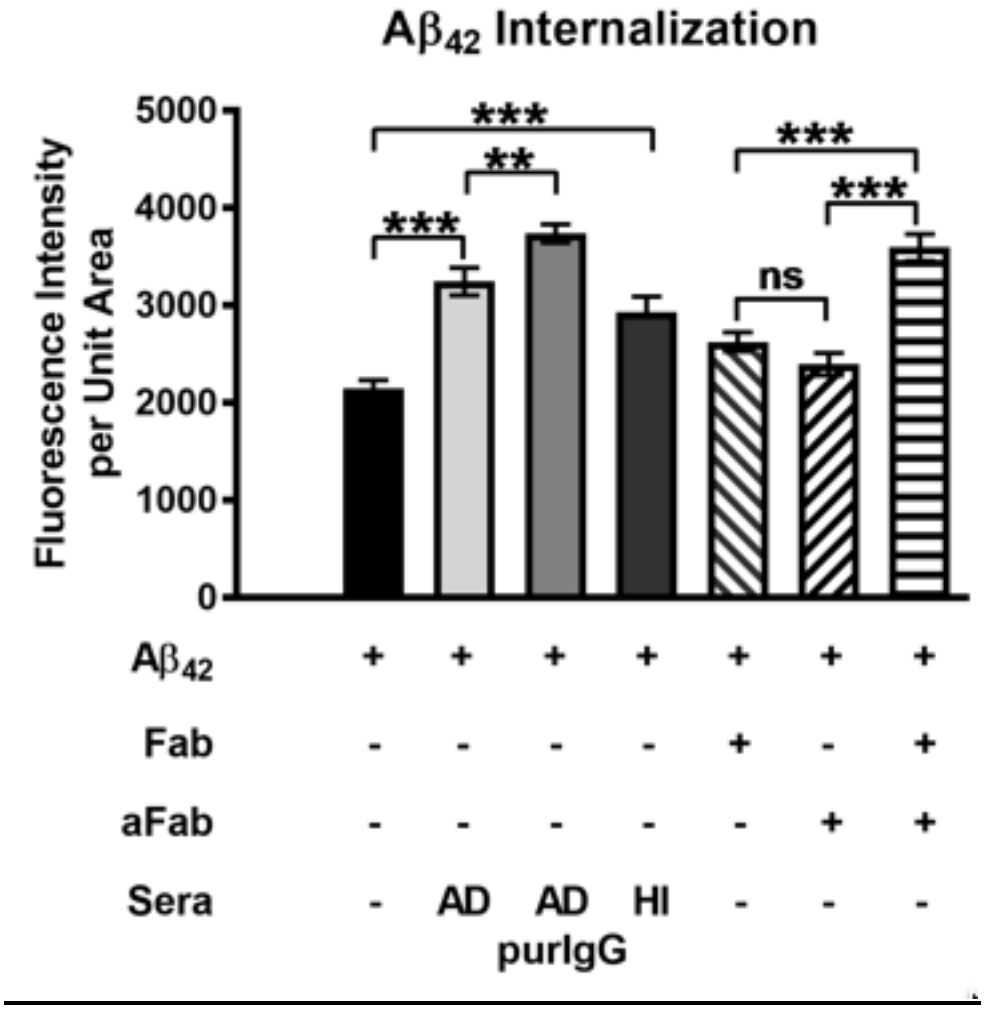

Figure 7: aAb-mediated endocytosis requires a cross-linking step prior to internalization.

Cells were treated with monovalent F(ab) fragments, incapable of cross-linking, in conjunction with $A\beta_{42}$. Next, media was supplemented with antibodies directed to the F(ab) fragment, thus restoring cross-linking abilities with the now divalent antibody complex. Heat inactivated (HI) serum was used to exclude complement-mediated internalization mechanisms as a means of $A\beta_{42}$ entry into the cell.

Supplemental Fig 3. F(ab) fragment preparation using papain.

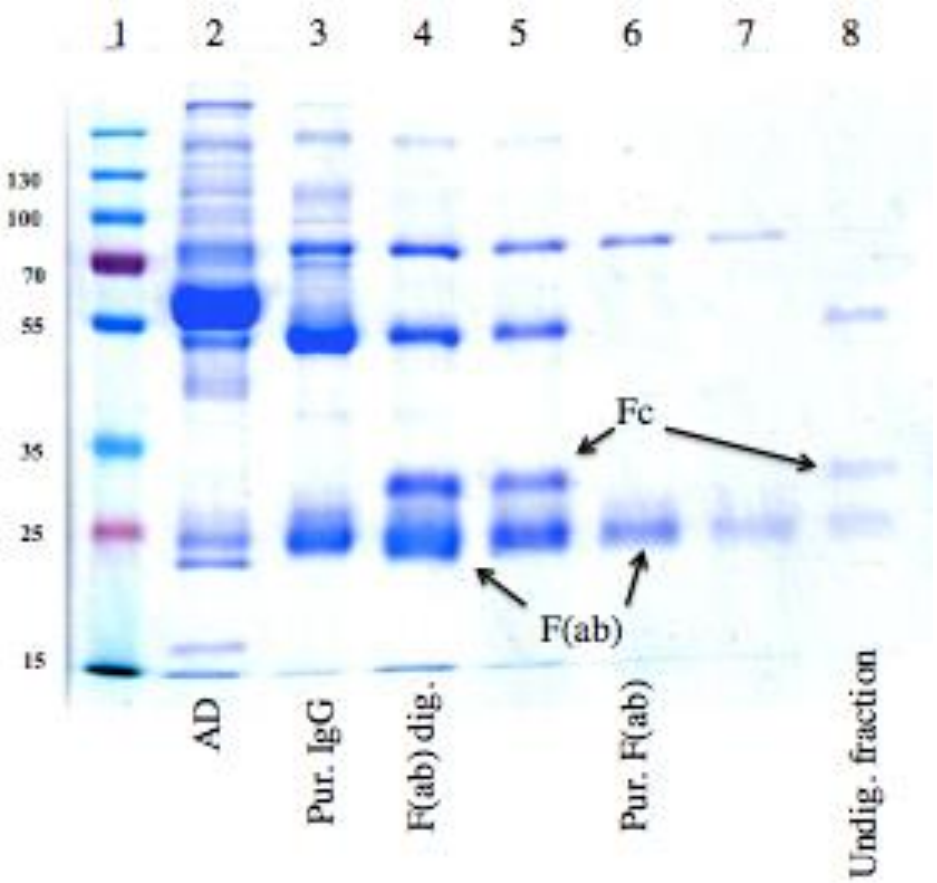

Supplemental Figure 3: F(ab) fragment preparation confirmed with reducing SDS-PAGE condition.

Using immobilized papain treatment according to manufacturer's protocol (Pierce Fab Micro Preparation Kit), purified IgG (lane 3) from AD serum (lane 2) was successfully digested into F(ab) fragments (lanes 4-5), and then purified (lanes 6-7). Undigested fraction was removed from the column after F(ab) purification step to confirm the presence of undigested IgG and Fc portions. Bands of ~27kDa and ~25kDa correspond to the Fc and F(ab) fragments, respectively. Note the removal of the Fc portion in the purified F(ab) fraction (lanes 6-7) was used for experimental conditions.

Table 1: Top 50 most prevalent aAb targets.

Young-aged non-demented control	Old-aged non-demented control	Old-aged matched AD
N-methylpurine-DNA glycosylase (MPG)	elaC homolog 1 (E. coli) (ELAC1)	protein phosphatase 1, regulatory (inhibitor) subunit 10 (PPP1R10)
NRP1 / Neuropilin-1 Protein	UBX domain containing 1 (UBXD1)	NRP1 / Neuropilin-1 Protein
Interferon alpha 7 / IFNA7 Protein	BMPR1A Recombinant Human Protein	S100A1 Protein
EphrinB2 / EFNB2 Protein	Interferon beta / IFN-beta / IFNB Protein	Isocitrate dehydrogenase [NADP] cytoplasmic
Interferon beta / IFN-beta / IFNB Protein	N-methylpurine-DNA glycosylase (MPG)	Interferon beta / IFN-beta / IFNB Protein
Interferon alpha 10 / IFNA10 Protein	folliculin (FLCN), transcript variant 2	chromatin assembly factor 1, subunit B (p60) (CHAF1B)
IL2Ra / CD25 Protein	Interferon alpha 7 / IFNA7 Protein	N-methylpurine-DNA glycosylase (MPG)
phosphorylase kinase, gamma 2 (testis)	EphrinB2 / EFNB2 Protein	CD27 / TNFRSF7 Protein
interferon, alpha-inducible protein 6 (IFI6)	IL1R1 / CD121a Protein	PD1 / PDCD1 Protein
leukocyte receptor cluster (LRC) member 1 (LENG1)	tripartite motif-containing 21 (TRIM21)	Serine/threonine-protein kinase PAK 1
TREM1 Protein	Kelch-like ECH-associated protein 1	EphrinB2 / EFNB2 Protein
PD-L2 / B7-DC / CD273 Protein	synaptotagmin-like 2 (SYTL2), transcript variant a	folliculin (FLCN), transcript variant 2
IL2RB Protein	LIM and senescent cell antigen-like-containing domain protein 1	KIAA1143 (KIAA1143)
cDNA clone MGC:27376 IMAGE:4688477, complete cds	tubulin polymerization promoting protein (TPPP)	Interferon alpha 7 / IFNA7 Protein
PD-L1 Protein	bromodomain adjacent to zinc finger domain, 2B, mRNA (cDNA clone IMAGE:4290975), complete cds.	Wolf-Hirschhorn syndrome candidate 2 (WHSC2)
endosulfine alpha (ENSA), transcript variant 3	PREDICTED: Homo sapiens hypothetical protein LOC283663 (LOC283663), mRNA	IL2RB Protein

myosin, light chain 9, regulatory (MYL9), transcript variant 2, mRNA.	cDNA clone MGC:32654 IMAGE:4701898, complete cds	prune homolog 2 (Drosophila) (PRUNE2)
cDNA clone MGC:22645 IMAGE:4700961, complete cds	cDNA clone MGC:22645 IMAGE:4700961, complete cds	ubiquitin associated protein 1 (UBAP1)
oligonucleotide/oligosaccharide-binding fold containing 2A (OBFC2A)	Interferon alpha 10 / IFNA10 Protein	IL1R1 / CD121a Protein
Endoglin / CD105 / ENG Protein	cDNA clone MGC:23888 IMAGE:4704496, complete cds	Mucin-1 / MUC-1 Protein (Fc Tag)
Transcription cofactor HES-6	phosphorylase kinase, gamma 2 (testis)	tripartite motif-containing 21 (TRIM21)
membrane protein, palmitoylated 3 (MAGUK p55 subfamily member 3) (MPP3), transcript variant 1	interferon, alpha-inducible protein 6 (IFI6)	PD-L1 Protein
folliculin (FLCN), transcript variant 2	cDNA clone MGC:27376 IMAGE:4688477, complete cds	LIM and senescent cell antigen-like-containing domain protein 1
CD27 / TNFRSF7 Protein	Mucin-1 / MUC-1 Protein (Fc Tag)	IL2Ra / CD25 Protein
Splicing factor 1	cDNA clone MGC:31936 IMAGE:4765518, complete cds	cDNA clone MGC:32654 IMAGE:4701898, complete cds
ACE2 / ACEH Protein	Acti-Vin R1b Recombinant Human Protein	CD14 Protein
IL27Ra / TCCR / WSX1 Protein	IL2Ra / CD25 Protein	hypothetical protein LOC403312 (MGC39545)
Calpastatin	TREM1 Protein	Dual specificity mitogen-activated protein kinase kinase 6
cDNA clone MGC:32654 IMAGE:4701898, complete cds	serine/threonine kinase 40 (STK40)	Interferon alpha 10 / IFNA10 Protein
piccolo (presynaptic cytomatrix protein) (PCLO)	CD14 Protein	cDNA clone MGC:22645 IMAGE:4700961, complete cds
BMPR1A Recombinant Human Protein	melanoma antigen family B, 4 (MAGEB4)	JAG1 / JAGL1 / CD339 Protein

BCL2-associated athanogene 3 (BAG3)	B-NGF / Beta-NGF Protein (Native)	Syntaxin-10
IL3RA / CD123 Protein	cDNA clone MGC:88796 IMAGE:6295732, complete cds	WAS/WASL-interacting protein family member 1
5'-nucleotidase domain containing 1 (NT5DC1)	ubiquitin associated protein 1 (UBAP1)	cDNA clone MGC:27376 IMAGE:4688477, complete cds
cDNA clone MGC:40426 IMAGE:5178085, complete cds	RD RNA binding protein (RDBP)	chromosome 19 open reading frame 40 (C19orf40)
3-hydroxybutyrate dehydrogenase, type 2 (BDH2)	IL27Ra / TCCR / WSX1 Protein	interferon, alpha-inducible protein 6 (IFI6)
cyclin-dependent kinase 5, regulatory subunit 1 (p35) (CDK5R1)	cDNA clone MGC:88813 IMAGE:6302307, complete cds	cDNA clone MGC:31936 IMAGE:4765518, complete cds
RNA binding motif protein 12 (RBM12), transcript variant 1, mRNA	ACE2 / ACEH Protein	TREM1 Protein
microtubule-associated protein, RP/EB family, member 2 (MAPRE2)	cDNA clone MGC:12418 IMAGE:3934658, complete cds	Acti-Vin R1b Recombinant Human Protein
musculoskeletal, embryonic nuclear protein 1 (MUSTN1)	cDNA clone IMAGE:3050953, **** WARNING: chimeric clone ****	leukocyte receptor cluster (LRC) member 1 (LENG1)
mannosyl (alpha-1,6-)-glycoprotein beta-1,6-N-acetyl-glucosaminyltransferase, isozyme B (MGAT5B)	coiled-coil-helix-coiled-coil-helix domain containing 2 (CHCHD2)	cDNA clone MGC:88796 IMAGE:6295732, complete cds
doublecortin-like kinase 1 (DCLK1)	zinc binding alcohol dehydrogenase, domain containing 2 (ZADH2)	Usher syndrome 1C (autosomal recessive, severe) (USH1C)
cyclin B3 (CCNB3), transcript variant 2	CD27 / TNFRSF7 Protein	Family with sequence similarity 9, member B (FAM9B), mRNA
cDNA clone MGC:31944 IMAGE:4878869, complete cds	2',5'-oligoadenylate synthetase 1, 40/46kDa (OAS1), transcript variant 1	PD-L2 / B7-DC / CD273 Protein
cDNA clone MGC:31936 IMAGE:4765518, complete cds	twinfilin, actin-binding protein, homolog 1 (Drosophila) (TWF1)	thioredoxin 2 (TXN2), nuclear gene encoding mitochondrial protein

Table 1: Potential candidate aAb targets.

Human protein microarray data of IgG aAbs present in serum across age and disease gives rise to candidate aAb targets. Further data will be needed to begin narrowing down potential targets with those of surface (specifically neuronal surface) proteins. The 50 most prevalently expressed aAb targets amongst young-aged non-demented control (green), old-aged non-demented control (blue), and AD patient serum (yellow) were chosen and listed in order of decreasing prevalence.

DISCUSSION

The blood-brain barrier (BBB) compartmentalizes the peripheral blood from the immunoprivileged brain. With that function comes the responsibility to stringently control what enters into the brain parenchyma, as neuronal homeostatic balance is highly sensitive to minor perturbations. Consequent to a compromised BBB is the indiscriminate leakage of blood components, like amyloid proteins (namely $A\beta_{42}$) and immunoglobulins (namely IgG), including neuron-binding autoantibodies (aAbs). We have proposed a novel mechanism of amyloid plaque (AP) development in the early stages of Alzheimer's disease (AD), whereby chronic loading of $A\beta_{42}$ in the neurons is what eventually causes lysis and gives rise to the APs. Given that neuron-binding aAbs and $A\beta_{42}$ binding to the surface of neurons can both independently cause endocytosis, we sought to address if the $A\beta_{42}$ loading is enhanced, and by what physiologic mechanism does this process occur.

Following in the footsteps of other diseases with known aAb components to them, like NMDAR encephalitis (a classical autoimmune disorder), experiments were designed to address the role that aAbs play in neuronal endocytosis of $A\beta_{42}$ bound to their surfaces. We have successfully demonstrated that the autoreactive IgG species of antibodies (autoantibodies) within human serum, irrespective of age and disease, were able to bind the surfaces of differentiated SH-SY5Y cells, a translatable model system established to probe into the cellular aspects of various neuronal functions. We showed that exogenous $A\beta_{42}$ like that entering into the brain from the blood in

vivo, proceeds through the endosome-lysosome pathway likely en route to eventual degradation within the lysosomal system. However, within the low pH environment of the lysosome, the internalized $A\beta_{42}$ begins to aggregate and fibrillize, forming non-digestible and insoluble amyloid deposits that progressively increase in volume over time. Furthermore, the endocytic machinery used predominantly by this pathway was shown, using our series of inhibitors, to likely proceed through a dynamin1/2-dependent, clathrin-mediated form of internalization. However, it is thought that $A\beta_{42}$ may undergo internalization by several different mechanisms, depending on its state of aggregation at the time of contact (i.e. monomeric, oligomeric, or fibrillary). Given the increased hydrophobicity of the transmembrane domain of the $A\beta_{42}$, a caveolin-mediated, clathrin-independent pathway has been hypothesized, and is an active area of research to better understand this mechanism. Taken together, the data presented here suggests that $A\beta_{42}$ enters neurons primarily through a clathrin-dependent pathway, but that a lesser amount may also be continually entering cells via another independent pathway. This aspect is further complicated when seen in a more physiological context of serum supplementing the $A\beta_{42}$ effect on internalization. Although the $A\beta_{42}$ internalization is re-established, it no longer co-localizes with the AD serum IgG aAbs. It is conceivable that this latter clathrin-independent pathway may be operating as the primary means of entry in situations where the individual is lacking aAbs that target abundant neuronal surface proteins.

Thousands of aAbs are present in the sera of individuals, and can be used for diagnostic purposes. From a mechanistic standpoint, however, we are interested in

knowing the cognate receptors to which the aAbs bind on the surface of neurons in the presence of soluble, exogenous $A\beta_{42}$, also bound to neuronal cell surface membranes that could participate in the observed enhanced endocytosis. Protein microarray platforms have been extensively used for the purposes of characterizing the aAb profiles present in the serum, and make for an equally sensitive and specific means to assay aAbs in this context as well. Unfortunately, very little is known about the specific aAb candidate biomarkers that have thus far been identified in our microarray studies, and as such, it will be the focus of future studies to discern associated from causative protein targets.

In conclusion, our study has helped to solidify a hypothesis that describes the pathoetiology of AD, in particular the mode of $A\beta_{42}$ entry into the brain and neurons, leading to amyloid plaque formation, one of the pathological hallmarks of AD. Furthermore, our results give strength to the concept that BBB breakdown may be the disease trigger for AD, thus highlighting this aspect of AD as a new treatment target.

REFERENCES

Acharya, N. K., E. C. Levin, P. M. Clifford, M. Han, R. Tourtellotte, D. Chamberlain, M. Pollaro, N. J. Coretti, M. C. Kosciuk, E. P. Nagele, C. Demarshall, T. Freeman, Y. Shi, C. Guan, C. H. Macphee, R. L. Wilensky, and R. G. Nagele. 2013. "Diabetes and hypercholesterolemia increase blood-brain barrier permeability and brain amyloid deposition: beneficial effects of the LpPLA2 inhibitor darapladib." *J Alzheimers Dis* 35 (1):179-98. doi: 10.3233/JAD-122254.

Bouras, C., B. M. Riederer, E. Kovari, P. R. Hof, and P. Giannakopoulos. 2005. "Humoral immunity in brain aging and Alzheimer's disease." *Brain Res Brain Res Rev* 48 (3):477-87. doi: S0165-0173(04)00126-2 [pii]10.1016/j.brainresrev.2004.09.009.

Carey, R. M., B. A. Balcz, I. Lopez-Coviella, and B. E. Slack. 2005. "Inhibition of dynamin-dependent endocytosis increases shedding of the amyloid precursor protein ectodomain and reduces generation of amyloid beta protein." *BMC Cell Biol* 6:30. doi: 10.1186/1471-2121-6-30.

Chyung, J. H., and D. J. Selkoe. 2003. "Inhibition of receptor-mediated endocytosis demonstrates generation of amyloid beta-protein at the cell surface." *J Biol Chem* 278 (51):51035-43. doi: 10.1074/jbc.M304989200.

Clifford, P. M., G. Siu, M. Kosciuk, E. C. Levin, V. Venkataraman, M. R. D'Andrea, and R. G. Nagele. 2008. "Alpha7 nicotinic acetylcholine receptor expression by vascular smooth muscle cells facilitates the deposition of Abeta peptides and promotes cerebrovascular amyloid angiopathy." *Brain Res* 1234:158-71. doi: S0006-8993(08)01811-8 [pii]10.1016/j.brainres.2008.07.092 [doi].

Clifford, P. M., S. Zarrabi, G. Siu, K. J. Kinsler, M. C. Kosciuk, V. Venkataraman, M. R. D'Andrea, S. Dinsmore, and R. G. Nagele. 2007. "Abeta peptides can enter the brain through a defective blood-brain barrier and bind selectively to neurons." *Brain Res* 1142:223-36. doi: S0006-8993(07)00127-8 [pii]10.1016/j.brainres.2007.01.070 [doi].

Cossec, J. C., A. Simon, C. Marquer, R. X. Moldrich, C. Leterrier, J. Rossier, C. Duyckaerts, Z. Lenkei, and M. C. Potier. 2010. "Clathrin-dependent APP endocytosis and Abeta secretion are highly sensitive to the level of plasma membrane cholesterol." *Biochim Biophys Acta* 1801 (8):846-52. doi: 10.1016/j.bbalip.2010.05.010.

D'Andrea, M. R., Nagele, R. G., Wang, H-Y., Peterson, P. A., Lee, D. H. 2001. "Evidence that neurones accumulating amyloid can undergo lysis to form amyloid plaques in Alzheimer's disease." *Histopathology* 38:120-134.

DeMarshall, C. A., M. Han, E. P. Nagele, A. Sarkar, N. K. Acharya, G. Godsey, E. L. Goldwaser, M. Kosciuk, U. Thayasivam, B. Belinka, and R. G. Nagele. 2015. "Potential utility of autoantibodies as blood-based biomarkers for early detection and diagnosis of Parkinson's disease." *Immunol Lett* 168 (1):80-8. doi: 10.1016/j.imlet.2015.09.010.

Doherty, G. J., and H. T. McMahon. 2009. "Mechanisms of endocytosis." *Annu Rev Biochem* 78:857-902. doi: 10.1146/annurev.biochem.78.081307.110540.

Elkin, S. R., A. M. Lakoduk, and S. L. Schmid. 2016. "Endocytic pathways and endosomal trafficking: a primer." *Wien Med Wochenschr*. doi: 10.1007/s10354-016-0432-7.

Goldwaser, E. L., Acharya, N. K., Nagele, R. G. 2015. "Cerebrovascular and Blood-brain barrier compromise: A mechanistic link between Vascular disease and Alzheimer's disease subtypes of Neurocognitive disorders." *J Parkinsons Dis Alzheimer Dis* 2 (2):10.

Hammer, C., B. Stepniak, A. Schneider, S. Papiol, M. Tantra, M. Begemann, A. L. Siren, L. A. Pardo, S. Sperling, S. Mohd Jofrry, A. Gurvich, N. Jensen, K. Ostmeier, F. Luhder, C. Probst, H. Martens, M. Gillis, G. Saher, F. Assogna, G. Spalletta, W. Stocker, T. F. Schulz, K. A. Nave, and H. Ehrenreich. 2014. "Neuropsychiatric disease relevance of circulating anti-NMDA receptor autoantibodies depends on blood-brain barrier integrity." *Mol Psychiatry* 19 (10):1143-9. doi: 10.1038/mp.2013.110.

Han, M., E. Nagele, C. DeMarshall, N. Acharya, and R. Nagele. 2012. "Diagnosis of Parkinson's disease based on disease-specific autoantibody profiles in human sera." *PLoS One* 7 (2):e32383. doi: 10.1371/journal.pone.0032383.

Harris, V. K., and S. A. Sadiq. 2014. "Biomarkers of therapeutic response in multiple sclerosis: current status." *Mol Diagn Ther* 18 (6):605-17. doi: 10.1007/s40291-014-0117-0.

Hughes, E. G., X. Peng, A. J. Gleichman, M. Lai, L. Zhou, R. Tsou, T. D. Parsons, D. R. Lynch, J. Dalmau, and R. J. Balice-Gordon. 2010. "Cellular and synaptic mechanisms of anti-NMDA receptor encephalitis." *J Neurosci* 30 (17):5866-75. doi: 10.1523/jneurosci.0167-10.2010.

Jang, S. K., J. M. Yu, S. T. Kim, G. H. Kim, W. Park da, I. Lee do, and S. S. Joo. 2015. "An Abeta42 uptake and degradation via Rg3 requires an activation of caveolin, clathrin and Abeta-degrading enzymes in microglia." *Eur J Pharmacol* 758:1-10. doi: 10.1016/j.ejphar.2015.03.071.

Kandimalla, K. K., O. G. Scott, S. Fulzele, M. W. Davidson, and J. F. Poduslo. 2009. "Mechanism of neuronal versus endothelial cell uptake of Alzheimer's disease amyloid beta protein." *PLoS One* 4 (2):e4627. doi: 10.1371/journal.pone.0004627.

Koo, E. H., and S. L. Squazzo. 1994. "Evidence that production and release of amyloid beta-protein involves the endocytic pathway." *J Biol Chem* 269 (26):17386-9.

Kuboyama, T., Y. A. Lee, H. Nishiko, and C. Tohda. 2015. "Inhibition of clathrin-mediated endocytosis prevents amyloid beta-induced axonal damage." *Neurobiol Aging* 36 (5):1808-19. doi: 10.1016/j.neurobiolaging.2015.02.005.

Lana, E., M. Khanbolouki, C. Degavre, E. B. Samuelsson, E. Akesson, B. Winblad, E. Alici, C. U. Lithner, and H. Behbahani. 2016. "Perforin Promotes Amyloid Beta Internalisation in Neurons." *Mol Neurobiol*. doi: 10.1007/s12035-016-9685-9.

Leech, S., J. Kirk, J. Plumb, and S. McQuaid. 2007. "Persistent endothelial abnormalities and blood-brain barrier leak in primary and secondary progressive multiple sclerosis." *Neuropathol Appl Neurobiol* 33 (1):86-98. doi: NAN781 [pii]10.1111/j.1365-2990.2006.00781.x.

Mecocci, P., L. Parnetti, G. Romano, A. Scarelli, F. Chionne, R. Cecchetti, M. C. Polidori, B. Palumbo, A. Cherubini, and U. Senin. 1995. "Serum anti-GFAP and anti-S100 autoantibodies in brain aging, Alzheimer's disease and vascular dementia." *J Neuroimmunol* 57 (1-2):165-70.

Nagele, E., M. Han, C. Demarshall, B. Belinka, and R. Nagele. 2011. "Diagnosis of Alzheimer's disease based on disease-specific autoantibody profiles in human sera." *PLoS One* 6 (8):e23112. doi: 10.1371/journal.pone.0023112.

Nagele, E. P., M. Han, N. K. Acharya, C. DeMarshall, M. C. Kosciuk, and R. G. Nagele. 2013. "Natural IgG autoantibodies are abundant and ubiquitous in human sera, and their number is influenced by age, gender, and disease." *PLoS One* 8 (4):e60726. doi: 10.1371/journal.pone.0060726.

Nagele, R. G., P. M. Clifford, G. Siu, E. C. Levin, N. K. Acharya, M. Han, M. C. Kosciuk, V. Venkataraman, S. Zavareh, S. Zarrabi, K. Kinsler, N. G. Thaker, E. P. Nagele, J. Dash, H. Y. Wang, and A. Levitas. 2011. "Brain-reactive autoantibodies prevalent in human sera increase intraneuronal amyloid-beta(1-42) deposition." *J Alzheimers Dis* 25 (4):605-22. doi: 10.3233/JAD-2011-110098.

Nagele, R. G., M. R. D'Andrea, W. J. Anderson, and H. Y. Wang. 2002. "Intracellular accumulation of beta-amyloid(1-42) in neurons is facilitated by the alpha 7 nicotinic acetylcholine receptor in Alzheimer's disease." *Neuroscience* 110 (2):199-211. doi: S0306452201004602 [pii].

Nagele, R. G., M. R. D'Andrea, H. Lee, V. Venkataraman, and H. Y. Wang. 2003. "Astrocytes accumulate A beta 42 and give rise to astrocytic amyloid plaques in Alzheimer disease brains." *Brain Res* 971 (2):197-209. doi: S0006899303023618 [pii].

Rasband, W.S. 1997-2015. "ImageJ." U.S. National Institutes of Health. http://imagej.nih.gov/ij/.

Roche, S., Y. Dauvilliers, L. Tiers, C. Couderc, M. T. Piva, M. Provansal, A. Gabelle, and S. Lehmann. 2008. "Autoantibody profiling on high-density protein microarrays for biomarker discovery in the cerebrospinal fluid." *J Immunol Methods* 338 (1-2):75-8. doi: 10.1016/j.jim.2008.07.002.

Schott, K., H. Wormstall, M. Dietrich, R. Klein, and A. Batra. 1996. "Autoantibody reactivity in serum of patients with Alzheimer's disease and other age-related dementias." *Psychiatry Res* 59 (3):251-4. doi: 0165-1781(95)02703-3 [pii].

Singh, V. K., and H. H. Fudenberg. 1989. "Increase of immunoglobulin G3 subclass is related to brain autoantibody in Alzheimer's disease but not in Down's syndrome." *Autoimmunity* 3 (2):95-101.

Sui, Y. T., K. M. Bullock, M. A. Erickson, J. Zhang, and W. A. Banks. 2014. "Alpha synuclein is transported into and out of the brain by the blood-brain barrier." *Peptides* 62:197-202. doi: 10.1016/j.peptides.2014.09.018.

Terryberry, J. W., G. Thor, and J. B. Peter. 1998. "Autoantibodies in neurodegenerative diseases: antigen-specific frequencies and intrathecal analysis." *Neurobiol Aging* 19 (3):205-16. doi: S0197458098000499 [pii].

Wang, H. Y., D. H. Lee, M. R. D'Andrea, P. A. Peterson, R. P. Shank, and A. B. Reitz. 2000. "beta-Amyloid(1-42) binds to alpha7 nicotinic acetylcholine receptor with high affinity. Implications for Alzheimer's disease pathology." *J Biol Chem* 275 (8):5626-32.

Whitton, P. S. 2007. "Inflammation as a causative factor in the aetiology of Parkinson's disease." *Br J Pharmacol* 150 (8):963-76. doi: 0707167 [pii]10.1038/sj.bjp.0707167.

Zhao, Z., A. P. Sagare, Q. Ma, M. R. Halliday, P. Kong, K. Kisler, E. A. Winkler, A. Ramanathan, T. Kanekiyo, G. Bu, N. C. Owens, S. V. Rege, G. Si, A. Ahuja,

D. Zhu, C. A. Miller, J. A. Schneider, M. Maeda, T. Maeda, T. Sugawara, J. K. Ichida, and B. V. Zlokovic. 2015. "Central role for PICALM in amyloid-beta blood-brain barrier transcytosis and clearance." *Nat Neurosci* 18 (7):978-87. doi: 10.1038/nn.4025.

Zlokovic, B. V. 2008. "The blood-brain barrier in health and chronic neurodegenerative disorders." *Neuron* 57 (2):178-201. doi: 10.1016/j.neuron.2008.01.003.

Zlokovic, B. V. 2011. "Neurovascular pathways to neurodegeneration in Alzheimer's disease and other disorders." *Nat Rev Neurosci* 12 (12):723-38. doi: 10.1038/nrn3114.

ATTRIBUTIONS

Authors

Eric L Goldwaser[1, 2], Nimish K Acharya[4], Hao Wu[2], George Godsey[1, 2], Abhirup Sarkar[1, 2], Cassandra DeMarshall[1, 2], Mary Kosciuk[1, 2], and Robert G Nagele[1, 2, 3]

Affiliations

[1]Biomarker Discovery Center, New Jersey Institute for Successful Aging, Rowan University School of Osteopathic Medicine, Stratford, NJ 08084

[2]Graduate School of Biomedical Sciences, Rowan University, Stratford, NJ 08084

[3]Department of Geriatrics and Gerontology, Rowan University School of Osteopathic Medicine, Stratford, NJ 08084

[4]Department of Neurosurgery, University of Pennsylvania, Philadelphia, Pennsylvania, PA 19104

Funding disclosure

The authors wish to thank the Osteopathic Heritage Foundation and the Dean's endowment for primary care research for support of this project.

Running headline

Autoantibody-mediated endocytosis of $A\beta_{42}$

Figure 1. ELG, GG, NKA, AS helped in the culturing and maintaining the cell lines, as well as establishing protocol adapted for ICC experiments. ELG imaged, analyzed, and quantified data.

Figure 1 Supplemental. ELG, GG, NKA, AS helped in the culturing and maintaining the cell lines, as well as establishing protocol adapted for ICC

experiments. ELG imaged, analyzed, and quantified data. HW helped in construction of the graphical representation.

Figure 2. ELG, GG, NKA, AS helped in the culturing and maintaining the cell lines, as well as establishing protocol adapted for ICC experiments. ELG imaged, analyzed, and quantified data.

Figure 3. ELG, GG, NKA, AS helped in the culturing and maintaining the cell lines, as well as establishing protocol adapted for ICC experiments. ELG imaged, analyzed, and quantified data. HW helped in construction of the graphical representations.

Figure 4. ELG, GG, NKA, AS helped in the culturing and maintaining the cell lines, as well as establishing protocol adapted for ICC experiments. ELG imaged, analyzed, and quantified data. HW helped in construction of the graphical representations.

Figure 5. ELG, GG, NKA, AS helped in the culturing and maintaining the cell lines, as well as establishing protocol adapted for ICC experiments. ELG imaged, analyzed, and quantified data. HW helped in construction of the graphical representations.

Figure 6. ELG, GG, NKA, AS helped in the culturing and maintaining the cell lines, as well as establishing protocol adapted for ICC experiments. ELG imaged, analyzed, and quantified data. HW helped in construction of the graphical representations.

Figure 7. ELG, GG, NKA, AS helped in the culturing and maintaining the cell lines, as well as establishing protocol adapted for ICC experiments. ELG imaged,

analyzed, and quantified data. HW helped in construction of the graphical representations.

Figure 3 Supplemental. ELG, AS, and NKA helped in antibody purification and papain digestion, as well as performing the SDS-PAGE.

Table 1. ELG, CD, and NKA helped in running the microarrays and interpreting the data. RGN, MK, and AS helped in conception and implementing the idea.

Chapter VII

Perspectives

SUMMARY

Brain homeostasis can be affected in a number of ways that lead to gross anatomical, cellular, and molecular disturbances. Subsequent neurological, cognitive, and behavioral symptoms are manifest and constitute an array of diseases, including Alzheimer's disease (AD) and related dementias. Unfortunately, the mechanistic pathoetiology of AD that culminates in its hallmark features of cerebral amyloid plaque buildup, synaptic loss, and neuronal death are still disputed. Current literature directs more attention to the vasculature that nourishes the brain as paramount in maintaining normal functioning of neurons (Anderson and Nedergaard 2003, Clifford et al. 2008, de la Torre 2006, Deane et al. 2003, Deane and Zlokovic 2007, Drake and Iadecola 2007). Inherent in the brain vasculature is the blood-brain barrier (BBB) tasked with compartmentalizing blood-borne components, including immunoglobulins and pathogens, from access to cerebral parenchyma, an otherwise immunoprivileged site. Recent findings have implicated a permeable BBB, as evidenced by extravasated plasma components, in all stages of AD (Acharya et al. 2013, Amaducci, Falcini, and Lippi 1992, Bouras et al. 2005, Goldwaser 2015, Hsu and Kanoski 2014, Kandimalla et al. 2009, Nagele et al. 2011, Pflanzner et al. 2011, Romanitan et al. 2007, Shams et al. 2016, Wisniewski, Vorbrodt, and Wegiel 1997, Zlokovic 2011, 2008). Past findings in our lab have shown immunoglobulin G (IgG) to undergo neuronal binding and internalization in $A\beta_{42}$-burdened, especially those that find themselves within the plasma leak clouds (Clifford et al. 2007, D'Andrea 2001, Nagele et al. 2002, Nagele et al. 2003).

The work I have presented here continues the trend of providing evidence that points to an autoantibody-mediated endocytic mechanism that facilitates $A\beta_{42}$ entry into neurons that are vulnerable to AD pathological changes. Furthermore, we show that, within the vast antibody repertoire that any individual has in his or her possession, there exists hundreds of autoantibodies, and some of these are now known to bind to neurons once access is given via a disrupted BBB (Nagele et al. 2013, Nagele et al. 2011). Like other antibodies, upon binding to their cognate receptor, these will induce endocytosis. In the context of AD and the work we have shown here, we have filled a critical gap in the mechanism that relates to our working hypothesis. Previous works by Peter Clifford DO/PhD, Gilbert Siu DO/PhD, Michael D'Andrea PhD, Nimish Acharya PhD, and Eli Levin DO/PhD in this laboratory have elucidated many of the steps involved in this process, but these have not been judiciously tested in a cell-based system.

At the beginning of the proposed mechanism, the single most important factor crucial for maintenance of overall brain homeostasis is the blood-brain barrier (BBB) – more specifically, the tight junctions of the BBB (Acharya et al. 2013). During inflammatory conditions, brought on either acutely (as in during general anesthesia) or chronically (as in disorders like diabetes, hypertension, cancer), the BBB becomes leaky. In the elderly, there appears to be a high incidence of non-recovery from these acute BBB insults (Strom, Rasmussen, and Sieber 2014, Vasilevskis et al. 2012). Once this occurs, indiscriminate leakage of blood components small enough to fit

through the now-porous BBB, can readily be detected using immunohistochemistry, unambiguously, and unequivocally. Next, the neurons, which display cognate receptors on their surface, will bind autoantibodies that recognize them; the ones without any cognate receptors will remain unscathed. Upon binding, autoantibodies will cross-link surface membrane proteins, presumably of similar class, avidity, and affinity, and rigidify regions of surface membrane. The cell responds to this stimulus by internalizing the region of surface membrane that includes these autoantibody-receptor complexes, as well as nearby membrane within clathrin-coated pits. This receptor and antibody-mediated endocytosis pathway was described by past scientists like Michael Brown, PhD and Joe Goldstein, PhD, who won their Nobel Prize for their work on LDL receptor-mediated endocytosis and receptor recycling (Herz et al. 1990). Next, the newly formed endocytic vesicle buds off from the surface membrane and enters the cytoplasm, carrying the autoantibody-receptor complex as it is trafficked through the endosomes. The intravesicular pH within endosomes begins to drop as they fuse with other endosomes at similar stages of maturation. After several minutes to hours of this acidification process, the endosome will begin to activate pH-sensitive enzymes and will transition to an endolysosome intermediate and eventually a lysosome as it progresses through this maturation process. Once in the lysosome, most proteins are normally degraded in the low pH and with enzymatic activity. However, in cases of proteinopathies like AD, $A\beta_{42}$ is resistant to degradation and can build up as a fibrillized aggregate with a more β-pleated sheet secondary structure. Although the receptors to which $A\beta_{42}$ binds may vary, their visualization with the amyloid plaques is telling for one in particular, the α7nAChR

(D'Andrea 2001, Nagele et al. 2002, Nagele et al. 2003, Wang et al. 2012, Wang et al. 2000, Wang et al. 2009). As the $A\beta_{42}$ continues to accrue, the lysosomal compartment expands due to the coalescing of non-digestible fibrillized $A\beta_{42}$-burdened vesicles. If this process continues chronically, the lysosomal compartment will encroach on other vital organelles in the cell, perturbing function, and initiating the earliest forms of AD, also called mild cognitive impairment (Bouras et al. 1994, Braak and Braak 1991, Castellani and Perry 2014, D'Andrea et al. 2001, Giannakopoulos et al. 1997, Gomez-Isla et al. 1997, Gouras, Almeida, and Takahashi 2005, Ikonomovic et al. 2008). As the cell accumulates more and more $A\beta_{42}$, it will eventually undergo lysis, presumably through a necrotic mechanism, and disperse its cellular contents out as a plaque. The inflammatory state that ensues locally is thought to be due to the effect of dsDNA on glial activation. Unfortunately, the microglia cannot digest the $A\beta_{42}$ in its fibrillized form (or ubiquitin or hyperphosophorylated Tau), and thus these are what remains within the plaque after microglial activity has subsided, since they could not be digested by the lysosomal compartment's onslaught of proteases.

CONCLUSIONS AND FUTURE DIRECTIONS

The part of the aforementioned proposed mechanism that still remained to be elucidated was the major thrust of my thesis work – demonstrating in living cells that cellular and mechanistic descriptions for autoantibody and $A\beta_{42}$ internalization are valid. I have shown that the autoantibody component of serum does in fact bind to the surface of neurons and induces a global receptor-stripping phenomenon, and co-localizes with $A\beta_{42}$, endosome, and lysosome at varying points during endocytosis. The lysosomal compartment grows, both in human AD and in vitro under conditions of extended $A\beta_{42}$ treatment. Although various possible mechanisms exist for $A\beta_{42}$ internalization, the use of a series of different inhibitors of various aspects of endocytosis here has helped to characterize the dynamin-dependent, clathrin-mediated endocytosis that operates to bring $A\beta_{42}$ and autoantibodies into the cell, predominantly. I also describe the necessity for cross-linking that a bivalent autoantibody can achieve in order to induce endocytosis.

Other disorders of the central nervous system have also cited the presence of a disrupted BBB functional integrity and subsequent IgG leakage into the surrounding brain parenchyma (Odoardi et al. 2007, Bauman et al. 2013, Burgoon et al. 1999, Dahm et al. 2014, Engelhardt and Appel 1990, Kumar, Cohen, and Eisdorfer 1988, Nagele et al. 2011, Ortiz et al. 2014). Classical examples of such conditions are N-methyl D-aspartate receptor (NMDAR) encephalitis and multiple sclerosis, whereby a patient's autoantibodies target neuronal surface proteins or other components, gaining

entry presumably through a broken BBB (Hammer et al. 2014, Hughes et al. 2010). However, recently, other disorders not typically associated with autoimmune disease have surfaced where BBB breakdown and aAb may also play a key role – epilepsy, post-ictal psychosis, schizophrenia, and Parkinson's disease to name a few (Sui et al. 2014). NMDAR encephalitis was described in cellular and molecular mechanistic detail by Drs. Dalmau, Moscato, Hughes, and colleagues (Hughes et al. 2010, Moscato et al. 2014). Other similar research findings regarding NMDAR autoantibodies and their role in schizophrenia has been described by Dr. Ehrenreich's group (Dahm et al. 2014, Hammer et al. 2014). Essentially, what we can conclude from the research I am presenting here is that AD can fall along a spectrum of diseases that include classical autoimmune diseases as sharing pathoetiological underpinnings – including BBB breakdown and autoantibody binding and internalizing. The key difference is that in AD, a protein aggregation pathway exists. Unlike NMDAR encephalitis in which symptoms appear in response to NMDA receptor depletion on the surface, AD pathology also includes protein accumulation on the lysosomal side. In AD, $A\beta_{42}$ "hijacks" this system and accumulates within the cell. This again agrees with the BBB breakdown as the initiating event, which occurs prior to neuronal dysfunction in all of the diseases mentioned above. To consider autoimmunity as a genre of disease may misclassify a spectrum of disorders that actually have much in common regarding their most upstream inciting factors (that is, BBB damage). More importantly, treatment options may overlap for seemingly unrelated disorders. Perhaps a redefinition of our concept of autoimmune diseases is warranted in light of the growing field of research across the neurosciences.

In a pilot study investigating the acute effects of inhaled anesthetics on the structural and functional integrity of the BBB, we demonstrated that exposure to anesthetics favor an acute and dramatic disruption of BBB integrity, leading to a leakage of IgG into the cerebral cortex. As in our AD models and pathological specimens, the autoantibodies bound to subsets of neurons and were increased in regions of anesthetic-induced BBB breakdown. The extent of this effect was directly proportional to the age of the animal, which parallels the incidence of post-operative delirium (POD) seen in the elderly in the clinical setting, thus posing as a potential link to post-operative cognitive decline and later AD in these same subjects. Furthermore, sevoflurane may be more damaging to the BBB than isoflurane, which agrees with clinical observations in which sevoflurane more quickly induces a surgical plane of anesthesia in the patient than many other anesthetics (sevoflurane is more potent). This piece of inference is quite impactful, in that it not only describes, for the first time, a difference in efficacy, but also it advocates for more individualized approaches to anesthesia administration. Sevoflurane, a third-generation anesthetic, enables a patient to more quickly emerge from anesthesia than isoflurane, a second-generation anesthetic, as well. Perhaps inhaled anesthetics should be studied for their POD effects, rather than the immediate induction/emergence in perioperative care.

Lastly, the ability of BBB integrity (or the lack of it) to be visualized or detected clinically has remained elusive, yet is invaluable for pre-symptomatic diagnoses and

thus treatment efforts, given the aforementioned data. In a previously published study using a diabetic young pig model, pathological changes were demonstrated in the brain parenchyma that faithfully recapitulated AD-type changes. The retinas of these pigs were also investigated for regions of blood-retinal barrier (BRB) leakage and neuronal pathology in the ganglion cell layer. As a final part of my thesis objective, this project was able to show categorical similarities between the BRB and BBB. By allowing for a juxtaposed comparison between the BBB and the BRB, it opens up doors clinically to use the BRB as a surrogate system to detect ongoing BBB pathology. Given the previously mentioned phenomenon of BBB demise across many neurocognitive and neurological disorders, this notion may have highly impactful clinical relevance. Fluorescein angiograms have fallen out of style in academic ophthalmological studies, supplanted by Optical Coherence Tomography, which can detect finer details regarding the cellularity and thicknesses of layers, but does not detect the vasculature whatsoever. Fluorescence photometry can detect minute amounts of fluorescein leakage into the vitreous of the eye, however traditional slit-lamps do not have such resolving abilities. Thus, fluorophotometry may have a place in the future for diagnostics of neurodegenerative diseases at a very early stage, making treatments more amenable to work. Taken together, these research endeavors help to broaden the landscape of mechanistic knowledge surrounding AD and other neurological diseases, and have provided new perspectives on pathogenesis, diagnosis, and treatment efforts.

REFERENCES

Acharya, N. K., E. C. Levin, P. M. Clifford, M. Han, R. Tourtellotte, D. Chamberlain, M. Pollaro, N. J. Coretti, M. C. Kosciuk, E. P. Nagele, C. Demarshall, T. Freeman, Y. Shi, C. Guan, C. H. Macphee, R. L. Wilensky, and R. G. Nagele. 2013. "Diabetes and hypercholesterolemia increase blood-brain barrier permeability and brain amyloid deposition: beneficial effects of the LpPLA2 inhibitor darapladib." *J Alzheimers Dis* 35 (1):179-98. doi: 10.3233/JAD-122254.

Amaducci, L., M. Falcini, and A. Lippi. 1992. "Humoral and cellular immunologic repertoire in Alzheimer's disease." *Ann N Y Acad Sci* 663:349-56.

Anderson, C. M., and M. Nedergaard. 2003. "Astrocyte-mediated control of cerebral microcirculation." *Trends Neurosci* 26 (7):340-4; author reply 344-5. doi: S0166223603001413 [pii].

Bauman, M. D., A. M. Iosif, P. Ashwood, D. Braunschweig, A. Lee, C. M. Schumann, J. Van de Water, and D. G. Amaral. 2013. "Maternal antibodies from mothers of children with autism alter brain growth and social behavior development in the rhesus monkey." *Transl Psychiatry* 3:e278. doi: 10.1038/tp.2013.47.

Bouras, C., P. R. Hof, P. Giannakopoulos, J. P. Michel, and J. H. Morrison. 1994. "Regional distribution of neurofibrillary tangles and senile plaques in the cerebral cortex of elderly patients: a quantitative evaluation of a one-year autopsy population from a geriatric hospital." *Cereb Cortex* 4 (2):138-50.

Bouras, C., B. M. Riederer, E. Kovari, P. R. Hof, and P. Giannakopoulos. 2005. "Humoral immunity in brain aging and Alzheimer's disease." *Brain Res Brain Res Rev* 48 (3):477-87. doi: S0165-0173(04)00126-2 [pii]10.1016/j.brainresrev.2004.09.009.

Braak, H., and E. Braak. 1991. "Neuropathological stageing of Alzheimer-related changes." *Acta Neuropathol* 82 (4):239-59.

Burgoon, M. P., G. P. Owens, T. Smith-Jensen, D. Walker, and D. H. Gilden. 1999. "Cloning the antibody response in humans with inflammatory central nervous system disease: analysis of the expressed IgG repertoire in subacute sclerosing panencephalitis brain reveals disease-relevant antibodies that recognize specific measles virus antigens." *J Immunol* 163 (6):3496-502. doi: ji_v163n6p3496 [pii].

Castellani, R. J., and G. Perry. 2014. "The complexities of the pathology-pathogenesis relationship in Alzheimer disease." *Biochem Pharmacol* 88 (4):671-6. doi: 10.1016/j.bcp.2014.01.009.

Clifford, P. M., G. Siu, M. Kosciuk, E. C. Levin, V. Venkataraman, M. R. D'Andrea, and R. G. Nagele. 2008. "Alpha7 nicotinic acetylcholine receptor expression by vascular smooth muscle cells facilitates the deposition of Abeta peptides and promotes cerebrovascular amyloid angiopathy." *Brain Res* 1234:158-71. doi: S0006-8993(08)01811-8 [pii]10.1016/j.brainres.2008.07.092 [doi].

Clifford, P. M., S. Zarrabi, G. Siu, K. J. Kinsler, M. C. Kosciuk, V. Venkataraman, M. R. D'Andrea, S. Dinsmore, and R. G. Nagele. 2007. "Abeta peptides can enter the brain through a defective blood-brain barrier and bind selectively to neurons." *Brain Res* 1142:223-36. doi: S0006-8993(07)00127-8 [pii]10.1016/j.brainres.2007.01.070 [doi].

D'Andrea, M. R., R. G. Nagele, H. Y. Wang, P. A. Peterson, and D. H. Lee. 2001. "Evidence that neurones accumulating amyloid can undergo lysis to form amyloid plaques in Alzheimer's disease." *Histopathology* 38 (2):120-34. doi: his1082 [pii].

D'Andrea, M. R., Nagele, R. G., Wang, H-Y., Peterson, P. A., Lee, D. H. 2001. "Evidence that neurones accumulating amyloid can undergo lysis to form amyloid plaques in Alzheimer's disease." *Histopathology* 38:120-134.

Dahm, L., C. Ott, J. Steiner, B. Stepniak, B. Teegen, S. Saschenbrecker, C. Hammer, K. Borowski, M. Begemann, S. Lemke, K. Rentzsch, C. Probst, H. Martens, J. Wienands, G. Spalletta, K. Weissenborn, W. Stocker, and H. Ehrenreich. 2014. "Seroprevalence of autoantibodies against brain antigens in health and disease." *Ann Neurol* 76 (1):82-94. doi: 10.1002/ana.24189.

de la Torre, J. C. 2006. "How do heart disease and stroke become risk factors for Alzheimer's disease?" *Neurol Res* 28 (6):637-44. doi: 10.1179/016164106X130362.

Deane, R., S. Du Yan, R. K. Submamaryan, B. LaRue, S. Jovanovic, E. Hogg, D. Welch, L. Manness, C. Lin, J. Yu, H. Zhu, J. Ghiso, B. Frangione, A. Stern, A. M. Schmidt, D. L. Armstrong, B. Arnold, B. Liliensiek, P. Nawroth, F. Hofman, M. Kindy, D. Stern, and B. Zlokovic. 2003. "RAGE mediates amyloid-beta peptide transport across the blood-brain barrier and accumulation in brain." *Nat Med* 9 (7):907-13. doi: 10.1038/nm890nm890 [pii].

Deane, R., and B. V. Zlokovic. 2007. "Role of the blood-brain barrier in the pathogenesis of Alzheimer's disease." *Curr Alzheimer Res* 4 (2):191-7.

Drake, C. T., and C. Iadecola. 2007. "The role of neuronal signaling in controlling cerebral blood flow." *Brain Lang* 102 (2):141-52. doi: S0093-934X(06)00357-9 [pii]10.1016/j.bandl.2006.08.002.

Engelhardt, J. I., and S. H. Appel. 1990. "IgG reactivity in the spinal cord and motor cortex in amyotrophic lateral sclerosis." *Arch Neurol* 47 (11):1210-6.

Giannakopoulos, P., P. R. Hof, J. P. Michel, J. Guimon, and C. Bouras. 1997. "Cerebral cortex pathology in aging and Alzheimer's disease: a quantitative survey of large hospital-based geriatric and psychiatric cohorts." *Brain Res Brain Res Rev* 25 (2):217-45. doi: S0165017397000234 [pii].

Goldwaser, E. L., Acharya, N. K., Nagele, R. G. 2015. "Cerebrovascular and Blood-brain barrier compromise: A mechanistic link between Vascular disease and Alzheimer's disease subtypes of Neurocognitive disorders." *J Parkinsons Dis Alzheimer Dis* 2 (2):10.

Gomez-Isla, T., R. Hollister, H. West, S. Mui, J. H. Growdon, R. C. Petersen, J. E. Parisi, and B. T. Hyman. 1997. "Neuronal loss correlates with but exceeds neurofibrillary tangles in Alzheimer's disease." *Ann Neurol* 41 (1):17-24. doi: 10.1002/ana.410410106.

Gouras, G. K., C. G. Almeida, and R. H. Takahashi. 2005. "Intraneuronal Abeta accumulation and origin of plaques in Alzheimer's disease." *Neurobiol Aging* 26 (9):1235-44. doi: 10.1016/j.neurobiolaging.2005.05.022.

Hammer, C., B. Stepniak, A. Schneider, S. Papiol, M. Tantra, M. Begemann, A. L. Siren, L. A. Pardo, S. Sperling, S. Mohd Jofrry, A. Gurvich, N. Jensen, K. Ostmeier, F. Luhder, C. Probst, H. Martens, M. Gillis, G. Saher, F. Assogna, G. Spalletta, W. Stocker, T. F. Schulz, K. A. Nave, and H. Ehrenreich. 2014. "Neuropsychiatric disease relevance of circulating anti-NMDA receptor autoantibodies depends on blood-brain barrier integrity." *Mol Psychiatry* 19 (10):1143-9. doi: 10.1038/mp.2013.110.

Herz, J., R. C. Kowal, Y. K. Ho, M. S. Brown, and J. L. Goldstein. 1990. "Low density lipoprotein receptor-related protein mediates endocytosis of monoclonal antibodies in cultured cells and rabbit liver." *J Biol Chem* 265 (34):21355-62.

Hsu, T. M., and S. E. Kanoski. 2014. "Blood-brain barrier disruption: mechanistic links between Western diet consumption and dementia." *Front Aging Neurosci* 6:88. doi: 10.3389/fnagi.2014.00088.

Hughes, E. G., X. Peng, A. J. Gleichman, M. Lai, L. Zhou, R. Tsou, T. D. Parsons, D. R. Lynch, J. Dalmau, and R. J. Balice-Gordon. 2010. "Cellular and synaptic mechanisms of anti-NMDA receptor encephalitis." *J Neurosci* 30 (17):5866-75. doi: 10.1523/jneurosci.0167-10.2010.

Ikonomovic, M. D., W. E. Klunk, E. E. Abrahamson, C. A. Mathis, J. C. Price, N. D. Tsopelas, B. J. Lopresti, S. Ziolko, W. Bi, W. R. Paljug, M. L. Debnath, C. E. Hope, B. A. Isanski, R. L. Hamilton, and S. T. DeKosky. 2008. "Post-mortem correlates of in vivo PiB-PET amyloid imaging in a typical case of Alzheimer's disease." *Brain* 131 (Pt 6):1630-45. doi: 10.1093/brain/awn016.

Kandimalla, K. K., O. G. Scott, S. Fulzele, M. W. Davidson, and J. F. Poduslo. 2009. "Mechanism of neuronal versus endothelial cell uptake of Alzheimer's disease amyloid beta protein." *PLoS One* 4 (2):e4627. doi: 10.1371/journal.pone.0004627.

Kumar, M., D. Cohen, and C. Eisdorfer. 1988. "Serum IgG brain reactive antibodies in Alzheimer disease and Down syndrome." *Alzheimer Dis Assoc Disord* 2 (1):50-5.

Moscato, E. H., X. Peng, A. Jain, T. D. Parsons, J. Dalmau, and R. J. Balice-Gordon. 2014. "Acute mechanisms underlying antibody effects in anti-N-methyl-D-aspartate receptor encephalitis." *Ann Neurol* 76 (1):108-19. doi: 10.1002/ana.24195.

Nagele, E. P., M. Han, N. K. Acharya, C. DeMarshall, M. C. Kosciuk, and R. G. Nagele. 2013. "Natural IgG autoantibodies are abundant and ubiquitous in human sera, and their number is influenced by age, gender, and disease." *PLoS One* 8 (4):e60726. doi: 10.1371/journal.pone.0060726.

Nagele, R. G., P. M. Clifford, G. Siu, E. C. Levin, N. K. Acharya, M. Han, M. C. Kosciuk, V. Venkataraman, S. Zavareh, S. Zarrabi, K. Kinsler, N. G. Thaker, E. P. Nagele, J. Dash, H. Y. Wang, and A. Levitas. 2011. "Brain-reactive autoantibodies prevalent in human sera increase intraneuronal amyloid-beta(1-42) deposition." *J Alzheimers Dis* 25 (4):605-22. doi: 10.3233/JAD-2011-110098.

Nagele, R. G., M. R. D'Andrea, W. J. Anderson, and H. Y. Wang. 2002. "Intracellular accumulation of beta-amyloid(1-42) in neurons is facilitated by the alpha 7 nicotinic acetylcholine receptor in Alzheimer's disease." *Neuroscience* 110 (2):199-211. doi: S0306452201004602 [pii].

Nagele, R. G., M. R. D'Andrea, H. Lee, V. Venkataraman, and H. Y. Wang. 2003. "Astrocytes accumulate A beta 42 and give rise to astrocytic amyloid plaques

in Alzheimer disease brains." *Brain Res* 971 (2):197-209. doi: S0006899303023618 [pii].

Odoardi, F., N. Kawakami, W. E. Klinkert, H. Wekerle, and A. Flugel. 2007. "Blood-borne soluble protein antigen intensifies T cell activation in autoimmune CNS lesions and exacerbates clinical disease." *Proc Natl Acad Sci U S A* 104 (47):18625-30. doi: 0705033104 [pii]10.1073/pnas.0705033104.

Ortiz, G. G., F. P. Pacheco-Moises, M. A. Macias-Islas, L. J. Flores-Alvarado, M. A. Mireles-Ramirez, E. D. Gonzalez-Renovato, V. E. Hernandez-Navarro, A. L. Sanchez-Lopez, and M. A. Alatorre-Jimenez. 2014. "Role of the blood-brain barrier in multiple sclerosis." *Arch Med Res* 45 (8):687-97. doi: 10.1016/j.arcmed.2014.11.013.

Pflanzner, T., M. C. Janko, B. Andre-Dohmen, S. Reuss, S. Weggen, A. J. Roebroek, C. R. Kuhlmann, and C. U. Pietrzik. 2011. "LRP1 mediates bidirectional transcytosis of amyloid-beta across the blood-brain barrier." *Neurobiol Aging* 32 (12):2323.e1-11. doi: 10.1016/j.neurobiolaging.2010.05.025.

Romanitan, M. O., B. O. Popescu, B. Winblad, O. A. Bajenaru, and N. Bogdanovic. 2007. "Occludin is overexpressed in Alzheimer's disease and vascular dementia." *J Cell Mol Med* 11 (3):569-79. doi: JCMM047 [pii]10.1111/j.1582-4934.2007.00047.x.

Shams, S., T. Granberg, J. Martola, X. Li, M. Shams, S. M. Fereshtehnejad, L. Cavallin, P. Aspelin, M. Kristoffersen-Wiberg, and L. O. Wahlund. 2016. "Cerebrospinal fluid profiles with increasing number of cerebral microbleeds in a continuum of cognitive impairment." *J Cereb Blood Flow Metab* 36 (3):621-8. doi: 10.1177/0271678X15606141.

Strom, C., L. S. Rasmussen, and F. E. Sieber. 2014. "Should general anaesthesia be avoided in the elderly?" *Anaesthesia* 69 Suppl 1:35-44. doi: 10.1111/anae.12493.

Sui, Y. T., K. M. Bullock, M. A. Erickson, J. Zhang, and W. A. Banks. 2014. "Alpha synuclein is transported into and out of the brain by the blood-brain barrier." *Peptides* 62:197-202. doi: 10.1016/j.peptides.2014.09.018.

Vasilevskis, E. E., J. H. Han, C. G. Hughes, and E. W. Ely. 2012. "Epidemiology and risk factors for delirium across hospital settings." *Best Pract Res Clin Anaesthesiol* 26 (3):277-87. doi: 10.1016/j.bpa.2012.07.003.

Wang, H. Y., K. Bakshi, M. Frankfurt, A. Stucky, M. Goberdhan, S. M. Shah, and L. H. Burns. 2012. "Reducing amyloid-related Alzheimer's disease pathogenesis

by a small molecule targeting filamin A." *J Neurosci* 32 (29):9773-84. doi: 10.1523/JNEUROSCI.0354-12.2012.

Wang, H. Y., D. H. Lee, M. R. D'Andrea, P. A. Peterson, R. P. Shank, and A. B. Reitz. 2000. "beta-Amyloid(1-42) binds to alpha7 nicotinic acetylcholine receptor with high affinity. Implications for Alzheimer's disease pathology." *J Biol Chem* 275 (8):5626-32.

Wang, H. Y., A. Stucky, J. Liu, C. Shen, C. Trocme-Thibierge, and P. Morain. 2009. "Dissociating beta-amyloid from alpha 7 nicotinic acetylcholine receptor by a novel therapeutic agent, S 24795, normalizes alpha 7 nicotinic acetylcholine and NMDA receptor function in Alzheimer's disease brain." *J Neurosci* 29 (35):10961-73. doi: 10.1523/JNEUROSCI.6088-08.2009.

Wisniewski, H. M., A. W. Vorbrodt, and J. Wegiel. 1997. "Amyloid angiopathy and blood-brain barrier changes in Alzheimer's disease." *Ann N Y Acad Sci* 826:161-72.

Zlokovic, B. V. 2008. "The blood-brain barrier in health and chronic neurodegenerative disorders." *Neuron* 57 (2):178-201. doi: 10.1016/j.neuron.2008.01.003.

Zlokovic, B. V. 2011. "Neurovascular pathways to neurodegeneration in Alzheimer's disease and other disorders." *Nat Rev Neurosci* 12 (12):723-38. doi: 10.1038/nrn3114.

Appendix

Abbreviations list

Alzheimer's disease = AD
Amyloid-β_{1-42} = $A\beta_{42}$
Immunoglobulin = Ig
Blood-brain barrier = BBB
Autoantibody = aAb
Blood-retina barrier = BRB
Diagnostic and Statistical Manual = DSM
Neurocognitive disorder = NCD
Vascular dementia = VaD
Cerebrospinal fluid = CSF
Neurofibrillary tangle = NFT
Computed tomography = CT
Positron emission tomography = PET
Magnetic resonance imaging = MRI
Fluorescein isothiocyanate = FITC
Minimum alveolar concentration = MAC
Post-operative delirium = POD
Diabetes mellitus = DM
Hypercholesterolemia = HC
Receptors for advanced glycation end products = RAGE
Cardiovascular disease = CVD
Diabetic retinopathy = DR
RPE = retinal pigment epithelial
Alpha 7 nicotinic acetylcholine receptor = α7nAChR
Amyloid plaque = AP
Immunohistochemistry = IHC
Dynasore = Dyn
Genistein = Gen
Cytochalasin D = CytD
Phenylarsine oxide = PAO
Retinoic acid = RA